Elucidating Mechanisms of Post-Transcriptional Regulation in *Mycobacterium smegmatis*

by

Diego Alonso Vargas Blanco

A Dissertation
Submitted to the Faculty of the
WORCESTER POLYTECHNIC INSTITUTE
in partial fulfillment of the requirements for the degree of

Doctor of Philosophy
in
Biology and Biotechnology

December 18th, 2020

APPROVED BY:

Prof. José Argüello, Committee Member
Chemistry and Biochemistry, WPI

Prof. Reeta Rao, Committee Member
Biology and Biotechnology, WPI

Prof. Joseph Duffy, Committee Member
Biology and Biotechnology, WPI

Prof. Scarlet Shell, Advisor
Biology and Biotechnology, WPI

Abstract

One of the deadliest diseases in the world is tuberculosis, caused by the bacillus *Mycobacterium tuberculosis*. In contrast to most bacterial infections, treatment for tuberculosis requires of multidrug regimes that can extend from six months to over a year. Importantly, the exceptional capability of *M. tuberculosis* to survive stress conditions, such as low energy environments and the host immune response, has been shown to confer drug tolerance and drug resistance, two factors that impact treatment length and limit the selection of available antimicrobials, particularly when only a reduced number of drugs are effective against *M. tuberculosis*. Therefore, understanding the biology behind the microbial stress response becomes fundamental for drug development. Mycobacteria employ diverse transcriptional and posttranscriptional mechanisms that allow them to survive stressful environments. One of these is global RNA stabilization, a conserved microbial stress response usually associated with non-growing states. However, while there is extensive research on transcriptional regulation as a response to stress, only limited information is available on regulation of mRNA degradation. Here we sought to address this gap.

Because *M. tuberculosis* is a slow-growing bacteria, we conducted our studies on *Mycobacterium smegmatis*, a non-pathogenic and fast-growing relative. In Chapter 2, we show that it is possible to alter translation efficiency, transcript stability, and transcription rates in *M. smegmatis* by altering the 5' UTR in reporter constructs. The relative efficiency of leadered vs leaderless translation depended on the nature of the 5' UTR. Combined with a global proteome and transcriptome analysis, our results suggest that leaderless genes are globally translated with a similar range of efficiencies as leadered genes.

In Chapter 3 we show that mRNA stabilization as a response to stress is a reversible mechanism. The stable transcriptome of *M. smegmatis* in hypoxia can be rapidly degraded upon re-exposure to oxygen. This discovery led us to stablish a connection between mRNA degradation and metabolic status. We investigated distinct mechanisms that could stabilize the mRNA pool in response to stress. We found that

global stabilization could not be explained by RNA-degradation protein abundance, the stringent response, or changes in transcript abundance. However, we discovered that we could modulate mRNA degradation in growth-arrested *M. smegmatis* as a response to energy metabolism. These exciting findings provided evidence that mRNA degradation is not necessarily dependent on cell growth status, as previously conceived, and instead responds directly to energy metabolism status. These findings will help reorient studies on transcriptome stabilization, bringing us a step closer to identify the mechanism(s) responsible for mRNA stabilization under stress.

Work in other bacteria has shown that ribosome occupancy and translation can regulate mRNA degradation, at least in a transcript-specific manner. Therefore, we wondered if increased ribosome occupancy was responsible for global mRNA stabilization during stress. We used diverse approaches to investigate the impacts of translation and ribosome occupancy on mRNA degradation. Our results, detailed in Chapter 4, show that changes in ribosome occupancy do not explain global mRNA stabilization in energy stress. Interestingly, while we explored ribosome occupancy, we serendipitously accumulated data consistent with the idea that transcription and translation may be physically coupled in mycobacteria.

Understanding the universality of mRNA stabilization as part of the mycobacterial stress response has been a fascinating and challenging task, and an important one to undertake. As we aim to discover new antimicrobials, we must comprehend the biology of bacterial adaptation to stress. And because of increasing levels of antimicrobial resistance in *M. tuberculosis*, it is more important than ever to study different bacterial processes to reveal new drug targets. Here, we have compiled evidence that bring us closer to identifying the mechanism(s) by which mycobacteria can quickly stabilize their transcriptomes in response to stress.

Table of Contents

List of Figures and Supplemental Figures

List of Tables

List of Figures and Tables in Appendices

Acknowledgements

What a wonderful journey has been working on a Ph.D. in the Shell lab. Without a doubt, the years I spent in graduate school have been the best part of my life. For that, I am immensely grateful to you, Dr. Scarlet Shell. Your keen mind, your contagious passion for research, and your unconditional support have been instrumental in guiding me to this moment. You have pushed me to work harder, to be competitive, to enjoy giving talks, and to never give up. You have taught me how to be a scientist, how to be a teacher and how to be a better person. For that and much more I will always thank you.

I offer my gratitude to the members of my dissertation committee for their support and their critical role in shaping the scientist I wished to become. Dr. José Argüello, Dr. Reeta Rao and Dr. Joseph Duffy, you have encouraged me to think critically and to see the bigger picture beyond my research. Your excellent questions, feedback and insight have improved the quality of my research and dissertation. Furthermore, I thank you Dr. José Argüello for sharing your wisdom and perspectives on what awaits beyond graduate school; I will always remember your advice. And Dr. Reeta Rao, I would like to thank you again, this time for your support and guidance beyond graduate school.

To the current and past members of the Shell lab, thank you so much for your support, for your advice, for your happiness, for sharing your knowledge, and for your continual commitment to science. Dr. Carla Martini, Ying Zhou, Huaming Sun, and Julia Ryan, I will warmly treasure our time together. Thank you as well to the amazing Shell lab undergraduate scientists that are doing exceptional work. Specifically, to Sam Randall and Tien Nguyen for their friendship and their help with parts of my projects, I am joyful knowing you both are doing so well in your careers. For all the beautiful memories, thank you so much Shell lab.

Without a doubt I am extremely thankful to Dr. Tim Antonelli for his warm support throughout the years. Had you not encouraged me come to the United States, I would not have written this dissertation or

become who I am. You have been an important part of my life and for that I am so grateful. I value your friendship and I hope we can always count on each other.

I am also grateful to Dr. Rodney Macedo and Claudia “Gutich” Gutierrez for their support, advice, and eternal friendship; I am elated that we are in the same country once again, and I hope we do not have to keep chasing each other around the world. Thank you Dr. David Dolivo, Dr. Michelle McKee and soon-to-be Dr. Kevin Keating for your friendship, and for making my time as a graduate student more pleasant. To my friends in Peru: Arturo, Jorge and Paola Pinto, Alfredo Agüero, Claudia Calisaya, Claudia Gomez, Dorinha Castro and Rosalyn Diaz, thank you for your support and love. Thank you also to Alex Coleman, Mike Silvestri, Joshua Guzzi, Kelsey Alexander and Dr. Todd Alexander for their friendship and support, especially during the 2020 pandemic.

I would like to thank my uncle Hamilton Blanco and my parents, Alonso and Mitzi, who went above and beyond to enable my sisters and I to achieve our dreams, even though that required being miles apart. I am also grateful to my sisters Valeria and Daniela, for their love, support and help. Thank you so much Daniela, for always keeping an eye for me at home; I immensely appreciate it. Finally, thank you Dr. Steven Vandal; you have been the light in my life and I hope you will always be.

Chapter 1 : Regulation of mRNA stability during bacterial stress responses

Regulation of mRNA stability during bacterial stress responses

Diego A. Vargas-Blanco[1] and Scarlet S. Shell[1,2*]

[1]Department of Biology and Biotechnology, Worcester Polytechnic Institute, Worcester, MA, USA
[2]Program in Bioinformatics and Computational Biology, Worcester Polytechnic Institute, Worcester, MA, USA
Edited by: Omar Orellana. University of Chile, Chile

This chapter corresponds to a manuscript that was published as:

Vargas-Blanco, D.A., and Shell, S.S. (2020). Regulation of mRNA Stability During Bacterial Stress Responses. *Front Microbiol* 11**,** 2111. doi: 10.3389/fmicb.2020.02111.

Author Contributions

Conceptualization: D.A.V.-B. and S.S.S. Data Analysis: D.A.V.-B. and S.S.S. Writing – Original Draft: D.A.V.-B. Writing – Review and Editing: D.A.V.-B. and S.S.S.

Abstract

Bacteria have a remarkable ability to sense environmental changes, swiftly regulating their transcriptional and posttranscriptional machinery as a response. Under conditions that cause growth to slow or stop, bacteria typically stabilize their transcriptomes in what has been shown to be a conserved stress response. In recent years, diverse studies have elucidated many of the mechanisms underlying mRNA degradation, yet an understanding of the regulation of mRNA degradation under stress conditions remains elusive. In this review we discuss the diverse mechanisms that have been shown to affect mRNA stability in bacteria. While many of these mechanisms are transcript-specific, they provide insight into possible mechanisms of global mRNA stabilization. To that end, we have compiled information on how mRNA fate is affected by RNA secondary structures; interaction with ribosomes, RNA binding proteins, and small RNAs; RNA base modifications; the chemical nature of 5’ ends; activity and concentration of RNases and other degradation proteins; mRNA and RNase localization; and the stringent response. We also provide an

analysis of reported relationships between mRNA abundance and mRNA stability, and discuss the importance of stress-associated mRNA stabilization as a potential target for therapeutic development.

Introduction

Bacterial adaptation to stress is orchestrated by complex responses to specific environmental stimuli, capable of rapidly regulating transcription, transcript degradation, and translation, which increases the organism's survival opportunities. Historically, regulation mechanisms for transcriptional and translational pathways have been the most studied, providing insight into the genes and protein products needed for bacterial adaptation to unfavorable growth environments. These findings have been key for our understanding of bacterial biology, allowing us, for example, to develop tools to tune bacterial machinery for biotechnology processes (such as Tao et al., 2011; Courbet et al., 2015; Daeffler et al., 2017; Martinez et al., 2017; Riglar et al., 2017), and to discover and develop new antibacterial drugs (for example, Yarmolinsky and Haba, 1959; Wolfe and Hahn, 1965; Maggi et al., 1966; Olson et al., 2011). However, the role of RNA degradation in stress responses is not well understood.

Modulation of mRNA degradation has been associated with various stress conditions in bacteria, such as temperature changes, growth rate, nutrient starvation, and oxygen limitation (see Table 1-1). Transcript stability—also referred as mRNA or transcript half-life—was shown to be globally altered in response to some stressors, while in other cases, gene-specific modulation of transcript stability contributes to specific expression changes that bacteria need to adapt to and survive in new environments (Figure 1-1).

In this review we will discuss a range of reported situations in which bacterial mRNA stability is modulated in response to various stress conditions, with a focus on known and suspected mechanisms underlying such regulation. We will also discuss the ways in which known gene-specific mechanisms shape our thinking on the unanswered question of how mRNA pools are globally stabilized in response to energy

stress. Furthermore, we will discuss the ways in which regulation of mRNA stability in clinically relevant bacteria such as *Mycobacterium tuberculosis* shape their responses to the host environment.

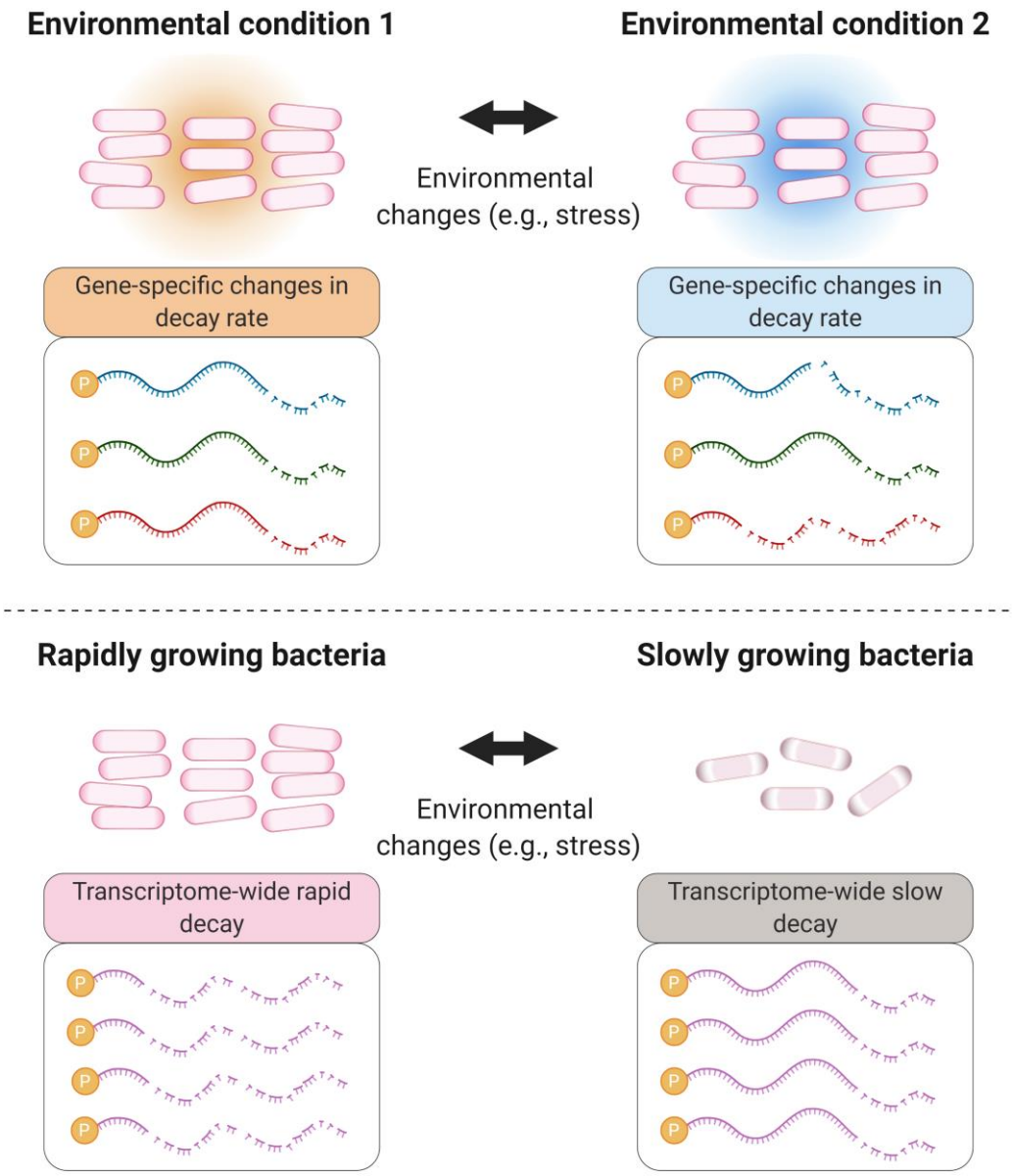

Figure 1-1. Environmental changes cause mRNA degradation rates to change in both global and gene-specific ways. Bacterial adaptation to many stressors, and other changes in environment, involve modulation of degradation rates of specific transcripts encoding proteins relevant to the changing conditions (top panel). Some stressors, particularly those causing severe energy stress, trigger global stabilization of the mRNA pool (bottom panel). These scenarios are not mutually exclusive; stressors that cause global transcriptome stabilization typically also cause gene-specific changes in relative degradation rates.

RNases and other degradation proteins

The degradosome

RNA degradation is carried out by a wide range of RNases, enzymes with strong activities and relatively low specificities towards their targets (reviewed in Carpousis, 2007). There are two main types of RNases: endonucleases and exonucleases. The former cleave RNA sequences at internal points, while the latter carry out nucleolytic attacks from either end of the RNA chain (deemed 5' or 3' exonucleases based on their enzymatic directionality). Some bacteria possess both 5' and 3' exonucleases—*M. tuberculosis* and *Mycobacterium smegmatis*, for example—while others such as *E. coli* have only 3' exonucleases.

With respect to RNA degradation systems, *E. coli* is perhaps the most studied organism. In fact, it was in *E. coli* that a multiprotein complex, deemed the degradosome (Figure 1-2), was first reported (Carpousis et al., 1994; Py et al., 1994). In *E. coli*, the main degradosome components are two RNases (RNase E and PNPase), a DEAD-box RNA helicase (RhlB), and a glycolytic enzyme (enolase) (Carpousis et al., 1994; Py et al., 1994; Marcaida et al., 2006; Carpousis, 2007). RhlB facilitates RNase activity by unwinding stem-loops within RNA targets (Py et al., 1996). Both RNases carry out RNA degradation (Mohanty and Kushner, 2000; Deutscher, 2006; Unciuleac and Shuman, 2013). Moreover, in this bacterium the C-terminal region of RNase E acts as a scaffold for other degradosome components (Kido et al., 1996; Vanzo et al., 1998; Lopez et al., 1999; Morita et al., 2004). However, not all of the degradosome components are well defined or have known roles. For example, enolase is suspected to have a regulatory role in mRNA degradation under low phosphosugar levels (Morita et al., 2004; Chandran and Luisi, 2006) and anaerobic conditions (Murashko and Lin-Chao, 2017).

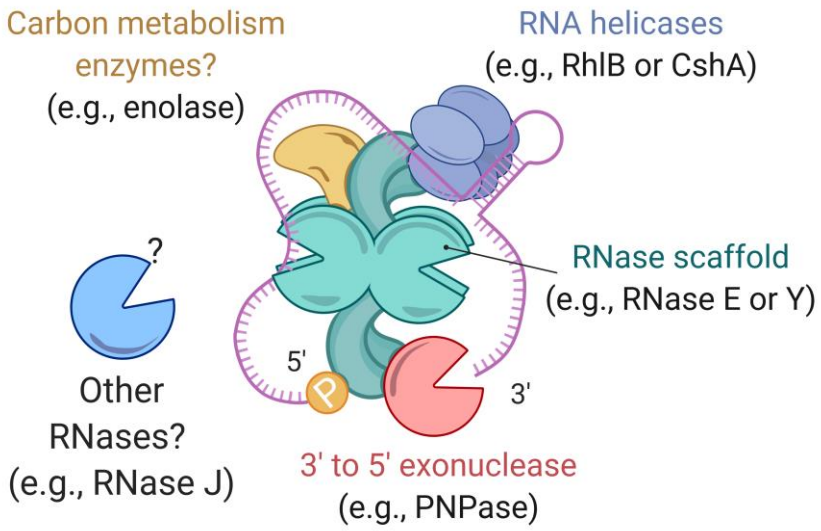

Figure 1-2. Bacterial degradosomes. The bacterial degradosome is scaffolded by an RNase such as RNase E in *E. coli* and RNase Y in *B. subtilis*. The RNase scaffolds have catalytic domains and natively disordered scaffold domains that bind other degradosome proteins. Typical degradosome components in both gram-positive and gram-negative bacteria are RNA helicases, carbon metabolism enzymes, and other RNases.

While RNases can degrade RNA substrates on their own, it has been suggested that degradosomes increase the efficiency of RNA degradation, for example by facilitating processing of structures such as stem-loops and repeated extragenic palindromic sequences (Newbury et al., 1987; McLaren et al., 1991; Py et al., 1996). Alteration of the degradosome components leads to changes in transcriptome stability; for example, deletion of RhlB in *E. coli* results in longer mRNA half-lives (Bernstein et al., 2004). Similarly, mRNA stability is dramatically increased when the arginine-rich RNA binding region or the scaffolding region of RNase E are deleted (Kido et al., 1996; Ow et al., 2000). While the RNA degradosome of *E. coli* has been extensively studied, the composition and function of degradosomes in other gram-negatives and in gram-positives may differ and new studies are still uncovering this information. In the Firmicute *Bacillus subtilis,* there is no RNase E homolog. Instead, RNase Y serves as a degradosome scaffold for PNPase, the helicase CshA (Lehnik-Habrink et al., 2010), phosphofructokinase (Commichau et al., 2009), and RNase J1 and RNase J2—two bifunctional enzymes with both endonucleolytic and 5’ to 3’ exoribonuclease activity (Even et al., 2005; Shahbabian et al., 2009; Mathy et al., 2010; Durand et al., 2012). Interestingly, the *B.*

subtilis degradosome interactions have been shown mainly by bacterial 2-hybrid assays and immunoprecipitation of complexes stabilized by formaldehyde crosslinking (Commichau et al., 2009; Lehnik-Habrink et al., 2010), in contrast to the *E. coli* degradosome which can be immunoprecipitated without a crosslinking agent (Carpousis et al., 1994; Py et al., 1994; Py et al., 1996). This suggests that *B. subtilis* degradosomes could be more transient in nature. A recent report on the Actinomycete *M. tuberculosis* provided insight into its elusive degradosome structure, which appears to be composed of RhlE (an RNA helicase), PNPase, RNase E, and RNase J (Plocinski et al., 2019). Overall, the degradosome is considered to be the ultimate effector of bulk mRNA degradation in bacterial cells, but it has also been implicated in regulating the stability of specific mRNAs and sRNAs as will be discussed in later sections. For further details on the degradosome, we encourage reading the following reviews (Carpousis, 2007; Bandyra et al., 2013; Ait-Bara and Carpousis, 2015; Cho, 2017; Tejada-Arranz et al., 2020).

An overview of RNase regulation

There are multiple ways in which transcript levels can be regulated. Alteration of mRNA steady-state abundance is ultimately a consequence of changes in transcription, changes in mRNA half-life, or both. In the process of mRNA degradation, the roles of different RNases may be defined in part by their preferred cleavage sequences. In *Staphylococcus aureus*, RNase Y cleavage is usually in the R↓W sequence, near AU rich regions (Khemici et al., 2015). This pattern seems to be conserved in *B. subtilis* (Shahbabian et al., 2009). Furthermore, in these two gram-positive organisms, RNase Y cleavage appears to be influenced by proximity to a secondary structure. In *E. coli*, RNase E cleaves single-stranded RNA with a strong preference for the +2 sites in RN↓AU (Mackie, 1992; McDowall et al., 1994), or in RN↓WUU in *Salmonella enterica* (Chao et al., 2017). In *M. smegmatis*, a strong preference for cleavage 5' of cytidines was detected in a transcriptome-wide RNA cleavage analysis (Martini et al., 2019). RNase E could be responsible for these cleavage events, given its major role in mycobacteria; however, we cannot yet exclude the possibility that they are produced by another endonuclease. In contrast, RNase III in *E. coli* has optimal

activity on double-stranded RNA, where the cleavage site is specified by both positive and negative sequence and secondary structure determinants (Pertzev and Nicholson, 2006). While the preferred cleavage sites of various RNases seem highly represented in the mRNA pool, some transcripts are more resistant to cleavage than others, indicating the presence of mechanisms that regulate not only bulk RNA stability, but also differential stabilities among transcripts.

Studies of various mRNAs have identified multiple features that confer protection against RNase cleavage (Figure 1-3 and Figure 1-4A). These include stem-loops (Emory et al., 1992; McDowall et al., 1995; Arnold et al., 1998; Hambraeus et al., 2002), 5' UTRs and leader/leaderless status (Chen et al., 1991; Arnold et al., 1998; Unniraman et al., 2002; Nguyen et al., 2020), subcellular compartmentalization (Khemici et al., 2008; Montero Llopis et al., 2010; Murashko et al., 2012; Khemici et al., 2015; Moffitt et al., 2016); 5' triphosphate groups (Bouvet and Belasco, 1992; Emory et al., 1992; Arnold et al., 1998; Mackie, 1998), 5' NAD^+/NADH/dephospho-coenzyme A caps (Chen et al., 2009; Kowtoniuk et al., 2009; Bird et al., 2016; Frindert et al., 2018), Np_nN caps (Luciano et al., 2019; Hudecek et al., 2020), and association with regulatory proteins and sRNAs (Braun et al., 1998; Gualerzi et al., 2003; Moll et al., 2003; Afonyushkin et al., 2005; Daou-Chabo et al., 2009; Nielsen et al., 2010; Morita and Aiba, 2011; Faner and Feig, 2013; Liang and Deutscher, 2013; Deng et al., 2014; Sinha et al., 2018; Zhao et al., 2018; Cameron et al., 2019; Chen et al., 2019a; Richards and Belasco, 2019). For example, in *Streptococcus pyogenes* the sRNA FasX binds to the 5' end of *ska*—a transcript coding for streptokinase—increasing its mRNA half-life, thus allowing an extended period of time in which translation of streptokinase can occur (Ramirez-Pena et al., 2010). In other cases, the product of an mRNA can regulate its own transcript stability. In *E. coli*, the fate of the *lysC* transcript is regulated by a dual-acting riboswitch that, under low levels of lysine, promotes translation initiation while simultaneously sequestering RNase E cleavage sites. In the presence of lysine, the riboswitch folds into an alternative conformation that exposes RNase E cleavage motifs, in addition to

blocking translation (Caron et al., 2012). In these examples, it is ultimately the conformational structure of the mRNA that allows regulation of its half-life, independently from the stability of the bulk mRNA pool.

The activity of RNases does not always result in RNA decay. Some mRNA precursors can be processed by RNases to create mature, functional forms of the transcript (Condon et al., 1996). In a similar manner, polycistronic transcripts can be cleaved by endonucleases to produce transcripts with varying degrees of stability; some examples include (Belasco et al., 1985; Baga et al., 1988; Nilsson and Uhlin, 1991; Nilsson et al., 1996; Ludwig et al., 2001; Esquerre et al., 2014; Xu et al., 2015). While this is a fascinating mechanism of gene-specific regulation, it is beyond the scope of this review.

mRNA stabilization as a response to stress

When bacteria are forced to slow or stop growth in response to stress, they must reduce their rates of protein synthesis. This can be done by direct modulation of translation or by regulation of transcription and transcript degradation rates. In recent decades, there have been many reports of mRNA stabilization as a response to different stressors, usually conditions that alter growth rate (see Table 1-1). In *E. coli*, the outer membrane protein A precursor transcript, *ompA*, is very stable in rapidly growing cells (Nilsson et al., 1984), but its half-life is significantly decreased in conditions of slow growth rate (Nilsson et al., 1984; Emory et al., 1992; Vytvytska et al., 2000). An inverse phenomenon was observed in stationary phase *E. coli* cells for *rpoS* and *rmf*, transcripts coding for the transcription factor σ38 and the ribosome modulation factor, respectively (Zgurskaya et al., 1997; Aiso et al., 2005). Research conducted in other organisms also showed regulation of degradation rates of specific mRNAs according to growth rate: *sdh*, coding for succinate dehydrogenase in *B. subtilis*, and *rpoS* in *Salmonella dublin* had mRNA half-lives negatively correlated with growth rate (Melin et al., 1989; Paesold and Krause, 1999). Furthermore, cell growth studies using chemostats revealed that most transcripts in *E. coli* stabilize at low growth rates (Esquerre et al., 2014), with those belonging to the COGs “Coenzyme transport and metabolism” and “Intracellular

trafficking, secretion and vesicular transport" being enriched among the most highly stabilized transcripts. On the other hand, genes in "Cell motility" and "Secondary metabolites biosynthesis, transport and catabolism" had shorter half-lives than the transcript population mean (Esquerre et al., 2015). This reinforces the ideas that transcript half-lives may be linked to gene function and can be regulated as conditions require. For example, in *E. coli,* genes from the COGs "Carbohydrate transport and metabolism" and "Nucleotide transport and metabolism" are amongst the most stable at normal growth rates (Esquerre et al., 2014; Esquerre et al., 2015; Esquerre et al., 2016). Although these findings propose a link between growth rate and mRNA stability, it is possible that metabolic status rather than growth rate per se is the key determinant of global mRNA stability. In *M. smegmatis*, a drug-induced increase in metabolic activity resulted in accelerated mRNA decay and vice versa, even though growth was halted in both conditions (Vargas-Blanco et al., 2019). Another study supported these findings, showing that mRNA stabilization upon changes in nutrient availability could be dissociated from changes in growth rate (Morin et al, 2020).

Growth rate is altered as a consequence of metabolic changes as bacteria adapt to different environments. Because the ultimate goal of an organism is to survive and multiply, we can assume that in stress conditions—such as low-nutrient environments—bacteria trigger mechanisms that regulate energy usage and preserve energetically expensive macromolecules, such as mRNA. Thus, transcript stabilization is a logical response to various forms of energy stress. Indeed, *E. coli* stabilizes most of its transcriptome in anaerobic conditions (Georgellis et al., 1993) as well as in carbon starvation and stationary phase (Esquerre et al., 2014; Chen et al., 2015; Morin et al, 2020). Studies on *Rhizobium leguminosarum*, *Vibrio sp. S14,* and *Lactococcus lactis* also showed increased transcriptome half-lives when the bacteria are subjected to nutrient starvation (Albertson et al., 1990; Thorne and Williams, 1997; Redon et al., 2005a; Redon et al., 2005b). *S. aureus* induces global mRNA stabilization in response to low and high

temperatures, as well as during the stringent response (Anderson et al., 2006). Under hypoxic conditions, the median mRNA half-life in *M. tuberculosis* increases from ~9.5 min to more than 30 min, and cells shifted from 37°C to room temperature stabilized their transcriptomes so dramatically that half-lives could not be measured (Rustad et al., 2013). Similarly, transcript stabilization occurs in *M. smegmatis* in response to carbon starvation and hypoxia (Smeulders et al., 1999; Vargas-Blanco et al., 2019). Intriguingly, transcript destabilization can be resumed within seconds upon re-oxygenation of hypoxic *M. smegmatis* cultures, suggesting a highly sensitive mechanism regulating mRNA degradation in response to stress and energy status (Vargas-Blanco et al., 2019).

This response seems to be conserved even in some eukaryotes such as *Saccharomyces cerevisiae*, where the mRNA turnover rate is slower under stress than in log phase (Jona et al., 2000), and in plants as part of their immune response (Yu et al., 2019). However, the adaptive mechanism(s) underlying global mRNA stabilization as a stress response remain unknown. In the following sections we will discuss in more detail diverse bacterial strategies that contribute to global and gene-specific regulation of RNA stability. Our intent is to highlight recent findings on regulation of RNA degradation, to serve as a base for development of experiments to uncover how mRNA stabilization occurs as a response to stress.

Regulation of RNA degradation proteins

In this section we will discuss factors that have been shown to regulate the abundance and activity of endo- and exonucleases. We invite the reader to consult some excellent reviews (Condon, 2003; Arraiano et al., 2010; Bechhofer and Deutscher, 2019) for additional information on the roles and activities of RNases.

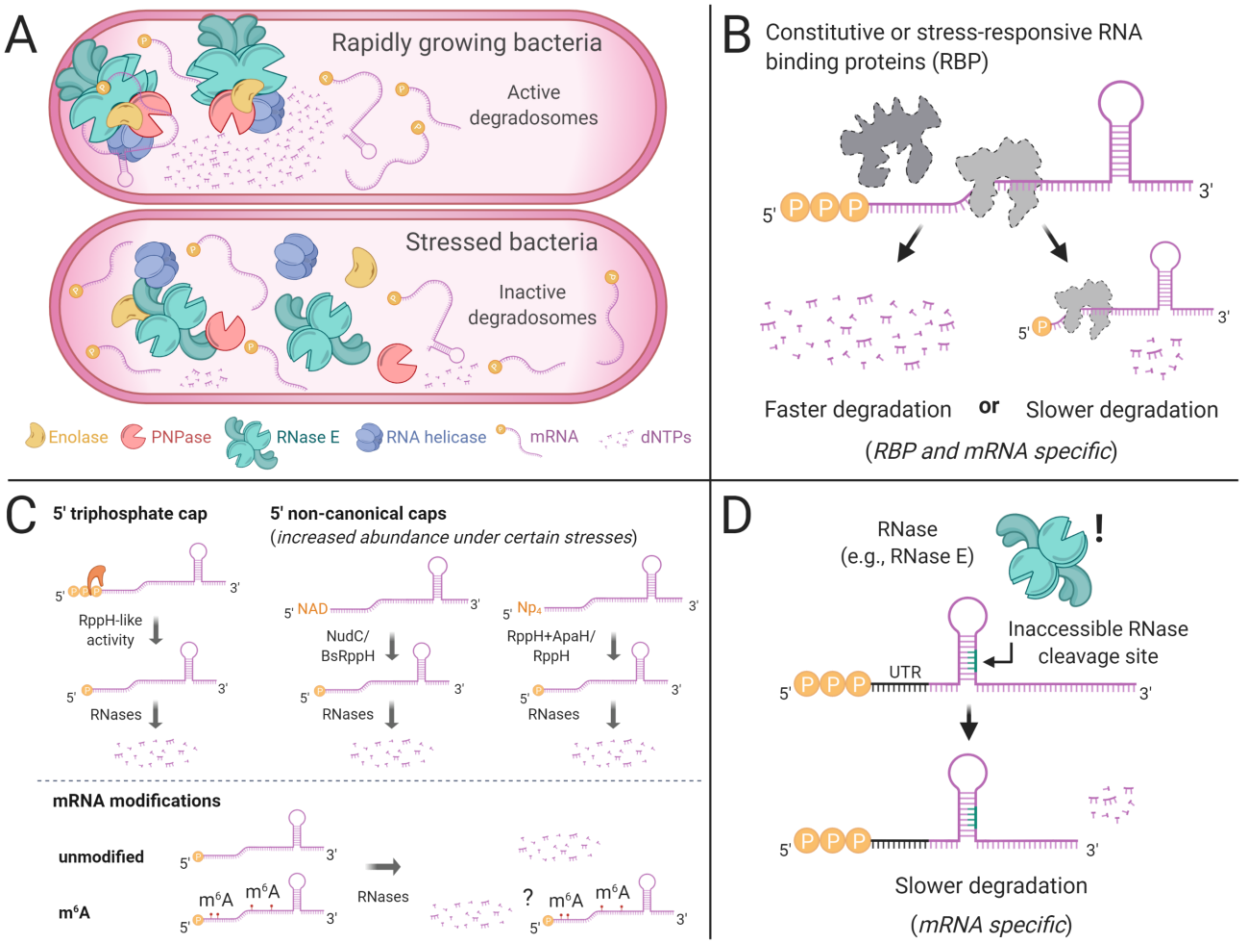

Figure 1-3. Common mechanisms that can protect mRNAs from degradation. (A) Degradosome localization can influence its RNA degradation activity. In *E. coli*, the degradosome is anchored to the cytoplasmic membrane via RNase E's N-terminal domain, where it displays higher RNA processing activity in degradation foci. A cytoplasmic RNase E is less efficient in degradosome assembly and RNA processing. In *B. subtilis*, RNase Y is associated with the membrane and is more active when in smaller foci and less active when in larger foci. (B) RNA binding proteins can modulate mRNA degradation. Some of them, such as CsrA in γ-Proteobacteria, have regulatory roles as a response to environmental changes. (C) The chemical nature of mRNA 5′ ends can protect transcripts from degradation. These caps may vary depending on stress conditions. Nucleotide modifications in the bodies of transcripts have also been reported, but they have not been shown to alter mRNA stability. (D) RNA degradation depends on RNase accessibility to cleavage sites. Secondary structures that block cleavage sites can result in slower RNA degradation.

As we described in a previous section, RNases have preferred cleavage sequences. These patterns can be either masked or exposed by alternative RNA folding configurations as a result of intracellular changes, allowing modulation of specific cleavage events, e.g., the *lysC* riboswitch which is sensitive to lysine concentration (Caron et al., 2012). However, this regulatory paradigm tends to be used to control specific

messages rather than the overall transcriptome stability. Hence, a major open question is: Are there elements that control RNase abundance or RNase activity that regulate transcriptome stability globally?

Abundance of key RNases that catalyze rate-limiting steps in mRNA degradation can affect bulk mRNA decay. For example, depletion or mutation of RNase E caused bulk mRNA stabilization in *E. coli* (Lopez et al., 1999; Sousa et al., 2001); depletion or mutation of RNase Y caused bulk mRNA stabilization in *B. subtilis* and *S. pyogenes* (Shahbabian et al., 2009; Chen et al., 2013); depletion of RNase J caused bulk mRNA stabilization in *Helicobacter pylori* (Redko et al. 2016); and deletion of RNases J1 and J2 caused mRNA stabilization in *B. subtilis* (Evan et al., 2005). Mechanisms for regulation of RNase abundance have been reported in some bacteria. In *E. coli*, RNase III autoregulates its abundance by cleaving its own operon to induce its degradation when RNase III protein levels are high (Bardwell et al., 1989; Matsunaga et al., 1996; 1997; Xu et al., 2008). Similarly, in *E. coli* a stem-loop located in the 5' UTR of *rne* responds to changes in RNase E levels, allowing this enzyme to autoregulate its own production (Diwa et al., 2000; Diwa and Belasco, 2002). There is evidence that in some cases, stability of other mRNAs can be regulated by changes in RNase abundance. In *E. coli*, the *betT* and *proP* transcripts, encoding osmoregulators, showed increased abundance and stability when cells were subject to osmotic stress, apparently as a consequence of lower RNase III concentrations (Sim et al., 2014). However, there is not yet evidence that global stress-induced mRNA stabilization can be attributed to reduced RNase abundance. In *M. tuberculosis,* a quantitative proteomics study comparing exponentially growing and hypoxic cultures showed no alteration in levels of RNase E, RNase J, RNase III, PNPase, or the helicase HelY even after 20 days under hypoxia (Schubert et al., 2015). Only one RNA helicase, RhlE, had reduced levels in hypoxia (Schubert et al., 2015). Similarly, a study of *M. smegmatis* showed no variation in levels of RNase E, PNPase, or the predicted RNA helicase msmeg_1930 under hypoxia, reaeration, or exponential growth (Vargas-Blanco et al., 2019). Because mycobacterial transcriptomes are rapidly stabilized upon

encountering hypoxia and other stress conditions (Rustad et al., 2013; Vargas-Blanco et al., 2019), it is unlikely that alteration of RNase abundance is part of the early RNA stabilization responses in these organisms.

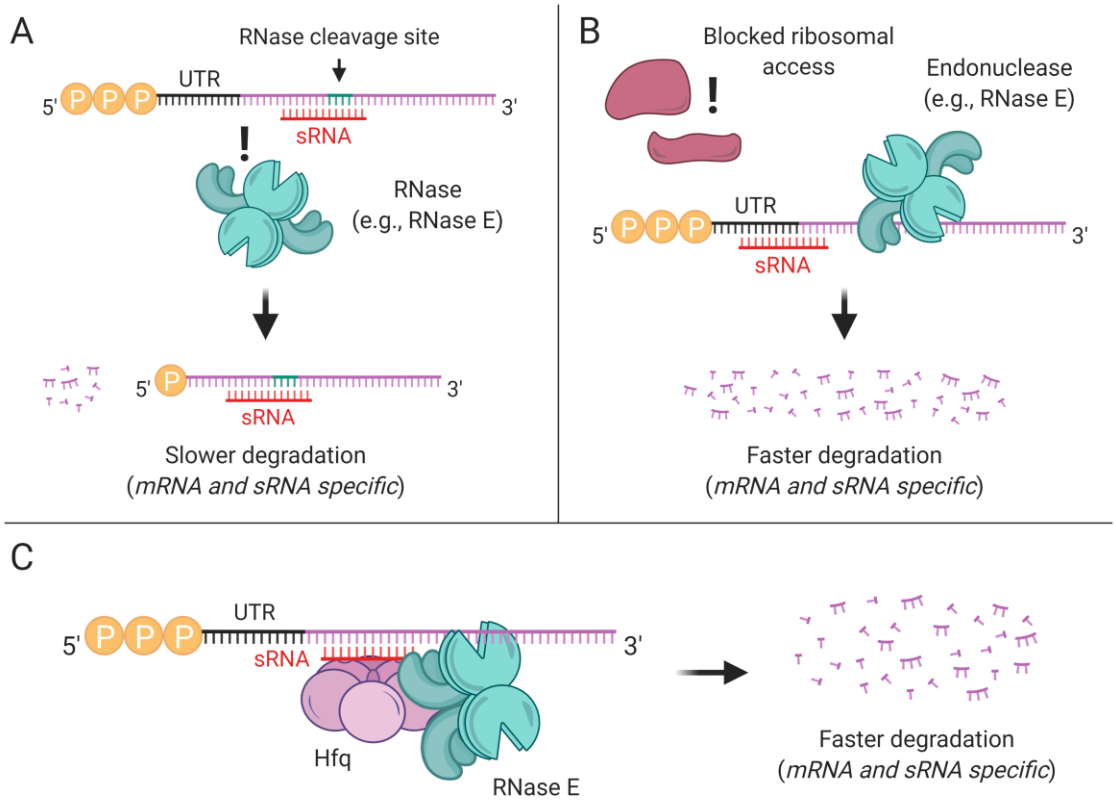

Figure 1-4. sRNAs can affect mRNA stability through multiple mechanisms. (A) sRNA binding can mask preferred RNase cleavage sites, thereby stabilizing transcripts. (B) sRNA binding can block ribosome access to Shine-Dalgarno sites, reducing translation and typically destabilizing transcripts. (C) In *E. coli* and some other gram-negative bacteria, sRNA-mRNA pairing is often mediated by Hfq, which typically leads to mRNA degradation.

It is possible that the activity of existing RNA degradation enzymes is regulated. RNA helicases are ATP-dependent, and ATP levels decrease in some bacteria in severe energy stress (Rao et al., 2008; Vargas-Blanco et al., 2019). This raises the possibility that RNA degradation could be directly modulated by ATP levels. However, when this hypothesis was tested in *M. smegmatis,* mRNA stabilization was found to occur prior to a decrease in intracellular ATP levels upon exposure to hypoxic conditions (Vargas-Blanco et al., 2019). While these findings suggest that nucleotide sensing—particularly changes in ATP concentrations—

does not influence the initial global stabilization response in mycobacteria, it is possible that ATP concentrations or ATP/ADP ratios could be responsible for further stabilization in later stages of dormancy, and/or that ATP levels contribute to global mRNA stabilization in other bacteria. The roles of nucleotides associated with the stringent response are discussed separately below.

In *E. coli,* inhibition of RNase E activity by RraA and RraB (Regulator of ribonuclease activity A and B) result in increased bulk mRNA half-life (Lee et al., 2003). However, in the case of RraA, the effect was observed after a significant overexpression of the inhibitor (Lee et al., 2003), something not observed under stress. Alternatively, inhibition of RNase activity by other factors may regulate transcript degradation. RNase E was recently shown to have a 5' linear scanning function, and its cleavage activity is impaired upon encountering obstacles, such as sRNAs or ribosomes (Richards and Belasco, 2019). Furthermore, in *E. coli*, the activity of RNase E has been shown to depend on its anchorage to the inner membrane (Figure 1-3A). YFP-tagged RNase E forms small foci localized at the inner membrane (Strahl et al., 2015) which are dependent on metabolic activity; in anaerobic conditions RNase E rapidly dissociates from the membrane and diffuses in the cytoplasm, a response apparently dependent on enolase (Murashko and Lin-Chao, 2017). A cytoplasmic version of RNase E was unstable, and led to increased mRNA half-lives (Hadjeras et al., 2019). Interestingly, the cytoplasmic RNase E was able to assemble a degradosome and had a comparable *in vitro* activity to wild type RNase E, supporting the role of membrane attachment and cellular localization in RNase E activity (Moffitt et al., 2016; Hadjeras et al., 2019). Conversely, in *Caulobacter crescentus*, RNase E is cytoplasmic and forms bacterial ribonucleoprotein (BR) bodies, which dynamically assemble and disassemble in the presence of mRNA (Al-Husini et al., 2018). BR body formation was dependent on the RNase E scaffold domains and the presence of mRNA, while disassembly of the bodies required mRNA cleavage (Al-Husini et al., 2018). Intriguingly, the formation of BR-bodies increased under some stress conditions but was unaffected by others, suggesting they play an as-yet

undefined role in stress response (Al-Husini et al., 2018). Further work is needed to understand the extent to which RNase localization contributes to regulation of mRNA degradation rates in various species.

In *B. subtilis*, the activity of RNase Y appears to be regulated by both subcellular localization and association with proteins termed the Y-complex (YaaT, YlbF, and YmcA). The Y-complex affects expression of genes involved in biofilm formation, sporulation, and competence, and in some cases, this was shown to be a direct consequence of altered mRNA degradation rates for the relevant genes (Tortosa et al., 2000; Carabetta et al., 2013; DeLoughery et al., 2016; Dubnau et al., 2016). The Y complex has been viewed as a specificity factor for RNase Y, required in particular for processing of polycistronic transcripts (DeLoughery et al., 2018). RNase Y also localizes in the cell membrane, where it can form RNase Y foci (Hunt et al., 2006; Lehnik-Habrink et al., 2011; Hamouche et al., 2020). These foci seem to represent a less active form of the enzyme, as they increased in size in absence of RNA or in Y-complex mutants (Hamouche et al., 2020).

The stringent response and mRNA degradation

The stringent response is perhaps one of the most well-studied mechanisms of prokaryotic stress adaptation. This response is modulated by guanosine-3',5'-bisphosphate (ppGpp) and/or guanosine-3'-diphosphate-5'-triphosphate (pppGpp), alarmones collectively referred to as (p)ppGpp. In gram-negative bacteria, (p)ppGpp is synthesized by RelA in response to uncharged-tRNAs binding ribosomes, or by SpoT, a (p)ppGpp synthase/hydrolase, during fatty acid starvation (Seyfzadeh et al., 1993; Battesti and Bouveret, 2009). In some gram-positive bacteria, (p)ppGpp is synthesized by a dual RelA/SpoT homolog (Atkinson et al., 2011; Frederix and Downie, 2011; Corrigan et al., 2016). Once produced, (p)ppGpp halts the synthesis of stable RNA (tRNAs and ribosomes) while upregulating stress-associated genes and downregulating those associated with cell growth (Gentry et al., 1993; Chakraburtty and Bibb, 1997; Martinez-Costa et al., 1998; Avarbock et al., 2000; Artsimovitch et al., 2004; Corrigan et al., 2016). Intriguingly, (p)ppGpp was

reported to inhibit PNPase in the actinomycetes *Nonomuraea sp* and *Streptomyces coelicolor* but not in *E. coli* (Gatewood and Jones, 2010; Siculella et al., 2010), suggesting the stringent response may have a previously overlooked role in directly regulating mRNA degradation in some groups of bacteria. However, a recent study on the stringent response in *M. smegmatis* showed that (p)ppGpp was not required for mRNA stabilization in response to carbon starvation or hypoxia (Vargas-Blanco et al., 2019).

In the pathogen *Borrelia burgdorferi*, a connection between the stringent response and the expression of 241 sRNAs was recently stablished, 187 of which were upregulated during nutrient stress (Drecktrah et al., 2018). The authors of the aforementioned study described potential mechanisms of regulation by Rel_{Bbu} on transcription and fate of some transcripts, such as destabilization of the glycerol uptake facilitator transcript, *glpF*. The SR0546 sRNA is among the sRNAs induced by nutrient starvation; the upregulation of its target, *bosR*, encoding a transcriptional regulator, may suggest a regulatory role of (p)ppGpp on specific mRNA stabilization. However, the effects of these stringent response-induced sRNAs on mRNA stability have not yet been directly tested.

A surprising role of RelZ (initially called MS_RHII-RSD), a dual (p)ppGpp synthase and RNase HII, was reported for *M. smegmatis* (Murdeshwar and Chatterji, 2012). R-loops (RNA/DNA hybrids) are harmful structures that cause replication stress and can be removed by the RNase H domain of RelZ, while stalled ribosome removal is attributed to their alarmone synthase domain. RelZ was shown to be upregulated under short UV exposure in *M. smegmatis* (Krishnan et al., 2016), and while its role is suspected to increase cell viability under stress conditions (Petchiappan et al., 2020), the stringent response seems to not intervene in transcriptome stability regulation. This pathway leads to degradation of transcripts involved in R-loops, but given the low frequency of R-loop formation, the effects on mRNA pools are likely to be minimal.

Overall, there is much evidence that the stringent response regulates expression of specific transcripts in various bacteria. However, the extent to which control of mRNA stability contributes to these effects is mostly untested. The stringent response also plays important roles in mediating global responses to starvation and other forms of energy stress, but there is not yet evidence that it contributes to global mRNA stabilization, which is a consistent component of these stress responses. This suggests that the stringent response may not be the mediator of global mRNA stabilization in response to stress, or that its involvement in this process is species-specific.

Transcript modifications as regulators of mRNA decay

Bacterial mRNA is primarily transcribed using nucleoside triphosphates as initiating nucleotides, making mRNAs triphosphorylated at their 5' ends. In *S. aureus,* RNase J1 exhibits strong *in vitro* exo- and endonucleolytic activities on 5' triphosphorylated transcripts (Hausmann et al., 2017). However, in most other organisms studied to date, RNases E, J, and Y more efficiently cleave mRNAs with 5' monophosphates (Figure 1-3C). RNase E is an endoribonuclease, but has a binding pocket for monophosphorylated 5' ends (Callaghan et al., 2005) that strongly stimulates its activity in organisms including *E. coli* and *M. tuberculosis* (Mackie, 1998; Zeller et al., 2007). Similarly, in *B. subtilis*, RNase J1, and to a lesser extent J2, show a strong preference towards 5' monophosphorylated substrates (Even et al., 2005). RNase Y also shows preference towards monophosphorylated 5' substrates, but to a lesser extent (Shahbabian et al., 2009). These findings contributed to the discovery of RppH, an RNA pyrophosphohydrolase. Similar enzymes were later found in other bacteria, such as *Bdellovibrio bacteriovorus* (Messing et al., 2009) and *B. subtilis* (Richards et al., 2011). However, while the role of 5' triphosphate pyrophosphohydrolysis was initially attributed to RppH (Celesnik et al., 2007; Deana et al., 2008), recent findings have shown that the primary substrate of RppH in *E. coli* is 5' diphosphorylated RNAs, and that 5' diphosphorylated RNAs are abundant in the transcriptome (Luciano et al., 2017). As

RppH cannot convert 5’ triphosphates to diphosphates, this suggests the existence of an unknown 5’ triphosphate to diphosphate phosphorylase. Given that 5’ monophosphates make transcripts more susceptible to degradation in multiple organisms, one could envision regulation of 5’ triphosphate pyrophosphohydrolysis as a potential mechanism for regulation of mRNA stability. However, to our knowledge there are not yet reports of if and how pyrophosphohydrolysis or γ-phosphate removal are regulated.

The presence of non-canonical mRNA 5’ ends has recently been reported for subsets of mRNAs in several bacterial species, suggesting another possible mechanism for regulation of mRNA stability (Figure 1-3C). Examples include NADH and NAD+ (Chen et al., 2009; Cahova et al., 2015), and less commonly, dephospho-CoA, succinyl-CoA, acetyl-CoA, and methylmalonyl-CoA (Kowtoniuk et al., 2009). We will refer to these as 5’ caps, with the understanding that they are structurally and functionally distinct from eukaryotic mRNA caps. Other studies have shown additional types of 5’ capping, as well as potential mechanisms behind it (Bird et al., 2016; Zhang et al., 2016; Julius and Yuzenkova, 2017). In most cases, bacterial caps are incorporated directly into mRNAs during transcription initiation. RNA polymerase can initiate transcription with non-canonical nucleotides such as NAD in *E. coli* (Bird et al., 2016; Vvedenskaya et al., 2018) and *B. subtilis* (Frindert et al., 2018). Furthermore, *E. coli* RNA polymerase seems to initiate with dinucleoside tetraphosphates (Np_4N), Np_4A in particular, with an efficiency almost 60 times higher than for NAD (Luciano and Belasco, 2020). Alternative, posttranscriptional mechanisms may also contribute to Np_4 capping formation, as *in vitro* experiments using LysU (lysyl-tRNA synthetase) from *E. coli* suggest (Luciano et al., 2019).

The intracellular concentration of Np_4As were shown to be affected by overproduction of aminoacyl-tRNA synthetases (Brevet et al., 1989). Interestingly, some stress conditions also induce higher levels of Np_4Ns, for example heat shock (Lee et al., 1983), oxidative stress (Bochner et al., 1984), cadmium stress (Coste

et al., 1987; Luciano et al., 2019) and disulfide stress (Bochner et al., 1984; Luciano et al., 2019). 5' mRNA decapping was shown to require Nudix enzymes, such as NudC and BsRppH, to hydrolyze NAD-RNA substrates (Hofer et al., 2016; Frindert et al., 2018). On the other hand, hydrolysis of Np_4As requires RppH and ApaH, the latter carrying out the hydrolysis of Np_4As into two NDPs (Farr et al., 1989); in this context ApaH generates a diphosphorylated 5' end that can be readily converted to monophosphate 5' end by RppH (Figure 1-3C). Non-canonical mRNA 5' ends also occur when transcription initiates with short RNA degradation products, resulting in mRNAs with 5' hydroxyls (Druzhinin et al., 2015). Such transcripts have been found in *E. coli* and *Vibrio cholerae* and are present at increased abundance in stationary phase (Vvedenskaya et al., 2012; Druzhinin et al., 2015). However, the effects of these alternate 5' ends on transcript stability have not been reported.

Some mRNA caps have been shown to stabilize mRNAs in *E. coli* (Bird et al., 2016; Luciano et al., 2019) and in *B. subtilis* (Frindert et al., 2018). For example, after increasing the cellular concentration of Np_4Ns in cadmium-stressed cells and in Δ*apaH* mutants, RNA stability was increased, suggesting that Np_4 caps have a stabilizing role (Luciano et al., 2019). Additionally, in this study Np_4 caps were suggested to be more abundant than NAD caps. Similarly, in the *E. coli* Δ*nudC* mutant strain there is an increase of up to four-fold in RNA stability for transcripts with non-canonical 5' caps (Bird et al., 2016). Furthermore, NAD 5' caps were almost two-fold more abundant for cells in stationary phase when compared to exponential phase (Bird et al., 2016). Together, these findings present a potential mechanism for stabilization of mRNA under stress conditions. An interesting regulatory mechanism behind Np_4 decapping in *E. coli* was recently linked to methylation in m^7Gp_4Gm and m^6Ap_3A 5' caps, which protects them from RppH cleavage but not from AppH (Hudecek et al., 2020). Methylated Np_nN caps were shown to be more abundant in stationary phase than exponential phase (Hudecek et al., 2020), consistent with the idea that these caps protect mRNA from degradation. Interestingly, the Np_nN caps found in that study did not include Ap_4N (Hudecek et al.,

2020), presumably due to different stress conditions and detection techniques than those in (Luciano et al., 2019). Since capped mRNAs appear to be generally more stable than canonical mRNAs, it is logical to infer that when stress conditions cause growth to slow or stop and transcription to slow or stop concomitantly, the proportion of capped mRNAs will increase as a result of their inherently longer half-lives. One could therefore speculate that the global mRNA stabilization observed in non-growing bacteria is due in part to an mRNA pool that is largely protected by 5' caps. This is plausible assuming capping frequency remains constant or increases under stress. But, a recent study argues against this idea. Rapid transcript destabilization occurred in hypoxic *M. smegmatis* cultures after re-exposure to oxygen, even when transcription was blocked prior to reaeration (Vargas-Blanco et al., 2019). Thus, mRNA capping does not explain the transcript stabilization observed in these conditions (early-stage hypoxia)—at least in *M. smegmatis*—but could be involved in mRNA stabilization in other conditions and/or other bacteria.

Another possible mechanism of mRNA stabilization involves posttranscriptional nucleotide modifications (Figure 1-3C). N^6-methyladenosine (m^6A) is a common base modification in mice and humans (Meyer et al., 2012; Linder et al., 2015). This methylation is enriched near stop codons and in 3' UTRs (Yue et al., 2018), and is dependent on the consensus motif DRACH (Linder et al., 2015). Recent studies revealed m^6A to be an important part of a transcript stability regulatory mechanism, as it facilitates mRNA degradation in association with RBP in mice, zebra fish, and human cells (Schwartz et al., 2014; Wang et al., 2014; Zhao et al., 2017). Moreover, the levels of m^6A methylation are responsive to stress conditions, as shown for human cancer cells under hypoxic conditions (Panneerdoss et al., 2018), suggesting a posttranscriptional regulatory role. In *E. coli* and *Pseudomonas aeruginosa*, m^6A is present at similar levels, ~0.2% to ~0.3% of adenines (Deng et al., 2015b), to those reported for yeast and other eukaryotes (Wei et al., 1975; Bodi et al., 2010). However, in contrast to mammals, m^6A appears distributed throughout the gene, with modest enrichments near the 5' ends and centers of transcripts, and with a similar m^6A motif for *E. coli*

and *P. aeruginosa* (UGCCAG and GGYCAG, respectively) (Deng et al., 2015b). Contrary to eukaryotes, m^6A methylation has not been shown to have a global role in mRNA degradation in bacterial stress responses. A deep analysis in *E. coli* and *P. aeruginosa* revealed no difference in the m^6A levels for cells growing in LB when compared to other (unspecified) growth media, or oxidative stress; interestingly, increasing the temperature from 37 to 45°C lowered m^6A methylation levels, but only for *P. aeruginosa* (Deng et al., 2015b). Furthermore, the m^6A levels were lower in other bacteria (~0.02% to ~0.08%, for *S. aureus*, *B. subtilis*, *Anabaena* sp. and *Synechocystis* sp.) (Deng et al., 2015b), suggesting that this particular base modification may not be conserved across bacteria. In *E. coli*, codon modifications of the *ermCL* mRNA with m^6A blocked translation, though it had no impact on mRNA degradation rates (Hoernes et al., 2016). While it is conceivable that m^6A has a role in the regulation of bacterial translation, current evidence does not suggest it regulates mRNA fate.

5-methylcytosine (m^5C) has also been found in mRNA. In eukaryotes, m^5C has been shown to increase transcript stability (Arango et al., 2018; Chen et al., 2019b; Yang et al., 2019; Schumann et al., 2020), while reports on translation regulation are controversial (Huang et al., 2019; Yang et al., 2019; Schumann et al., 2020). m^5C modifications have been found in mRNA and 23S rRNA in the archaeon *Solfolobus solfataricus* (Edelheit et al., 2013). However, there is no defined role of m^5C in *S. solfataricus*, and evidence of m^5C in bacteria or regulatory roles in RNA degradation have not been reported.

Another modification, and perhaps the most abundant in RNA, is pseudouridine (Ψ) (Rozenski et al., 1999). Ψ is present at the position U55 in all *E. coli* tRNAs (Gutgsell et al., 2000), and is widespread across kingdoms (Nishikura and De Robertis, 1981; Becker et al., 1997; Ishida et al., 2011). In *E. coli,* deletion of *truB*, encoding a tRNA Ψ 55 synthase (Nurse et al., 1995), was shown reduce viability after a temperature shock (37 to 50°C); however, no viability changes were observed during exponential growth at 37°C (Kinghorn et al., 2002). In *Thermus thermophilus*, a Δ*truB* mutant showed a growth defect when cultured

at 50°C (Ishida et al., 2011). Thus, it is possible that the presence of tRNA modifications under stress conditions contributes to survival in other bacteria. Other tRNA modifications have been also reported in bacteria and yeast during stress, contributing to a translational bias with implications for translation regulation (Chan et al., 2010; Chan et al., 2012; Laxman et al., 2013; Deng et al., 2015a; Chionh et al., 2016). However, while stress may alter tRNA modifications, ultimately these changes lead to translational regulation without clear evidence, at least in bacteria, of effects on mRNAs. On the other hand, Ψ modifications on mRNA have been shown to increase mRNA stability in yeast and human cells (Carlile et al., 2014) and in *Toxoplasma gondii* (Nakamoto et al., 2017). A broad study involving *E. coli* and human cells found that even a single replacement of U with Ψ in mRNA can interfere with translation (Eyler et al., 2019). Whether these modifications ultimately regulate mRNA stability in bacteria as a response to stress is an open question. Based on evidence aforementioned for *M. smegmatis* regarding the rapidity of transcript destabilization after stress alleviation (Vargas-Blanco et al., 2019), we speculate that base modifications are unlikely to be the primary mechanism of mRNA stabilization in hypoxic mycobacteria, although it could play roles in other organisms or conditions.

Roles of ribosomes, translation, sRNAs and RNA-binding proteins in regulation of mRNA decay

Experiments conducted by Bechhofer and others in *B. subtilis* showed that ribosome stalling can increase *ermC* half-life. In this scenario, ribosomes acted as obstacles at the 5’ ends of transcripts, resulting in protection from endonucleolytic cleavage downstream (Shivakumar et al., 1980; Bechhofer and Dubnau, 1987; Bechhofer and Zen, 1989). These findings would become early evidence of a 5’ to 3’ polarity for endonucleolytic activity, dependent upon or enhanced by 1) interaction with a 5’ monophosphate, and 2) RNase linear scanning mechanisms, as it would be later reported by others (Bouvet and Belasco, 1992; Jourdan and McDowall, 2008; Kime et al., 2010; Richards and Belasco, 2016; 2019). In *E. coli*, the use of puromycin or kasugamycin—translation inhibitors that cause ribosomes to dissociate from transcripts—

caused faster mRNA decay in the absence of new transcription (Varmus et al., 1971; Pato et al., 1973; Schneider et al., 1978). On the other hand, the use of chloramphenicol, fusidic acid or tetracycline—elongation inhibitors that cause ribosomes to stall on transcripts—resulted in transcript stabilization (Varmus et al., 1971; Fry et al., 1972; Pato et al., 1973; Schneider et al., 1978), findings also later shown in *M. smegmatis* (Vargas-Blanco et al., 2019). These results are consistent with ribosome binding having a protective effect on mRNAs (Figure 1-5). In experiments where transcription was not blocked, it is possible that the mRNA stabilization seen in response to elongation inhibitors may also be conferred in part by the sudden increase in rRNA synthesis that these drugs cause, which increases the abundance of potential RNase substrates and could therefore titrate the activity of RNases such as PNPase and RNase E (Lopez et al., 1998). However, the increase in rRNA synthesis cannot fully explain these effects.

In *B. subtilis,* the stability of *gsiB,* encoding general stress protein, and *ermC,* encoding erythromycin resistance leader peptide, are associated with ribosome binding (Sandler and Weisblum, 1989; Hambraeus et al., 2000). Mutations to the RBS sites of *gsiB*, *aprE* (coding for subtilisin), and SP82 phage mRNA resulted in reductions of their mRNA half-lives (Hue et al., 1995; Jurgen et al., 1998; Hambraeus et al., 2002). Transcript stability conferred by ribosomes does not always require productive translation, at least for *ermC* (Hambraeus et al., 2002) and *ompA* (Emory and Belasco, 1990), where transcripts were stable in the absence of start codons as long as strong Shine-Dalgarno (SD) sequences were present (Arnold et al., 1998). A later study also in *E. coli* reported that ribosome protection is independent of translation for another transcript (Wagner et al., 1994). Transcript stabilization in a translation-independent manner was also shown for *B. subtilis*, with the insertion of an alternative SD (not involved in translation) to the gene reporter *cryIII* (Agaisse and Lereclus, 1996). These findings suggest that binding of a 30S subunit to a transcript, regardless of translation, may suffice to impair RNase degradation.

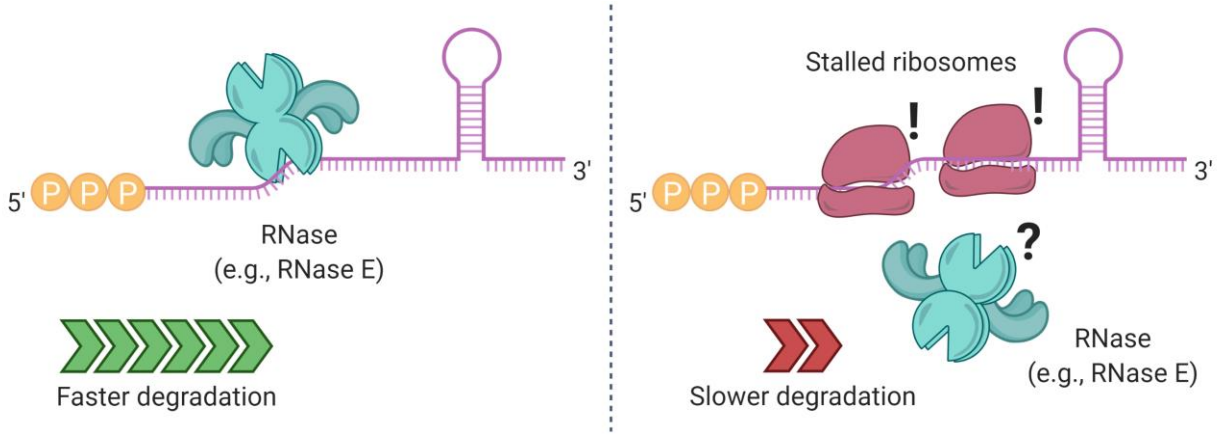

Figure 1-5. Ribosome binding and stalling can alter mRNA degradation. In some cases, ribosome stalling can mask RNase cleavage sites, increasing the half-life of a transcript. Elements that prevent ribosome binding, such as translation initiation inhibitors, lead to shorter mRNA half-lives.

However, other studies did find a correlation between translation itself and stability. In *E. coli*, codon composition can influence translation rate and mRNA stability; codon-optimized transcripts were more stable than their corresponding non-modified, inefficiently-translated versions (Boel et al., 2016). Similar results were shown for *S. cerevisiae* (Presnyak et al., 2015). A transcriptome-wide analysis in *E. coli* also identified a positive correlation between mRNA stability and codon content optimality, for bacteria growing at different rates (Esquerre et al., 2015). This directly contradicted a previous report that codon optimality and half-life were inversely correlated (Lenz et al., 2011), possibly due to use of different codon optimality metrics. In *B. subtilis*, translation initiation is necessary to prevent swift degradation of the *hbs* transcript, which encodes the DNA binding protein HBsu (Daou-Chabo et al., 2009; Braun et al., 2017). In *M. smegmatis* and *M. tuberculosis*, RNase E cleaves the *furA-katG* operon, producing an unstable *furA* message that is rapidly degraded while the *katG* transcript is stabilized as it becomes readily accessible for translation (Sala et al., 2008). Overall, regulation of mRNA stability by translation initiation and SD strength seems to be gene-specific.

While it is generally accepted in *E. coli* that occlusion of RNase cleavage sites by ribosome occupancy may protect a transcript from degradation (Joyce and Dreyfus, 1998), ribosome association with mRNA has not been shown to regulate mRNA stability globally in response to stress. However, data from *B. subtilis* suggest an interesting mechanism by which RNase activity could affect translation and therefore mRNA degradation on a transcriptome-wide scale (Bruscella et al., 2011). The *infC-rpmI-rplT* operon, which encodes translation initiation factor 3 (IF-3) along with two ribosomal proteins, is expressed from two promoters. The resulting transcripts have different sensitivities to RNase Y, and the RNase Y-sensitive transcript is not competent for translation of IF-3. As a result, inhibition of RNase Y expression alters the relative abundance of the two transcript and causes reduced translation of IF-3. If this were to cause globally reduced translation due to IF-3 deficiency, mRNA decay could be globally increased as a result, although this effect would presumably be counteracted by the globally reduced RNase Y activity. Complex interplays between RNase levels and translation may therefore have the potential to globally impact mRNA decay in *B. subtilis*.

RNA-binding proteins (RBPs), stalled ribosomes, and SD-like sequences in close proximity to transcript 5' ends can also alter mRNA fate (Sharp and Bechhofer, 2005). In *B. subtilis,* interaction of the RBP Glp with the 5' UTR of *glpD*, encoding glycerol-3-phosphate dehydrogenase, increases the transcript's stability (Glatz et al., 1996). Other RBPs can modulate the stability of target genes during stress conditions (Figure 1-3B). For example, H-NS, a histone-like protein, regulates the RNA stability of *rpoS* in *E. coli* and *V. cholerae* in stressful environments (Brescia et al., 2004; Silva et al., 2008; Wang et al., 2012). The carbon storage regulator CsrA is an RBP that regulates gene expression posttranscriptionally in *E. coli* and other γ-Proteobacteria in response to environmental changes, described in (Timmermans and Van Melderen, 2010; Romeo and Babitzke, 2018). CsrA regulatory roles are best studied in *E. coli*. The *glgCAP* transcript, encoding genes implicated in the biosynthesis of glycogen, is destabilized when bound by CsrA (Liu et al.,

1995). This response is halted when *E. coli* enters stationary phase, where CsrA is sequestered by the sRNA CsrB in a ribonucleoprotein complex (Liu et al., 1997). Conversely, CsrA was shown to stabilize some transcripts. CsrA directly binds the *pgaA* transcript, increasing its half-life along with the rest of the *pgaABC* polycistron, encoding genes associated to biofilm formation (Wang et al., 2005). Similarly, CsrA stabilizes the *flhDC* transcript, encoding the flagellar activation genes $FlhD_2C_2$ (Wei et al., 2001). More recently, a transcriptome-wide study together with bioinformatics predictions showed a major role for CsrA as an mRNA stabilization factor in *E. coli* (M9 minimal media, doubling time of 6.9 h) for more than a thousand transcripts, of which many were predicted to have at least one putative CsrA binding site (Esquerre et al., 2016). CsrA could directly bind transcripts and protect them from RNases, or could affect mRNA stability indirectly by modulating expression or activity of other post-transcriptional regulators, e.g., the RNA chaperone Hfq, encoded by *hfq*. In *E. coli*, CsrA can bind the *hfq* mRNA at a single binding site that overlaps its SD region, preventing ribosome access and decreasing its half-life; however, in stationary phase CsrA is sequestered, allowing higher expression of Hfq (Baker et al., 2007). Regulatory roles for CsrA in gram-positive bacteria have only recently been reported. In *B. subtilis*, CsrA mediates the interaction of the sRNA SR1 and the *ahrC* mRNA, encoding a transcription regulator of arginine metabolism, to regulate the expression of the arginine catabolic operons (Muller et al., 2019). However, CsrA-SR1 only mildly increased *ahrC* half-life, and it had no impact on SR1 degradation, indicating that the regulation was primarily at the level of protein synthesis (Muller et al., 2019).

The homohexameric Hfq, highly studied in *E. coli* and present in a large number of bacteria (Sun et al., 2002), is an important regulator of mRNA-sRNA pairing. The multiple roles of Hfq include modulation of sRNA-mediated translation blockage or promotion, and regulation of transcript degradation as a direct consequence of altered translation or through translation-independent mechanisms. For example, guiding a cognate sRNA to the 5’ region of mRNAs can result either in translation disruption by preventing

the 30S subunit from binding (Figure 1-4B), or the opposite outcome by disruption of stem-loops that inhibit its binding (Wassarman et al., 2001; Arluison et al., 2002; Moller et al., 2002; Schumacher et al., 2002; Zhang et al., 2003; Afonyushkin et al., 2005; Sittka et al., 2008). Hfq can also allow RNase E access to specific mRNAs, or modulate the synthesis of Poly(A) tails, assisting PNPase in 3' to 5' degradation, as it will be discussed shortly. The physical properties, sequence specificity, protein interaction partners, sRNAs/mRNAs binding kinetics, and other important aspects of Hfq function will not be described here, as they are well described elsewhere; we refer the reader to the following detailed reviews (Vogel and Luisi, 2011; Updegrove et al., 2016; Kavita et al., 2018; Santiago-Frangos and Woodson, 2018).

A common outcome of Hfq sRNA/mRNA interactions is specific regulation of mRNA half-life (Figure 1-4C). For example, the destabilization of *ptsG*, encoding a glucose permease, in *E. coli* is mediated by the sRNA SgrS as a response to phosphosugar accumulation (Vanderpool and Gottesman, 2004). Similarly, degradation of *ompA* was also shown to be impacted by the specific binding of the sRNA MicA to its translational start site, blocking binding of the 30S ribosomal subunit and recruiting Hfq to promote RNase E cleavage (Lundberg et al., 1990; Vytvytska et al., 2000; Udekwu et al., 2005). While the regulatory roles of Hfq are widely accepted for other gram-negative bacteria as well (Sonnleitner et al., 2006; Cui et al., 2013), in gram-positive bacteria Hfq is less well characterized. Hfq rescue experiments in *E. coli* and *S. enterica* serovar Typhimurium using Hfq from *B. subtilis* and *S. aureus*, respectively, failed at rescuing the phenotypes (Vecerek et al., 2008; Rochat et al., 2012). These findings suggest important structural and/or functional differences in Hfq across evolutionarily divergent groups of bacteria. A study in *B. subtilis* found that the absence of Hfq does not impair growth under almost 2000 conditions including different carbon, nitrogen, phosphorus and sulfur sources, osmolarity or pH changes in a large phenotypic analysis (Rochat et al., 2015). Similar findings were shown for *S. aureus* (Bohn et al., 2007). However, Hfq became necessary for survival in stationary phase (Hammerle et al., 2014; Rochat et al., 2015). Surprisingly, the absence of

Hfq in rich media conditions did not alter the transcriptome of *B. subtilis* (Rochat et al., 2015), while in minimal media, 68 mRNAs and a single sRNA were affected (Hammerle et al., 2014). Both of these studies reported transcriptome changes in the absence of Hfq for *B. subtilis* in stationary phase, particularly for sporulation and TA systems. Nevertheless, these changes do not necessarily confer fitness or increased survival (Rochat et al., 2015). Overall, while Hfq was shown to impact the *B. subtilis* transcriptome under certain stress conditions, its role as a regulator of transcript stability seems to greatly vary across species. In another gram-positive, the pathogen *Listeria monocytogenes*, Hfq interacts with the sRNA LhrA, increasing its stability and controlling the fate of its target mRNAs. But, ~50 other sRNA seem to function in an Hfq-independent manner (Christiansen et al., 2006; Nielsen et al., 2010; Nielsen et al., 2011). Unexpectedly, hypoxia, stationary phase and low temperature (30°C) did not affect sRNA levels in a Δ*hfq* strain (Toledo-Arana et al., 2009). Hence, it seems that Hfq may have a smaller role in control of mRNA stability, and an overall restricted role in sRNA/mRNA regulation in gram-positive bacteria; and it appears to not be required at all in some bacteria, such as mycobacteria, that lack identified Hfq orthologs (Sun et al., 2002).

mRNA folding alters mRNA decay

mRNA secondary structures can modulate translation and transcript stability (Figure 1-3D). Previously, we have discussed how specific 5' UTR folding prevents RNase and ribosome accessibility to the *lysC* transcript (Caron et al., 2012). In other transcripts, secondary structures can also prevent RNase E from carrying out the first endonucleolytic cleavage, delaying subsequent steps in the decay pathways. In *Rhodobacter capsulatus*, formation of multiple hairpins can prevent endonucleolytic cleavage of the *puf* operon (Klug and Cohen, 1990). A stem-loop at the 5' UTR confers stability to *recA*, coding for the nucleoprotein filament RecA in *Acinetobacter baumannii* (Ching et al., 2017), as well as *vacA*, coding for vacuolating cytotoxin A in *Helicobacter pylori* (Amilon et al., 2015). In the case of *vacA*, the stem-loop is also essential

for transcript stabilization in acidic and osmotic stress (Amilon et al., 2015). The distance between the start codon and secondary structures can also affect mRNA half-life, as was shown for the ΔermC mRNA in *B. subtilis*, where placing a stem-loop too close to the SD decreased transcript stability (Sharp and Bechhofer, 2005). Secondary structure at transcript 3' ends also affects stability. The mRNA 3' end hairpins formed by Rho-independent transcriptional terminators typically stabilize transcripts, as 3' to 5' RNases have difficulty initiating decay without a single-stranded substrate (Adhya et al., 1979; Farnham and Platt, 1981; Abe and Aiba, 1996). In *E. coli*, the poly(A) polymerase (PAP I) is an enzyme responsible for synthesizing poly(A) tails in mRNA (Li et al., 1998). The addition of poly(A) tails to bacterial mRNAs facilitates degradation of transcripts with 3' hairpins, allowing PNPase—an enzyme that also has a minor polyadenylation role—and other enzymes to carry out exonucleolytic activity (Donovan and Kushner, 1986; Blum et al., 1999) (Figure 1-6).

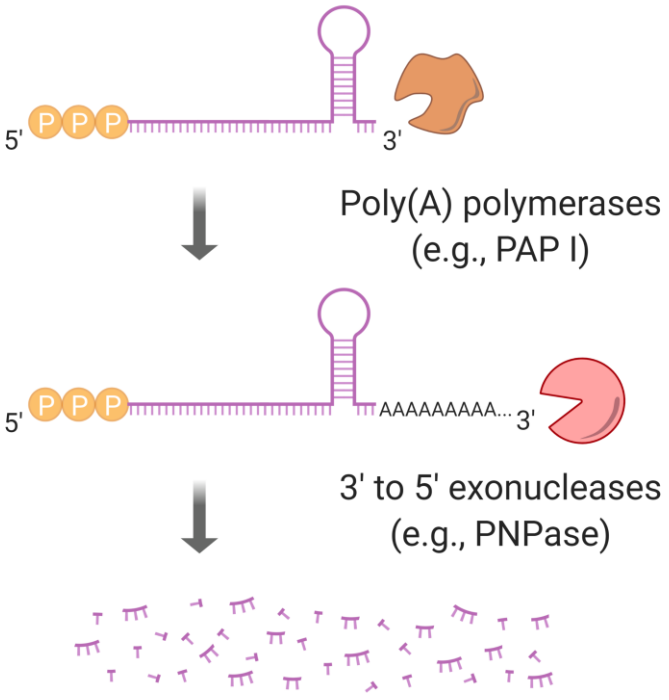

Figure 1-6. Polyadenylation regulates mRNA half-life. Stem-loops at mRNA 3′ ends block 3′–5′ exoribonucleases such as PNPase. PAP I, a poly(A) polymerase, can facilitate an exoribonuclease "grip" by synthesizing a poly(A) tail.

Regulation of PNPase abundance has been shown for *E. coli*, as its transcript *pnp* is post-transcriptionally regulated by its own product and RNase III. This mechanism can be disrupted by transcript association with the ribosomal protein S1 (Briani et al., 2008; Carzaniga et al., 2015). Moreover, an increase of the pool of polyadenylated transcripts increases *pnp* half-life, an effect attributed to PNPase titration (Mohanty and Kushner, 2000; 2002). Regardless of this autoregulatory characteristic, changes in PNPase abundance were not detected as a response to hypoxic stress in *M. smegmatis* (Vargas-Blanco et al., 2019), despite increased mRNA stability. While these findings suggest that regulation by mRNA polyadenylation via PNPase abundance is not a mechanism of transcriptome stabilization in mycobacteria, it is possible that polyadenylation activity by other enzymes, such as PcnA and PcnB, (Adilakshmi et al., 2000) might have a role in regulation of mRNA turnover in stress. Further research is needed to investigate this possibility.

The relationship between mRNA abundance and mRNA decay rates

In bacteria, the steady-state mRNA concentration is a function of transcription rates and transcript degradation rates, and to a lesser extent, of mRNA dilution. The contribution of mRNA dilution occurring during cell growth is usually ignored, given that doubling times are significantly longer than the median mRNA half-life. For example, in *L. lactis* mRNA half-lives complied with this assumption for 85% of the measured transcripts, at multiple growth rates (Dressaire et al., 2013). In stress conditions, bacterial growth is generally impaired, making the impact of mRNA dilution even smaller and reinforcing the roles of transcription and RNA turnover as the major determinants of mRNA abundance. Also under stress conditions, transcript abundance per cell is typically lower than in conditions of rapid growth. For example, low transcript abundance was observed for *S. aureus* in cold shock, heat shock, and stringent response when compared to unstressed exponential phase (Anderson et al., 2006). The per-cell mRNA concentration decreased in *L. lactis* during progressive adaptation to carbon starvation (Redon et al.,

2005b) or isoleucine starvation (Dressaire et al., 2013). The mRNA concentration was three times higher for *E. coli* growing in LB when compared to growth in in minimal media (Bartholomaus et al., 2016). For *M. smegmatis* in early hypoxic stress, the levels of *atpB*, *atpE*, *rnj*, *rraA* and *sigA* ranged between ~5% and 75% of those in cells growing in aerobic conditions, and after extended periods of hypoxic or carbon starvation stress, mRNA levels dropped to under 5% of those in log phase (Vargas-Blanco et al., 2019). Given the generally longer half-lives of mRNAs in stressed bacteria, the observation of reduced mRNA concentrations in these conditions may seem counter-intuitive. However, these observations can be reconciled if transcription is also greatly reduced. It is possible that maintaining lower overall mRNA abundance in stress conditions is an adaptive mechanism to favor translation of genes needed for survival of that particular stressor. For example, in a transcriptome-wide study in *E. coli*, mRNA abundance decreased in response to osmotic stress (from ~2,400 to ~1,600 transcripts per cell), a change that may allow specific transcripts—associated with stress response—to be more accessible to ribosomes and translated (Bartholomaus et al., 2016). Interestingly, transcripts with higher copy numbers per cell in normal conditions (> 2 copies/cell) were downregulated the most in osmotic stress (Bartholomaus et al., 2016).

The question has arisen if lower mRNA concentrations can actually cause their degradation to be slowed. This idea is suggested by an observation made by several groups, in several species, that in log phase growth, mRNA half-lives are inversely correlated with steady-state abundance (Figure 1-7). For example, a weak negative correlation was shown between mRNA concentration and mRNA half-life for *E. coli* cells in exponential phase (Bernstein et al., 2002). Stronger negative correlations were reported in *L. lactis* (Redon et al., 2005a), and in *M. tuberculosis* (Rustad et al., 2013), both in exponentially growing bacteria. Moreover, in the latter study the overexpression of genes in the DosR regulon resulted in transcripts with shorter half-lives. Other reports in *E. coli* and *L. lactis* showed that cells growing at different growth rates

also show a negative correlation between these parameters (Dressaire et al., 2013; Esquerre et al., 2015). For example, changes in growth rate from 0.1 h^{-1} to 0.63 h^{-1}—using chemostats—resulted in increased mRNA levels and a decreased median mRNA half-life from 4.2 min to 2.8 min, respectively (Esquerre et al., 2014; Esquerre et al., 2015). Transcription modulation using five constructs with distinct 5' UTRs in *lacLM* mRNA also depicted a similar trend in *L. lactis* in exponential phase, and a similar outcome was obtained for *lacZ* in *E. coli*, using P_{BAD}-mediated transcription regulation (Nouaille et al., 2017). Two of the studies described here (Rustad et al., 2013; Nouaille et al., 2017) reported inverse relationships between mRNA abundance and half-life in defined systems where expression was modulated by inducible promotors and growth rate was not affected. This strongly suggested that transcription rate can directly influence degradation rate. However, contradictory findings have been reported.

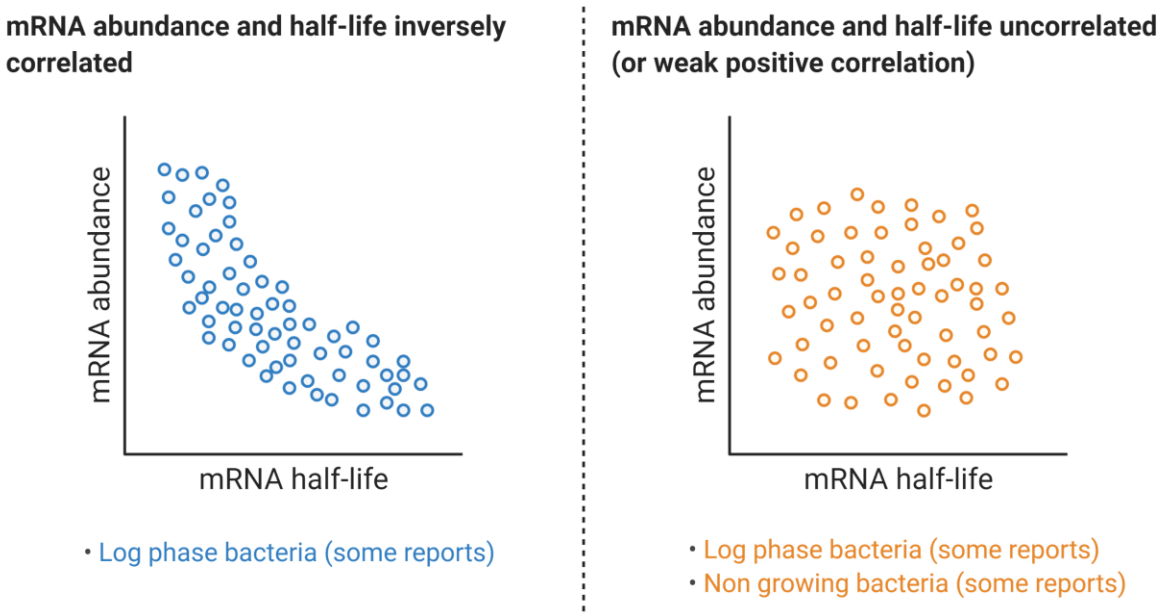

Figure 1-7. Relationships between mRNA abundance and mRNA decay rates. While some reports have shown a clear negative correlation between a transcript half-life and its abundance, a similar number of reports have found no correlation at all or a modest positive correlation, even for the same organism. Table 1-1 compiles transcriptome-wide analyses of mRNA decay in different organisms, techniques used, and information on the reported relationships between mRNA abundance and mRNA half-life.

An *E. coli* transcriptome-wide mRNA half-life study by a different group reported that the rate of mRNA degradation had a very weak positive correlation with mRNA abundance for both exponential phase (R^2 = 0.07) and stationary phase (R^2 = 0.19) (Chen et al., 2015), in contrast to other *E. coli* studies (Bernstein et al., 2002; Esquerre et al., 2014; Esquerre et al., 2015). In *Bacillus cereus*, mRNA half-life had a positive correlation with expression level (Kristoffersen et al., 2012), while in *Stenotrophomonas maltophilia* and *Chlamydia trachomatis* trachoma and lymphogranuloma venereum biovars no correlations were found (Bernardini and Martinez, 2017; Ferreira et al., 2017). In *M. smegmatis*, induced overexpression of *dCas9* (in the absence of a gene-targeting sgRNA) did not alter its half-life in log phase (Vargas-Blanco et al., 2019). Surprisingly, overexpressing *dCas9* under hypoxic stress increased its mRNA stability by approximately two-fold (Vargas-Blanco et al., 2019). Moreover, re-exposure of hypoxic *M. smegmatis* cultures to oxygen caused half-lives of several tested genes to immediately return to log-phase like levels, despite transcription being blocked by rifampicin and transcript levels therefore remaining low (Vargas-Blanco et al., 2019). Other reports have indicated that the relationship between mRNA abundance and half-life differs in various stress conditions. In carbon-starved *L. lactis* there was a positive correlation between mRNA degradation and abundance (Redon et al., 2005a), while the opposite was observed during isoleucine starvation (Dressaire et al., 2013). Work in eukaryotes suggests complexities that could conceivably occur in bacteria as well. In *S. cerevisiae*, under DNA damaging conditions, upregulated genes are usually stabilized and repressed genes are prone to degradation (Shalem et al., 2008). Conversely, under oxidative stress upregulated genes are destabilized, with the opposite scenario for repressed genes (Shalem et al., 2008). Furthermore, an in-depth analysis in that work revealed a trend between these two stress conditions: Genes with a rapid transcriptional regulation show a negative correlation between mRNA abundance and mRNA degradation. On the other hand, genes subject to a slow transcriptional response follow a positive correlation between mRNA abundance and degradation (Shalem et al., 2008).

Clearly, further work is needed to reconcile contradictory findings in bacteria with respect to the relationships between mRNA abundance and stability. Some reported differences may be attributable to differences between species, while others may result from differences in methodology for measuring half-life. Most studies measure half-life by measuring decreases in mRNA abundance following transcription blockage by rifampicin. Variability may arise from the time-points chosen to assay abundance following transcriptional block, given that we and others have reported multiphasic decay kinetics (Hambraeus et al., 2003; Selinger et al., 2003; Chen et al., 2015; Nguyen et al., 2020). Methodology for normalization and for calculating half-lives also vary (see Table 1-1).

The importance of RNA decay in clinically important species

Pathogenic bacteria have developed mechanisms that allow them to survive often-hostile host environments by sensing cues and mounting specific responses at both transcriptional and posttranscriptional levels. These pathogens exhibit highly specific responses to some stressors, as well as broader responses to conditions such as energy stress, where resources are preserved by global modulation of processes including translation, protein degradation, transcription, and RNA stabilization (Bohne et al., 1994; Sherman et al., 2001; Park et al., 2003; Christiansen et al., 2004; Wood et al., 2005; Papenfort et al., 2006; Liu et al., 2010; Fritsch et al., 2011; Galagan et al., 2013; Guo et al., 2014; Sievers et al., 2015; Quereda et al., 2018; Ignatov et al., 2020).

In *L. monocytogenes*, PrfA serves as a transcriptional regulator of multiple virulence factors, such as phospholipases PlcA and PlcB, and the toxin listeriolysin O (Leimeister-Wachter et al., 1990; Leimeister-Wachter et al., 1991; Quereda et al., 2018). Expression of PrfA itself is regulated by several mechanisms at the translational and transcriptional level. For example, PrfA translation is temperature-regulated by a stem-loop in its transcript, *prfA*, that prevents ribosome access to the SD sequence at 30°C but not at 37°C (Johansson et al., 2002). *prfA* is also regulated by an S-adenosylmethionine riboswitch and its product, the

sRNA SreA, that blocks translation after binding the 5' UTR (Loh et al., 2009). Additionally, while the stem-loop increases *prfA* stability (Loh et al., 2012), the binding of SreA to *prfA* triggers transcript degradation (Loh et al., 2009). Also in *L. monocytogenes*, posttranscriptional regulation of Tcsa, the T cell-stimulating antigen encoded by *tcsA*, was recently reported to be under the control of the sRNA LhrC in a translation-independent manner, by recruiting an undefined RNase (Ross et al., 2019). In *S. aureus* SarA, a histone-like protein, influences mRNA turnover of virulence factors, such as protein A (*spa*) and the collagen adhesion protein (*cna*) during exponential growth (Roberts et al., 2006; Morrison et al., 2012). Also in *S. aureus*, the multifunctional RNAIII binds other RNAs, recruiting RNase III to initiate transcript degradation. Some of RNAIII's targets are *spa*, *coa* (encoding coagulase), *sbi* (encoding the IgG-binding protein Sbi), and *SA1000* (encoding the fibrinogen-binding protein SA1000) (Huntzinger et al., 2005; Boisset et al., 2007; Chevalier et al., 2010), playing an important role in *S. aureus* virulence and response to stress. In *S. enterica*, under low Mg^{2+} conditions synthesis of the antisense AmgR RNA leads to interaction and destabilization of the *mgtC* transcript (encoding the virulence protein MgtC), in an RNase E-dependent manner (Lee and Groisman, 2010). Hence, regulation of the stabilities of specific mRNAs has a major role in the survival and virulence responses of pathogens.

Recent reports have suggested unexpected relationships between RNases and drug resistance. Nonsense and INDEL mutations in *Rv2752c*, encoding RNase J, were associated with drug resistance in a GWAS study that identified resistance-associated mutations in whole-genome sequences of hundreds of *M. tuberculosis* clinical isolates (Hicks et al., 2018), as well as an earlier study performing similar analyses on a smaller set of clinical isolates (Zhang et al., 2013). Another study, reporting whole-genome sequences of 154 *M. leprae* clinical isolates from 25 countries, found a disproportionately high number of polymorphisms in *ML1040c*, encoding RNase D, and *ML1512c*, encoding RNase J (Benjak et al., 2018).

These mutations were not directly associated with drug resistance, but appeared to be under positive selection (Benjak et al., 2018).

Global mRNA stabilization is another feature associated with bacterial stress response and non-growing conditions (see Table 1-1). Cells in quiescent states contain relatively low levels of mRNA, with greatly reduced transcriptional and translational activity (Betts et al., 2002; Wood et al., 2005; Kumar et al., 2012; Rittershaus et al., 2013). In some cases, these states share similarities with *B. subtilis* spores, in which the bacteria have dramatically reduced mRNA turnover (Segev et al., 2012). This can be interpreted as a concerted cellular effort to downregulate global gene expression and preserve cellular resources, until encountering a suitable environment to resume growth. At the same time, having paused translational machinery may permit allocation of resources towards specific responses needed to survive a given condition, such as those described in the previous paragraph. Importantly, stress responses that establish and maintain non-growing states not only allow pathogens to survive these stressors, but also induce broad antibiotic tolerance, since most antibiotics are relatively ineffective at killing non-growing cells [for example, (Rao et al., 2008)]. This relationship between growth arrest and antibiotic tolerance may be one of the reasons why months of multidrug therapy are required to prevent relapse in tuberculosis patients, where large numbers of bacteria are likely semi-dormant in hypoxic granulomas (Garton et al., 2008). The apparent universality of mRNA stabilization as a response to energy stress and other stressors that inhibit growth, compared to gene-specific mRNA regulation, brings up fascinating possibilities as a prospective target for therapeutic development. There has been a surge in antimicrobial resistance in recent decades, prompting collaborative efforts between academia and industry to develop new antimicrobials (Ventola, 2015a; Ventola, 2015b; WHO, 2019). As we approach an understanding of the mechanisms behind mRNA turnover—and strive to unveil how transcript fate is regulated under stress conditions—we would like to emphasize the essentiality of mRNA degradation in bacteria, and the roles of RNases in the virulence and

survival responses of pathogens. Many clinically important antibiotics target transcription and translation, highlighting the potential of targeting these central dogma processes from the opposite angle. In early steps in this direction, a protein degradation inhibitor was found to have strong activity against mycobacteria (Gavrish et al., 2014) and inhibitors of RNase E have been reported (Kime et al., 2015).

Conclusions

Transcriptome stabilization as a stress response is widespread across the bacterial domain. This globally concerted response is implicated in gene regulation and survival, as well as pathogenesis in bacteria. We have described and discussed various mechanisms of mRNA degradation and stabilization, many of which have established roles in regulation of specific genes, but have not yet been able to explain transcriptome-wide half-life alterations. We hope that the information presented here helps to inspire further study that will uncover the mechanism(s) behind global transcriptome stabilization in stress, which so far remains elusive. Finally, we hope to inspire the reader to find these mysteries as scientifically stimulating as we do.

Acknowledgments

This work was supported by the NSF CAREER award 1652756 to SS. DV-B was partially supported by the Fulbright Foreign Student Program.

We thank all members of the Shell lab for technical assistance and helpful discussions. Figures were created with BioRender.com.

References

Abe, H., and Aiba, H. (1996). Differential contributions of two elements of rho-independent terminator to transcription termination and mRNA stabilization. *Biochimie* 78(11-12)**,** 1035-1042. doi: 10.1016/s0300-9084(97)86727-2.

Adhya, S., Sarkar, P., Valenzuela, D., and Maitra, U. (1979). Termination of transcription by *Escherichia coli* RNA polymerase: influence of secondary structure of RNA transcripts on rho-independent and rho-dependent termination. *Proc Natl Acad Sci U S A* 76(4)**,** 1613-1617. doi: 10.1073/pnas.76.4.1613.

Adilakshmi, T., Ayling, P.D., and Ratledge, C. (2000). Polyadenylylation in mycobacteria: evidence for oligo(dT)-primed cDNA synthesis. *Microbiology* 146 (Pt 3)**,** 633-638. doi: 10.1099/00221287-146-3-633.

Afonyushkin, T., Vecerek, B., Moll, I., Blasi, U., and Kaberdin, V.R. (2005). Both RNase E and RNase III control the stability of sodB mRNA upon translational inhibition by the small regulatory RNA RyhB. *Nucleic Acids Res* 33(5)**,** 1678-1689. doi: 10.1093/nar/gki313.

Agaisse, H., and Lereclus, D. (1996). STAB-SD: a Shine-Dalgarno sequence in the 5' untranslated region is a determinant of mRNA stability. *Mol Microbiol* 20(3)**,** 633-643. doi: 10.1046/j.1365-2958.1996.5401046.x.

Aiso, T., Yoshida, H., Wada, A., and Ohki, R. (2005). Modulation of mRNA stability participates in stationary-phase-specific expression of ribosome modulation factor. *J Bacteriol* 187(6)**,** 1951-1958. doi: 10.1128/JB.187.6.1951-1958.2005.

Ait-Bara, S., and Carpousis, A.J. (2015). RNA degradosomes in bacteria and chloroplasts: classification, distribution and evolution of RNase E homologs. *Mol Microbiol* 97(6)**,** 1021-1135. doi: 10.1111/mmi.13095.

Al-Husini, N., Tomares, D.T., Bitar, O., Childers, W.S., and Schrader, J.M. (2018). alpha-proteobacterial RNA degradosomes assemble liquid-liquid phase-separated RNP bodies. *Mol Cell* 71(6)**,** 1027-1039 e1014. doi: 10.1016/j.molcel.2018.08.003.

Albertson, M.H., Nyström, T., and Kjelleberg, S. (1990). Functional mRNA half-lives in the marine *Vibrio* sp. S14 during starvation and recovery. *Microbiology* 136(11)**,** 2195-2199.

Amilon, K.R., Letley, D.P., Winter, J.A., Robinson, K., and Atherton, J.C. (2015). Expression of the *Helicobacter pylori* virulence factor vacuolating cytotoxin A (vacA) is influenced by a potential stem-loop structure in the 5' untranslated region of the transcript. *Mol Microbiol* 98(5)**,** 831-846. doi: 10.1111/mmi.13160.

Anderson, K.L., Roberts, C., Disz, T., Vonstein, V., Hwang, K., Overbeek, R., et al. (2006). Characterization of the *Staphylococcus aureus* heat shock, cold shock, stringent, and SOS responses and their effects on log-phase mRNA turnover. *J Bacteriol* 188(19)**,** 6739-6756. doi: 10.1128/JB.00609-06.

Arango, D., Sturgill, D., Alhusaini, N., Dillman, A.A., Sweet, T.J., Hanson, G., et al. (2018). Acetylation of cytidine in mRNA promotes translation efficiency. *Cell* 175(7)**,** 1872-1886 e1824. doi: 10.1016/j.cell.2018.10.030.

Arluison, V., Derreumaux, P., Allemand, F., Folichon, M., Hajnsdorf, E., and Regnier, P. (2002). Structural modelling of the m-like protein Hfq from *Escherichia coli*. *J Mol Biol* 320(4)**,** 705-712. doi: 10.1016/s0022-2836(02)00548-x.

Arnold, T.E., Yu, J., and Belasco, J.G. (1998). mRNA stabilization by the ompA 5' untranslated region: two protective elements hinder distinct pathways for mRNA degradation. *RNA* 4(3)**,** 319-330.

Arraiano, C.M., Andrade, J.M., Domingues, S., Guinote, I.B., Malecki, M., Matos, R.G., et al. (2010). The critical role of RNA processing and degradation in the control of gene expression. *FEMS Microbiol Rev* 34(5)**,** 883-923. doi: 10.1111/j.1574-6976.2010.00242.x.

Artsimovitch, I., Patlan, V., Sekine, S., Vassylyeva, M.N., Hosaka, T., Ochi, K., et al. (2004). Structural basis for transcription regulation by alarmone ppGpp. *Cell* 117(3)**,** 299-310.

Atkinson, G.C., Tenson, T., and Hauryliuk, V. (2011). The RelA/SpoT homolog (RSH) superfamily: distribution and functional evolution of ppGpp synthetases and hydrolases across the tree of life. *PLoS One* 6(8)**,** e23479. doi: 10.1371/journal.pone.0023479.

Avarbock, D., Avarbock, A., and Rubin, H. (2000). Differential regulation of opposing RelMtb activities by the aminoacylation state of a tRNA.ribosome.mRNA.RelMtb complex. *Biochemistry* 39(38)**,** 11640-11648.

Baga, M., Goransson, M., Normark, S., and Uhlin, B.E. (1988). Processed mRNA with differential stability in the regulation of *E. coli* pilin gene expression. *Cell* 52(2)**,** 197-206. doi: 10.1016/0092-8674(88)90508-9.

Baker, C.S., Eory, L.A., Yakhnin, H., Mercante, J., Romeo, T., and Babitzke, P. (2007). CsrA inhibits translation initiation of *Escherichia coli* hfq by binding to a single site overlapping the Shine-Dalgarno sequence. *J Bacteriol* 189(15)**,** 5472-5481. doi: 10.1128/JB.00529-07.

Bandyra, K.J., Bouvier, M., Carpousis, A.J., and Luisi, B.F. (2013). The social fabric of the RNA degradosome. *Biochim Biophys Acta* 1829(6-7)**,** 514-522. doi: 10.1016/j.bbagrm.2013.02.011.

Bardwell, J.C., Regnier, P., Chen, S.M., Nakamura, Y., Grunberg-Manago, M., and Court, D.L. (1989). Autoregulation of RNase III operon by mRNA processing. *EMBO J* 8(11)**,** 3401-3407.

Bartholomaus, A., Fedyunin, I., Feist, P., Sin, C., Zhang, G., Valleriani, A., et al. (2016). Bacteria differently regulate mRNA abundance to specifically respond to various stresses. *Philos Trans A Math Phys Eng Sci* 374(2063). doi: 10.1098/rsta.2015.0069.

Battesti, A., and Bouveret, E. (2009). Bacteria possessing two RelA/SpoT-like proteins have evolved a specific stringent response involving the acyl carrier protein-SpoT interaction. *J Bacteriol* 191(2)**,** 616-624. doi: 10.1128/JB.01195-08.

Bechhofer, D.H., and Deutscher, M.P. (2019). Bacterial ribonucleases and their roles in RNA metabolism. *Crit Rev Biochem Mol Biol* 54(3)**,** 242-300. doi: 10.1080/10409238.2019.1651816.

Bechhofer, D.H., and Dubnau, D. (1987). Induced mRNA stability in *Bacillus subtilis*. *Proc Natl Acad Sci U S A* 84(2)**,** 498-502. doi: 10.1073/pnas.84.2.498.

Bechhofer, D.H., and Zen, K.H. (1989). Mechanism of erythromycin-induced ermC mRNA stability in *Bacillus subtilis*. *J Bacteriol* 171(11)**,** 5803-5811. doi: 10.1128/jb.171.11.5803-5811.1989.

Becker, H.F., Motorin, Y., Planta, R.J., and Grosjean, H. (1997). The yeast gene YNL292w encodes a pseudouridine synthase (Pus4) catalyzing the formation of psi55 in both mitochondrial and cytoplasmic tRNAs. *Nucleic Acids Res* 25(22)**,** 4493-4499. doi: 10.1093/nar/25.22.4493.

Belasco, J.G., Beatty, J.T., Adams, C.W., von Gabain, A., and Cohen, S.N. (1985). Differential expression of photosynthesis genes in R. capsulata results from segmental differences in stability within the polycistronic rxcA transcript. *Cell* 40(1)**,** 171-181.

Benjak, A., Avanzi, C., Singh, P., Loiseau, C., Girma, S., Busso, P., et al. (2018). Phylogenomics and antimicrobial resistance of the leprosy bacillus *Mycobacterium leprae*. *Nat Commun* 9(1)**,** 352. doi: 10.1038/s41467-017-02576-z.

Bernardini, A., and Martinez, J.L. (2017). Genome-wide analysis shows that RNase G plays a global role in the stability of mRNAs in *Stenotrophomonas maltophilia*. *Sci Rep* 7(1)**,** 16016. doi: 10.1038/s41598-017-16091-0.

Bernstein, J.A., Khodursky, A.B., Lin, P.H., Lin-Chao, S., and Cohen, S.N. (2002). Global analysis of mRNA decay and abundance in *Escherichia coli* at single-gene resolution using two-color fluorescent DNA microarrays. *Proc Natl Acad Sci U S A* 99(15)**,** 9697-9702. doi: 10.1073/pnas.112318199.

Bernstein, J.A., Lin, P.H., Cohen, S.N., and Lin-Chao, S. (2004). Global analysis of *Escherichia coli* RNA degradosome function using DNA microarrays. *Proc Natl Acad Sci U S A* 101(9)**,** 2758-2763. doi: 10.1073/pnas.0308747101.

Betts, J.C., Lukey, P.T., Robb, L.C., McAdam, R.A., and Duncan, K. (2002). Evaluation of a nutrient starvation model of *Mycobacterium tuberculosis* persistence by gene and protein expression profiling. *Mol Microbiol* 43(3)**,** 717-731.

Bird, J.G., Zhang, Y., Tian, Y., Panova, N., Barvik, I., Greene, L., et al. (2016). The mechanism of RNA 5' capping with NAD+, NADH and desphospho-CoA. *Nature* 535(7612)**,** 444-447. doi: 10.1038/nature18622.

Blum, E., Carpousis, A.J., and Higgins, C.F. (1999). Polyadenylation promotes degradation of 3'-structured RNA by the *Escherichia coli* mRNA degradosome in vitro. *J Biol Chem* 274(7)**,** 4009-4016. doi: 10.1074/jbc.274.7.4009.

Bochner, B.R., Lee, P.C., Wilson, S.W., Cutler, C.W., and Ames, B.N. (1984). AppppA and related adenylylated nucleotides are synthesized as a consequence of oxidation stress. *Cell* 37(1)**,** 225-232. doi: 10.1016/0092-8674(84)90318-0.

Bodi, Z., Button, J.D., Grierson, D., and Fray, R.G. (2010). Yeast targets for mRNA methylation. *Nucleic Acids Res* 38(16)**,** 5327-5335. doi: 10.1093/nar/gkq266.

Boel, G., Letso, R., Neely, H., Price, W.N., Wong, K.H., Su, M., et al. (2016). Codon influence on protein expression in *E. coli* correlates with mRNA levels. *Nature* 529(7586)**,** 358-363. doi: 10.1038/nature16509.

Bohn, C., Rigoulay, C., and Bouloc, P. (2007). No detectable effect of RNA-binding protein Hfq absence in *Staphylococcus aureus*. *BMC Microbiol* 7**,** 10. doi: 10.1186/1471-2180-7-10.

Bohne, J., Sokolovic, Z., and Goebel, W. (1994). Transcriptional regulation of prfA and PrfA-regulated virulence genes in *Listeria monocytogenes*. *Mol Microbiol* 11(6)**,** 1141-1150. doi: 10.1111/j.1365-2958.1994.tb00390.x.

Boisset, S., Geissmann, T., Huntzinger, E., Fechter, P., Bendridi, N., Possedko, M., et al. (2007). *Staphylococcus aureus* RNAIII coordinately represses the synthesis of virulence factors and the transcription regulator Rot by an antisense mechanism. *Genes Dev* 21(11)**,** 1353-1366. doi: 10.1101/gad.423507.

Bouvet, P., and Belasco, J.G. (1992). Control of RNase E-mediated RNA degradation by 5'-terminal base pairing in *E. coli*. *Nature* 360(6403)**,** 488-491. doi: 10.1038/360488a0.

Braun, F., Durand, S., and Condon, C. (2017). Initiating ribosomes and a 5'/3'-UTR interaction control ribonuclease action to tightly couple B. subtilis hbs mRNA stability with translation. *Nucleic Acids Res* 45(19)**,** 11386-11400. doi: 10.1093/nar/gkx793.

Braun, F., Le Derout, J., and Regnier, P. (1998). Ribosomes inhibit an RNase E cleavage which induces the decay of the rpsO mRNA of *Escherichia coli*. *EMBO J* 17(16)**,** 4790-4797. doi: 10.1093/emboj/17.16.4790.

Brescia, C.C., Kaw, M.K., and Sledjeski, D.D. (2004). The DNA binding protein H-NS binds to and alters the stability of RNA in vitro and in vivo. *J Mol Biol* 339(3)**,** 505-514. doi: 10.1016/j.jmb.2004.03.067.

Brevet, A., Chen, J., Leveque, F., Plateau, P., and Blanquet, S. (1989). In vivo synthesis of adenylylated bis(5'-nucleosidyl) tetraphosphates (Ap4N) by Escherichia coli aminoacyl-tRNA synthetases. *Proc Natl Acad Sci U S A* 86(21)**,** 8275-8279. doi: 10.1073/pnas.86.21.8275.

Briani, F., Curti, S., Rossi, F., Carzaniga, T., Mauri, P., and Deho, G. (2008). Polynucleotide phosphorylase hinders mRNA degradation upon ribosomal protein S1 overexpression in *Escherichia coli*. *RNA* 14(11)**,** 2417-2429. doi: 10.1261/rna.1123908.

Bruscella, P., Shahbabian, K., Laalami, S., and Putzer, H. (2011). RNase Y is responsible for uncoupling the expression of translation factor IF3 from that of the ribosomal proteins L35 and L20 in *Bacillus subtilis*. *Mol Microbiol* 81(6), 1526-1541. doi: 10.1111/j.1365-2958.2011.07793.x.

Cahova, H., Winz, M.L., Hofer, K., Nubel, G., and Jaschke, A. (2015). NAD captureSeq indicates NAD as a bacterial cap for a subset of regulatory RNAs. *Nature* 519(7543)**,** 374-377. doi: 10.1038/nature14020.

Callaghan, A.J., Marcaida, M.J., Stead, J.A., McDowall, K.J., Scott, W.G., and Luisi, B.F. (2005). Structure of *Escherichia coli* RNase E catalytic domain and implications for RNA turnover. *Nature* 437(7062)**,** 1187-1191. doi: 10.1038/nature04084.

Cameron, T.A., Matz, L.M., Sinha, D., and De Lay, N.R. (2019). Polynucleotide phosphorylase promotes the stability and function of Hfq-binding sRNAs by degrading target mRNA-derived fragments. *Nucleic Acids Res* 47(16)**,** 8821-8837. doi: 10.1093/nar/gkz616.

Campos-Guillen, J., Bralley, P., Jones, G.H., Bechhofer, D.H., and Olmedo-Alvarez, G. (2005). Addition of poly(A) and heteropolymeric 3' ends in *Bacillus subtilis* wild-type and polynucleotide phosphorylase-deficient strains. *J Bacteriol* 187(14)**,** 4698-4706. doi: 10.1128/JB.187.14.4698-4706.2005.

Carabetta, V. J., Tanner, A. W., Greco, T. M., Defrancesco, M., Cristea, I. M. and Dubnau, D. (2013). A complex of YlbF, YmcA and YaaT regulates sporulation, competence and biofilm formation by accelerating the phosphorylation of Spo0A. *Mol microbiol*, 88(2). 283–300. doi: 10.1111/mmi.12186

Carlile, T.M., Rojas-Duran, M.F., Zinshteyn, B., Shin, H., Bartoli, K.M., and Gilbert, W.V. (2014). Pseudouridine profiling reveals regulated mRNA pseudouridylation in yeast and human cells. *Nature* 515(7525)**,** 143-146. doi: 10.1038/nature13802.

Caron, M.P., Bastet, L., Lussier, A., Simoneau-Roy, M., Masse, E., and Lafontaine, D.A. (2012). Dual-acting riboswitch control of translation initiation and mRNA decay. *Proc Natl Acad Sci U S A* 109(50)**,** E3444-3453. doi: 10.1073/pnas.1214024109.

Carpousis, A.J. (2007). The RNA degradosome of Escherichia coli: an mRNA-degrading machine assembled on RNase E. *Annu Rev Microbiol* 61**,** 71-87. doi: 10.1146/annurev.micro.61.080706.093440.

Carpousis, A.J., Van Houwe, G., Ehretsmann, C., and Krisch, H.M. (1994). Copurification of E. coli RNAase E and PNPase: evidence for a specific association between two enzymes important in RNA processing and degradation. *Cell* 76(5)**,** 889-900.

Carzaniga, T., Deho, G., and Briani, F. (2015). RNase III-independent autogenous regulation of *Escherichia coli* polynucleotide phosphorylase via translational repression. *J Bacteriol* 197(11)**,** 1931-1938. doi: 10.1128/JB.00105-15.

Celesnik, H., Deana, A., and Belasco, J.G. (2007). Initiation of RNA decay in *Escherichia coli* by 5' pyrophosphate removal. *Mol Cell* 27(1)**,** 79-90. doi: 10.1016/j.molcel.2007.05.038.

Chakraburtty, R., and Bibb, M. (1997). The ppGpp synthetase gene (relA) of *Streptomyces coelicolor* A3(2) plays a conditional role in antibiotic production and morphological differentiation. *J Bacteriol* 179(18)**,** 5854-5861.

Chan, C.T., Dyavaiah, M., DeMott, M.S., Taghizadeh, K., Dedon, P.C., and Begley, T.J. (2010). A quantitative systems approach reveals dynamic control of tRNA modifications during cellular stress. *PLoS Genet* 6(12)**,** e1001247. doi: 10.1371/journal.pgen.1001247.

Chan, C.T., Pang, Y.L., Deng, W., Babu, I.R., Dyavaiah, M., Begley, T.J., et al. (2012). Reprogramming of tRNA modifications controls the oxidative stress response by codon-biased translation of proteins. *Nat Commun* 3**,** 937. doi: 10.1038/ncomms1938.

Chandran, V., and Luisi, B.F. (2006). Recognition of enolase in the *Escherichia coli* RNA degradosome. *J Mol Biol* 358(1)**,** 8-15. doi: 10.1016/j.jmb.2006.02.012.

Chao, Y., Li, L., Girodat, D., Forstner, K.U., Said, N., Corcoran, C., et al. (2017). *In vivo* cleavage map illuminates the central role of RNase E in coding and non-coding RNA pathways. *Mol Cell* 65(1)**,** 39-51. doi: 10.1016/j.molcel.2016.11.002.

Chen, Z., Itzek, A., Malke, H., Ferretti, J. J., and Kreth, J. (2013). Multiple roles of RNase Y in *Streptococcus pyogenes* mRNA processing and degradation. *J Bacteriol*, 195(11). 2585–2594. doi: 10.1128/JB.00097-13.

Chen, H., Previero, A., and Deutscher, M.P. (2019a). A novel mechanism of ribonuclease regulation: GcvB and Hfq stabilize the mRNA that encodes RNase BN/Z during exponential phase. *J Biol Chem* 294(52)**,** 19997-20008. doi: 10.1074/jbc.RA119.011367.

Chen, H., Shiroguchi, K., Ge, H., and Xie, X.S. (2015). Genome-wide study of mRNA degradation and transcript elongation in *Escherichia coli*. *Mol Syst Biol* 11(1)**,** 781. doi: 10.15252/msb.20145794.

Chen, L.H., Emory, S.A., Bricker, A.L., Bouvet, P., and Belasco, J.G. (1991). Structure and function of a bacterial mRNA stabilizer: analysis of the 5' untranslated region of ompA mRNA. *J Bacteriol* 173(15)**,** 4578-4586. doi: 10.1128/jb.173.15.4578-4586.1991.

Chen, X., Li, A., Sun, B.F., Yang, Y., Han, Y.N., Yuan, X., et al. (2019b). 5-methylcytosine promotes pathogenesis of bladder cancer through stabilizing mRNAs. *Nat Cell Biol* 21(8)**,** 978-990. doi: 10.1038/s41556-019-0361-y.

Chen, Y.G., Kowtoniuk, W.E., Agarwal, I., Shen, Y., and Liu, D.R. (2009). LC/MS analysis of cellular RNA reveals NAD-linked RNA. *Nat Chem Biol* 5(12)**,** 879-881. doi: 10.1038/nchembio.235.

Chevalier, C., Boisset, S., Romilly, C., Masquida, B., Fechter, P., Geissmann, T., et al. (2010). *Staphylococcus aureus* RNAIII binds to two distant regions of coa mRNA to arrest translation and promote mRNA degradation. *PLoS Pathog* 6(3)**,** e1000809. doi: 10.1371/journal.ppat.1000809.

Ching, C., Gozzi, K., Heinemann, B., Chai, Y., and Godoy, V.G. (2017). RNA-Mediated cis Regulation in *Acinetobacter baumannii* Modulates Stress-Induced Phenotypic Variation. *J Bacteriol* 199(11). doi: 10.1128/JB.00799-16.

Chionh, Y.H., McBee, M., Babu, I.R., Hia, F., Lin, W., Zhao, W., et al. (2016). tRNA-mediated codon-biased translation in mycobacterial hypoxic persistence. *Nat Commun* 7**,** 13302. doi: 10.1038/ncomms13302.

Cho, K.H. (2017). The structure and function of the gram-positive bacterial RNA degradosome. *Front Microbiol* 8**,** 154. doi: 10.3389/fmicb.2017.00154.

Christiansen, J.K., Larsen, M.H., Ingmer, H., Sogaard-Andersen, L., and Kallipolitis, B.H. (2004). The RNA-binding protein Hfq of *Listeria monocytogenes*: role in stress tolerance and virulence. *J Bacteriol* 186(11)**,** 3355-3362. doi: 10.1128/JB.186.11.3355-3362.2004.

Christiansen, J.K., Nielsen, J.S., Ebersbach, T., Valentin-Hansen, P., Sogaard-Andersen, L., and Kallipolitis, B.H. (2006). Identification of small Hfq-binding RNAs in *Listeria monocytogenes*. *RNA* 12(7)**,** 1383-1396. doi: 10.1261/rna.49706.

Commichau, F.M., Rothe, F.M., Herzberg, C., Wagner, E., Hellwig, D., Lehnik-Habrink, M., et al. (2009). Novel activities of glycolytic enzymes in *Bacillus subtilis*: interactions with essential proteins involved in mRNA processing. *Mol Cell Proteomics* 8(6)**,** 1350-1360. doi: 10.1074/mcp.M800546-MCP200.

Condon, C. (2003). RNA processing and degradation in *Bacillus subtilis*. *Microbiol Mol Biol Rev* 67(2)**,** 157-174, table of contents. doi: 10.1128/mmbr.67.2.157-174.2003.

Condon, C., Putzer, H., and Grunberg-Manago, M. (1996). Processing of the leader mRNA plays a major role in the induction of thrS expression following threonine starvation in *Bacillus subtilis*. *Proc Natl Acad Sci U S A* 93(14)**,** 6992-6997.

Corrigan, R.M., Bellows, L.E., Wood, A., and Grundling, A. (2016). ppGpp negatively impacts ribosome assembly affecting growth and antimicrobial tolerance in Gram-positive bacteria. *Proc Natl Acad Sci U S A* 113(12)**,** E1710-1719. doi: 10.1073/pnas.1522179113.

Coste, H., Brevet, A., Plateau, P., and Blanquet, S. (1987). Non-adenylylated bis(5'-nucleosidyl) tetraphosphates occur in Saccharomyces cerevisiae and in *Escherichia coli* and accumulate upon temperature shift or exposure to cadmium. *J Biol Chem* 262(25)**,** 12096-12103.

Courbet, A., Endy, D., Renard, E., Molina, F., and Bonnet, J. (2015). Detection of pathological biomarkers in human clinical samples via amplifying genetic switches and logic gates. *Sci Transl Med* 7(289)**,** 289ra283. doi: 10.1126/scitranslmed.aaa3601.

Cui, M., Wang, T., Xu, J., Ke, Y., Du, X., Yuan, X., et al. (2013). Impact of Hfq on global gene expression and intracellular survival in *Brucella melitensis*. *PLoS One* 8(8)**,** e71933. doi: 10.1371/journal.pone.0071933.

Daeffler, K.N., Galley, J.D., Sheth, R.U., Ortiz-Velez, L.C., Bibb, C.O., Shroyer, N.F., et al. (2017). Engineering bacterial thiosulfate and tetrathionate sensors for detecting gut inflammation. *Mol Syst Biol* 13(4)**,** 923. doi: 10.15252/msb.20167416.

Daou-Chabo, R., Mathy, N., Benard, L., and Condon, C. (2009). Ribosomes initiating translation of the hbs mRNA protect it from 5'-to-3' exoribonucleolytic degradation by RNase J1. *Mol Microbiol* 71(6)**,** 1538-1550. doi: 10.1111/j.1365-2958.2009.06620.x.

Deana, A., Celesnik, H., and Belasco, J.G. (2008). The bacterial enzyme RppH triggers messenger RNA degradation by 5' pyrophosphate removal. *Nature* 451(7176)**,** 355-358. doi: 10.1038/nature06475.

DeLoughery, A., Dengler, V., Chai, Y. and Losick, R. (2016). Biofilm formation by *Bacillus subtilis* requires an endoribonuclease-containing multisubunit complex that controls mRNA levels for the matrix gene repressor SinR. *Mol Microbiol* 99(2), 425–437. doi: 10.1111/mmi.13240.

DeLoughery, A., Jean-Benoît, L., Losick, R., and Gene-Wei, L. (2018). Maturation of polycistronic mRNAs by the endoribonuclease RNase Y and its associated Y-complex in *Bacillus subtilis*. *Proc Natl Acad Sci U S A* 115(24), E5585-E5594. doi: 10.1073/pnas.1803283115.

Deng, W., Babu, I.R., Su, D., Yin, S., Begley, T.J., and Dedon, P.C. (2015a). Trm9-catalyzed tRNA modifications regulate global protein expression by codon-biased translation. *PLoS Genet* 11(12)**,** e1005706. doi: 10.1371/journal.pgen.1005706.

Deng, X., Chen, K., Luo, G.Z., Weng, X., Ji, Q., Zhou, T., et al. (2015b). Widespread occurrence of N6-methyladenosine in bacterial mRNA. *Nucleic Acids Res* 43(13)**,** 6557-6567. doi: 10.1093/nar/gkv596.

Deng, Z., Liu, Z., Bi, Y., Wang, X., Zhou, D., Yang, R., et al. (2014). Rapid degradation of Hfq-free RyhB in *Yersinia pestis* by PNPase independent of putative ribonucleolytic complexes. *Biomed Res Int* 2014**,** 798918. doi: 10.1155/2014/798918.

Deutscher, M.P. (2006). Degradation of RNA in bacteria: comparison of mRNA and stable RNA. *Nucleic Acids Res* 34(2)**,** 659-666. doi: 10.1093/nar/gkj472.

Diwa, A., Bricker, A.L., Jain, C., and Belasco, J.G. (2000). An evolutionarily conserved RNA stem-loop functions as a sensor that directs feedback regulation of RNase E gene expression. *Genes Dev* 14(10)**,** 1249-1260.

Diwa, A.A., and Belasco, J.G. (2002). Critical features of a conserved RNA stem-loop important for feedback regulation of RNase E synthesis. *J Biol Chem* 277(23)**,** 20415-20422. doi: 10.1074/jbc.M202313200.

Donovan, W.P., and Kushner, S.R. (1986). Polynucleotide phosphorylase and ribonuclease II are required for cell viability and mRNA turnover in *Escherichia coli* K-12. *Proc Natl Acad Sci U S A* 83(1)**,** 120-124.

Drecktrah, D., Hall, L.S., Rescheneder, P., Lybecker, M., and Samuels, D.S. (2018). The Stringent Response-Regulated sRNA Transcriptome of *Borrelia burgdorferi*. *Front Cell Infect Microbiol* 8**,** 231. doi: 10.3389/fcimb.2018.00231.

Dressaire, C., Picard, F., Redon, E., Loubiere, P., Queinnec, I., Girbal, L., et al. (2013). Role of mRNA stability during bacterial adaptation. *PLoS One* 8(3)**,** e59059. doi: 10.1371/journal.pone.0059059.

Druzhinin, S.Y., Tran, N.T., Skalenko, K.S., Goldman, S.R., Knoblauch, J.G., Dove, S.L., et al. (2015). A conserved pattern of primer-dependent transcription initiation in escherichia coli and *Vibrio cholerae* revealed by 5' RNA-seq. *PLoS Genet* 11(7)**,** e1005348. doi: 10.1371/journal.pgen.1005348.

Dubnau, E.J., Carabetta, V.J., Tanner, A.W., Miras, M., Diethmaier, C., and Dubnau, D. (2016). A protein complex supports the production of Spo0A-P and plays additional roles for biofilms and the K-state in *Bacillus subtilis*. *Mol Microbiol* 101(4), 606-624. doi: 10.1111/mmi.13411.

Durand, S., Gilet, L., Bessieres, P., Nicolas, P., and Condon, C. (2012). Three essential ribonucleases-RNase Y, J1, and III-control the abundance of a majority of *Bacillus subtilis* mRNAs. *PLoS Genet* 8(3)**,** e1002520. doi: 10.1371/journal.pgen.1002520.

Edelheit, S., Schwartz, S., Mumbach, M.R., Wurtzel, O., and Sorek, R. (2013). Transcriptome-wide mapping of 5-methylcytidine RNA modifications in bacteria, archaea, and yeast reveals m5C within archaeal mRNAs. *PLoS Genet* 9(6)**,** e1003602. doi: 10.1371/journal.pgen.1003602.

Emory, S.A., and Belasco, J.G. (1990). The ompA 5' untranslated RNA segment functions in *Escherichia coli* as a growth-rate-regulated mRNA stabilizer whose activity is unrelated to translational efficiency. *J Bacteriol* 172(8)**,** 4472-4481. doi: 10.1128/jb.172.8.4472-4481.1990.

Emory, S.A., Bouvet, P., and Belasco, J.G. (1992). A 5'-terminal stem-loop structure can stabilize mRNA in *Escherichia coli*. *Genes Dev* 6(1)**,** 135-148. doi: 10.1101/gad.6.1.135.

Esquerre, T., Bouvier, M., Turlan, C., Carpousis, A.J., Girbal, L., and Cocaign-Bousquet, M. (2016). The Csr system regulates genome-wide mRNA stability and transcription and thus gene expression in *Escherichia coli*. *Sci Rep* 6**,** 25057. doi: 10.1038/srep25057.

Esquerre, T., Laguerre, S., Turlan, C., Carpousis, A.J., Girbal, L., and Cocaign-Bousquet, M. (2014). Dual role of transcription and transcript stability in the regulation of gene expression in *Escherichia coli* cells cultured on glucose at different growth rates. *Nucleic Acids Res* 42(4)**,** 2460-2472. doi: 10.1093/nar/gkt1150.

Esquerre, T., Moisan, A., Chiapello, H., Arike, L., Vilu, R., Gaspin, C., et al. (2015). Genome-wide investigation of mRNA lifetime determinants in *Escherichia coli* cells cultured at different growth rates. *BMC Genomics* 16**,** 275. doi: 10.1186/s12864-015-1482-8.

Even, S., Pellegrini, O., Zig, L., Labas, V., Vinh, J., Brechemmier-Baey, D., et al. (2005). Ribonucleases J1 and J2: two novel endoribonucleases in *B. subtilis* with functional homology to *E.coli* RNase E. *Nucleic Acids Res* 33(7)**,** 2141-2152. doi: 10.1093/nar/gki505.

Eyler, D.E., Franco, M.K., Batool, Z., Wu, M.Z., Dubuke, M.L., Dobosz-Bartoszek, M., et al. (2019). Pseudouridinylation of mRNA coding sequences alters translation. *Proc Natl Acad Sci U S A* 116(46)**,** 23068-23074. doi: 10.1073/pnas.1821754116.

Faner, M.A., and Feig, A.L. (2013). Identifying and characterizing Hfq-RNA interactions. *Methods* 63(2)**,** 144-159. doi: 10.1016/j.ymeth.2013.04.023.

Farnham, P.J., and Platt, T. (1981). Rho-independent termination: dyad symmetry in DNA causes RNA polymerase to pause during transcription in vitro. *Nucleic Acids Res* 9(3)**,** 563-577. doi: 10.1093/nar/9.3.563.

Farr, S.B., Arnosti, D.N., Chamberlin, M.J., and Ames, B.N. (1989). An apaH mutation causes AppppA to accumulate and affects motility and catabolite repression in *Escherichia coli*. *Proc Natl Acad Sci U S A* 86(13)**,** 5010-5014. doi: 10.1073/pnas.86.13.5010.

Ferreira, R., Borges, V., Borrego, M.J., and Gomes, J.P. (2017). Global survey of mRNA levels and decay rates of *Chlamydia trachomatis* trachoma and lymphogranuloma venereum biovars. *Heliyon* 3(7)**,** e00364. doi: 10.1016/j.heliyon.2017.e00364.

Folichon, M., Allemand, F., Regnier, P., and Hajnsdorf, E. (2005). Stimulation of poly(A) synthesis by *Escherichia coli* poly(A)polymerase I is correlated with Hfq binding to poly(A) tails. *FEBS J* 272(2)**,** 454-463. doi: 10.1111/j.1742-4658.2004.04485.x.

Frederix, M., and Downie, A.J. (2011). Quorum sensing: regulating the regulators. *Adv Microb Physiol* 58**,** 23-80. doi: 10.1016/B978-0-12-381043-4.00002-7.

Frindert, J., Zhang, Y., Nubel, G., Kahloon, M., Kolmar, L., Hotz-Wagenblatt, A., et al. (2018). Identification, biosynthesis, and decapping of NAD-capped RNAs in B. *subtilis*. *Cell Rep* 24(7)**,** 1890-1901 e1898. doi: 10.1016/j.celrep.2018.07.047.

Fritsch, F., Mauder, N., Williams, T., Weiser, J., Oberle, M., and Beier, D. (2011). The cell envelope stress response mediated by the LiaFSRLm three-component system of *Listeria monocytogenes* is controlled via the phosphatase activity of the bifunctional histidine kinase LiaSLm. *Microbiology* 157(Pt 2)**,** 373-386. doi: 10.1099/mic.0.044776-0.

Fry, M., Israeli-Reches, M., and Artman, M. (1972). Stabilization and breakdown of *Escherichia coli* messenger ribonucleic acid in the presence of chloramphenicol. *Biochemistry* 11(16)**,** 3054-3059. doi: 10.1021/bi00766a017.

Galagan, J.E., Minch, K., Peterson, M., Lyubetskaya, A., Azizi, E., Sweet, L., et al. (2013). The *Mycobacterium tuberculosis* regulatory network and hypoxia. *Nature* 499(7457)**,** 178-183. doi: 10.1038/nature12337.

Garton, N.J., Waddell, S.J., Sherratt, A.L., Lee, S.M., Smith, R.J., Senner, C., et al. (2008). Cytological and transcript analyses reveal fat and lazy persister-like bacilli in tuberculous sputum. *PLoS Med* 5(4)**,** e75. doi: 10.1371/journal.pmed.0050075.

Gatewood, M.L., and Jones, G.H. (2010). (p)ppGpp inhibits polynucleotide phosphorylase from streptomyces but not from *Escherichia coli* and increases the stability of bulk mRNA in Streptomyces coelicolor. *J Bacteriol* 192(17)**,** 4275-4280. doi: 10.1128/JB.00367-10.

Gavrish, E., Sit, C.S., Cao, S., Kandror, O., Spoering, A., Peoples, A., et al. (2014). Lassomycin, a ribosomally synthesized cyclic peptide, kills *Mycobacterium tuberculosis* by targeting the ATP-dependent protease ClpC1P1P2. *Chem Biol* 21(4)**,** 509-518. doi: 10.1016/j.chembiol.2014.01.014.

Gentry, D.R., Hernandez, V.J., Nguyen, L.H., Jensen, D.B., and Cashel, M. (1993). Synthesis of the stationary-phase sigma factor sigma s is positively regulated by ppGpp. *J Bacteriol* 175(24)**,** 7982-7989.

Georgellis, D., Barlow, T., Arvidson, S., and von Gabain, A. (1993). Retarded RNA turnover in *Escherichia coli*: a means of maintaining gene expression during anaerobiosis. *Mol Microbiol* 9(2)**,** 375-381.

Glatz, E., Nilsson, R.P., Rutberg, L., and Rutberg, B. (1996). A dual role for the *Bacillus subtilis* glpD leader and the GlpP protein in the regulated expression of glpD: antitermination and control of mRNA stability. *Mol Microbiol* 19(2)**,** 319-328. doi: 10.1046/j.1365-2958.1996.376903.x.

Gualerzi, C.O., Giuliodori, A.M., and Pon, C.L. (2003). Transcriptional and post-transcriptional control of cold-shock genes. *J Mol Biol* 331(3)**,** 527-539. doi: 10.1016/s0022-2836(03)00732-0.

Guo, M.S., Updegrove, T.B., Gogol, E.B., Shabalina, S.A., Gross, C.A., and Storz, G. (2014). MicL, a new sigmaE-dependent sRNA, combats envelope stress by repressing synthesis of Lpp, the major outer membrane lipoprotein. *Genes Dev* 28(14)**,** 1620-1634. doi: 10.1101/gad.243485.114.

Gutgsell, N., Englund, N., Niu, L., Kaya, Y., Lane, B.G., and Ofengand, J. (2000). Deletion of the *Escherichia coli* pseudouridine synthase gene truB blocks formation of pseudouridine 55 in tRNA in vivo, does not affect exponential growth, but confers a strong selective disadvantage in competition with wild-type cells. *RNA* 6(12)**,** 1870-1881. doi: 10.1017/s1355838200001588.

Hadjeras, L., Poljak, L., Bouvier, M., Morin-Ogier, Q., Canal, I., Cocaign-Bousquet, M., et al. (2019). Detachment of the RNA degradosome from the inner membrane of *Escherichia coli* results in a global slowdown of mRNA degradation, proteolysis of RNase E and increased turnover of ribosome-free transcripts. *Mol Microbiol* 111(6)**,** 1715-1731. doi: 10.1111/mmi.14248.

Hajnsdorf, E., and Regnier, P. (2000). Host factor Hfq of *Escherichia coli* stimulates elongation of poly(A) tails by poly(A) polymerase I. *Proc Natl Acad Sci U S A* 97(4)**,** 1501-1505. doi: 10.1073/pnas.040549897.

Hambraeus, G., Karhumaa, K., and Rutberg, B. (2002). A 5' stem-loop and ribosome binding but not translation are important for the stability of Bacillus subtilis aprE leader mRNA. *Microbiology* 148(Pt 6)**,** 1795-1803. doi: 10.1099/00221287-148-6-1795.

Hambraeus, G., Persson, M., and Rutberg, B. (2000). The aprE leader is a determinant of extreme mRNA stability in *Bacillus subtilis*. *Microbiology* 146 Pt 12**,** 3051-3059. doi: 10.1099/00221287-146-12-3051.

Hambraeus, G., von Wachenfeldt, C., and Hederstedt, L. (2003). Genome-wide survey of mRNA half-lives in *Bacillus subtilis* identifies extremely stable mRNAs. *Mol Genet Genomics* 269(5)**,** 706-714. doi: 10.1007/s00438-003-0883-6.

Hammerle, H., Amman, F., Vecerek, B., Stulke, J., Hofacker, I., and Blasi, U. (2014). Impact of Hfq on the *Bacillus subtilis* transcriptome. *PLoS One* 9(6)**,** e98661. doi: 10.1371/journal.pone.0098661.

Hamouche, L., Billaudeau, C., Rocca, A., Chastanet, A., Ngo, S., Laalami, S., et al. (2020). Dynamic Membrane Localization of RNase Y in *Bacillus subtilis*. *mBio* 11(1). doi: 10.1128/mBio.03337-19.

Hausmann, S., Guimaraes, V.A., Garcin, D., Baumann, N., Linder, P., and Redder, P. (2017). Both exo- and endo-nucleolytic activities of RNase J1 from *Staphylococcus aureus* are manganese dependent and active on triphosphorylated 5'-ends. *RNA Biol* 14(10)**,** 1431-1443. doi: 10.1080/15476286.2017.1300223.

Hicks, N.D., Yang, J., Zhang, X., Zhao, B., Grad, Y.H., Liu, L., et al. (2018). Clinically prevalent mutations in *Mycobacterium tuberculosis* alter propionate metabolism and mediate multidrug tolerance. *Nat Microbiol* 3(9)**,** 1032-1042. doi: 10.1038/s41564-018-0218-3.

Hoernes, T.P., Clementi, N., Faserl, K., Glasner, H., Breuker, K., Lindner, H., et al. (2016). Nucleotide modifications within bacterial messenger RNAs regulate their translation and are able to rewire the genetic code. *Nucleic Acids Res* 44(2)**,** 852-862. doi: 10.1093/nar/gkv1182.

Hofer, K., Li, S., Abele, F., Frindert, J., Schlotthauer, J., Grawenhoff, J., et al. (2016). Structure and function of the bacterial decapping enzyme NudC. *Nat Chem Biol* 12(9)**,** 730-734. doi: 10.1038/nchembio.2132.

Huang, T., Chen, W., Liu, J., Gu, N., and Zhang, R. (2019). Genome-wide identification of mRNA 5-methylcytosine in mammals. *Nat Struct Mol Biol* 26(5)**,** 380-388. doi: 10.1038/s41594-019-0218-x.

Hudecek, O., Benoni, R., Reyes-Gutierrez, P.E., Culka, M., Sanderova, H., Hubalek, M., et al. (2020). Dinucleoside polyphosphates act as 5'-RNA caps in bacteria. *Nat Commun* 11(1)**,** 1052. doi: 10.1038/s41467-020-14896-8.

Hue, K.K., Cohen, S.D., and Bechhofer, D.H. (1995). A polypurine sequence that acts as a 5' mRNA stabilizer in *Bacillus subtilis*. *J Bacteriol* 177(12)**,** 3465-3471. doi: 10.1128/jb.177.12.3465-3471.1995.

Hunt, A., Rawlins, J.P., Thomaides, H.B., and Errington, J. (2006). Functional analysis of 11 putative essential genes in *Bacillus subtilis*. *Microbiology* 152(Pt 10), 2895-2907. doi: 10.1099/mic.0.29152-0.

Huntzinger, E., Boisset, S., Saveanu, C., Benito, Y., Geissmann, T., Namane, A., et al. (2005). *Staphylococcus aureus* RNAIII and the endoribonuclease III coordinately regulate spa gene expression. *EMBO J* 24(4)**,** 824-835. doi: 10.1038/sj.emboj.7600572.

Ignatov, D., Vaitkevicius, K., Durand, S., Cahoon, L., Sandberg, S.S., Liu, X., et al. (2020). An mRNA-mRNA interaction couples expression of a virulence factor and its chaperone in *Listeria monocytogenes*. *Cell Rep* 30(12)**,** 4027-4040 e4027. doi: 10.1016/j.celrep.2020.03.006.

Ishida, K., Kunibayashi, T., Tomikawa, C., Ochi, A., Kanai, T., Hirata, A., et al. (2011). Pseudouridine at position 55 in tRNA controls the contents of other modified nucleotides for low-temperature adaptation in the extreme-thermophilic eubacterium *Thermus thermophilus*. *Nucleic Acids Res* 39(6)**,** 2304-2318. doi: 10.1093/nar/gkq1180.

Johansson, J., Mandin, P., Renzoni, A., Chiaruttini, C., Springer, M., and Cossart, P. (2002). An RNA thermosensor controls expression of virulence genes in *Listeria monocytogenes*. *Cell* 110(5)**,** 551-561. doi: 10.1016/s0092-8674(02)00905-4.

Jona, G., Choder, M., and Gileadi, O. (2000). Glucose starvation induces a drastic reduction in the rates of both transcription and degradation of mRNA in yeast. *Biochim Biophys Acta* 1491(1-3)**,** 37-48.

Jourdan, S.S., and McDowall, K.J. (2008). Sensing of 5' monophosphate by *Escherichia coli* RNase G can significantly enhance association with RNA and stimulate the decay of functional mRNA transcripts in vivo. *Mol Microbiol* 67(1)**,** 102-115. doi: 10.1111/j.1365-2958.2007.06028.x.

Joyce, S.A., and Dreyfus, M. (1998). In the absence of translation, RNase E can bypass 5' mRNA stabilizers in *Escherichia coli*. *J Mol Biol* 282(2)**,** 241-254. doi: 10.1006/jmbi.1998.2027.

Julius, C., and Yuzenkova, Y. (2017). Bacterial RNA polymerase caps RNA with various cofactors and cell wall precursors. *Nucleic Acids Res* 45(14)**,** 8282-8290. doi: 10.1093/nar/gkx452.

Jurgen, B., Schweder, T., and Hecker, M. (1998). The stability of mRNA from the gsiB gene of *Bacillus subtilis* is dependent on the presence of a strong ribosome binding site. *Mol Gen Genet* 258(5)**,** 538-545. doi: 10.1007/s004380050765.

Kavita, K., de Mets, F., and Gottesman, S. (2018). New aspects of RNA-based regulation by Hfq and its partner sRNAs. *Curr Opin Microbiol* 42**,** 53-61. doi: 10.1016/j.mib.2017.10.014.

Khemici, V., Poljak, L., Luisi, B.F., and Carpousis, A.J. (2008). The RNase E of *Escherichia coli* is a membrane-binding protein. *Mol Microbiol* 70(4)**,** 799-813. doi: 10.1111/j.1365-2958.2008.06454.x.

Khemici, V., Prados, J., Linder, P., and Redder, P. (2015). Decay-initiating endoribonucleolytic cleavage by RNase y is kept under tight control via sequence preference and sub-cellular localisation. *PLoS Genet* 11(10)**,** e1005577. doi: 10.1371/journal.pgen.1005577.

Kido, M., Yamanaka, K., Mitani, T., Niki, H., Ogura, T., and Hiraga, S. (1996). RNase E polypeptides lacking a carboxyl-terminal half suppress a mukB mutation in *Escherichia coli*. *J Bacteriol* 178(13)**,** 3917-3925. doi: 10.1128/jb.178.13.3917-3925.1996.

Kime, L., Jourdan, S.S., Stead, J.A., Hidalgo-Sastre, A., and McDowall, K.J. (2010). Rapid cleavage of RNA by RNase E in the absence of 5' monophosphate stimulation. *Mol Microbiol* 76(3)**,** 590-604. doi: 10.1111/j.1365-2958.2009.06935.x.

Kime, L., Vincent, H.A., Gendoo, D.M., Jourdan, S.S., Fishwick, C.W., Callaghan, A.J., et al. (2015). The first small-molecule inhibitors of members of the ribonuclease E family. *Sci Rep* 5**,** 8028. doi: 10.1038/srep08028.

Kinghorn, S.M., O'Byrne, C.P., Booth, I.R., and Stansfield, I. (2002). Physiological analysis of the role of truB in *Escherichia coli*: a role for tRNA modification in extreme temperature resistance. *Microbiology* 148(Pt 11)**,** 3511-3520. doi: 10.1099/00221287-148-11-3511.

Klug, G., and Cohen, S.N. (1990). Combined actions of multiple hairpin loop structures and sites of rate-limiting endonucleolytic cleavage determine differential degradation rates of individual segments within polycistronic puf operon mRNA. *J Bacteriol* 172(9)**,** 5140-5146. doi: 10.1128/jb.172.9.5140-5146.1990.

Kowtoniuk, W.E., Shen, Y., Heemstra, J.M., Agarwal, I., and Liu, D.R. (2009). A chemical screen for biological small molecule-RNA conjugates reveals CoA-linked RNA. *Proc Natl Acad Sci U S A* 106(19)**,** 7768-7773. doi: 10.1073/pnas.0900528106.

Krishnan, S., Petchiappan, A., Singh, A., Bhatt, A., and Chatterji, D. (2016). R-loop induced stress response by second (p)ppGpp synthetase in *Mycobacterium smegmatis*: functional and domain interdependence. *Mol Microbiol* 102(1)**,** 168-182. doi: 10.1111/mmi.13453.

Kristoffersen, S.M., Haase, C., Weil, M.R., Passalacqua, K.D., Niazi, F., Hutchison, S.K., et al. (2012). Global mRNA decay analysis at single nucleotide resolution reveals segmental and positional degradation patterns in a Gram-positive bacterium. *Genome Biol* 13(4)**,** R30. doi: 10.1186/gb-2012-13-4-r30.

Kumar, A., Majid, M., Kunisch, R., Rani, P.S., Qureshi, I.A., Lewin, A., et al. (2012). *Mycobacterium tuberculosis* DosR regulon gene Rv0079 encodes a putative, 'dormancy associated translation inhibitor (DATIN)'. *PLoS One* 7(6)**,** e38709. doi: 10.1371/journal.pone.0038709.

Laxman, S., Sutter, B.M., Wu, X., Kumar, S., Guo, X., Trudgian, D.C., et al. (2013). Sulfur amino acids regulate translational capacity and metabolic homeostasis through modulation of tRNA thiolation. *Cell* 154(2)**,** 416-429. doi: 10.1016/j.cell.2013.06.043.

Lee, E.J., and Groisman, E.A. (2010). An antisense RNA that governs the expression kinetics of a multifunctional virulence gene. *Mol Microbiol* 76(4)**,** 1020-1033. doi: 10.1111/j.1365-2958.2010.07161.x.

Lee, K., Zhan, X., Gao, J., Qiu, J., Feng, Y., Meganathan, R., et al. (2003). RraA. a protein inhibitor of RNase E activity that globally modulates RNA abundance in *E. coli*. *Cell* 114(5)**,** 623-634.

Lee, P.C., Bochner, B.R., and Ames, B.N. (1983). AppppA, heat-shock stress, and cell oxidation. *Proc Natl Acad Sci U S A* 80(24)**,** 7496-7500. doi: 10.1073/pnas.80.24.7496.

Lehnik-Habrink, M., Newman, J., Rothe, F.M., Solovyova, A.S., Rodrigues, C., Herzberg, C., et al. (2011). RNase Y in Bacillus subtilis: a Natively disordered protein that is the functional equivalent of RNase E from *Escherichia coli*. *J Bacteriol* 193(19), 5431-5441. doi: 10.1128/JB.05500-11

Lehnik-Habrink, M., Pfortner, H., Rempeters, L., Pietack, N., Herzberg, C., and Stulke, J. (2010). The RNA degradosome in *Bacillus subtilis*: identification of CshA as the major RNA helicase in the multiprotein complex. *Mol Microbiol* 77(4)**,** 958-971. doi: 10.1111/j.1365-2958.2010.07264.x.

Leimeister-Wachter, M., Domann, E., and Chakraborty, T. (1991). Detection of a gene encoding a phosphatidylinositol-specific phospholipase C that is co-ordinately expressed with listeriolysin in *Listeria monocytogenes*. *Mol Microbiol* 5(2)**,** 361-366. doi: 10.1111/j.1365-2958.1991.tb02117.x.

Leimeister-Wachter, M., Haffner, C., Domann, E., Goebel, W., and Chakraborty, T. (1990). Identification of a gene that positively regulates expression of listeriolysin, the major virulence factor of *Listeria monocytogenes*. *Proc Natl Acad Sci U S A* 87(21)**,** 8336-8340. doi: 10.1073/pnas.87.21.8336.

Lenz, G., Doron-Faigenboim, A., Ron, E.Z., Tuller, T., and Gophna, U. (2011). Sequence features of E. coli mRNAs affect their degradation. *PLoS One* 6(12)**,** e28544. doi: 10.1371/journal.pone.0028544.

Li, Z., Pandit, S., and Deutscher, M.P. (1998). Polyadenylation of stable RNA precursors in vivo. *Proc Natl Acad Sci U S A* 95(21)**,** 12158-12162. doi: 10.1073/pnas.95.21.12158.

Liang, W., and Deutscher, M.P. (2013). Ribosomes regulate the stability and action of the exoribonuclease RNase R. *J Biol Chem* 288(48)**,** 34791-34798. doi: 10.1074/jbc.M113.519553.

Linder, B., Grozhik, A.V., Olarerin-George, A.O., Meydan, C., Mason, C.E., and Jaffrey, S.R. (2015). Single-nucleotide-resolution mapping of m6A and m6Am throughout the transcriptome. *Nat Methods* 12(8)**,** 767-772. doi: 10.1038/nmeth.3453.

Liu, M.Y., Gui, G., Wei, B., Preston, J.F., 3rd, Oakford, L., Yuksel, U., et al. (1997). The RNA molecule CsrB binds to the global regulatory protein CsrA and antagonizes its activity in *Escherichia coli*. *J Biol Chem* 272(28)**,** 17502-17510. doi: 10.1074/jbc.272.28.17502.

Liu, M.Y., Yang, H., and Romeo, T. (1995). The product of the pleiotropic *Escherichia coli* gene csrA modulates glycogen biosynthesis via effects on mRNA stability. *J Bacteriol* 177(10)**,** 2663-2672. doi: 10.1128/jb.177.10.2663-2672.1995.

Liu, Y., Wu, N., Dong, J., Gao, Y., Zhang, X., Mu, C., et al. (2010). Hfq is a global regulator that controls the pathogenicity of *Staphylococcus aureus*. *PLoS One* 5(9). doi: 10.1371/journal.pone.0013069.

Loh, E., Dussurget, O., Gripenland, J., Vaitkevicius, K., Tiensuu, T., Mandin, P., et al. (2009). A trans-acting riboswitch controls expression of the virulence regulator PrfA in *Listeria monocytogenes*. *Cell* 139(4)**,** 770-779. doi: 10.1016/j.cell.2009.08.046.

Loh, E., Memarpour, F., Vaitkevicius, K., Kallipolitis, B.H., Johansson, J., and Sonden, B. (2012). An unstructured 5'-coding region of the prfA mRNA is required for efficient translation. *Nucleic Acids Res* 40(4)**,** 1818-1827. doi: 10.1093/nar/gkr850.

Lopez, P.J., Marchand, I., Joyce, S.A., and Dreyfus, M. (1999). The C-terminal half of RNase E, which organizes the *Escherichia coli* degradosome, participates in mRNA degradation but not rRNA processing in vivo. *Mol Microbiol* 33(1)**,** 188-199. doi: 10.1046/j.1365-2958.1999.01465.x.

Lopez, P.J., Marchand, I., Yarchuk, O., and Dreyfus, M. (1998). Translation inhibitors stabilize *Escherichia coli* mRNAs independently of ribosome protection. *Proc Natl Acad Sci U S A* 95(11)**,** 6067-6072.

Luciano, D.J., and Belasco, J.G. (2020). Np4A alarmones function in bacteria as precursors to RNA caps. *Proc Natl Acad Sci U S A* 117(7)**,** 3560-3567. doi: 10.1073/pnas.1914229117.

Luciano, D.J., Levenson-Palmer, R., and Belasco, J.G. (2019). Stresses that raise Np4A levels induce protective nucleoside tetraphosphate capping of bacterial RNA. *Mol Cell* 75(5)**,** 957-966 e958. doi: 10.1016/j.molcel.2019.05.031.

Luciano, D.J., Vasilyev, N., Richards, J., Serganov, A., and Belasco, J.G. (2017). A novel RNA phosphorylation state enables 5' end-dependent degradation in *Escherichia coli*. *Mol Cell* 67(1)**,** 44-54 e46. doi: 10.1016/j.molcel.2017.05.035.

Ludwig, H., Homuth, G., Schmalisch, M., Dyka, F.M., Hecker, M., and Stulke, J. (2001). Transcription of glycolytic genes and operons in *Bacillus subtilis*: evidence for the presence of multiple levels of control of the gapA operon. *Mol Microbiol* 41(2)**,** 409-422. doi: 10.1046/j.1365-2958.2001.02523.x.

Lundberg, U., von Gabain, A., and Melefors, O. (1990). Cleavages in the 5' region of the ompA and bla mRNA control stability: studies with an *E. coli* mutant altering mRNA stability and a novel endoribonuclease. *EMBO J* 9(9)**,** 2731-2741.

Mackie, G.A. (1992). Secondary structure of the mRNA for ribosomal protein S20. Implications for cleavage by ribonuclease E. *J Biol Chem* 267(2)**,** 1054-1061.

Mackie, G.A. (1998). Ribonuclease E is a 5'-end-dependent endonuclease. *Nature* 395(6703)**,** 720-723. doi: 10.1038/27246.

Maggi, N., Pasqualucci, C.R., Ballotta, R., and Sensi, P. (1966). Rifampicin: a new orally active rifamycin. *Chemotherapy* 11(5)**,** 285-292. doi: 10.1159/000220462.

Marcaida, M.J., DePristo, M.A., Chandran, V., Carpousis, A.J., and Luisi, B.F. (2006). The RNA degradosome: life in the fast lane of adaptive molecular evolution. *Trends Biochem Sci* 31(7)**,** 359-365. doi: 10.1016/j.tibs.2006.05.005.

Martinez-Costa, O.H., Fernandez-Moreno, M.A., and Malpartida, F. (1998). The relA/spoT-homologous gene in *Streptomyces coelicolor* encodes both ribosome-dependent (p)ppGpp-synthesizing and -degrading activities. *J Bacteriol* 180(16)**,** 4123-4132.

Martinez, I., El-Said Mohamed, M., Santos, V.E., Garcia, J.L., Garcia-Ochoa, F., and Diaz, E. (2017). Metabolic and process engineering for biodesulfurization in Gram-negative bacteria. *J Biotechnol* 262**,** 47-55. doi: 10.1016/j.jbiotec.2017.09.004.

Martini, M.C., Zhou, Y., Sun, H., and Shell, S.S. (2019). Defining the transcriptional and post-transcriptional landscapes of *Mycobacterium smegmatis* in aerobic growth and hypoxia. *Front Microbiol* 10**,** 591. doi: 10.3389/fmicb.2019.00591.

Mathy, N., Hebert, A., Mervelet, P., Benard, L., Dorleans, A., Li de la Sierra-Gallay, I., et al. (2010). *Bacillus subtilis* ribonucleases J1 and J2 form a complex with altered enzyme behaviour. *Mol Microbiol* 75(2)**,** 489-498. doi: 10.1111/j.1365-2958.2009.07004.x.

Matsunaga, J., Simons, E.L., and Simons, R.W. (1996). RNase III autoregulation: structure and function of rncO, the posttranscriptional "operator". *RNA* 2(12)**,** 1228-1240.

Matsunaga, J., Simons, E.L., and Simons, R.W. (1997). *Escherichia coli* RNase III (rnc) autoregulation occurs independently of rnc gene translation. *Mol Microbiol* 26(5)**,** 1125-1135. doi: 10.1046/j.1365-2958.1997.6652007.x.

McDowall, K.J., Kaberdin, V.R., Wu, S.W., Cohen, S.N., and Lin-Chao, S. (1995). Site-specific RNase E cleavage of oligonucleotides and inhibition by stem-loops. *Nature* 374(6519)**,** 287-290. doi: 10.1038/374287a0.

McDowall, K.J., Lin-Chao, S., and Cohen, S.N. (1994). A+U content rather than a particular nucleotide order determines the specificity of RNase E cleavage. *J Biol Chem* 269(14)**,** 10790-10796.

McLaren, R.S., Newbury, S.F., Dance, G.S., Causton, H.C., and Higgins, C.F. (1991). mRNA degradation by processive 3'-5' exoribonucleases in vitro and the implications for prokaryotic mRNA decay in vivo. *J Mol Biol* 221(1)**,** 81-95.

Melin, L., Rutberg, L., and von Gabain, A. (1989). Transcriptional and posttranscriptional control of the *Bacillus subtilis* succinate dehydrogenase operon. *J Bacteriol* 171(4)**,** 2110-2115. doi: 10.1128/jb.171.4.2110-2115.1989.

Messing, S.A., Gabelli, S.B., Liu, Q., Celesnik, H., Belasco, J.G., Pineiro, S.A., et al. (2009). Structure and biological function of the RNA pyrophosphohydrolase BdRppH from *Bdellovibrio bacteriovorus*. *Structure* 17(3)**,** 472-481. doi: 10.1016/j.str.2008.12.022.

Meyer, K.D., Saletore, Y., Zumbo, P., Elemento, O., Mason, C.E., and Jaffrey, S.R. (2012). Comprehensive analysis of mRNA methylation reveals enrichment in 3' UTRs and near stop codons. *Cell* 149(7)**,** 1635-1646. doi: 10.1016/j.cell.2012.05.003.

Moffitt, J.R., Pandey, S., Boettiger, A.N., Wang, S., and Zhuang, X. (2016). Spatial organization shapes the turnover of a bacterial transcriptome. *Elife* 5. doi: 10.7554/eLife.13065.

Mohanty, B.K., and Kushner, S.R. (2000). Polynucleotide phosphorylase functions both as a 3' right-arrow 5' exonuclease and a poly(A) polymerase in *Escherichia coli*. *Proc Natl Acad Sci U S A* 97(22)**,** 11966-11971. doi: 10.1073/pnas.220295997.

Mohanty, B.K., and Kushner, S.R. (2002). Polyadenylation of *Escherichia coli* transcripts plays an integral role in regulating intracellular levels of polynucleotide phosphorylase and RNase E. *Mol Microbiol* 45(5)**,** 1315-1324. doi: 10.1046/j.1365-2958.2002.03097.x.

Moll, I., Afonyushkin, T., Vytvytska, O., Kaberdin, V.R., and Blasi, U. (2003). Coincident Hfq binding and RNase E cleavage sites on mRNA and small regulatory RNAs. *RNA* 9(11)**,** 1308-1314. doi: 10.1261/rna.5850703.

Moller, T., Franch, T., Hojrup, P., Keene, D.R., Bachinger, H.P., Brennan, R.G., et al. (2002). Hfq: a bacterial Sm-like protein that mediates RNA-RNA interaction. *Mol Cell* 9(1)**,** 23-30. doi: 10.1016/s1097-2765(01)00436-1.

Montero Llopis, P., Jackson, A.F., Sliusarenko, O., Surovtsev, I., Heinritz, J., Emonet, T., et al. (2010). Spatial organization of the flow of genetic information in bacteria. *Nature* 466(7302)**,** 77-81. doi: 10.1038/nature09152.

Morin, M., Enjalbert, B., Ropers, D., Girbal, L., and Cocaign-Bousquet, M. (2020). Genomewide Stabilization of mRNA during a "Feast-to-Famine" Growth Transition in *Escherichia coli*. *mSphere* 5(3). doi: 10.1128/mSphere.00276-20.

Morita, T., and Aiba, H. (2011). RNase E action at a distance: degradation of target mRNAs mediated by an Hfq-binding small RNA in bacteria. *Genes Dev* 25(4)**,** 294-298. doi: 10.1101/gad.2030311.

Morita, T., Kawamoto, H., Mizota, T., Inada, T., and Aiba, H. (2004). Enolase in the RNA degradosome plays a crucial role in the rapid decay of glucose transporter mRNA in the response to phosphosugar stress in *Escherichia coli*. *Mol Microbiol* 54(4)**,** 1063-1075. doi: 10.1111/j.1365-2958.2004.04329.x.

Morrison, J.M., Anderson, K.L., Beenken, K.E., Smeltzer, M.S., and Dunman, P.M. (2012). The staphylococcal accessory regulator, SarA, is an RNA-binding protein that modulates the mRNA turnover properties of late-exponential and stationary phase *Staphylococcus aureus* cells. *Front Cell Infect Microbiol* 2**,** 26. doi: 10.3389/fcimb.2012.00026.

Muller, P., Gimpel, M., Wildenhain, T., and Brantl, S. (2019). A new role for CsrA: promotion of complex formation between an sRNA and its mRNA target in *Bacillus subtilis*. *RNA Biol* 16(7)**,** 972-987. doi: 10.1080/15476286.2019.1605811.

Murashko, O.N., Kaberdin, V.R., and Lin-Chao, S. (2012). Membrane binding of *Escherichia coli* RNase E catalytic domain stabilizes protein structure and increases RNA substrate affinity. *Proc Natl Acad Sci U S A* 109(18)**,** 7019-7024. doi: 10.1073/pnas.1120181109.

Murashko, O.N., and Lin-Chao, S. (2017). Escherichia coli responds to environmental changes using enolasic degradosomes and stabilized DicF sRNA to alter cellular morphology. *Proc Natl Acad Sci U S A* 114(38)**,** E8025-E8034. doi: 10.1073/pnas.1703731114.

Murdeshwar, M.S., and Chatterji, D. (2012). MS_RHII-RSD, a dual-function RNase HII-(p)ppGpp synthetase from *Mycobacterium smegmatis*. *J Bacteriol* 194(15)**,** 4003-4014. doi: 10.1128/JB.00258-12.

Nakamoto, M.A., Lovejoy, A.F., Cygan, A.M., and Boothroyd, J.C. (2017). mRNA pseudouridylation affects RNA metabolism in the parasite *Toxoplasma gondii*. *RNA* 23(12)**,** 1834-1849. doi: 10.1261/rna.062794.117.

Newbury, S.F., Smith, N.H., Robinson, E.C., Hiles, I.D., and Higgins, C.F. (1987). Stabilization of translationally active mRNA by prokaryotic REP sequences. *Cell* 48(2)**,** 297-310.

Nguyen, T.G., Vargas-Blanco, D.A., Roberts, L.A., and Shell, S.S. (2020). The impact of leadered and leaderless gene structures on translation efficiency, transcript stability, and predicted transcription rates in *Mycobacterium smegmatis*. *J Bacteriol*. doi: 10.1128/JB.00746-19.

Nielsen, J.S., Larsen, M.H., Lillebaek, E.M., Bergholz, T.M., Christiansen, M.H., Boor, K.J., et al. (2011). A small RNA controls expression of the chitinase ChiA in *Listeria monocytogenes*. *PLoS One* 6(4)**,** e19019. doi: 10.1371/journal.pone.0019019.

Nielsen, J.S., Lei, L.K., Ebersbach, T., Olsen, A.S., Klitgaard, J.K., Valentin-Hansen, P., et al. (2010). Defining a role for Hfq in Gram-positive bacteria: evidence for Hfq-dependent antisense regulation in *Listeria monocytogenes*. *Nucleic Acids Res* 38(3)**,** 907-919. doi: 10.1093/nar/gkp1081.

Nilsson, G., Belasco, J.G., Cohen, S.N., and von Gabain, A. (1984). Growth-rate dependent regulation of mRNA stability in *Escherichia coli*. *Nature* 312(5989)**,** 75-77. doi: 10.1038/312075a0.

Nilsson, P., Naureckiene, S., and Uhlin, B.E. (1996). Mutations affecting mRNA processing and fimbrial biogenesis in the *Escherichia coli* pap operon. *J Bacteriol* 178(3)**,** 683-690. doi: 10.1128/jb.178.3.683-690.1996.

Nilsson, P., and Uhlin, B.E. (1991). Differential decay of a polycistronic *Escherichia coli* transcript is initiated by RNaseE-dependent endonucleolytic processing. *Mol Microbiol* 5(7)**,** 1791-1799. doi: 10.1111/j.1365-2958.1991.tb01928.x.

Nishikura, K., and De Robertis, E.M. (1981). RNA processing in microinjected *Xenopus* oocytes. Sequential addition of base modifications in the spliced transfer RNA. *J Mol Biol* 145(2)**,** 405-420. doi: 10.1016/0022-2836(81)90212-6.

Nouaille, S., Mondeil, S., Finoux, A.L., Moulis, C., Girbal, L., and Cocaign-Bousquet, M. (2017). The stability of an mRNA is influenced by its concentration: a potential physical mechanism to regulate gene expression. *Nucleic Acids Res* 45(20)**,** 11711-11724. doi: 10.1093/nar/gkx781.

Nurse, K., Wrzesinski, J., Bakin, A., Lane, B.G., and Ofengand, J. (1995). Purification, cloning, and properties of the tRNA psi 55 synthase from *Escherichia coli*. *RNA* 1(1)**,** 102-112.

Olson, P.D., Kuechenmeister, L.J., Anderson, K.L., Daily, S., Beenken, K.E., Roux, C.M., et al. (2011). Small molecule inhibitors of *Staphylococcus aureus* RnpA alter cellular mRNA turnover, exhibit antimicrobial activity, and attenuate pathogenesis. *PLoS Pathog* 7(2)**,** e1001287. doi: 10.1371/journal.ppat.1001287.

Ow, M.C., Liu, Q., and Kushner, S.R. (2000). Analysis of mRNA decay and rRNA processing in *Escherichia coli* in the absence of RNase E-based degradosome assembly. *Mol Microbiol* 38(4)**,** 854-866. doi: 10.1046/j.1365-2958.2000.02186.x.

Paesold, G., and Krause, M. (1999). Analysis of rpoS mRNA in *Salmonella dublin*: identification of multiple transcripts with growth-phase-dependent variation in transcript stability. *J Bacteriol* 181(4)**,** 1264-1268.

Panneerdoss, S., Eedunuri, V.K., Yadav, P., Timilsina, S., Rajamanickam, S., Viswanadhapalli, S., et al. (2018). Cross-talk among writers, readers, and erasers of m(6)A regulates cancer growth and progression. *Sci Adv* 4(10)**,** eaar8263. doi: 10.1126/sciadv.aar8263.

Papenfort, K., Pfeiffer, V., Mika, F., Lucchini, S., Hinton, J.C., and Vogel, J. (2006). SigmaE-dependent small RNAs of *Salmonella* respond to membrane stress by accelerating global omp mRNA decay. *Mol Microbiol* 62(6)**,** 1674-1688. doi: 10.1111/j.1365-2958.2006.05524.x.

Park, H.D., Guinn, K.M., Harrell, M.I., Liao, R., Voskuil, M.I., Tompa, M., et al. (2003). Rv3133c/dosR is a transcription factor that mediates the hypoxic response of *Mycobacterium tuberculosis*. *Mol Microbiol* 48(3)**,** 833-843. doi: 10.1046/j.1365-2958.2003.03474.x.

Pato, M.L., Bennett, P.M., and von Meyenburg, K. (1973). Messenger ribonucleic acid synthesis and degradation in *Escherichia coli* during inhibition of translation. *J Bacteriol* 116(2)**,** 710-718.

Pertzev, A.V., and Nicholson, A.W. (2006). Characterization of RNA sequence determinants and antideterminants of processing reactivity for a minimal substrate of *Escherichia coli* ribonuclease III. *Nucleic Acids Res* 34(13)**,** 3708-3721. doi: 10.1093/nar/gkl459.

Petchiappan, A., Naik, S.Y., and Chatterji, D. (2020). RelZ-mediated stress response in *Mycobacterium smegmatis*: pGpp synthesis and its regulation. *J Bacteriol* 202(2). doi: 10.1128/JB.00444-19.

Plocinski, P., Macios, M., Houghton, J., Niemiec, E., Plocinska, R., Brzostek, A., et al. (2019). Proteomic and transcriptomic experiments reveal an essential role of RNA degradosome complexes in shaping the transcriptome of *Mycobacterium tuberculosis*. *Nucleic Acids Res* 47(11)**,** 5892-5905. doi: 10.1093/nar/gkz251.

Presnyak, V., Alhusaini, N., Chen, Y.H., Martin, S., Morris, N., Kline, N., et al. (2015). Codon optimality is a major determinant of mRNA stability. *Cell* 160(6)**,** 1111-1124. doi: 10.1016/j.cell.2015.02.029.

Py, B., Causton, H., Mudd, E.A., and Higgins, C.F. (1994). A protein complex mediating mRNA degradation in *Escherichia coli*. *Mol Microbiol* 14(4)**,** 717-729.

Py, B., Higgins, C.F., Krisch, H.M., and Carpousis, A.J. (1996). A DEAD-box RNA helicase in the *Escherichia coli* RNA degradosome. *Nature* 381(6578)**,** 169-172. doi: 10.1038/381169a0.

Quereda, J.J., Andersson, C., Cossart, P., Johansson, J., and Pizarro-Cerda, J. (2018). Role in virulence of phospholipases, listeriolysin O and listeriolysin S from epidemic *Listeria monocytogenes* using the chicken embryo infection model. *Vet Res* 49(1)**,** 13. doi: 10.1186/s13567-017-0496-4.

Ramirez-Pena, E., Trevino, J., Liu, Z., Perez, N., and Sumby, P. (2010). The group A *Streptococcus* small regulatory RNA FasX enhances streptokinase activity by increasing the stability of the ska mRNA transcript. *Mol Microbiol* 78(6)**,** 1332-1347. doi: 10.1111/j.1365-2958.2010.07427.x.

Rao, S.P., Alonso, S., Rand, L., Dick, T., and Pethe, K. (2008). The protonmotive force is required for maintaining ATP homeostasis and viability of hypoxic, nonreplicating *Mycobacterium tuberculosis*. *Proc Natl Acad Sci U S A* 105(33)**,** 11945-11950. doi: 10.1073/pnas.0711697105.

Redon, E., Loubiere, P., and Cocaign-Bousquet, M. (2005a). Role of mRNA stability during genome-wide adaptation of *Lactococcus lactis* to carbon starvation. *J Biol Chem* 280(43)**,** 36380-36385. doi: 10.1074/jbc.M506006200.

Redon, E., Loubiere, P., and Cocaign-Bousquet, M. (2005b). Transcriptome analysis of the progressive adaptation of *Lactococcus lactis* to carbon starvation. *J Bacteriol* 187(10)**,** 3589-3592. doi: 10.1128/JB.187.10.3589-3592.2005.

Redko, Y., Galtier, E., Arnion, H., Darfeuille, F., Sismeiro, O., Coppee, J.Y., et al. (2016). RNase J depletion leads to massive changes in mRNA abundance in *Helicobacter pylori*. *RNA Biol* 13(2)**,** 243-253. doi: 10.1080/15476286.2015.1132141.

Regnier, P., and Hajnsdorf, E. (2013). The interplay of Hfq, poly(A) polymerase I and exoribonucleases at the 3' ends of RNAs resulting from Rho-independent termination: A tentative model. *RNA Biol* 10(4)**,** 602-609. doi: 10.4161/rna.23664.

Richards, J., and Belasco, J.G. (2016). Distinct requirements for 5'-monophosphate-assisted RNA cleavage by *Escherichia coli* RNase E and RNase G. *J Biol Chem* 291(39)**,** 20825. doi: 10.1074/jbc.A115.702555.

Richards, J., and Belasco, J.G. (2019). Obstacles to scanning by RNase E govern bacterial mRNA lifetimes by hindering access to distal cleavage sites. *Mol Cell* 74(2)**,** 284-295 e285. doi: 10.1016/j.molcel.2019.01.044.

Richards, J., Liu, Q., Pellegrini, O., Celesnik, H., Yao, S., Bechhofer, D.H., et al. (2011). An RNA pyrophosphohydrolase triggers 5'-exonucleolytic degradation of mRNA in *Bacillus subtilis*. *Mol Cell* 43(6)**,** 940-949. doi: 10.1016/j.molcel.2011.07.023.

Riglar, D.T., Giessen, T.W., Baym, M., Kerns, S.J., Niederhuber, M.J., Bronson, R.T., et al. (2017). Engineered bacteria can function in the mammalian gut long-term as live diagnostics of inflammation. *Nat Biotechnol* 35(7)**,** 653-658. doi: 10.1038/nbt.3879.

Rittershaus, E.S., Baek, S.H., and Sassetti, C.M. (2013). The normalcy of dormancy: common themes in microbial quiescence. *Cell Host Microbe* 13(6)**,** 643-651. doi: 10.1016/j.chom.2013.05.012.

Roberts, C., Anderson, K.L., Murphy, E., Projan, S.J., Mounts, W., Hurlburt, B., et al. (2006). Characterizing the effect of the *Staphylococcus aureus* virulence factor regulator, SarA, on log-phase mRNA half-lives. *J Bacteriol* 188(7)**,** 2593-2603. doi: 10.1128/JB.188.7.2593-2603.2006.

Rochat, T., Bouloc, P., Yang, Q., Bossi, L., and Figueroa-Bossi, N. (2012). Lack of interchangeability of Hfq-like proteins. *Biochimie* 94(7)**,** 1554-1559. doi: 10.1016/j.biochi.2012.01.016.

Rochat, T., Delumeau, O., Figueroa-Bossi, N., Noirot, P., Bossi, L., Dervyn, E., et al. (2015). Tracking the elusive function of *Bacillus subtilis* Hfq. *PLoS One* 10(4)**,** e0124977. doi: 10.1371/journal.pone.0124977.

Romeo, T., and Babitzke, P. (2018). Global regulation by CsrA and its RNA antagonists. *Microbiol Spectr* 6(2). doi: 10.1128/microbiolspec.RWR-0009-2017.

Ross, J.A., Thorsing, M., Lillebaek, E.M.S., Teixeira Dos Santos, P., and Kallipolitis, B.H. (2019). The LhrC sRNAs control expression of T cell-stimulating antigen TcsA in *Listeria monocytogenes* by decreasing tcsA mRNA stability. *RNA Biol* 16(3)**,** 270-281. doi: 10.1080/15476286.2019.1572423.

Rozenski, J., Crain, P.F., and McCloskey, J.A. (1999). The RNA modification database: 1999 update. *Nucleic Acids Res* 27(1)**,** 196-197. doi: 10.1093/nar/27.1.196.

Rustad, T.R., Minch, K.J., Brabant, W., Winkler, J.K., Reiss, D.J., Baliga, N.S., et al. (2013). Global analysis of mRNA stability in *Mycobacterium tuberculosis*. *Nucleic Acids Res* 41(1)**,** 509-517. doi: 10.1093/nar/gks1019.

Sala, C., Forti, F., Magnoni, F., and Ghisotti, D. (2008). The katG mRNA of *Mycobacterium tuberculosis* and *Mycobacterium smegmatis* is processed at its 5' end and is stabilized by both a polypurine sequence and translation initiation. *BMC Mol Biol* 9**,** 33. doi: 10.1186/1471-2199-9-33.

Sandler, P., and Weisblum, B. (1989). Erythromycin-induced ribosome stall in the ermA leader: a barricade to 5'-to-3' nucleolytic cleavage of the ermA transcript. *J Bacteriol* 171(12)**,** 6680-6688.

Santiago-Frangos, A., and Woodson, S.A. (2018). Hfq chaperone brings speed dating to bacterial sRNA. *Wiley Interdiscip Rev RNA* 9(4)**,** e1475. doi: 10.1002/wrna.1475.

Schneider, E., Blundell, M., and Kennell, D. (1978). Translation and mRNA decay. *Mol Gen Genet* 160(2)**,** 121-129.

Schubert, O.T., Ludwig, C., Kogadeeva, M., Zimmermann, M., Rosenberger, G., Gengenbacher, M., et al. (2015). Absolute proteome composition and dynamics during dormancy and resuscitation of *Mycobacterium tuberculosis*. *Cell Host Microbe* 18(1)**,** 96-108. doi: 10.1016/j.chom.2015.06.001.

Schumacher, M.A., Pearson, R.F., Moller, T., Valentin-Hansen, P., and Brennan, R.G. (2002). Structures of the pleiotropic translational regulator Hfq and an Hfq-RNA complex: a bacterial Sm-like protein. *EMBO J* 21(13)**,** 3546-3556. doi: 10.1093/emboj/cdf322.

Schumann, U., Zhang, H.N., Sibbritt, T., Pan, A., Horvath, A., Gross, S., et al. (2020). Multiple links between 5-methylcytosine content of mRNA and translation. *BMC Biol* 18(1)**,** 40. doi: 10.1186/s12915-020-00769-5.

Schwartz, S., Mumbach, M.R., Jovanovic, M., Wang, T., Maciag, K., Bushkin, G.G., et al. (2014). Perturbation of m6A writers reveals two distinct classes of mRNA methylation at internal and 5' sites. *Cell Rep* 8(1)**,** 284-296. doi: 10.1016/j.celrep.2014.05.048.

Segev, E., Smith, Y., and Ben-Yehuda, S. (2012). RNA dynamics in aging bacterial spores. *Cell* 148(1-2)**,** 139-149. doi: 10.1016/j.cell.2011.11.059.

Selinger, D.W., Saxena, R.M., Cheung, K.J., Church, G.M., and Rosenow, C. (2003). Global RNA half-life analysis in *Escherichia coli* reveals positional patterns of transcript degradation. *Genome Res* 13(2)**,** 216-223. doi: 10.1101/gr.912603.

Seyfzadeh, M., Keener, J., and Nomura, M. (1993). spoT-dependent accumulation of guanosine tetraphosphate in response to fatty acid starvation in *Escherichia coli*. *Proc Natl Acad Sci U S A* 90(23)**,** 11004-11008. doi: 10.1073/pnas.90.23.11004.

Shahbabian, K., Jamalli, A., Zig, L., and Putzer, H. (2009). RNase Y, a novel endoribonuclease, initiates riboswitch turnover in *Bacillus subtilis*. *EMBO J* 28(22)**,** 3523-3533. doi: 10.1038/emboj.2009.283.

Shalem, O., Dahan, O., Levo, M., Martinez, M.R., Furman, I., Segal, E., et al. (2008). Transient transcriptional responses to stress are generated by opposing effects of mRNA production and degradation. *Mol Syst Biol* 4**,** 223. doi: 10.1038/msb.2008.59.

Sharp, J.S., and Bechhofer, D.H. (2005). Effect of 5'-proximal elements on decay of a model mRNA in *Bacillus subtilis*. *Mol Microbiol* 57(2)**,** 484-495. doi: 10.1111/j.1365-2958.2005.04683.x.

Sherman, D.R., Voskuil, M., Schnappinger, D., Liao, R., Harrell, M.I., and Schoolnik, G.K. (2001). Regulation of the *Mycobacterium tuberculosis* hypoxic response gene encoding alpha -crystallin. *Proc Natl Acad Sci U S A* 98(13)**,** 7534-7539. doi: 10.1073/pnas.121172498.

Shivakumar, A.G., Hahn, J., Grandi, G., Kozlov, Y., and Dubnau, D. (1980). Posttranscriptional regulation of an erythromycin resistance protein specified by plasmic pE194. *Proc Natl Acad Sci U S A* 77(7)**,** 3903-3907. doi: 10.1073/pnas.77.7.3903.

Siculella, L., Damiano, F., di Summa, R., Tredici, S.M., Alduina, R., Gnoni, G.V., et al. (2010). Guanosine 5'-diphosphate 3'-diphosphate (ppGpp) as a negative modulator of polynucleotide phosphorylase activity in a 'rare' actinomycete. *Mol Microbiol* 77(3)**,** 716-729. doi: 10.1111/j.1365-2958.2010.07240.x.

Sievers, S., Lund, A., Menendez-Gil, P., Nielsen, A., Storm Mollerup, M., Lambert Nielsen, S., et al. (2015). The multicopy sRNA LhrC controls expression of the oligopeptide-binding protein OppA in *Listeria monocytogenes*. *RNA Biol* 12(9)**,** 985-997. doi: 10.1080/15476286.2015.1071011.

Silva, A.J., Sultan, S.Z., Liang, W., and Benitez, J.A. (2008). Role of the histone-like nucleoid structuring protein in the regulation of rpoS and RpoS-dependent genes in *Vibrio cholerae*. *J Bacteriol* 190(22)**,** 7335-7345. doi: 10.1128/JB.00360-08.

Sim, M., Lim, B., Sim, S.H., Kim, D., Jung, E., Lee, Y., et al. (2014). Two tandem RNase III cleavage sites determine betT mRNA stability in response to osmotic stress in *Escherichia coli*. *PLoS One* 9(6)**,** e100520. doi: 10.1371/journal.pone.0100520.

Sinha, D., Matz, L.M., Cameron, T.A., and De Lay, N.R. (2018). Poly(A) polymerase is required for RyhB sRNA stability and function in *Escherichia coli*. *RNA* 24(11)**,** 1496-1511. doi: 10.1261/rna.067181.118.

Sittka, A., Lucchini, S., Papenfort, K., Sharma, C.M., Rolle, K., Binnewies, T.T., et al. (2008). Deep sequencing analysis of small noncoding RNA and mRNA targets of the global post-transcriptional regulator, Hfq. *PLoS Genet* 4(8)**,** e1000163. doi: 10.1371/journal.pgen.1000163.

Smeulders, M.J., Keer, J., Speight, R.A., and Williams, H.D. (1999). Adaptation of *Mycobacterium smegmatis* to stationary phase. *J Bacteriol* 181(1)**,** 270-283.

Sonnleitner, E., Schuster, M., Sorger-Domenigg, T., Greenberg, E.P., and Blasi, U. (2006). Hfq-dependent alterations of the transcriptome profile and effects on quorum sensing in *Pseudomonas aeruginosa*. *Mol Microbiol* 59(5)**,** 1542-1558. doi: 10.1111/j.1365-2958.2006.05032.x.

Sousa, S., Marchand, I., and Dreyfus, M. (2001). Autoregulation allows *Escherichia coli* RNase E to adjust continuously its synthesis to that of its substrates. *Mol Microbiol* 42(3), 867-878. doi: 10.1046/j.1365-2958.2001.02687.x.

Steglich, C., Lindell, D., Futschik, M., Rector, T., Steen, R., and Chisholm, S.W. (2010). Short RNA half-lives in the slow-growing marine cyanobacterium *Prochlorococcus*. *Genome Biol* 11(5)**,** R54. doi: 10.1186/gb-2010-11-5-r54.

Strahl, H., Turlan, C., Khalid, S., Bond, P.J., Kebalo, J.M., Peyron, P., et al. (2015). Membrane recognition and dynamics of the RNA degradosome. *PLoS Genet* 11(2)**,** e1004961. doi: 10.1371/journal.pgen.1004961.

Sun, X., Zhulin, I., and Wartell, R.M. (2002). Predicted structure and phyletic distribution of the RNA-binding protein Hfq. *Nucleic Acids Res* 30(17)**,** 3662-3671. doi: 10.1093/nar/gkf508.

Tao, F., Liu, Y., Luo, Q., Su, F., Xu, Y., Li, F., et al. (2011). Novel organic solvent-responsive expression vectors for biocatalysis: application for development of an organic solvent-tolerant biodesulfurizing strain. *Bioresour Technol* 102(20)**,** 9380-9387. doi: 10.1016/j.biortech.2011.08.015.

Tejada-Arranz, A., de Crecy-Lagard, V., and de Reuse, H. (2020). Bacterial RNA Degradosomes: molecular machines under tight control. *Trends Biochem Sci* 45(1)**,** 42-57. doi: 10.1016/j.tibs.2019.10.002.

Thorne, S.H., and Williams, H.D. (1997). Adaptation to nutrient starvation in *Rhizobium leguminosarum* bv. phaseoli: analysis of survival, stress resistance, and changes in macromolecular synthesis during entry to and exit from stationary phase. *J Bacteriol* 179(22)**,** 6894-6901.

Timmermans, J., and Van Melderen, L. (2010). Post-transcriptional global regulation by CsrA in bacteria. *Cell Mol Life Sci* 67(17)**,** 2897-2908. doi: 10.1007/s00018-010-0381-z.

Toledo-Arana, A., Dussurget, O., Nikitas, G., Sesto, N., Guet-Revillet, H., Balestrino, D., et al. (2009). The *Listeria* transcriptional landscape from saprophytism to virulence. *Nature* 459(7249)**,** 950-956. doi: 10.1038/nature08080.

Tortosa, P., Albano, M., and Dubnau, D. (2000). Characterization of ylbF, a new gene involved in competence development and sporulation in *Bacillus subtilis*. *Mol Microbiol* 35(5), 1110-1119. doi: 10.1046/j.1365-2958.2000.01779.x.

Udekwu, K.I., Darfeuille, F., Vogel, J., Reimegard, J., Holmqvist, E., and Wagner, E.G. (2005). Hfq-dependent regulation of OmpA synthesis is mediated by an antisense RNA. *Genes Dev* 19(19)**,** 2355-2366. doi: 10.1101/gad.354405.

Unciuleac, M.C., and Shuman, S. (2013). Distinctive effects of domain deletions on the manganese-dependent DNA polymerase and DNA phosphorylase activities of *Mycobacterium smegmatis* polynucleotide phosphorylase. *Biochemistry* 52(17)**,** 2967-2981. doi: 10.1021/bi400281w.

Unniraman, S., Chatterji, M., and Nagaraja, V. (2002). A hairpin near the 5' end stabilises the DNA gyrase mRNA in *Mycobacterium smegmatis*. *Nucleic Acids Res* 30(24)**,** 5376-5381. doi: 10.1093/nar/gkf697.

Updegrove, T.B., Zhang, A., and Storz, G. (2016). Hfq: the flexible RNA matchmaker. *Curr Opin Microbiol* 30**,** 133-138. doi: 10.1016/j.mib.2016.02.003.

Vanderpool, C.K., and Gottesman, S. (2004). Involvement of a novel transcriptional activator and small RNA in post-transcriptional regulation of the glucose phosphoenolpyruvate phosphotransferase system. *Mol Microbiol* 54(4)**,** 1076-1089. doi: 10.1111/j.1365-2958.2004.04348.x.

Vanzo, N.F., Li, Y.S., Py, B., Blum, E., Higgins, C.F., Raynal, L.C., et al. (1998). Ribonuclease E organizes the protein interactions in the *Escherichia coli* RNA degradosome. *Genes Dev* 12(17)**,** 2770-2781.

Vargas-Blanco, D.A., Zhou, Y., Zamalloa, L.G., Antonelli, T., and Shell, S.S. (2019). mRNA degradation rates are coupled to metabolic status in *Mycobacterium smegmatis*. *mBio* 10(4). doi: 10.1128/mBio.00957-19.

Varmus, H.E., Perlman, R.L., and Pastan, I. (1971). Regulation of lac transcription in antibiotic-treated *E. coli*. *Nat New Biol* 230(10)**,** 41-44. doi: 10.1038/newbio230041a0.

Vecerek, B., Rajkowitsch, L., Sonnleitner, E., Schroeder, R., and Blasi, U. (2008). The C-terminal domain of *Escherichia coli* Hfq is required for regulation. *Nucleic Acids Res* 36(1)**,** 133-143. doi: 10.1093/nar/gkm985.

Ventola, C.L. (2015a). The antibiotic resistance crisis: part 1: causes and threats. *P T* 40(4)**,** 277-283.

Ventola, C.L. (2015b). The antibiotic resistance crisis: part 2: management strategies and new agents. *P T* 40(5)**,** 344-352.

Vogel, J., and Luisi, B.F. (2011). Hfq and its constellation of RNA. *Nat Rev Microbiol* 9(8)**,** 578-589. doi: 10.1038/nrmicro2615.

Vvedenskaya, I.O., Bird, J.G., Zhang, Y., Zhang, Y., Jiao, X., Barvik, I., et al. (2018). CapZyme-seq comprehensively defines promoter-sequence determinants for rna 5' capping with NAD. *Mol Cell* 70(3)**,** 553-564 e559. doi: 10.1016/j.molcel.2018.03.014.

Vvedenskaya, I.O., Sharp, J.S., Goldman, S.R., Kanabar, P.N., Livny, J., Dove, S.L., et al. (2012). Growth phase-dependent control of transcription start site selection and gene expression by nanoRNAs. *Genes Dev* 26(13)**,** 1498-1507. doi: 10.1101/gad.192732.112.

Vytvytska, O., Moll, I., Kaberdin, V.R., von Gabain, A., and Blasi, U. (2000). Hfq (HF1) stimulates ompA mRNA decay by interfering with ribosome binding. *Genes Dev* 14(9)**,** 1109-1118.

Wagner, L.A., Gesteland, R.F., Dayhuff, T.J., and Weiss, R.B. (1994). An efficient Shine-Dalgarno sequence but not translation is necessary for lacZ mRNA stability in *Escherichia coli*. *J Bacteriol* 176(6)**,** 1683-1688. doi: 10.1128/jb.176.6.1683-1688.1994.

Wang, H., Ayala, J.C., Benitez, J.A., and Silva, A.J. (2012). Interaction of the histone-like nucleoid structuring protein and the general stress response regulator RpoS at *Vibrio cholerae* promoters that regulate motility and hemagglutinin/protease expression. *J Bacteriol* 194(5)**,** 1205-1215. doi: 10.1128/JB.05900-11.

Wang, X., Dubey, A.K., Suzuki, K., Baker, C.S., Babitzke, P., and Romeo, T. (2005). CsrA post-transcriptionally represses pgaABCD, responsible for synthesis of a biofilm polysaccharide adhesin of *Escherichia coli*. *Mol Microbiol* 56(6)**,** 1648-1663. doi: 10.1111/j.1365-2958.2005.04648.x.

Wang, Y., Li, Y., Toth, J.I., Petroski, M.D., Zhang, Z., and Zhao, J.C. (2014). N6-methyladenosine modification destabilizes developmental regulators in embryonic stem cells. *Nat Cell Biol* 16(2)**,** 191-198. doi: 10.1038/ncb2902.

Wassarman, K.M., Repoila, F., Rosenow, C., Storz, G., and Gottesman, S. (2001). Identification of novel small RNAs using comparative genomics and microarrays. *Genes Dev* 15(13)**,** 1637-1651. doi: 10.1101/gad.901001.

Wei, B.L., Brun-Zinkernagel, A.M., Simecka, J.W., Pruss, B.M., Babitzke, P., and Romeo, T. (2001). Positive regulation of motility and flhDC expression by the RNA-binding protein CsrA of *Escherichia coli*. *Mol Microbiol* 40(1)**,** 245-256. doi: 10.1046/j.1365-2958.2001.02380.x.

Wei, C.M., Gershowitz, A., and Moss, B. (1975). Methylated nucleotides block 5' terminus of HeLa cell messenger RNA. *Cell* 4(4)**,** 379-386. doi: 10.1016/0092-8674(75)90158-0.

Wolfe, A.D., and Hahn, F.E. (1965). Mode of action of chloramphenicol. Ix. Effects of chloramphenicol upon a ribosomal amino acid polymerization system and its binding to bacterial ribosome. *Biochim Biophys Acta* 95**,** 146-155.

Wood, D.N., Chaussee, M.A., Chaussee, M.S., and Buttaro, B.A. (2005). Persistence of *Streptococcus pyogenes* in stationary-phase cultures. *J Bacteriol* 187(10)**,** 3319-3328. doi: 10.1128/JB.187.10.3319-3328.2005.

World Health Organization [WHO] (2019). No Time to Wait: Securing the Future from Drug-Resistant Infections. Available online at: https://www.who.int/antimicrobial-resistance/interagency-coordination-group/final-report/en/ (accessed April 17, 2020).

Xu, C., Huang, R., Teng, L., Jing, X., Hu, J., Cui, G., et al. (2015). Cellulosome stoichiometry in *Clostridium cellulolyticum* is regulated by selective RNA processing and stabilization. *Nat Commun* 6**,** 6900. doi: 10.1038/ncomms7900.

Xu, W., Huang, J., and Cohen, S.N. (2008). Autoregulation of AbsB (RNase III) expression in *Streptomyces coelicolor* by endoribonucleolytic cleavage of absB operon transcripts. *J Bacteriol* 190(15)**,** 5526-5530. doi: 10.1128/JB.00558-08.

Yang, Y., Wang, L., Han, X., Yang, W.L., Zhang, M., Ma, H.L., et al. (2019). RNA 5-methylcytosine facilitates the maternal-to-zygotic transition by preventing maternal mRNA Decay. *Mol Cell* 75(6)**,** 1188-1202 e1111. doi: 10.1016/j.molcel.2019.06.033.

Yarmolinsky, M.B., and Haba, G.L. (1959). Inhibition by Puromycin of Amino Acid Incorporation into Protein. *Proc Natl Acad Sci U S A* 45(12)**,** 1721-1729. doi: 10.1073/pnas.45.12.1721.

Yu, X., Li, B., Jang, G.J., Jiang, S., Jiang, D., Jang, J.C., et al. (2019). Orchestration of Processing body dynamics and mrna decay in *Arabidopsis* immunity. *Cell Rep* 28(8)**,** 2194-2205 e2196. doi: 10.1016/j.celrep.2019.07.054.

Yue, Y., Liu, J., Cui, X., Cao, J., Luo, G., Zhang, Z., et al. (2018). VIRMA mediates preferential m(6)A mRNA methylation in 3'UTR and near stop codon and associates with alternative polyadenylation. *Cell Discov* 4**,** 10. doi: 10.1038/s41421-018-0019-0.

Zeller, M.E., Csanadi, A., Miczak, A., Rose, T., Bizebard, T., and Kaberdin, V.R. (2007). Quaternary structure and biochemical properties of mycobacterial RNase E/G. *Biochem J* 403(1)**,** 207-215. doi: 10.1042/BJ20061530.

Zgurskaya, H.I., Keyhan, M., and Matin, A. (1997). The sigma S level in starving Escherichia coli cells increases solely as a result of its increased stability, despite decreased synthesis. *Mol Microbiol* 24(3)**,** 643-651. doi: 10.1046/j.1365-2958.1997.3961742.x.

Zhang, A., Wassarman, K.M., Rosenow, C., Tjaden, B.C., Storz, G., and Gottesman, S. (2003). Global analysis of small RNA and mRNA targets of Hfq. *Mol Microbiol* 50(4)**,** 1111-1124. doi: 10.1046/j.1365-2958.2003.03734.x.

Zhang, D., Liu, Y., Wang, Q., Guan, Z., Wang, J., Liu, J., et al. (2016). Structural basis of prokaryotic NAD-RNA decapping by NudC. *Cell Res* 26(9)**,** 1062-1066. doi: 10.1038/cr.2016.98.

Zhang, H., Li, D., Zhao, L., Fleming, J., Lin, N., Wang, T., et al. (2013). Genome sequencing of 161 *Mycobacterium tuberculosis* isolates from China identifies genes and intergenic regions associated with drug resistance. *Nat Genet* 45(10)**,** 1255-1260. doi: 10.1038/ng.2735.

Zhao, B.S., Wang, X., Beadell, A.V., Lu, Z., Shi, H., Kuuspalu, A., et al. (2017). m(6)A-dependent maternal mRNA clearance facilitates zebrafish maternal-to-zygotic transition. *Nature* 542(7642)**,** 475-478. doi: 10.1038/nature21355.

Zhao, J.P., Zhu, H., Guo, X.P., and Sun, Y.C. (2018). AU-rich long 3' untranslated region regulates gene expression in bacteria. *Front Microbiol* 9**,** 3080. doi: 10.3389/fmicb.2018.03080.

Tables

Table 1-1. Transcriptome-wide studies on mRNA half-life in bacteria.

Organism	Growth/stress condition	Response to stress/condition (transcriptome stability)	mRNA quantification method	Correlation between mRNA abundance and half-life	Source
Bacillus cereus ATCC 10987, ATCC 14579	Exponential phase	-	RNA-seq	Positive	(Kristoffersen et al., 2012)
Bacillus subtilis	Early stationary phase	Stable*	Microarray	Not calculated	(Hambraeus et al., 2003)
Chlamydia trachomatis biovars: trachoma, lymphogranuloma venereum	Mid-phase stage of developmental cycle	-	RNA-seq	None	(Ferreira et al., 2017)
Escherichia coli	Exponential phase	-	Microarray	Negative	(Bernstein et al., 2002)
Escherichia coli	Exponential phase	-	Microarray	Not calculated	(Selinger et al., 2003)
Escherichia coli	0.1 h^{-1} growth rate	Stabilization at slower growth rates	Microarray	Negative	(Esquerre et al., 2014; Esquerre et al., 2015)
	0.2 h^{-1} growth rate				
	0.4 h^{-1} growth rate				
	0.63 h^{-1} growth rate				
Escherichia coli	Exponential phase	Stabilization in stationary phase	RNA-seq	Positive	(Chen et al., 2015)
	Stationary phase				
Escherichia coli	Exponential phase	Destabilization in Δ*csrA51*	Microarray	Negative	(Esquerre et al., 2016)
	Exponential phase (Δ*csrD*)				
	Exponential phase (Δ*csrA51*)				
Escherichia coli	Exponential phase	Stabilization in Ksm	RNA-seq	None for either condition†	(Moffitt et al., 2016)
	Exponential phase + Ksm (initiation inhibitor)				
Escherichia coli, Lactococcus lactis	Multiple‡	Stabilization at low growth rates and stress	Microarray, Nylon membrane-based macroarray	Negative	(Nouaille et al., 2017)
Escherichia coli	Exponential phase	Stabilization in *rneΔMTS*	Microarray	Not calculated	(Hadjeras et al, 2019)
	Exponential phase (*rneΔMTS*)				
Escherichia coli	Exponential phase	Stabilization in stress	Microarray	Negative†	(Morin et al, 2020)
	Glucose exhaustion				
	Acetate consumption				
	Carbon starvation				

Lactococcus lactis	Exponential phase	Stabilization at slower growth rates	Nylon membrane-based macroarray	Negative	(Redon et al., 2005a; Redon et al., 2005b)
	Deceleration phase			None	
	Starvation phase			Positive	
Lactococcus lactis	Isoleucine limitation, 0.11 h^{-1} growth rate	Stabilization at slower growth rates	Nylon membrane-based macroarrays	Negative	(Dressaire et al., 2013)
	Isoleucine limitation, 0.51 h^{-1} growth rate				
	Isoleucine limitation, 0.8 h^{-1} growth rate				
Stenotrophomonas maltophilia	Exponential phase	Stabilization	RNA-seq	None	(Bernardini and Martinez, 2017)
	Exponential phase (*rng*-defective mutant)				
Mycobacterium tuberculosis	Exponential phase	Stabilization in stress	Microarray	Negative	(Rustad et al., 2013)
	Hypoxic stress			Not calculated	
	Cold-induced stress			Not calculated	
Prochlorococcus MED4	0.325 day^{-1} growth rate	-	Microarray	Not calculated	(Steglich et al., 2010)
Staphylococcus aureus	Exponential phase	Stabilization in stress	Microarray	Not calculated	(Anderson et al., 2006)
	Cold-induced stress				
	Heat-induced stress				
	Mupirocin (isoleucyl-tRNA synthetase inhibitor, induces stringent response)				
	DNA damage (SOS response)	Destabilization in stress			

*Not compared to an exponential phase culture within the same study. Stabilization report based on previously reported studies.

†Our analysis of the source data.

‡ Includes data for *L. lactis* at growth rates of 0.09, 0.24, 0.35 and 0.47 h^{-1} (Dressaire et al., 2013); and unpublished and previously published data for *E. coli* at growth rates of 0.04, 0.11, 0.38, 0.51 and 0.80 h^{-1} and stationary phase (Esquerre et al., 2014).

Chapter 2 : The impact of leadered and leaderless gene structures on translation efficiency, transcript stability, and predicted transcription rates in *Mycobacterium smegmatis*

The impact of leadered and leaderless gene structures on translation efficiency, transcript stability, and predicted transcription rates in *Mycobacterium smegmatis*

Tien G. Nguyen[1], Diego A. Vargas-Blanco[1], Louis A. Roberts[1], Scarlet S. Shell[1,2]

[1]Department of Biology and Biotechnology, Worcester Polytechnic Institute, Worcester, MA, USA
[2]Program in Bioinformatics and Computational Biology, Worcester Polytechnic Institute, Worcester, MA, USA
Edited by: Tina M. Henkin. Ohio State University, Ohio

This chapter corresponds to a manuscript that was published as:

Nguyen, T.G., Vargas-Blanco, D.A., Roberts, L.A., and Shell, S.S. (2020). The impact of leadered and leaderless gene structures on translation efficiency, transcript stability, and predicted transcription rates in *Mycobacterium smegmatis*. *J Bacteriol*. doi: 10.1128/JB.00746-19.

Author Contributions

Conceptualization: T.G.N., L.A.R., and S.S.S. Methodology: D.A.V.-B. and T.G.N. Data Analysis: D.A.V.-B., T.G.N., and S.S.S. Writing – Original Draft: D.A.V.-B., S.S.S, and T.G.N. Writing – Review and Editing: D.A.V.-B., L.A.R., and S.S.S.

Abstract

Regulation of gene expression is critical for *Mycobacterium tuberculosis* to tolerate stressors encountered during infection and for nonpathogenic mycobacteria such as *Mycobacterium smegmatis* to survive environmental stressors. Unlike better-studied models, mycobacteria express ~14% of their genes as leaderless transcripts. However, the impacts of leaderless transcript structures on mRNA half-life and translation efficiency in mycobacteria have not been directly tested. For leadered transcripts, the contributions of 5′ untranslated regions (UTRs) to mRNA half-life and translation efficiency are similarly unknown. In *M. tuberculosis* and *M. smegmatis*, the essential sigma factor, SigA, is encoded by a transcript with a relatively short half-life. We hypothesized that the long 5′ UTR of *sigA* causes this instability. To test

this, we constructed fluorescence reporters and measured protein abundance, mRNA abundance, and mRNA half-life and calculated relative transcript production rates. The *sigA* 5′ UTR conferred an increased transcript production rate, shorter mRNA half-life, and decreased apparent translation rate compared to a synthetic 5′ UTR commonly used in mycobacterial expression plasmids. Leaderless transcripts appeared to be translated with similar efficiency as those with the *sigA* 5′ UTR but had lower predicted transcript production rates. A global comparison of *M. tuberculosis* mRNA and protein abundances failed to reveal systematic differences in protein/mRNA ratios for leadered and leaderless transcripts, suggesting that variability in translation efficiency is largely driven by factors other than leader status. Our data are also discussed in light of an alternative model that leads to different conclusions and suggests leaderless transcripts may indeed be translated less efficiently.

IMPORTANCE. Tuberculosis, caused by *Mycobacterium tuberculosis*, is a major public health problem killing 1.5 million people globally each year. During infection, *M. tuberculosis* must alter its gene expression patterns to adapt to the stress conditions it encounters. Understanding how *M. tuberculosis* regulates gene expression may provide clues for ways to interfere with the bacterium's survival. Gene expression encompasses transcription, mRNA degradation, and translation. Here, we used *Mycobacterium smegmatis* as a model organism to study how 5′ untranslated regions affect these three facets of gene expression in multiple ways. We furthermore provide insight into the expression of leaderless mRNAs, which lack 5′ untranslated regions and are unusually prevalent in mycobacteria.

Introduction

The pathogen *Mycobacterium tuberculosis* has evolved numerous strategies to survive in different niches within the human host. Bacterial adaptation to these harsh environments is usually achieved by gene regulation, both transcriptionally and posttranscriptionally. While promoters play critical roles in gene

regulation, other gene features and mechanisms have additional important regulatory roles. One such important gene feature is the 5′ untranslated region (5′ UTR), which contains the Shine-Dalgarno (SD) sequence within the ribosome binding site (RBS) and, therefore, can serve as a translation regulator (Shine and Dalgarno, 1974; Ringquist et al., 1992; Habib and Jackson, 1993; Chen et al., 1994; Sterk et al., 2018). For example, 5′ UTR interactions with *cis* and *trans* elements, such as complementary sequences within the UTR or coding sequence, small RNAs (sRNAs), and RNA-binding proteins, can modulate protein synthesis by blocking or improving accessibility to the RBS (Lease and Belfort, 2000; Mutalik et al., 2012; Takahashi and Lucks, 2013; Jagodnik et al., 2017). Importantly, it has been shown in *Escherichia coli* and other bacteria that transcription and translation are physically coupled, and thus 5′ UTR-mediated modulation of translation could have repercussions on transcription rate as well (Miller et al., 1970; Burmann et al., 2010; Proshkin et al., 2010; Zhang et al., 2014; Fan et al., 2017). Translation blocks in *Mycobacterium smegmatis* have been shown to decrease transcription as well (Vargas-Blanco et al., 2019), suggesting that transcription-translation coupling occurs in mycobacteria, although the extent and consequences are unknown.

The 5′ UTRs can also regulate gene expression by altering mRNA turnover rates. This can be a consequence of altered translation rates, as impairments to translation often lead to faster mRNA decay (Pato et al., 1973; Wagner et al., 1994; Arnold et al., 1998; Braun et al., 1998; Jurgen et al., 1998; Hambraeus et al., 2002; Sharp and Bechhofer, 2003). In other cases, mRNA stability is directly affected by sRNA binding to 5′ UTRs or by UTR secondary structure (Unniraman et al., 2001; Moll et al., 2003; Skorski et al., 2006; Anderson and Dunman, 2009; Link et al., 2009; Pedersen et al., 2011; Jagodnik et al., 2017). In *E. coli*, the half-life of the short-lived transcript *bla* can be significantly increased when its native 5′ UTR is replaced with the 5′ UTR of *ompA*, a long-lived transcript (Belasco et al., 1986; Emory and Belasco, 1990; Chen et al., 1991). Conversely, deletion of *ompA*'s native 5′ UTR decreased its half-life by 5-fold (Emory and

Belasco, 1990). The longevity conferred by the *ompA* 5′ UTR was attributed to the presence of a nonspecific stem-loop as well as the specific RBS sequence (Emory and Belasco, 1990; Chen et al., 1991; Emory et al., 1992). Secondary structure formation in 5′ UTRs has been shown to play a major role in transcript stability in other bacteria as well, such as for *ermC* in *Bacillus subtilis* (Bechhofer and Dubnau, 1987; Hambraeus et al., 2000) and *pufBA* in *Rhodobacter capsulatus* (Chen and Belasco, 1990; Heck et al., 1996; Heck et al., 1999). Moreover, obstacles that hinder the linear 5′ scanning function of RNase E (a major RNase in *E. coli* and mycobacteria) can prevent access to downstream cleavage sites, increasing transcript half-life (Richards and Belasco, 2019). Such obstacles include the 30S ribosomal subunit bound to an SD-like site far upstream of the translation start site in one case (Agaisse and Lereclus, 1996). UTRs can also contain binding sites for the global regulator CsrA, which can both promote and prevent mRNA decay in *E. coli* (Romeo and Babitzke, 2018). Although effects of 5′ UTRs on mRNA stability, translation, and transcription rate have been widely studied in more common bacterial systems, there is a paucity of information of the regulatory effects of 5′ UTRs in mycobacteria.

Compared to *E. coli* and most other well-studied bacteria, mycobacteria possess a large number of leaderless transcripts; approximately 14% of annotated genes are leaderless in both *M. smegmatis* and *M. tuberculosis* (Cortes et al., 2013; Shell et al., 2015; Martini et al., 2019). Studies in *E. coli* have shown that translation of leadered and leaderless transcripts is functionally distinct (Tedin et al., 1999; Grill et al., 2000; Grill et al., 2002; Moll et al., 2002; O'Donnell and Janssen, 2002; Moll et al., 2004; Udagawa et al., 2004), suggesting fundamental differences in their mechanisms of regulation. In contrast to *E. coli*, where leaderless transcripts are generally translated less efficiently (Baumeister et al., 1991; Van Etten and Janssen, 1998; O'Donnell and Janssen, 2001; Shell et al., 2015; Beck et al., 2016), leaderless transcripts in mycobacteria appear to be translated robustly (Cortes et al., 2013; Shell et al., 2015). However, direct

comparisons of translation rates for leadered versus leaderless transcripts in mycobacteria have yet to be reported.

Among leadered transcripts, 5′ UTR lengths vary. We hypothesized that longer 5′ UTRs were more likely to play regulatory roles through modulation of translation, transcription rate, and mRNA turnover. One such long-leadered transcript in both *M. tuberculosis* and *M. smegmatis* encodes sigma factor alpha (*sigA*), the primary sigma factor in mycobacteria (Gomez et al., 1998; Manganelli et al., 2004). Here, we used the mycobacterial model *M. smegmatis* and a series of yellow fluorescent protein (YFP) reporters to investigate the effects of the *sigA* 5′ UTR as well as leaderless gene structures on transcription, translation, and mRNA half-life. We found that the *sigA* 5′ UTR caused lower translation efficiency, reduced mRNA half-life, and a higher predicted transcript production rate compared to those of a control 5′ UTR. Leaderless transcripts were translated at similar rates as those of transcripts bearing the *sigA* 5′ UTR and had similar half-lives but appeared to be transcribed less efficiently, leading to lower steady-state mRNA and protein abundances. Our results highlight the potential of 5′ UTRs to affect transcription efficiency as well as translation and mRNA half-life and support the idea that leaderless translation can be either more or less efficient than leadered translation in mycobacteria, depending on the characteristics of the leader. Alternative interpretations of our data are possible and would lead to different conclusions, particularly with respect to the efficiency of leaderless translation. These will be discussed.

Results

Validation of the *sigA* 5′ UTR boundaries.

Transcription start site mapping has defined the 5′ ends of 5′ UTRs on a transcriptome-wide basis in both *M. smegmatis* and *M. tuberculosis* (Shell et al., 2015; Martini et al., 2019). Using annotated translation start sites to define the 3′ ends of the 5′ UTRs, the median 5′ UTR lengths in *M.*

smegmatis and *M. tuberculosis* are 48 and 56 nucleotides (nt), respectively, after excluding leaderless genes (Figure 2-1A; see also Table S1 in the supplemental material) (Shell et al., 2015; Martini et al., 2019). The 5′ UTR length distributions are skewed, with a mode of approximately 40 nt (Figure 2-1A). We hypothesized that longer-than-average 5′ UTRs are more likely to have regulatory roles and sought to investigate the role of the 5′ UTR of the *M. smegmatis sigA* gene. The *M. tuberculosis sigA* 5′ UTR (128 nt) is also predicted to be longer than the median. To ensure that the predicted 5′ UTR boundaries of *M. smegmatis sigA* were correct, we experimentally validated the predicted start codon at genome coordinate 2827625 in GenBank accession number NC_008596, which resulted in a 123-nt UTR. A second GTG codon 39 nt downstream at 2827586 also had an appropriately positioned Shine-Dalgarno-like sequence and could conceivably be used as a start codon. We therefore made reporter constructs in which the strong constitutive promoter p_{myc1}*tetO* (Ehrt et al., 2005) drove expression of a transcript containing the *sigA* 5′ UTR and the sequence encoding YFP, with a C-terminal 6×His tag and an N-terminal fusion of the sequence encoded by the first 54 nt of the annotated *sigA* coding sequence. We then individually mutated each of the two putative GTG start codons to GTC (Figure 2-1B). Mutations of the first GTG to GTC reduced fluorescence to levels indistinguishable from autofluorescence in a strain that lacked the *yfp* gene (Figure 2-1C and D, no plasmid). In contrast, mutation of the second GTG to GTC reduced fluorescence to an intermediate level (Figure 2-1C and D). We therefore concluded that the first GTG is likely to be the predominant site of translation initiation, while the second GTG may affect expression levels but is not by itself sufficient to produce above-background expression. For subsequent experiments, we considered the first GTG to be the most likely start of the coding sequence and thereby define the *sigA* 5′ UTR as 123 nt in length.

Assumptions made in subsequent data analysis.

In subsequent sections, we will report data on mRNA abundance, mRNA half-life, and protein abundance for a series of reporter constructs. We will also report predicted transcription rates and apparent translation efficiencies, which are calculated from the abundance and half-life data. These calculated values rest upon a key assumption that most of the mRNA synthesized in the cell contributes to the measured abundance and half-life values. If this is not true, the data could be interpreted differently and different conclusions reached (Nogueira et al., 2001). These alternate interpretations are offered in Discussion.

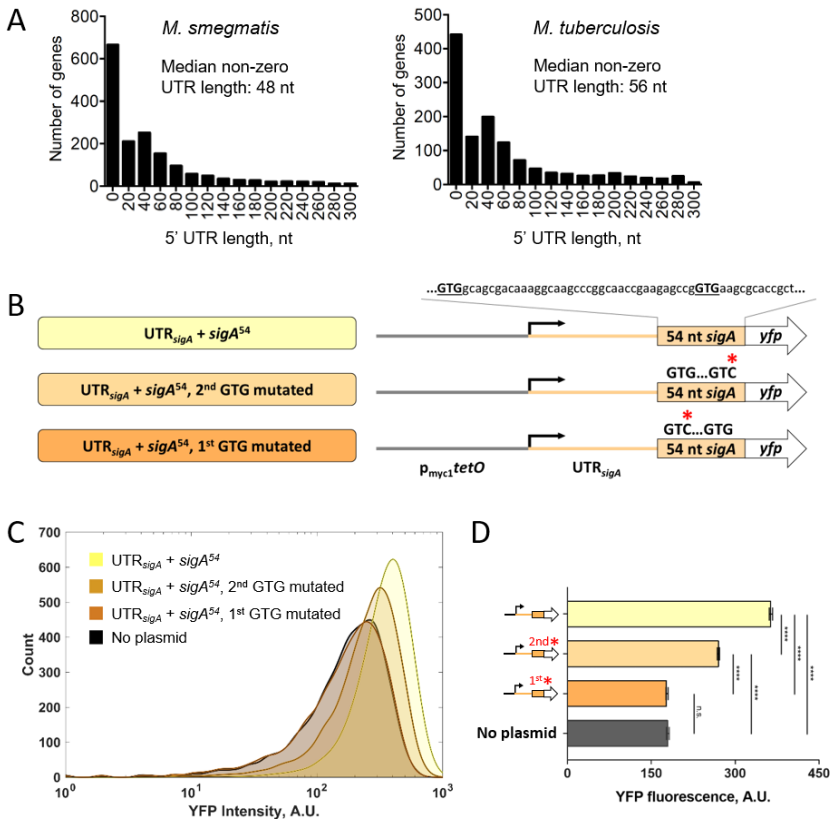

Figure 2-1. The *M. smegmatis sigA* gene has a longer-than-typical 5′ UTR. (A) Distributions of 5′ UTR lengths for *M. smegmatis* and *M. tuberculosis* genes reported to be transcribed from a single TSS (41, 42). (B) Constructs to confirm the predicted *sigA* translation start site. p$_{myc1}$*tetO* was described in reference 57. UTR$_{sigA}$ denotes the 123-nt sequence between the experimentally determined TSS (41) and the annotated translation start site. (C) Flow cytometry with YFP-expressing constructs diagrammed in panel B. (D) Median fluorescence intensities determined by flow cytometry. Error bars denote 95% confidence interval (CI). Fluorescence intensities were compared by Kruskal-Wallis test followed by Dunn's multiple-comparison test. ****, $P<0.0001$; ns, $P>0.05$.

The initial portion of the sigA coding sequence affects mRNA half-life and predicted transcript production rate.

To capture 5′ UTR-dependent effects on transcription, mRNA stability, and translation, we sought to investigate the role of the *sigA* 5′ UTR (UTR_{sigA}) in the context of a *yfp* transcript. UTR-mediated regulation of translation sometimes involves base pairing of 5′ UTR sequences with elements in the early portion of the coding sequence. Thus, we decided to include in our investigation the first 54 nt from the coding region of *sigA* (*sigA*^{54}). To determine if *sigA*^{54} alone affected expression, we compared fluorescence from our YFP reporters with or without the *sigA*^{54} N-terminal extension, independent from UTR_{sigA}. Transcription was driven by the p_{myc1}*tetO* promoter for these and all constructs used in this study. While this semisynthetic promoter contains TetR binding sites, the strains used in this study did not encode the corresponding Tet repressor, and the promoter was therefore constitutively active. Where indicated, constructs included the p_{myc1}*tetO*-associated 5′ UTR ($UTR_{pmyc1tetO}$) as initially described in reference (Ehrt et al., 2005). To ensure that expression initiated only from the annotated promoter and not from spurious promoter-like sequences in $UTR_{pmyc1tetO}$ or *sigA*^{54}, we built a control strain in which nt −53 through −1 of the promoter were deleted (Δp_{myc1}*tetO*) (Figure 2-2A).

We first tested the impact of *sigA*^{54} on YFP fluorescence intensity using $UTR_{pmyc1tetO}$. Interestingly, the *sigA*^{54} strain was ~9-fold less fluorescent than the strain in which YFP lacked this N-terminal extension (Figure 2-2B). To confirm that the reduced YFP fluorescence in the presence of *sigA*^{54} indeed reflected reduced protein levels rather than altered YFP structure or intrinsic fluorescence, we measured protein levels directly by Western blotting. The Western blotting data were consistent with the flow cytometry result, showing an approximately 16-fold reduction of YFP levels with the inclusion of *sigA*^{54} compared to the no-*sigA*^{54} strain (Figure 2-2C; see also Figure S2-1).

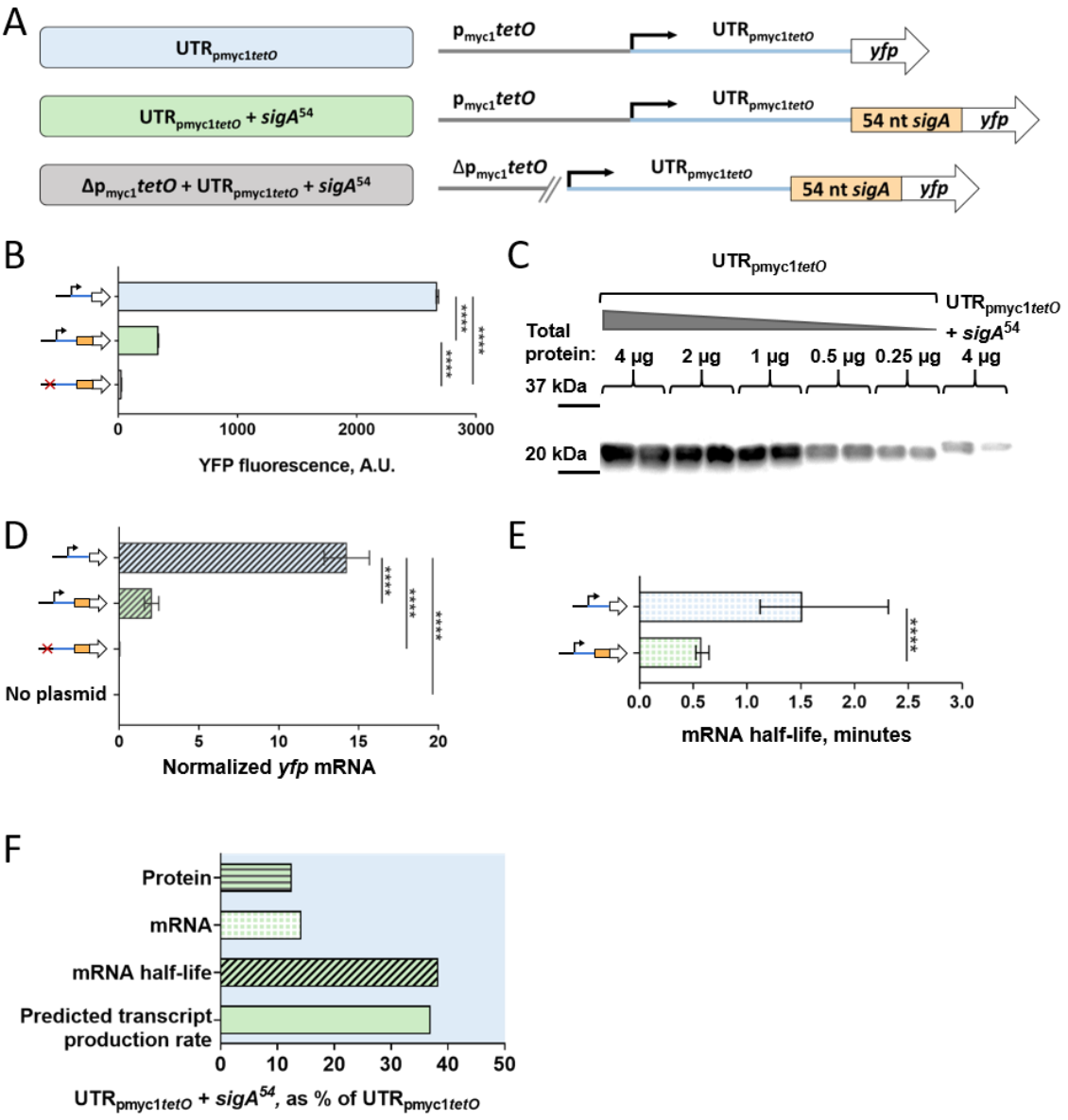

Figure 2-2. The first 54 nt of the *sigA* coding sequence affects transcript production rate and mRNA half-life.
(A) Constructs transformed into *M. smegmatis* to determine the impact of the first 54 nt of the *sigA* coding sequence (*sigA*^{54}) on expression of a YFP reporter. (B) Median YFP fluorescence of strains bearing the constructs in panel A, determined by flow cytometry. Error bars denote 95% CI. Strains were compared by Kruskal-Wallis test followed by Dunn's multiple-comparison test. (C) Lysates from strains bearing constructs with and without *sigA*^{54} were subject to Western blotting to detect the C-terminal 6×His tag on the YFP. The mass of total protein loaded per lane is stated. (D) *yfp* mRNA abundance for strains bearing the indicated constructs, determined by qPCR and normalized to expression of endogenous *sigA*. Error bars denote standard deviation. Strains were compared by analysis of variance (ANOVA) with Tukey's honestly significant difference (HSD) test. (E) The half-lives of *yfp* mRNA produced from the indicated constructs were measured. Error bars denote 95% CI. Half-lives were compared using linear regression analysis (n=3). (F) Protein abundance, mRNA abundance, mRNA half-life, and calculated transcript production rate for the construct containing *sigA*^{54} are shown as a percentage of the values produced by a construct that lacks *sigA*^{54} but is otherwise identical. ****, P<0.0001.

To assess if the presence of *sigA*^{54} affected *yfp* transcript levels, we conducted quantitative PCR (qPCR) for the same set of strains. Indeed, *sigA*^{54} *yfp* levels were approximately 6-fold lower than those of the *yfp* strain (Figure 2-2D). This suggested that the decrease in YFP protein levels could be due to a reduction in *yfp* mRNA levels. Alternatively, the *sigA*^{54} *yfp* transcript could be translated less efficiently, leading to reduced mRNA stability and thus lower steady-state abundance.

We then wondered if *sigA*^{54} affected transcript abundance by increasing the rate of transcript decay or by decreasing the rate of transcription. Thus, we determined mRNA half-life for *yfp* with and without *sigA*^{54}. As shown in Figure 2-2E, we estimated the half-life of *yfp* alone to be ∼1.5 min and the half-life of *yfp* plus *sigA*^{54} to be ∼0.6 min. We concluded that the first 54 nt of *sigA* made the *yfp* transcript more susceptible to degradation. Knowing the abundance and decay rate of a transcript, the rate of transcription can be predicted mathematically (Esquerré et al., 2014). This predicted transcription rate encompasses initiation, elongation, and termination, and changes in the apparent transcription rate could therefore theoretically result from changes in any of those three facets. We will henceforth refer to this calculated rate as the predicted transcript production rate. The insertion of *sigA*^{54} as an N-terminal extension for YFP appeared to reduce the *yfp* transcript production rate by approximately 60% (Figure 2-2F).

The sigA 5′ UTR affects transcript half-life, translation, and predicted transcript production rate.

In order to assess the effects of UTR$_{sigA}$ on transcription, mRNA stability, and translation, we replaced UTR$_{pmyc1tetO}$ with UTR$_{sigA}$ in our *sigA*^{54} *yfp* reporters as shown in Figure 2-3A. The presence of UTR$_{sigA}$ led to an approximately 2-fold reduction in YFP fluorescence intensity when compared to the UTR$_{pmyc1tetO}$ reporter strain (Figure 2-3B). We wondered if the reduction in fluorescence attributed to UTR$_{sigA}$ was associated with reduced *yfp* transcript abundance. However, qPCR revealed equivalent

transcript levels for strains with UTR_{sigA} and $UTR_{pmyc1tetO}$ (Figure 2-3C), indicating that the reduced protein levels were more likely a consequence of reduced translation efficiency. Interestingly, *yfp* mRNA half-life was reduced to 0.28 min by the presence of UTRsigA (Figure 2-3D), suggesting that a higher transcript production rate is required to maintain the steady-state mRNA abundance that we observed (Figure 2-3E). Taken together, our findings suggest that UTR_{sigA} may affect transcription, transcript decay, and translation. In Figure 2-3E, we summarize these results as percentages of *yfp* transcript production rate, mRNA abundance, mRNA half-life, and YFP protein levels relative to the $UTR_{pmyc1tetO}$ $sigA^{54}$ strain.

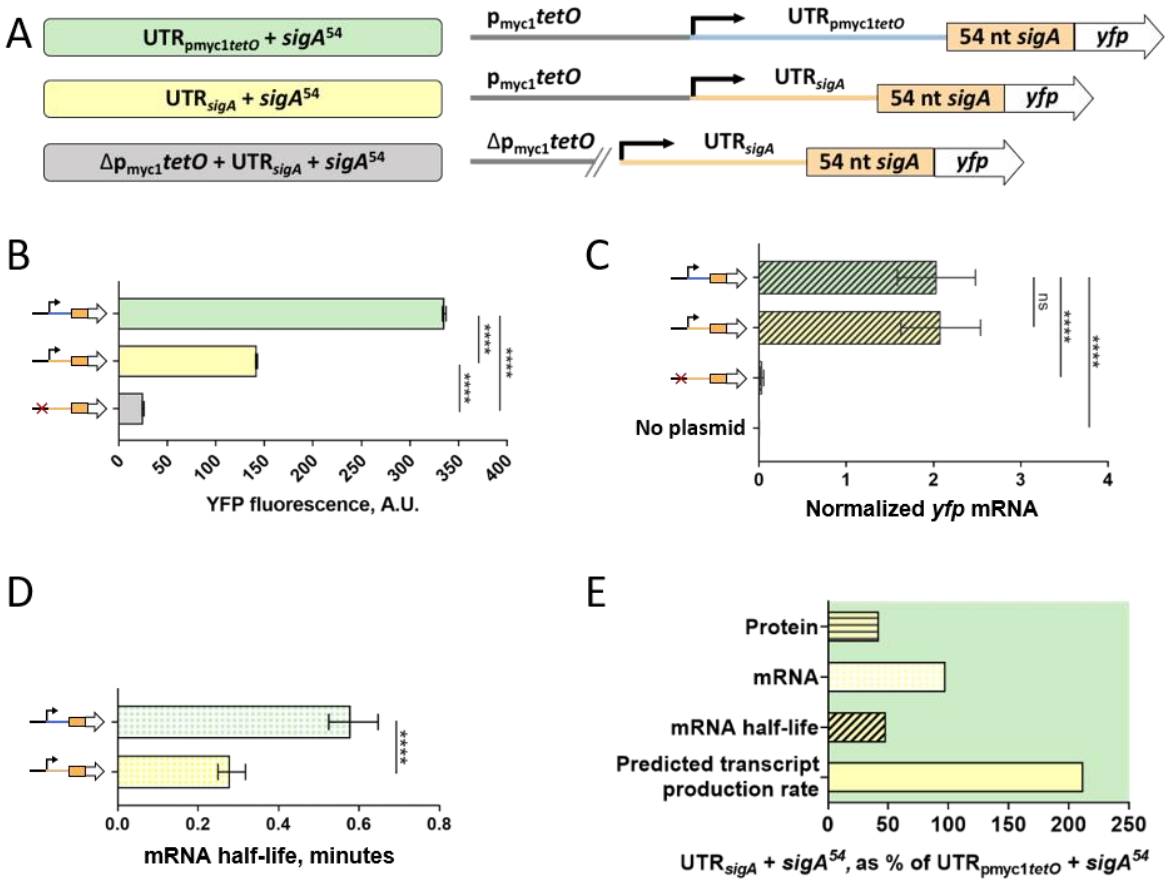

Figure 2-3. The *sigA* 5′ UTR affects translation efficiency, mRNA half-life, and transcript production rate. (A) Constructs transformed into *M. smegmatis* to determine the impact of the *sigA* 5′ UTR on expression of a YFP reporter. (B) Median YFP fluorescence of strains bearing the constructs in panel A, determined by flow cytometry. Error bars denote 95% CI. Strains were compared by Kruskal-Wallis test followed by Dunn's multiple-comparison test. (C) *yfp* mRNA abundance for strains bearing the indicated constructs, determined by qPCR and normalized to expression of endogenous *sigA*. Error bars denote standard deviation. Strains were compared by ANOVA with Tukey's HSD.

(continued on next page)

We analyzed the sequences and predicted secondary structures of UTR*sigA* and UTR$_{pmyc1}$*tetO* to investigate possible causes of the apparent difference in translation efficiency. The ribosome binding sites (RBSs) of these two UTRs have similar degrees of identity to a theoretically perfect mycobacterial SD sequence (the reverse complement of the 3' end of the 16S rRNA) (see Figure S2-2A). We noted that the spacing between the SD and start codon differed between the two UTRs (see Figure S2A). However, both spacings are common among native *M. smegmatis* transcripts harboring these SD sequences (Figure S2B), suggesting that neither spacing is particularly extreme. Secondary structure predictions by Sfold (Ding et al., 2004; 2005) suggested that the UTR$_{pmyc1}$*tetO* SD is likely to be in a single-stranded loop while the UTR*sigA* SD is likely to be partially base-paired (Figure S2-2C and D), suggesting that there may be differences in SD accessibility for ribosome binding. Either the differences in SD start codon spacing or the differences in predicted secondary structure could potentially be responsible for the observed differences in apparent translation efficiency.

Leaderless mRNAs may be transcribed less efficiently.

Leaderless transcripts are common in mycobacteria and were found to be associated with reduced protein abundance compared to that of leadered transcripts with near-consensus Shine-Dalgarno sites (Cortes et al., 2013), suggesting that leaderless translation may be generally less efficient as was shown in *E. coli* (Van Etten and Janssen, 1998; O'Donnell and Janssen, 2001; Beck et al., 2016). However, this hypothesis was not experimentally tested in mycobacteria. We therefore built two leaderless *yfp* reporters under the control of the p$_{myc1}$*tetO* promoter, with and without the *sigA*^{54} N-terminal extension (Figure 2-4A).

Figure 2-3. Legend (Continued)

(D) The half-lives of *yfp* mRNA produced from the indicated constructs were measured. Error bars denote 95% CI. Half-lives were compared using linear regression analysis ($n=3$). (E) Protein abundance, mRNA abundance, mRNA half-life, and calculated transcript production rate for the construct containing the *sigA* 5′ UTR are shown as a percentage of the values produced by a construct that contains the p$_{myc1}$*tetO*-associated 5′ UTR. Note that some data shown in Figure 2-2 are reproduced here to facilitate comparisons. ****, $P<0.0001$; ns, $P > 0.05$.

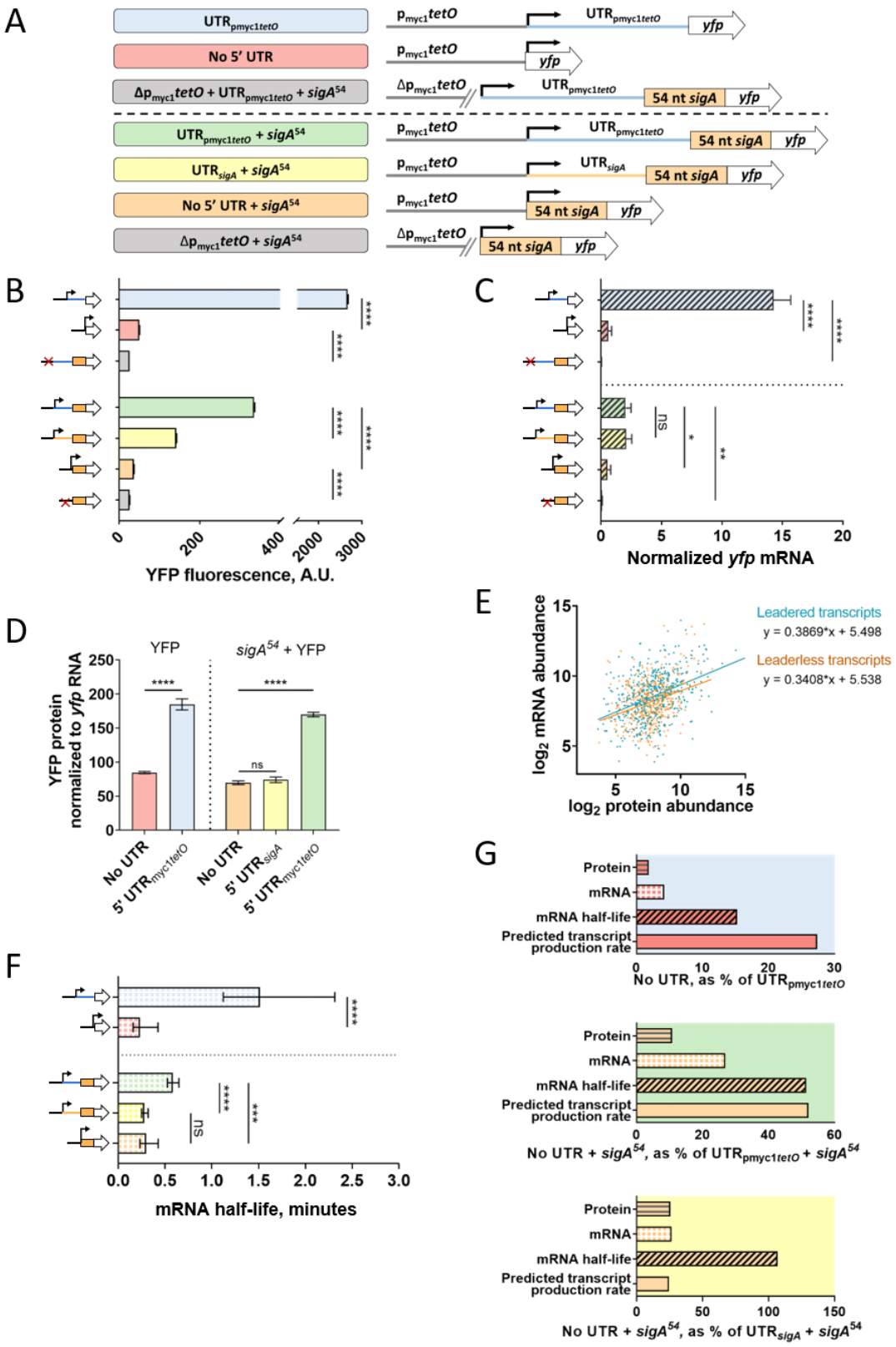

Figure 2-4. Leaderless transcripts have altered translation efficiencies, mRNA half-lives, and predicted transcript production rates compared to those of leadered controls. (Legend on next page)

When we compared YFP fluorescence between the leadered and leaderless reporters, we found that the leaderless fusions were substantially less fluorescent than those containing either 5′ UTR, regardless of the presence of $sigA^{54}$ (Figure 2-4B). The leaderless constructs also had reduced *yfp* mRNA levels compared to those of all of the leadered constructs (Figure 2-4C). When comparing the leaderless constructs to the UTR_{pmyc1}*tetO* construct, protein levels were decreased to a greater extent than mRNA levels, (Figure 2-4D), suggesting that the leaderless mRNAs were indeed translated less efficiently than mRNAs bearing UTR_{pmyc1}*tetO*. However, the difference in protein abundance from constructs without leaders and with UTR*sigA* could be largely explained by the difference in mRNA levels (Figure 2-4D), suggesting that leaderless and UTR*sigA*-leadered mRNAs are translated with similar efficiencies.

To further evaluate the relationship between leader status and translation efficiency, we compared the relative abundances of proteins and mRNAs in *M. tuberculosis* using published quantitative proteomics data (Schubert et al., 2015) and transcriptome sequencing (RNA-seq) data (Shell et al., 2015). For both leaderless transcripts and transcripts with 5′ UTRs ≥15 nt in length, mRNA abundance and protein abundance were significantly correlated ($P < 0.0001$, Spearman's ρ) (Figure 2-4E).

Figure 2-4. Legend (Continued)

(A) Constructs transformed into *M. smegmatis* to compare leaderless versus leadered gene structures. (B) Median YFP fluorescence of strains bearing the constructs in panel A, determined by flow cytometry. Error bars denote 95% CI. Strains were compared by Kruskal-Wallis test followed by Dunn's multiple-comparison test. (C) *yfp* mRNA abundance for strains bearing the indicated constructs, determined by qPCR and normalized to expression of endogenous *sigA*. Error bars denote standard deviation. Strains were compared by ANOVA with Tukey's HSD. (D) Transcripts containing the p_{myc1}*tetO*-associated 5′ UTR are translated more efficiently than leaderless transcripts or those containing the *sigA* 5′ UTR. (E) Published *M. tuberculosis* mRNA abundance (42) and protein abundance (62) levels for genes that have a single TSS and are leaderless or have 5′ UTRs of ≥15 nt. Protein and mRNA abundance were significantly correlated for both gene structures ($P<0.0001$, Spearman's ρ). Linear regression analysis revealed that the slopes were statistically indistinguishable ($P=0.44$). (F) The half-lives of *yfp* mRNA produced from the indicated constructs were measured. Error bars denote 95% CI. Half-lives were compared using linear regression analysis ($n=3$). (G) Protein abundance, mRNA abundance, mRNA half-life, and calculated transcript production rate for leaderless transcripts compared to transcripts with 5′ UTRs. Note that some data shown in Figure 2-2 and Figure 2-3 are reproduced here to facilitate comparisons. ****, $P<0.0001$; ***, $P<0.001$; ns, $P>0.05$.

We omitted transcripts with 1- to 14-nt UTRs because it is unknown if these behave more like leadered transcripts or more like leaderless transcripts with respect the mechanisms of translation initiation. Linear regression of these correlations revealed that they were statistically indistinguishable for leadered versus leaderless transcripts, consistent with the idea that variability in translation efficiency among mycobacterial genes is largely driven by factors other than the presence or absence of a leader.

We wondered if the reduced abundance of the leaderless *yfp* transcripts relative to the $UTR_{pmyc1tetO}$-leadered transcripts was associated with reduced mRNA stability. Indeed, *yfp* half-lives for the $UTR_{pmyc1tetO}$ leadered transcripts were longer than their leaderless counterparts (Figure 2-4F). In contrast, the leaderless transcripts had half-lives similar to the transcript bearing UTR_{sigA} (Figure 2-4F). Interestingly, leaderless transcripts with and without the $sigA^{54}$ N-terminal extension had equivalent half-lives. Taken together, the data indicate that the destabilizing effect of $sigA^{54}$ observed in Figure 2-2F is dependent on the $UTR_{pmyc1tetO}$ present in those constructs.

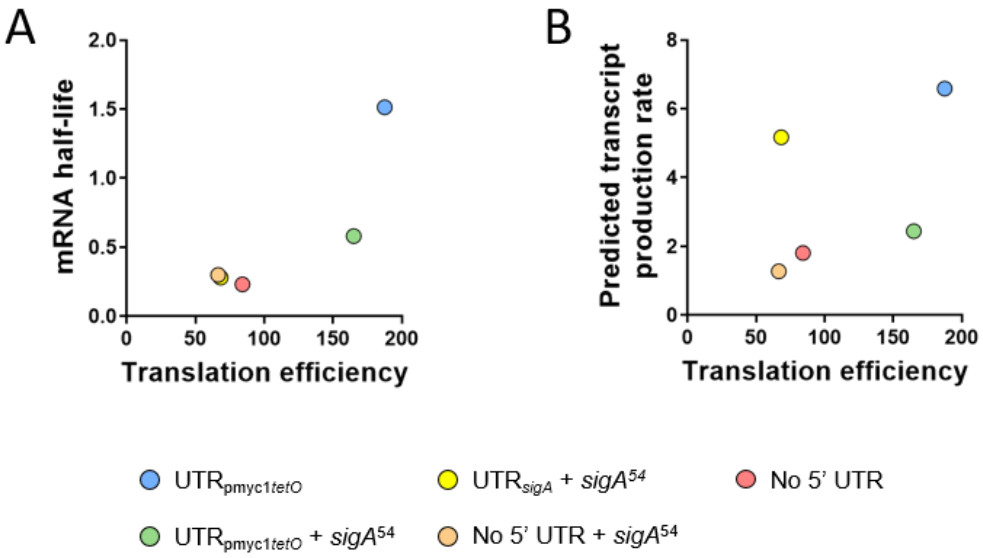

Figure 2-5. Translation efficiency is poorly correlated with mRNA half-life and predicted transcript production rate. Translation efficiency was defined as the ratio of protein abundance to mRNA abundance (arbitrary units). (A) Variability in mRNA half-life is largely not explained by variability in translation efficiency. (B) Variability in predicted transcript production rate is uncorrelated with translation efficiency.

The predicted *yfp* transcript production rates of the leaderless constructs were lower than those of their leadered counterparts (Figure 2-4G). This is consistent with the idea that transcription-translation coupling can cause transcription rates to be altered as a function of translation efficiency (Proshkin et al., 2010). However, the UTR_{sigA}-leadered transcript appeared to be translated with a similar efficiency as the leaderless constructs (Figure 2-4D) and yet had a substantially higher transcript production rate.

Translation efficiency is a poor predictor of mRNA half-life and transcript production rate.

The five constructs described above had identical promoters but produced strains that varied widely with respect to protein abundance, mRNA abundance, mRNA half-life, translation efficiency, and predicted transcript production rates. Given the reported impacts of translation efficiency on mRNA stability in bacteria (Pato et al., 1973; Wagner et al., 1994; Arnold et al., 1998; Braun et al., 1998; Jurgen et al., 1998; Hambraeus et al., 2002; Sharp and Bechhofer, 2003), we wondered to what extent the differences in half-life among our constructs were explained by differences in translation efficiency. We defined translation efficiency as follows:

$$\text{Translation efficiency} = \frac{protein\ abundance}{[mRNA]}$$

However, the relationship between translation efficiency and mRNA half-life was weak (Figure 2-5A), indicating that the variability in mRNA half-life was largely due to other factors. Translation rate has also been reported to affect transcription rate (Proshkin et al., 2010), but these two properties did not appear to be correlated in our constructs (Figure 2-5B), suggesting that the differences in transcript production rate were not a consequence of differences in translation rate. Alternative interpretations of these and other analyses are discussed below.

Discussion

The *sigA* transcripts in both *M. tuberculosis* and *M. smegmatis* were reported to have relatively short half-lives (Rustad et al., 2012; Vargas-Blanco et al., 2019), and we hypothesized that this property was conferred in part by the 5′ UTR. We therefore sought to determine the impacts of the *M. smegmatis sigA* 5′ UTR on expression and mRNA stability. Compared to a 5′ UTR associated with high levels of protein expression and commonly used in mycobacterial expression vectors (Ehrt et al., 2005), the *sigA* UTR indeed conferred a shorter half-life as well as reduced translation efficiency (which could be the cause of the reduced half-life). However, the half-life of a *sigA*-leadered transcript was similar to that of a leaderless transcript. Insertion of part of the *sigA* coding sequence as an N-terminal translational fusion to our YFP reporter also caused a reduction in mRNA half-life. These findings suggest that the relative instability of the native *sigA* transcript is a product of multiple features, including the 5′ UTR and regions of the coding sequence. However, this effect was not observed for a leaderless version of the translational fusion, indicating the effect is context dependent.

Our mRNA abundance and half-life data allowed us to calculate predicted transcript production rates. These calculated transcript production rates reflect the combined contributions of transcription initiation, elongation, and termination (with initiation and termination likely being the largest contributors), and our methodology did not allow us to distinguish between these processes. It is important to note that these rates were not directly measured but rather inferred from direct measurements of mRNA abundance and half-life; other interpretations of the data are therefore possible, as described below. Interestingly, the *sigA* 5′ UTR appeared to increase transcript production rates compared to the p_{myc1}*tetO*-associated UTR or leaderless transcripts. The promoter sequence upstream of the transcription start site (TSS) was identical for all constructs. The effect of the 5′ UTR on transcript production rate could therefore be mediated by at least three possible mechanisms. First, the sequence downstream of the TSS could affect

RNA polymerase binding and therefore initiation as has been reported in *E. coli* (Berg et al., 2009). This is consistent with the finding that the *E. coli* RNA polymerase footprint extends 20 nt downstream of the TSS in both the open and closed initiation complexes (Davis et al., 2007) and advises caution when using TSS data to predict promoters. Second, the composition of the 5′ UTR could affect rates of premature termination and therefore rates of production of full-length transcript as has also been reported (Hambraeus et al., 2002; Lale et al., 2011). We also note that the qPCR primers that we used to measure transcript abundance and half-life anneal to the coding sequence, so we only quantify transcripts that extend at least 89 nt into the coding sequence. Transcripts that terminate before this point are not detected in our experimental setup. Third, elongation rates could vary among constructs due to presence or absence of pause sites (Davenport et al., 2000) or DNA binding proteins that form roadblocks (Epshtein et al., 2003). Viewed broadly, this result highlights the complexity of bacterial transcription.

An alternative interpretation of these data is possible if one considers the idea that newly synthesized mRNAs may be degraded nearly instantaneously if not immediately engaged by the translation machinery. To our knowledge first proposed in detail in (Nogueira et al., 2001), this hypothesis invokes a population of “dark matter” mRNAs that are synthesized but decay so rapidly that they are not detected by abundance and half-life measurements. In this model, measured half-lives reflect primarily the decay of those transcripts that are quickly engaged by ribosomes and therefore long enough lived to contribute to steady-state abundance. The model implies that steady-state abundance is a function not only of transcription rate and measured half-life, as assumed in our transcript production rate calculations, but also of partitioning between the translated pool and the “dark matter” pool. If more mRNA is partitioned into the translated pool, greater steady-state abundance could be achieved without increased transcription rates and vice versa. Importantly, changes in partitioning between these pools need not correspond with predictable changes in measured mRNA half-life or protein levels. For example,

transcripts containing the *sigA* 5′ UTR could conceivably engage ribosomes more quickly than transcripts containing the p_{myc1}*tetO*-associated UTR and therefore enter the translated pool at higher rates yet be more susceptible to degradation during or after translation, resulting in shorter half-lives and thus similar steady-state mRNA abundance as we observed (Figure 2-3).

The relative efficiency of leaderless versus leadered translation in mycobacteria has not been experimentally established. Proteomics data from *M. tuberculosis* suggested that proteins encoded on leaderless transcripts were less abundant than those encoded on leadered transcripts with evident SD sequences, but this difference appeared to be explained by differences in mRNA levels (Cortes et al., 2013). A subsequently reported quantitative proteomics data set (Schubert et al., 2015) allows for a more rigorous assessment of the relationship between mRNA abundance and protein abundance in *M. tuberculosis*. When comparing leaderless genes to leadered genes with a single TSS, we found that leaderless genes indeed on average had slightly but significantly lower levels of both mRNA and protein (Mann-Whitney tests for both, $P < 0.01$). However, the relationships between mRNA abundance and protein abundance did not differ for these two groups.

There are at least two ways to interpret protein/mRNA ratios. In Results and the figures, we refer to these ratios as a measure of translation efficiency on the grounds that they reflect the number of protein molecules produced per mRNA molecule. This interpretation rests upon the assumption that most mRNAs are stable enough to contribute to measurements of steady-state abundance. There are various reports of mutations or modifications that affect mRNA levels and protein levels differently (Baumeister et al., 1991; Hambraeus et al., 2002; Sharp and Bechhofer, 2003; Lale et al., 2011; Bhattacharyya et al., 2018), supporting the idea that translation efficiency can indeed be estimated by comparing protein levels to mRNA levels. Using this assumption and definition of translation efficiency, the *M. tuberculosis* data imply that there is no global difference in translation efficiency for leadered versus leaderless transcripts. Using

the same assumptions, the small number of controlled comparisons that we report here support that idea; transcripts with the p_{myc1}*tetO*-associated UTR were translated more efficiently than leaderless transcripts, but a transcript with the *sigA* UTR was translated with similar efficiency as its leaderless counterpart. Notably, the difference in translation efficiency between the two leadered transcripts might be attributable to differences in secondary structure rather than differences in favorability of the SD sequences.

A positive correlation between mRNA half-life and translation efficiency was reported for E. coli (Boel et al., 2016), consistent with the idea that translation may protect mRNAs from degradation. We did not observe such a correlation within our set of five transcripts, indicating that translation efficiency is not the primary driver of the variability in half-lives that we observed. However, a broad analysis of this relationship in mycobacteria is warranted.

The protein and mRNA abundance data must be interpreted differently if there is a "dark matter" mRNA pool that does not contribute to the mRNA abundance measurements. In this model, steady-state mRNA abundance is affected by translation efficiency as a consequence of partitioning between the translated pool and the "dark matter" pool. Translation efficiency would therefore affect steady-state mRNA abundance to a greater extent than that predicted by measured mRNA half-lives. Importantly, in this model, the relationship between protein abundance and mRNA abundance is not a reliable indicator of translation efficiency. In *M. tuberculosis*, lower average levels of both mRNA and protein from leaderless genes could therefore be a consequence of slower engagement of ribosomes and greater partitioning of mRNAs into the undetected "dark matter" pool.

It is prudent to note the assumptions underlying our definition of mRNA half-life. We assume that following transcription block by rifampin, the initial rapid decrease in *yfp* transcript abundance that we

observe (see Figure S2-3) indeed reflects the degradation rate for most *yfp* transcripts produced in an unperturbed cell. This assumption could be invalid if rifampin immediately alters mRNA degradation rates. If there are populations of "dark matter" mRNAs, the measured half-lives presumably reflect only the decay rate of those mRNAs that are engaged by ribosomes. We also note that, for most constructs, we observed a second, slow phase of mRNA decay (see Figure S2-3 and Materials and Methods). This could reflect changes in mRNA decay in response to rifampin or reflect the presence of a second pool of transcripts with an inherently slower decay rate. As we could not distinguish between these possibilities, and the slow-decaying pool appeared to comprise at most 10% of the total, we did not further analyze it in this study. However, we cannot exclude the possibility that it is real and physiologically relevant.

Materials and methods

Strains and culture conditions.

All experiments were done using a *Mycobacterium smegmatis* Δ*MSMEG_2952* strain (Yang et al., 2017), which is less prone to aggregation (clumping) than its parent strain mc^2155 and therefore permits higher confidence measurements by flow cytometry. This strain and its derivatives (Table 2-1) were grown in Middlebrook 7H9 medium with albumin-dextrose-catalase (ADC) supplementation (final concentrations, 5 g/liter bovine serum albumin fraction V, 2 g/liter dextrose, 0.85 g/liter NaCl, and 3 mg/liter catalase), 0.2% glycerol, and 0.05% Tween 80. Cultures were shaken at 200 rpm and 37°C to an optical density at 600 nm (OD_{600}) of ~0.8 at the time of harvest.

Plasmid construction.

Plasmid pSS303 was built on a backbone derived from pGH1000A (Morris et al., 2008) by inserting a *yfp* cassette containing the gene sequence of a YFP reporter (sfYFP, obtained from Ivy Fitzgerald and Benjamin Glick) with a 6×His tag at the C terminus (complete amino acid sequence,

MASDSTESLFTGVVPILVELDGDVNGHKFSVRGEGEGDATNGKLTLKLICTTGKLPVPWPTLVTTLGYGVQCFARYPDH
MKQHDFFKSAMPEGYVQERTITFKDDGTYKTRAEVKFEGDTLVNRIELKGIDFKEDGNILGHKLEYNFNSHNVYITADK
QKNGIKANFKIRHNVEDGGVQLADHYQQNTPIGDGPVLLPDNHYLSYQSKLSKDPNEKRDHMVLLEFVTAAGITHGSS
GSSGCHHHHHH). Two synthetic transcriptional terminators were inserted flanking the cassette as follows: *tsynA* (Czyz et al., 2014) upstream and *ttsbiB* (Huff et al., 2010) downstream. Transcription was initiated by the p_{myc1}*tetO* promoter, which was constitutively active in our strains due to the absence of the corresponding *tet* repressor (Ehrt et al., 2005). All constructs (pSS303 and derivatives noted in Table 2-1) were built using NEBuilder HiFi DNA assembly master mix (catalog number E2621). Each assembled plasmid was integrated in *M. smegmatis* Δ*MSMEG_2952* (Yang et al., 2017) at the Giles phage site and selected with 200 µg/mL hygromycin.

Cell fixation and flow cytometry.

Several 1.5-mL aliquots of *M. smegmatis* cultures were pelleted, resuspended in 500 µL 2% paraformaldehyde in phosphate-buffered saline (PBS), and incubated at room temperature for 30 min. Cells were rinsed twice using 900 µL PBS + 0.1% Tween 20 and resuspended to a calculated OD_{600} of 15. Prior to flow cytometry analysis, cells were filtered using an 18-gauge 5-µm filter needle and diluted with Middlebrook 7H9 to an OD_{600} of 0.015. YFP fluorescence intensity was measured per manufacturer's instructions using a BD Accuri C6 flow cytometer collecting 100,000 events per sample (Figure 2-1B and C) or a BD LSR II flow cytometer collecting 50,000 events per sample (Figure 2-2B, Figure 2-3B, and Figure 2-4B) using appropriate controls and thresholds. FlowJo v10.6 was used to draw tight forward scatter and side scatter gates to limit analysis to similarly sized cells, and GraphPad Prism 8 was used for statistical analysis.

RNA extraction and determination of mRNA abundance and stability.

RNA extraction, measurement of mRNA abundance, and mRNA stability analyses from *M. smegmatis* cultures were conducted in biological triplicates as described in reference (Vargas-Blanco et al., 2019) Briefly, mRNA abundance was measured by quantitative PCR (qPCR) using iTaq SYBR green (Bio-Rad) on an Applied Biosystems 7500 with 400 pg of cDNA and 0.25 µM each primer in 10-µL reaction mixtures. Cycle parameters were 95°C for 15 s and 61°C for 60 s. Primers used to determine mRNA abundance are listed in Table 2-2.

For mRNA stability analysis, 5-mL *M. smegmatis* cultures were treated with rifampin at a final concentration of 150 µg/mL to halt transcription and snap-frozen in liquid nitrogen after 0, 1, 2, or 4 min. Abundance over time was determined for *sigA* and *yfp* using qPCR and used to estimate mRNA half-lives essentially as in reference (Vargas-Blanco et al., 2019). For each sample, the negative of the threshold cycle (C_T) represents transcript abundance on a $\log_2$ scale. For each strain and gene, linear regression was performed on a plot of $-C_T$ versus time. Half-life was defined as −1/slope. *sigA* half-lives were equivalent in all strains and not shown. As we have observed for many other genes in mycobacteria, plotting $\log_2$ abundance over time produced a biphasic decay curve consistent with a period of faster exponential decay, followed by a period of much slower exponential decay (see Figure S2-3A). Similar biphasic decay curves have been reported by others for some *E. coli* genes (Hambraeus et al., 2003; Brescia et al., 2004; Chen et al., 2015; Sinha et al., 2018). The initial rapid decay phase reflects the rate of decay for at least 90% of the *yfp* RNA present in our samples. We therefore used only this initial phase for mRNA half-life calculations (0, 1, and 2 min for strain SS-M_0489 and 0 and 1 min for strains SS-M_0493 and SS-M_0626) (see Figure S2-3B). The slower decay phase could reflect the presence of minority transcript species that inherently decay more slowly or could reflect perturbation of cellular physiology due to rifampin.

Calculation of transcript production rates.

The rate of transcript production was estimated as described in reference (Esquerré et al., 2014). Briefly, transcript production rate (*Vt*) is described as follows:

$$V_t = k \cdot [mRNA] + \mu \cdot [mRNA]$$

Where [mRNA] is a given transcript's concentration, μ is the growth rate of the cells (ln_2/doubling time), and *k* is the degradation rate constant (ln_2/half-life). Note that because [mRNA] is derived from our qPCR data and is therefore a relative value rather than absolute value, the calculated transcript production rate is also a relative rather than absolute value.

Protein extraction and BCA assay.

M. smegmatis cells were pelleted; rinsed three times with Middlebrook 7H9, 0.2% glycerol, and 0.05% Tween 80 at 4°C; resuspended in PBS + 2% SDS + protease inhibitor cocktail (VWR; catalog number 97063-972); and transferred to 2-mL disruption tubes (OPS Diagnostics; 100-μm zirconium lysing matrix, molecular grade). Cultures were lysed using a FastPrep-24 5G instrument (MP Biomedical) using four cycles of 6.5 m/s for 30 s with 1 min on ice between cycles. Samples were clarified by centrifugation at 21,130 × *g* at 4°C for 10 min, and the supernatant containing protein was recovered and stored at –20°C. Protein concentrations were calculated using the Pierce BCA protein assay (Thermo Scientific; catalog number 23225) according to the manufacturer's instructions.

Western blotting.

Protein was normalized to the indicated masses in a final volume of 9 μL combined with 4 μL of 4× protein loading dye (200 mM Tris-HCl [pH 6.8], 400 mM dithiothreitol [DTT], 8% SDS, 0.4% bromophenol blue, 40% glycerol) and heated to 95°C for 10 min. Using gradient gels (4 to 15% Mini-Protean TGX precast

protein gels; Bio-Rad; catalog number 4561086), the samples were electrophoresed for 60 min at 140 V and then transferred to a polyvinylidene difluoride (PVDF) membrane. The membrane was incubated in blocking solution (PBS plus 5% nonfat milk) for 30 min and washed once for 5 min using washing buffer (PBS 1× buffer plus 0.1% Tween 20). The membrane was probed with 1 µg/mL His tag antibody (polyclonal antibody, rabbit; GenScript; catalog number A00174) in blocking solution for 60 min at room temperature. The membrane was then rinsed twice with wash buffer and once with 1× PBS and incubated with anti-rabbit IgG–peroxidase (Sigma-Aldrich; catalog number A4914), 1:30,000 in blocking solution, for 60 min at room temperature. The membrane was rinsed as previously described and incubated with horseradish peroxidase (HRP) substrate (Radiance Q; Azure Biosystems; catalog number AC2101) as recommended by the manufacturer. Imaging was done using an Azure C200 imaging system (Azure Biosystems).

Software.

GraphPad Prism was used for all linear regressions and comparisons (GraphPad Software, La Jolla, CA). The Srna program within Sfold was used for RNA secondary structure predictions (Ding et al., 2004; 2005).

Acknowledgments

This work was supported by NSF CAREER award 1652756 to S.S.S. Thanks go to Ivy Fitzgerald and Benjamin Glick for providing the sfYFP construct. We thank all members of the Shell lab for technical assistance and helpful discussions.

References

Agaisse, H., and Lereclus, D. (1996). STAB-SD: a Shine-Dalgarno sequence in the 5' untranslated region is a determinant of mRNA stability. *Mol Microbiol* 20(3)**,** 633-643. doi: 10.1046/j.1365-2958.1996.5401046.x.

Anderson, K.L., and Dunman, P.M. (2009). Messenger RNA Turnover Processes in *Escherichia coli*, *Bacillus subtilis*, and Emerging Studies in *Staphylococcus aureus*. *Int J Microbiol* 2009**,** 525491. doi: 10.1155/2009/525491.

Arnold, T.E., Yu, J., and Belasco, J.G. (1998). mRNA stabilization by the ompA 5' untranslated region: two protective elements hinder distinct pathways for mRNA degradation. *RNA* 4(3)**,** 319-330.

Baumeister, R., Flache, P., Melefors, O., von Gabain, A., and Hillen, W. (1991). Lack of a 5'; non-coding region in Tn1721 encoded tetR mRNA is associated with a low efficiency of translation and a short half-life in *Escherichia coli*. *Nucleic Acids Research* 19(17)**,** 4595-4600.

Bechhofer, D.H., and Dubnau, D. (1987). Induced mRNA stability in *Bacillus subtilis*. *Proc Natl Acad Sci U S A* 84(2)**,** 498-502. doi: 10.1073/pnas.84.2.498.

Beck, H.J., Fleming, I.M., and Janssen, G.R. (2016). 5'-Terminal AUGs in *Escherichia coli* mRNAs with Shine-Dalgarno Sequences: Identification and Analysis of Their Roles in Non-Canonical Translation Initiation. *PLoS One* 11(7)**,** e0160144. doi: 10.1371/journal.pone.0160144.

Belasco, J.G., Nilsson, G., von Gabain, A., and Cohen, S.N. (1986). The stability of *E. coli* gene transcripts is dependent on determinants localized to specific mRNA segments. *Cell* 46(2)**,** 245-251. doi: 10.1016/0092-8674(86)90741-5.

Berg, L., Lale, R., Bakke, I., Burroughs, N., and Valla, S. (2009). The expression of recombinant genes in *Escherichia coli* can be strongly stimulated at the transcript production level by mutating the DNA-region corresponding to the 5'-untranslated part of mRNA. *Microb Biotechnol* 2(3)**,** 379-389. doi: 10.1111/j.1751-7915.2009.00107.x.

Bhattacharyya, S., Jacobs, W.M., Adkar, B.V., Yan, J., Zhang, W., and Shakhnovich, E.I. (2018). Accessibility of the Shine-Dalgarno Sequence Dictates N-Terminal Codon Bias in *E. coli*. *Mol Cell* 70(5)**,** 894-905 e895. doi: 10.1016/j.molcel.2018.05.008.

Boel, G., Letso, R., Neely, H., Price, W.N., Wong, K.H., Su, M., et al. (2016). Codon influence on protein expression in *E. coli* correlates with mRNA levels. *Nature* 529(7586)**,** 358-363. doi: 10.1038/nature16509.

Braun, F., Le Derout, J., and Regnier, P. (1998). Ribosomes inhibit an RNase E cleavage which induces the decay of the rpsO mRNA of *Escherichia coli*. *EMBO J* 17(16)**,** 4790-4797. doi: 10.1093/emboj/17.16.4790.

Brescia, C.C., Kaw, M.K., and Sledjeski, D.D. (2004). The DNA binding protein H-NS binds to and alters the stability of RNA in vitro and in vivo. *Journal of Molecular Biology* 339(3)**,** 505-514. doi: 10.1016/j.jmb.2004.03.067.

Burmann, B.M., Schweimer, K., Luo, X., Wahl, M.C., Stitt, B.L., Gottesman, M.E., et al. (2010). A NusE:NusG complex links transcription and translation. *Science* 328(5977)**,** 501-504. doi: 10.1126/science.1184953.

Chen, C.Y., and Belasco, J.G. (1990). Degradation of pufLMX mRNA in *Rhodobacter capsulatus* is initiated by nonrandom endonucleolytic cleavage. *J Bacteriol* 172(8)**,** 4578-4586. doi: 10.1128/jb.172.8.4578-4586.1990.

Chen, H., Bjerknes, M., Kumar, R., and Jay, E. (1994). Determination of the optimal aligned spacing between the Shine-Dalgarno sequence and the translation initiation codon of *Escherichia coli* mRNAs. *Nucleic Acids Res* 22(23)**,** 4953-4957. doi: 10.1093/nar/22.23.4953.

Chen, H., Shiroguchi, K., Ge, H., and Xie, X.S. (2015). Genome-wide study of mRNA degradation and transcript elongation in *Escherichia coli*. *Molecular systems biology* 11(1)**,** 781.

Chen, L.H., Emory, S.A., Bricker, A.L., Bouvet, P., and Belasco, J.G. (1991). Structure and function of a bacterial mRNA stabilizer: analysis of the 5' untranslated region of ompA mRNA. *J Bacteriol* 173(15)**,** 4578-4586. doi: 10.1128/jb.173.15.4578-4586.1991.

Cortes, T., Schubert, O.T., Rose, G., Arnvig, K.B., Comas, I., Aebersold, R., et al. (2013). Genome-wide Mapping of Transcriptional Start Sites Defines an Extensive Leaderless Transcriptome in *Mycobacterium tuberculosis*. *Cell reports*. doi: 10.1016/j.celrep.2013.10.031.

Czyz, A., Mooney, R.A., Iaconi, A., and Landick, R. (2014). Mycobacterial RNA polymerase requires a U-tract at intrinsic terminators and is aided by NusG at suboptimal terminators. *MBio* 5(2)**,** e00931. doi: 10.1128/mBio.00931-14.

Davenport, R.J., Wuite, G.J., Landick, R., and Bustamante, C. (2000). Single-molecule study of transcriptional pausing and arrest by *E. coli* RNA polymerase. *Science* 287(5462)**,** 2497-2500. doi: 10.1126/science.287.5462.2497.

Davis, C.A., Bingman, C.A., Landick, R., Record, M.T., Jr., and Saecker, R.M. (2007). Real-time footprinting of DNA in the first kinetically significant intermediate in open complex formation by *Escherichia coli* RNA polymerase. *Proc Natl Acad Sci U S A* 104(19)**,** 7833-7838. doi: 10.1073/pnas.0609888104.

Ding, Y., Chan, C.Y., and Lawrence, C.E. (2004). Sfold web server for statistical folding and rational design of nucleic acids. *Nucleic Acids Res* 32(Web Server issue)**,** W135-141. doi: 10.1093/nar/gkh449.

Ding, Y., Chan, C.Y., and Lawrence, C.E. (2005). RNA secondary structure prediction by centroids in a Boltzmann weighted ensemble. *RNA* 11(8)**,** 1157-1166. doi: 10.1261/rna.2500605.

Ehrt, S., Guo, X.V., Hickey, C.M., Ryou, M., Monteleone, M., Riley, L.W., et al. (2005). Controlling gene expression in mycobacteria with anhydrotetracycline and Tet repressor. *Nucleic Acids Research* 33(2)**,** e21. doi: 10.1093/nar/gni013.

Emory, S.A., and Belasco, J.G. (1990). The ompA 5' untranslated RNA segment functions in *Escherichia coli* as a growth-rate-regulated mRNA stabilizer whose activity is unrelated to translational efficiency. *J Bacteriol* 172(8)**,** 4472-4481. doi: 10.1128/jb.172.8.4472-4481.1990.

Emory, S.A., Bouvet, P., and Belasco, J.G. (1992). A 5'-terminal stem-loop structure can stabilize mRNA in *Escherichia coli*. *Genes Dev* 6(1)**,** 135-148. doi: 10.1101/gad.6.1.135.

Epshtein, V., Toulme, F., Rahmouni, A.R., Borukhov, S., and Nudler, E. (2003). Transcription through the roadblocks: the role of RNA polymerase cooperation. *EMBO J* 22(18)**,** 4719-4727. doi: 10.1093/emboj/cdg452.

Esquerré, T., Laguerre, S., Turlan, C., Carpousis, A.J., Girbal, L., and Cocaign-Bousquet, M. (2014). Dual role of transcription and transcript stability in the regulation of gene expression in *Escherichia coli* cells cultured on glucose at different growth rates. *Nucleic Acids Research* 42(4)**,** 2460-2472. doi: 10.1093/nar/gkt1150.

Fan, H., Conn, A.B., Williams, P.B., Diggs, S., Hahm, J., Gamper, H.B., Jr., et al. (2017). Transcription-translation coupling: direct interactions of RNA polymerase with ribosomes and ribosomal subunits. *Nucleic Acids Res* 45(19)**,** 11043-11055. doi: 10.1093/nar/gkx719.

Gomez, M., Doukhan, L., Nair, G., and Smith, I. (1998). *sigA* is an essential gene in *Mycobacterium smegmatis*. *Mol Microbiol* 29(2)**,** 617-628. doi: 10.1046/j.1365-2958.1998.00960.x.

Grill, S., Gualerzi, C.O., Londei, P., and Blasi, U. (2000). Selective stimulation of translation of leaderless mRNA by initiation factor 2: evolutionary implications for translation. *EMBO J* 19(15)**,** 4101-4110. doi: 10.1093/emboj/19.15.4101.

Grill, S., Moll, I., Giuliodori, A.M., Gualerzi, C.O., and Blasi, U. (2002). Temperature-dependent translation of leaderless and canonical mRNAs in *Escherichia coli*. *FEMS Microbiol Lett* 211(2)**,** 161-167. doi: 10.1111/j.1574-6968.2002.tb11219.x.

Habib, N.F., and Jackson, M.P. (1993). Roles of a ribosome-binding site and mRNA secondary structure in differential expression of Shiga toxin genes. *J Bacteriol* 175(3)**,** 597-603. doi: 10.1128/jb.175.3.597-603.1993.

Hambraeus, G., Karhumaa, K., and Rutberg, B. (2002). A 5' stem-loop and ribosome binding but not translation are important for the stability of *Bacillus subtilis* aprE leader mRNA. *Microbiology (Reading, England)* 148(Pt 6)**,** 1795-1803. doi: 10.1099/00221287-148-6-1795.

Hambraeus, G., Persson, M., and Rutberg, B. (2000). The aprE leader is a determinant of extreme mRNA stability in *Bacillus subtilis*. *Microbiology* 146 Pt 12**,** 3051-3059. doi: 10.1099/00221287-146-12-3051.

Hambraeus, G., von Wachenfeldt, C., and Hederstedt, L. (2003). Genome-wide survey of mRNA half-lives in *Bacillus subtilis* identifies extremely stable mRNAs. *Molecular genetics and genomics : MGG* 269(5)**,** 706-714. doi: 10.1007/s00438-003-0883-6.

Heck, C., Evguenieva-Hackenberg, E., Balzer, A., and Klug, G. (1999). RNase E enzymes from *Rhodobacter capsulatus* and *Escherichia coli* differ in context- and sequence-dependent in vivo cleavage within the polycistronic puf mRNA. *J Bacteriol* 181(24)**,** 7621-7625.

Heck, C., Rothfuchs, R., Jager, A., Rauhut, R., and Klug, G. (1996). Effect of the pufQ-pufB intercistronic region on puf mRNA stability in *Rhodobacter capsulatus*. *Mol Microbiol* 20(6)**,** 1165-1178. doi: 10.1111/j.1365-2958.1996.tb02637.x.

Huff, J., Czyz, A., Landick, R., and Niederweis, M. (2010). Taking phage integration to the next level as a genetic tool for mycobacteria. *Gene* 468(1-2)**,** 8-19. doi: 10.1016/j.gene.2010.07.012.

Jagodnik, J., Chiaruttini, C., and Guillier, M. (2017). Stem-Loop Structures within mRNA Coding Sequences Activate Translation Initiation and Mediate Control by Small Regulatory RNAs. *Mol Cell* 68(1)**,** 158-170 e153. doi: 10.1016/j.molcel.2017.08.015.

Jurgen, B., Schweder, T., and Hecker, M. (1998). The stability of mRNA from the *gsiB* gene of *Bacillus subtilis* is dependent on the presence of a strong ribosome binding site. *Mol Gen Genet* 258(5)**,** 538-545. doi: 10.1007/s004380050765.

Lale, R., Berg, L., Stuttgen, F., Netzer, R., Stafsnes, M., Brautaset, T., et al. (2011). Continuous control of the flow in biochemical pathways through 5' untranslated region sequence modifications in mRNA expressed from the broad-host-range promoter Pm. *Appl Environ Microbiol* 77(8)**,** 2648-2655. doi: 10.1128/AEM.02091-10.

Lease, R.A., and Belfort, M. (2000). A trans-acting RNA as a control switch in *Escherichia coli*: DsrA modulates function by forming alternative structures. *Proc Natl Acad Sci U S A* 97(18)**,** 9919-9924. doi: 10.1073/pnas.170281497.

Link, T.M., Valentin-Hansen, P., and Brennan, R.G. (2009). Structure of *Escherichia coli* Hfq bound to polyriboadenylate RNA. *Proc Natl Acad Sci U S A* 106(46)**,** 19292-19297. doi: 10.1073/pnas.0908744106.

Manganelli, R., Provvedi, R., Rodrigue, S., Beaucher, J., Gaudreau, L., and Smith, I. (2004). Sigma factors and global gene regulation in *Mycobacterium tuberculosis*. *J Bacteriol* 186(4)**,** 895-902. doi: 10.1128/jb.186.4.895-902.2004.

Martini, M.C., Zhou, Y., Sun, H., and Shell, S.S. (2019). Defining the Transcriptional and Post-transcriptional Landscapes of *Mycobacterium smegmatis* in Aerobic Growth and Hypoxia. *Front Microbiol* 10**,** 591. doi: 10.3389/fmicb.2019.00591.

Miller, O.L., Jr., Hamkalo, B.A., and Thomas, C.A., Jr. (1970). Visualization of bacterial genes in action. *Science* 169(3943)**,** 392-395.

Moll, I., Afonyushkin, T., Vytvytska, O., Kaberdin, V.R., and Blasi, U. (2003). Coincident Hfq binding and RNase E cleavage sites on mRNA and small regulatory RNAs. *RNA* 9(11)**,** 1308-1314. doi: 10.1261/rna.5850703.

Moll, I., Grill, S., Grundling, A., and Blasi, U. (2002). Effects of ribosomal proteins S1, S2 and the DeaD/CsdA DEAD-box helicase on translation of leaderless and canonical mRNAs in *Escherichia coli*. *Mol Microbiol* 44(5)**,** 1387-1396. doi: 10.1046/j.1365-2958.2002.02971.x.

Moll, I., Hirokawa, G., Kiel, M.C., Kaji, A., and Blasi, U. (2004). Translation initiation with 70S ribosomes: an alternative pathway for leaderless mRNAs. *Nucleic Acids Res* 32(11)**,** 3354-3363. doi: 10.1093/nar/gkh663.

Morris, P., Marinelli, L.J., Jacobs-Sera, D., Hendrix, R.W., and Hatfull, G.F. (2008). Genomic characterization of mycobacteriophage Giles: evidence for phage acquisition of host DNA by illegitimate recombination. *J Bacteriol* 190(6)**,** 2172-2182. doi: 10.1128/JB.01657-07.

Mutalik, V.K., Qi, L., Guimaraes, J.C., Lucks, J.B., and Arkin, A.P. (2012). Rationally designed families of orthogonal RNA regulators of translation. *Nat Chem Biol* 8(5)**,** 447-454. doi: 10.1038/nchembio.919.

Nogueira, T., de Smit, M., Graffe, M., and Springer, M. (2001). The relationship between translational control and mRNA degradation for the *Escherichia coli* threonyl-tRNA synthetase gene. *J Mol Biol* 310(4)**,** 709-722. doi: 10.1006/jmbi.2001.4796.

O'Donnell, S.M., and Janssen, G.R. (2001). The initiation codon affects ribosome binding and translational efficiency in *Escherichia coli* of cI mRNA with or without the 5' untranslated leader. *J Bacteriol* 183(4)**,** 1277-1283. doi: 10.1128/JB.183.4.1277-1283.2001.

O'Donnell, S.M., and Janssen, G.R. (2002). Leaderless mRNAs bind 70S ribosomes more strongly than 30S ribosomal subunits in *Escherichia coli*. *J Bacteriol* 184(23)**,** 6730-6733. doi: 10.1128/jb.184.23.6730-6733.2002.

Pato, M.L., Bennett, P.M., and von Meyenburg, K. (1973). Messenger ribonucleic acid synthesis and degradation in *Escherichia coli* during inhibition of translation. *Journal of Bacteriology* 116(2)**,** 710-718.

Pedersen, M., Nissen, S., Mitarai, N., Lo Svenningsen, S., Sneppen, K., and Pedersen, S. (2011). The functional half-life of an mRNA depends on the ribosome spacing in an early coding region. *J Mol Biol* 407(1)**,** 35-44. doi: 10.1016/j.jmb.2011.01.025.

Proshkin, S., Rahmouni, A.R., Mironov, A., and Nudler, E. (2010). Cooperation between translating ribosomes and RNA polymerase in transcription elongation. *Science* 328(5977)**,** 504-508. doi: 10.1126/science.1184939.

Richards, J., and Belasco, J.G. (2019). Obstacles to Scanning by RNase E Govern Bacterial mRNA Lifetimes by Hindering Access to Distal Cleavage Sites. *Mol Cell* 74(2)**,** 284-295 e285. doi: 10.1016/j.molcel.2019.01.044.

Ringquist, S., Shinedling, S., Barrick, D., Green, L., Binkley, J., Stormo, G.D., et al. (1992). Translation initiation in *Escherichia coli*: sequences within the ribosome-binding site. *Mol Microbiol* 6(9)**,** 1219-1229. doi: 10.1111/j.1365-2958.1992.tb01561.x.

Rock, J.M., Hopkins, F.F., Chavez, A., Diallo, M., Chase, M.R., Gerrick, E.R., et al. (2017). Programmable transcriptional repression in mycobacteria using an orthogonal CRISPR interference platform. *Nat Microbiol* 2**,** 16274. doi: 10.1038/nmicrobiol.2016.274.

Romeo, T., and Babitzke, P. (2018). Global Regulation by CsrA and Its RNA Antagonists. *Microbiol Spectr* 6(2). doi: 10.1128/microbiolspec.RWR-0009-2017.

Rustad, T.R., Minch, K.J., Brabant, W., Winkler, J.K., Reiss, D.J., Baliga, N.S., et al. (2012). Global analysis of mRNA stability in *Mycobacterium tuberculosis*. *Nucleic Acids Research* 41(1)**,** 509-517. doi: 10.1093/nar/gks1019.

Schubert, O.T., Ludwig, C., Kogadeeva, M., Zimmermann, M., Rosenberger, G., Gengenbacher, M., et al. (2015). Absolute Proteome Composition and Dynamics during Dormancy and Resuscitation of *Mycobacterium tuberculosis*. *Cell Host Microbe* 18(1)**,** 96-108. doi: 10.1016/j.chom.2015.06.001.

Sharp, J.S., and Bechhofer, D.H. (2003). Effect of translational signals on mRNA decay in *Bacillus subtilis*. *Journal of Bacteriology* 185(18)**,** 5372-5379.

Shell, S.S., Wang, J., Lapierre, P., Mir, M., Chase, M.R., Pyle, M.M., et al. (2015). Leaderless Transcripts and Small Proteins Are Common Features of the Mycobacterial Translational Landscape. *PLoS Genetics* 11(11)**,** e1005641. doi: 10.1371/journal.pgen.1005641.

Shine, J., and Dalgarno, L. (1974). The 3'-terminal sequence of *Escherichia coli* 16S ribosomal RNA: complementarity to nonsense triplets and ribosome binding sites. *Proc Natl Acad Sci U S A* 71(4)**,** 1342-1346. doi: 10.1073/pnas.71.4.1342.

Sinha, D., Matz, L.M., Cameron, T.A., and De Lay, N.R. (2018). Poly(A) polymerase is required for RyhB sRNA stability and function in *Escherichia coli*. *RNA* 24(11)**,** 1496-1511. doi: 10.1261/rna.067181.118.

Skorski, P., Leroy, P., Fayet, O., Dreyfus, M., and Hermann-Le Denmat, S. (2006). The highly efficient translation initiation region from the *Escherichia coli* rpsA gene lacks a shine-dalgarno element. *J Bacteriol* 188(17)**,** 6277-6285. doi: 10.1128/JB.00591-06.

Sterk, M., Romilly, C., and Wagner, E.G.H. (2018). Unstructured 5'-tails act through ribosome standby to override inhibitory structure at ribosome binding sites. *Nucleic Acids Res* 46(8)**,** 4188-4199. doi: 10.1093/nar/gky073.

Takahashi, M.K., and Lucks, J.B. (2013). A modular strategy for engineering orthogonal chimeric RNA transcription regulators. *Nucleic Acids Res* 41(15)**,** 7577-7588. doi: 10.1093/nar/gkt452.

Tedin, K., Moll, I., Grill, S., Resch, A., Graschopf, A., Gualerzi, C.O., et al. (1999). Translation initiation factor 3 antagonizes authentic start codon selection on leaderless mRNAs. *Mol Microbiol* 31(1)**,** 67-77. doi: 10.1046/j.1365-2958.1999.01147.x.

Udagawa, T., Shimizu, Y., and Ueda, T. (2004). Evidence for the translation initiation of leaderless mRNAs by the intact 70 S ribosome without its dissociation into subunits in eubacteria. *J Biol Chem* 279(10)**,** 8539-8546. doi: 10.1074/jbc.M308784200.

Unniraman, S., Prakash, R., and Nagaraja, V. (2001). Alternate paradigm for intrinsic transcription termination in eubacteria. *J Biol Chem* 276(45)**,** 41850-41855. doi: 10.1074/jbc.M106252200.

Van Etten, W.J., and Janssen, G.R. (1998). An AUG initiation codon, not codon-anticodon complementarity, is required for the translation of unleadered mRNA in *Escherichia coli*. *Mol Microbiol* 27(5)**,** 987-1001. doi: 10.1046/j.1365-2958.1998.00744.x.

Vargas-Blanco, D.A., Zhou, Y., Zamalloa, L.G., Antonelli, T., and Shell, S.S. (2019). mRNA Degradation Rates Are Coupled to Metabolic Status in *Mycobacterium smegmatis*. *MBio* 10(4). doi: 10.1128/mBio.00957-19.

Wagner, L.A., Gesteland, R.F., Dayhuff, T.J., and Weiss, R.B. (1994). An efficient Shine-Dalgarno sequence but not translation is necessary for lacZ mRNA stability in *Escherichia coli*. *J Bacteriol* 176(6)**,** 1683-1688. doi: 10.1128/jb.176.6.1683-1688.1994.

Yang, Y., Thomas, J., Li, Y., Vilcheze, C., Derbyshire, K.M., Jacobs, W.R., Jr., et al. (2017). Defining a temporal order of genetic requirements for development of mycobacterial biofilms. *Mol Microbiol* 105(5)**,** 794-809. doi: 10.1111/mmi.13734.

Zhang, Y., Mooney, R.A., Grass, J.A., Sivaramakrishnan, P., Herman, C., Landick, R., et al. (2014). DksA guards elongating RNA polymerase against ribosome-stalling-induced arrest. *Mol Cell* 53(5)**,** 766-778. doi: 10.1016/j.molcel.2014.02.005.

Tables

Table 2-1. Strains and plasmids used

Plasmid	Strain	Characteristics
-	*ΔMSMEG_2952*[1]	*mc²155, MSMEG2952::hyg*^{r}
pSS303	SS-M_0486	p_{myc1}*tetO* promoter + p_{myc1} 5' UTR + *yfp-6xHis*
pSS309	SS-M_0489	p_{myc1}*tetO* promoter + *sigA* 5' UTR + first 54 nt of *sigA* + *yfp-6xHis*
pSS310	SS-M_0493	p_{myc1}*tetO* promoter + no 5' UTR + *yfp-6xHis*
pSS314	SS-M_0497	p_{myc1}*tetO* promoter with a deletion of nt -53 through -1 + *yfp-6xHis*
pSS316	SS-M_0521	p_{myc1}*tetO* promoter + Δ1GTG *sigA* + first 54 nt of *sigA* + *yfp-6xHis*
pSS335	SS-M_0524	p_{myc1}*tetO* promoter + Δ2GTG *sigA* + first 54 nt of *sigA* + *yfp-6xHis*
pSS359	SS-M_0623	p_{myc1}*tetO* promoter + p_{myc1} 5' UTR + first 54 nt of *sigA* + *yfp-6xHis*
pSS360	SS-M_0626	p_{myc1}*tetO* promoter + no 5' UTR + first 54 nt of *sigA* + *yfp-6xHis*
pSS365	SS-M_0629	p_{myc1}*tetO* promoter with a deletion of nt -53 through -1 + first 54 nt of *sigA* + *yfp-6xHis*
pSS384	SS-M_0636	p_{myc1}*tetO* promoter with a deletion of nt -53 through -1 + *sigA* 5' UTR + first 54 nt of *sigA* + *yfp-6xHis*
pSS385	SS-M_0639	p_{myc1}*tetO* promoter with a deletion of nt -53 through -1 + p_{myc1} 5' UTR + first 54 nt of *sigA* + *yfp-6xHis*

[1] Strain source: (Yang et al., 2017)

Table 2-2. Primers for qPCR

Primer name	Gene	Directionality	Sequence 5' → 3'
JR273*	*sigA* (msmeg_2758)	Forward	GACTACACCAAGGGCTACAAG
JR274*	*sigA* (msmeg_2758)	Reverse	TTGATCACCTCGACCATGTG
SSS833	*yfp*	Forward	GATAGCACTGAGAGCCTGTT
SSS834	*yfp*	Reverse	CTGAACTTGTGGCCGTTTAC

*Sequence source: (Rock et al., 2017).

Supplemental Table

Table S1. *Mycobacterium tuberculosis* and *M. smegmatis* 5' UTR information

This table can be accessed online:

https://jb.asm.org/highwire/filestream/303803/field_highwire_adjunct_files/1/JB.00746-19-sd001.xlsx

Supplemental Figures

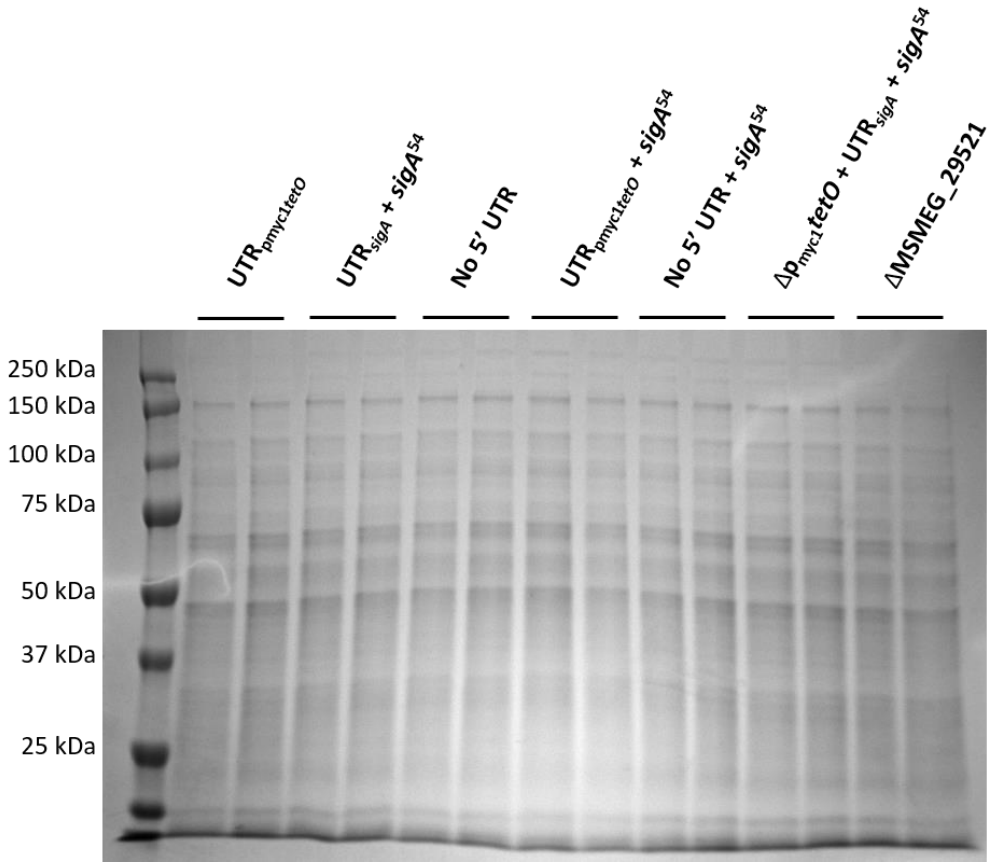

Figure S2-1. Expression of YFP constructs does not appear to globally affect protein levels in *M. smegmatis*. Coomassie stained gel loaded with duplicate lysates from strains expressing the indicated YFP constructs (first six strains) or from the parental strain into which the YFP constructs were transformed (last strain). YFP is approximately 27 kDa and does not appear to be expressed at high enough levels to be visible by Coomassie staining.

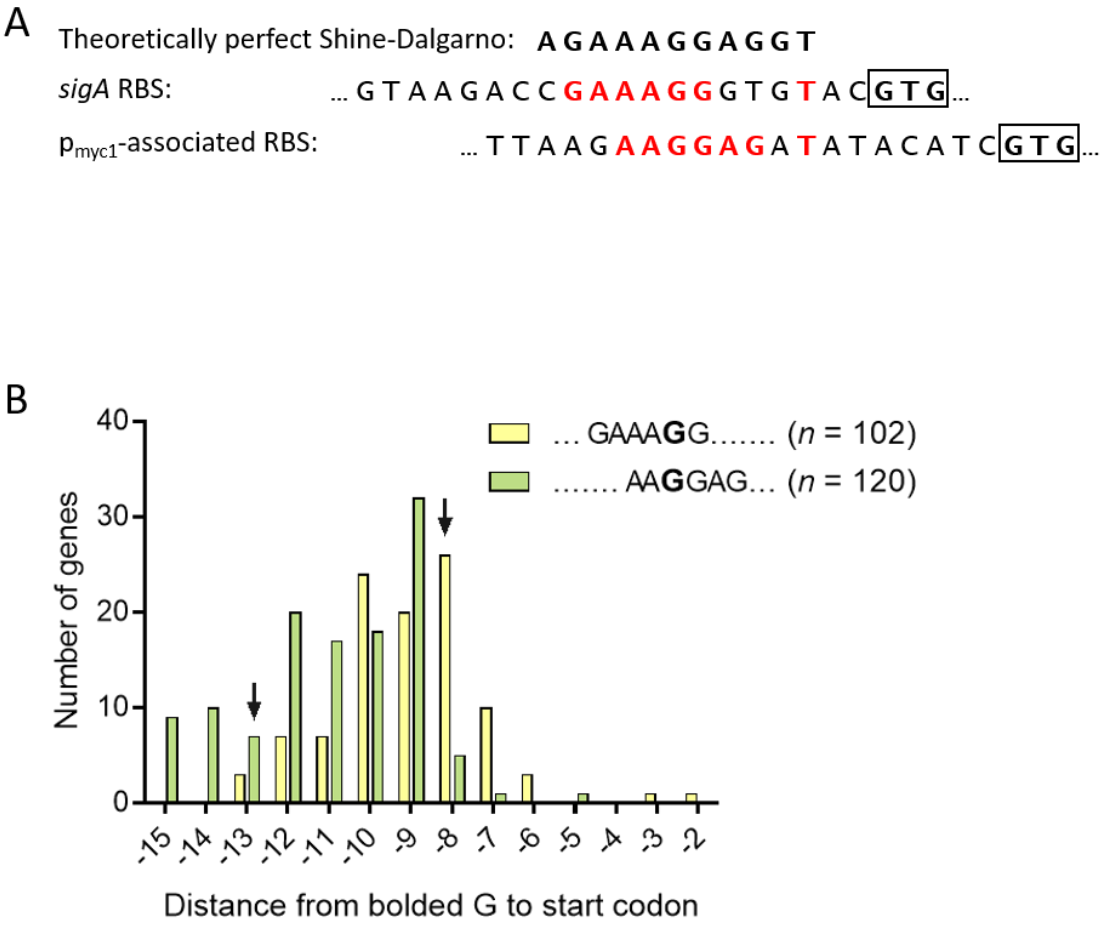

Figure S2-2. Comparison of Shine-Dalgarno (SD) sequences and predicted secondary structures for the *sigA* 5' UTR and the p_{myc1}*tetO*-associated 5' UTR. (A) The *sigA* and p_{myc1}*tetO*-associated RBSs are shown aligned to the reverse complement of the 3' end of the *M. smegmatis* 16S rRNA. Positions that match this theoretically perfect SD sequence are highlighted in red. Start codons are bolded and boxed. (B) Distributions of SD-start codon spacings for all genes that have the indicated SD sequences in the *M. smegmatis* genome. Yellow indicates the *sigA* SD sequence and green indicated the p_{myc1}*tetO*-associated SD sequence. Black arrows indicate the SD-start codon spacings for the *sigA* and p_{myc1}*tetO*-associated SD sequences. (C-D) Ensemble centroid predictions using Sfold (Ding et al, 2004) for secondary structures formed by the $p_{myc1tetO}$-associated (C) and *sigA* (D) 5' UTRs plus the first 15 nt of the *sigA* coding sequence. The predicted core SD sequences are highlighted in red. Start codons are highlighted in gray. The structures of the RBS regions were predicted to be the same when folding was performed using only the UTRs and start codons or using the UTRs and 54 nt of the *sigA* coding sequence.

(continued on next page)

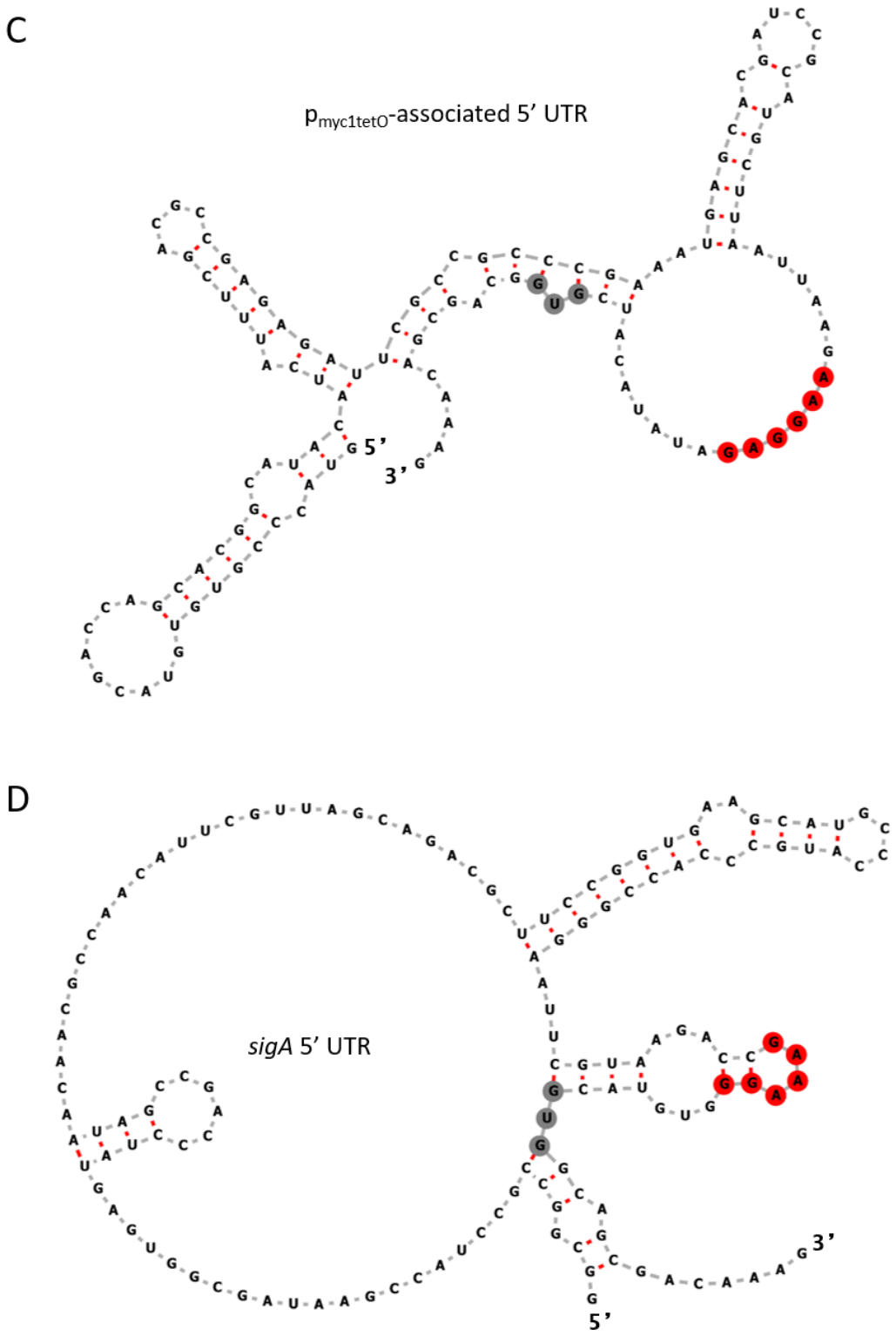

Figure S2. (Continued)

A

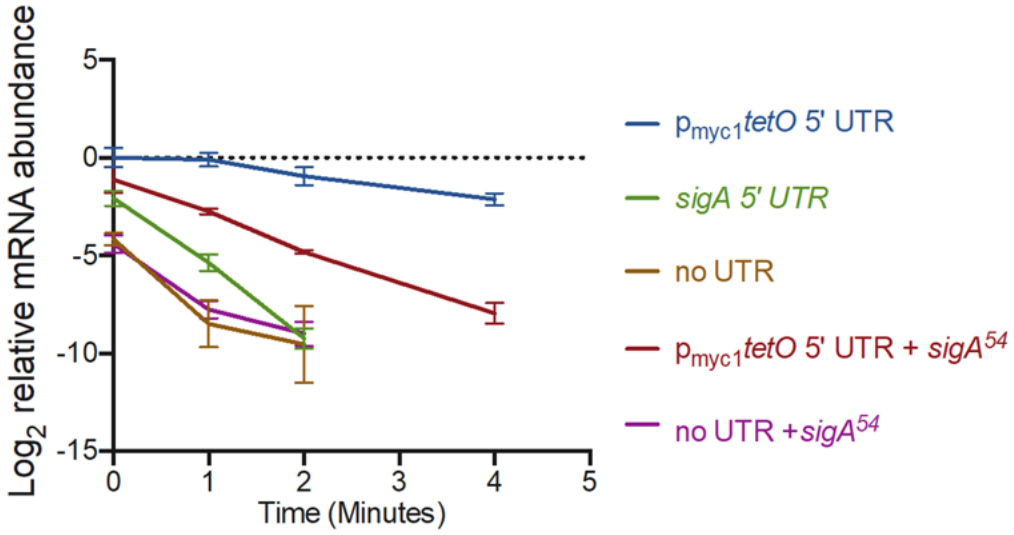

B

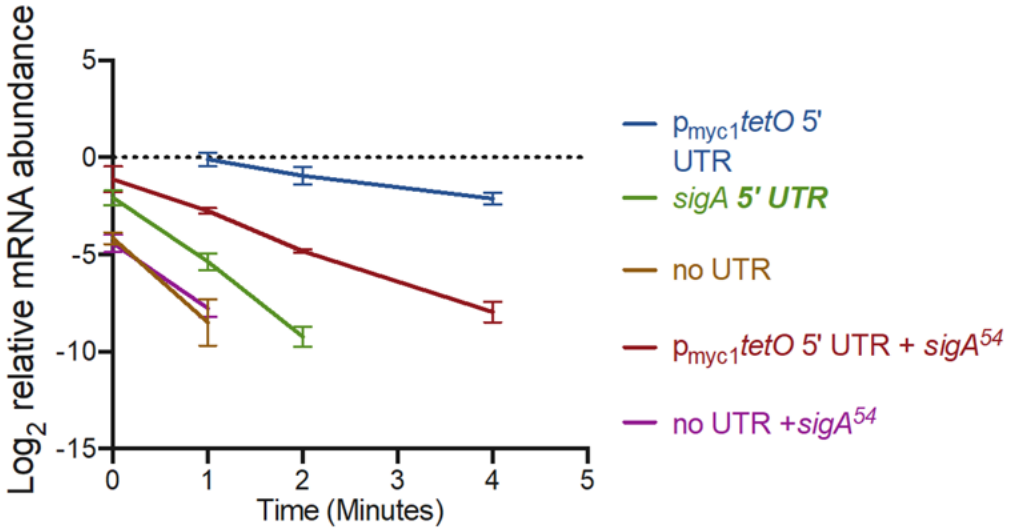

Figure S2-3. mRNA decay curves used to calculate the half-lives reported in the main text. (A) Quantitative PCR was used to measure *yfp* abundance following treatment of *M. smegmatis* cultures with 150 □g/mL rifampicin at time zero. The values displayed are normalized to the time zero abundance for the $p_{myc1}^{tetO5'UTR}$ construct and log_2 transformed. A single exponential decay is expected to produce a strain line for log_2 transformed values. In the main text we discuss possible reasons for the biphasic curves produced by some constructs. (B) The time-points used for calculating half-lives. The steepest portion of each curve was used, which in most cases was the earlier time-points. As further discussed in the main text, we predicted that the earlier, steeper decay rates were most likely to reflect the decay rates of the majority of the RNA molecules in cells not perturbed by rifampin.

Chapter 3 : mRNA Degradation Rates Are Coupled to Metabolic Status in *Mycobacterium smegmatis*

mRNA Degradation Rates Are Coupled to Metabolic Status in *Mycobacterium smegmatis*

Diego A. Vargas-Blanco[1], Ying Zhou[1], L. Gregory Zamalloa[1], Tim Antonelli[2], Scarlet S. Shell[1,3]

[1]Department of Biology and Biotechnology, Worcester Polytechnic Institute, Worcester, MA, USA
[2]Department of Mathematics, Worcester State University, Worcester, Massachusetts, USA
[3]Program in Bioinformatics and Computational Biology, Worcester Polytechnic Institute, Worcester, MA, USA
Edited by: Daniel Barkan. Hebrew University of Jerusalem, Israel

This chapter corresponds to a manuscript that was published as:

Vargas-Blanco, D.A., Zhou, Y., Zamalloa, L.G., Antonelli, T., and Shell, S.S. (2019). mRNA Degradation Rates Are Coupled to Metabolic Status in *Mycobacterium smegmatis*. *mBio* 10(4). doi: 10.1128/mBio.00957-19.

Author Contributions

Conceptualization: D.A.V.-B. and S.S.S. Methodology: D.A.V.-B. and Y.Z. Part of the experiments in Figure 3 were performed by L.G.Z. Data Analysis: D.A.V.-B., T.A., and S.S.S. Writing – Original Draft: D.A.V.-B and S.S.S. Writing – Review and Editing: D.A.V.-B, and S.S.S.

Abstract

The success of *Mycobacterium tuberculosis* as a human pathogen is due in part to its ability to survive stress conditions, such as hypoxia or nutrient deprivation, by entering non-growing states. In these low-metabolism states, *M. tuberculosis* can tolerate antibiotics and develop genetically encoded antibiotic resistance, making its metabolic adaptation to stress crucial for survival. Numerous bacteria, including *M. tuberculosis*, have been shown to reduce their rates of mRNA degradation under growth limitation and stress. While the existence of this response appears to be conserved across species, the underlying bacterial mRNA stabilization mechanisms remain unknown. To better understand the biology of non-growing mycobacteria, we sought to identify the mechanistic basis of mRNA stabilization in the

nonpathogenic model *Mycobacterium smegmatis*. We found that mRNA half-life was responsive to energy stress, with carbon starvation and hypoxia causing global mRNA stabilization. This global stabilization was rapidly reversed when hypoxia-adapted cultures were re-exposed to oxygen, even in the absence of new transcription. The stringent response and RNase levels did not explain mRNA stabilization, nor did transcript abundance. This led us to hypothesize that metabolic changes during growth cessation impact the activities of degradation proteins, increasing mRNA stability. Indeed, bedaquiline and isoniazid, two drugs with opposing effects on cellular energy status, had opposite effects on mRNA half-lives in growth-arrested cells. Taken together, our results indicate that mRNA stability in mycobacteria is not directly regulated by growth status but rather is dependent on the status of energy metabolism.

IMPORTANCE. The logistics of tuberculosis therapy are difficult, requiring multiple drugs for many months. *Mycobacterium tuberculosis* survives in part by entering non-growing states in which it is metabolically less active and thus less susceptible to antibiotics. Basic knowledge on how *M. tuberculosis* survives during these low-metabolism states is incomplete, and we hypothesize that optimized energy resource management is important. Here, we report that slowed mRNA turnover is a common feature of mycobacteria under energy stress but is not dependent on the mechanisms that have generally been postulated in the literature. Finally, we found that mRNA stability and growth status can be decoupled by a drug that causes growth arrest but increases metabolic activity, indicating that mRNA stability responds to metabolic status rather than to growth rate *per se*. Our findings suggest a need to reorient studies of global mRNA stabilization to identify novel mechanisms that are presumably responsible.

Introduction

Most bacteria periodically face environments that are unfavorable for growth. To overcome such challenges, bacteria must tune their gene expression and energy usage. Regulation of mRNA turnover can contribute to both of these. However, the mechanisms by which mRNA turnover is carried out and regulated remain poorly understood, particularly in mycobacteria.

During infection, the human pathogen *Mycobacterium tuberculosis* faces not only the immune response and antibiotics but also non-optimal microenvironments, such as hypoxia and starvation (Via et al., 2008; Belton et al., 2016). Regulation of mRNA turnover appears to contribute to adaptation to such conditions. A global study of mRNA decay in *M. tuberculosis* showed a dramatic increase in transcriptome stability (increased mRNA half-lives) in response to hypoxia, compared to that with aerobic growth (Rustad et al., 2013). This suggests that mRNA stabilization contributes to energy conservation in the energy-limited environments that *M. tuberculosis* encounters during infection. Similar responses have been shown for other bacteria under conditions that slow or halt growth, including carbon deprivation, stationary phase, and temperature shock (Albertson et al., 1990; Georgellis et al., 1993; Sakamoto and Bryant, 1997; Thorne and Williams, 1997; Redon et al., 2005; Anderson et al., 2006; Dressaire et al., 2013; Esquerre et al., 2014; Chen et al., 2015; Ignatov et al., 2015). However, the mechanisms responsible for global regulation of mRNA stability in prokaryotes remain unknown.

A conventional model for RNA decay in *Escherichia coli* starts with endonucleolytic cleavage by RNase E, particularly in 5'-end-monophosphorylated mRNAs (Tomcsanyi and Apirion, 1985; Bouvet and Belasco, 1992; McDowall et al., 1994). The resulting fragments are further cleaved by RNase E, producing fragments that are fully degraded by exonucleases, such as polynucleotide phosphorylase (PNPase), RNase II, and RNase R (Apirion and Gitelman, 1980; Donovan and Kushner, 1986). mRNA degradation is coordinated by the formation of a complex known as the degradosome. In *E. coli*, RNase E serves as the

scaffold for degradosomes containing RNA helicases, the glycolytic enzyme enolase, and PNPase (Carpousis et al., 1994; Py et al., 1994; Miczak et al., 1996; Py et al., 1996; Grunberg-Manago, 1999). Other organisms that encode RNase E form similar degradosomes (Vanzo et al., 1998; Ait-Bara and Carpousis, 2010). In bacteria lacking RNase E, other endonucleases assume the scaffold function (Commichau et al., 2009; Roux et al., 2011; Redko et al., 2013). Mycobacteria encode RNase E, but efforts to define the mycobacterial degradosome have produced inconsistent results (Kovacs et al., 2005; Csanadi et al., 2009). It is unclear if degradosome reorganization or dissolution contribute to the global regulation of mRNA degradation in any bacteria. Interestingly, the importance of degradosome formation in *E. coli* varies depending on the carbon sources provided, suggesting links between RNA degradation and metabolic capabilities (Tamura et al., 2013). Furthermore, the chaperones DnaK and CsdA associate with degradosomes in *E. coli* under certain stresses (Miczak et al., 1996; Prud'homme-Genereux et al., 2004; Regonesi et al., 2006).

Global transcript stabilization in stressed bacteria may plausibly result from reduced RNase abundance, reduced RNase activity, and/or reduced accessibility of transcripts to degradation proteins. In *E. coli*, multiple stressors upregulate RNase R, possibly to mitigate ribosome misassembly (Chen and Deutscher, 2005; 2010), and RNase III levels decrease under cold shock and stationary phase (Kim et al., 2008). Surprisingly, protein levels for most putative RNA degradation proteins in *M. tuberculosis* remain unaltered under hypoxic conditions (Schubert et al., 2015), suggesting that mRNA degradation is not necessarily regulated at the level of RNase abundance in mycobacteria. However, there is evidence that RNase activity may be regulated. For example, proteins such as RraA and RraB can alter the function of the RNase E-based degradosome in *E. coli* (Gao et al., 2006). Translating ribosomes can mask mRNA cleavage sites and stabilize mRNAs (Iost et al., 1992). In *Caulobacter crescentus*, subcellular localization of mRNA degradation proteins may affect global mRNA stability (Russell and Keiler, 2009; Bayas et al., 2018).

Furthermore, in some actinomycetes, PNPase might be regulated by the stringent response alarmones guanosine-3'-diphosphate-5'-triphosphate (pppGpp) and/or guanosine-3',5'-bisphosphate (ppGpp), collectively referred to as (p)ppGpp (Gatewood and Jones, 2010; Siculella et al., 2010). Many bacteria synthesize (p)ppGpp in response to energy stress (Battesti and Bouveret, 2006; Atkinson et al., 2011; Frederix and Downie, 2011; Corrigan et al., 2016), where it generally facilitates adaptation by upregulating stress-associated genes and downregulating those associated with growth (Gentry et al., 1993; Chakraburtty and Bibb, 1997; Martinez-Costa et al., 1998; Avarbock et al., 2000; Artsimovitch et al., 2004; Corrigan et al., 2016). (p)ppGpp was reported to inhibit the activity of PNPase in two actinomycetes, *Streptomyces coelicolor* and *Nonomuraea* (Gatewood and Jones, 2010; Siculella et al., 2010), suggesting that the stringent response may directly stabilize mRNA as part of a broader response to energy starvation.

Another explanation for stress-induced transcript stabilization may be that reduced transcript abundance directly leads to increased transcript stability. mRNA abundance and half-life were reported to be inversely correlated in multiple bacteria, including Mtb (Bernstein et al., 2002; Redon et al., 2005; Rustad et al., 2013; Nouaille et al., 2017), and mRNA abundance is lower on a per-cell basis for most transcripts in non-growing bacteria. Nevertheless, the causal relationships between translation, mRNA abundance, RNase expression, and mRNA stability in non-growing bacteria remain largely untested.

Given the importance of adaptation to energy starvation for mycobacteria, we sought to investigate the mechanisms by which mRNA stability is globally regulated. Here, we show that the global mRNA stabilization response occurs also in *Mycobacterium smegmatis*—a non-pathogenic model commonly used to study the basic biology of mycobacteria —under hypoxia and carbon starvation. Remarkably, we found that hypoxia-induced mRNA stability is rapidly reversible, with reaeration causing immediate mRNA destabilization even in the absence of protein synthesis. As expected, transcript levels from hypoxic cells

were lower on a per-cell basis than those from aerated cultures. However, our data are inconsistent with a model in which mRNA abundance dictates the degradation rate, as has been shown for log-phase *E. coli* (Bernstein et al., 2002) and *Lactococcus lactis* (Nouaille et al., 2017). Instead, our findings support the idea that mRNA stability is rapidly tuned in response to alterations in energy metabolism. This effect does not require the stringent response or changes in abundance of RNA degradation proteins and can be decoupled from growth status.

Results

mRNA is stabilized as a response to carbon starvation and hypoxic stress in *Mycobacterium smegmatis.*

The mRNA pools of *E. coli* and other well-studied bacteria were reported to be globally stabilized during conditions of stress, resulting in increased mRNA half-lives (Albertson et al., 1990; Georgellis et al., 1993; Sakamoto and Bryant, 1997; Thorne and Williams, 1997; Redon et al., 2005; Anderson et al., 2006; Dressaire et al., 2013; Rustad et al., 2013; Esquerre et al., 2014; Chen et al., 2015; Ignatov et al., 2015). Rustad *et al.* reported a similar phenomenon in *M. tuberculosis* under hypoxia and cold shock (Rustad et al., 2013). We sought to establish *M. smegmatis* as a model for study of the mechanistic basis of mRNA stabilization in mycobacteria under stress conditions. We therefore subjected *M. smegmatis* to hypoxia and carbon starvation and measured mRNA half-lives for a subset of genes by blocking transcription with rifampin (RIF) and measuring mRNA abundance at multiple time points using quantitative PCR (qPCR). We used a variation of the Wayne and Hayes model (Wayne and Hayes, 1996) to produce a gradual transition from aerated growth to hypoxia-induced growth arrest by sealing cultures in vials with defined headspace ratios and allowing them to slowly deplete the available oxygen (Figure 3-1A and B). We tested a set of mRNAs that included transcripts with and without leaders, monocistronic and polycistronic transcripts, and transcripts with both relatively short and relatively long half-lives in log phase. We observed that all

of the analyzed transcripts had increased half-lives under hypoxia compared to those of log-phase normoxic cultures, and similarly, transcripts were more stable under carbon starvation than in rich media (Figure 3-1C and D).

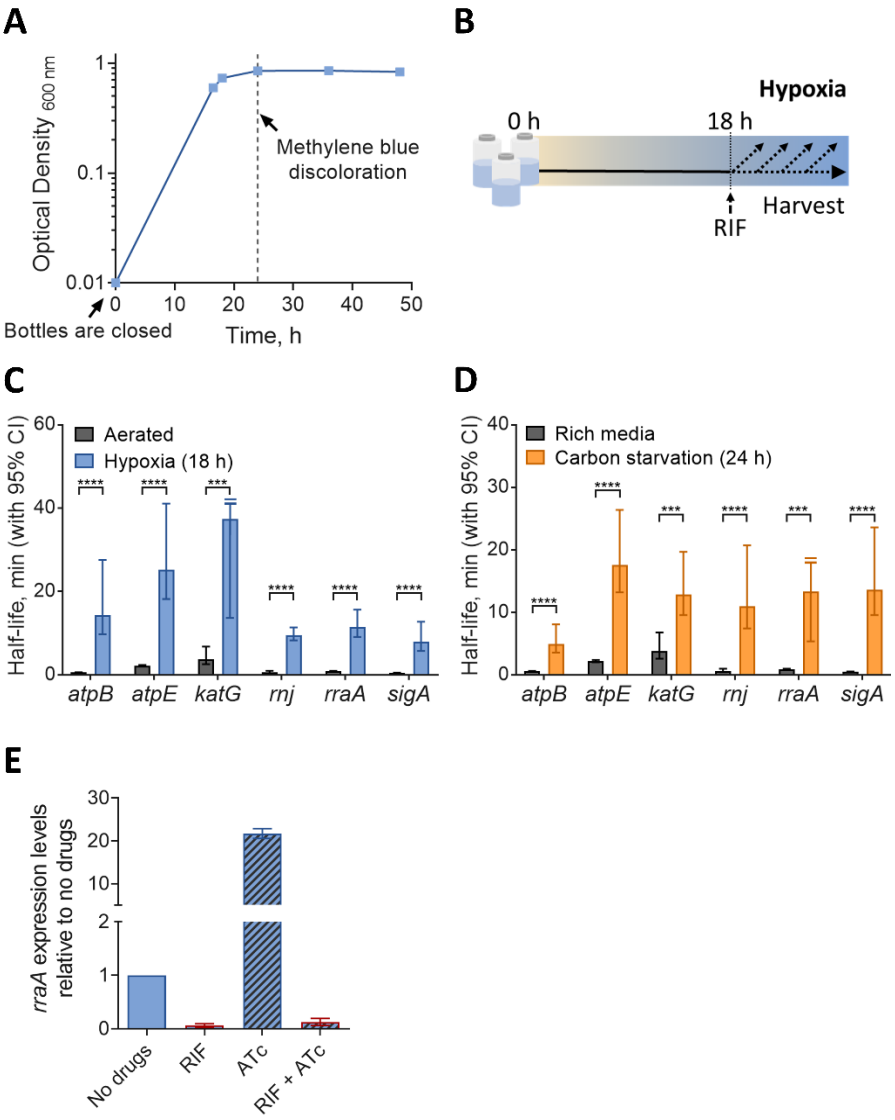

Figure 3-1. Transcript half-lives are increased in response to hypoxia and carbon starvation stress. (A) Growth kinetics for *M. smegmatis* under hypoxia using a variation of the Wayne and Hayes model (Wayne and Hayes, 1996), showing OD stabilization at 18 to 24 h. Oxygen depletion was assessed qualitatively by methylene blue discoloration. (B) *M. smegmatis* was sealed in vials to produce a hypoxic environment, and at 18 h, transcription was inhibited with RIF, and samples were collected thereafter. Transcript half-lives for the indicated genes were measured for *M. smegmatis* mc^{2}155 after blocking transcription with 150 µg/mL RIF. (C and D) RNA samples were collected during log-phase normoxia and hypoxia (18 h after closing the bottles) (C) or during log phase in 7H9 supplemented with ADC, glycerol, and Tween 80 (rich medium) or 7H9 with Tyloxapol only (carbon starvation, 24 h).

(continued on next page)

Thus, *M. smegmatis* appears to be a suitable model for investigating the mechanisms of stress-induced mRNA stabilization in mycobacteria. To ensure that the apparent mRNA stabilization was not an artifact of reduced RIF activity in non-growing cells, we confirmed that RIF indeed blocked transcription in hypoxia-arrested *M. smegmatis* (Figure 3-1E). We noted that transcripts became progressively more stable as oxygen levels dropped and growth ceased; 40 h after sealing the vials, mRNA half-lives were too long to be reliably measured by our methodology. We sought to focus our studies on the mechanisms that underlie the initial mRNA stabilization process during the transition into hypoxia-induced growth arrest. We therefore conducted most of our subsequent experiments 18 to 24 h after sealing the vials, when growth had nearly ceased and transcripts were 9-fold to 25-fold more stable than during log phase. We refer to these conditions as 18-h hypoxia and 24-h hypoxia.

(p)ppGpp does not contribute to mRNA stabilization under hypoxia or carbon starvation.

Given recent reports that (p)ppGpp may directly inhibit the enzymatic activity of the exoribonuclease PNPase (Gatewood and Jones, 2010; Siculella et al., 2010), we wondered whether mRNA stabilization as observed under carbon starvation and hypoxia is regulated by (p)ppGpp in mycobacteria. We obtained a double mutant strain of *M. smegmatis* (Weiss and Stallings, 2013) that lacks both genes implicated in the production of (p)ppGpp (*Δrel Δsas2*) and compared the mRNA half-lives of a subset of genes to those of wild-type mc^2155 under hypoxia, log-phase normoxia, and carbon starvation.

Figure 3-1. Legend (Continued)

(D). mRNA degradation rates were compared using linear regression ($n=3$), and half-lives were determined by the negative reciprocal of the best-fit slope. Error bars are 95% confidence intervals (CI). ***, $P<0.001$; ****, $P<0.0001$. When a slope of zero was included in the 95% CI (indicating no degradation), the upper limit for half-life was unbounded, indicated by a clipped error bar with a double line. (E) RIF blocks overexpression of an ATc-inducible gene (*rraA*) in hypoxic cultures. Forty hours after the bottles were sealed, cultures were treated with 50 ng/mL ATc and/or 150 µg/mL RIF or the drug vehicle (DMSO) for 1 h. Expression levels (qPCR) are displayed relative to those with no drugs (DMSO treatment). ATc, RIF, and DMSO solutions were degassed prior to addition. Error bars are standard deviations (SD).

The *Δrel Δsas2* strain had a growth defect during adaptation to hypoxia and carbon starvation (Figure 3-2A and C), as predicted (Dahl et al., 2005). However, we found no significant decrease in mRNA stabilization in the mutant strain (Figure 3-2B and D), indicating that the mRNA stabilization observed under hypoxia and carbon starvation is independent from the stringent response. Interestingly, the mutant strain displayed increased mRNA stabilization for a few transcripts under carbon starvation conditions, which may be an indirect consequence of altered transcription rates (see Discussion).

Hypoxia-induced mRNA stability is reversible and independent of mRNA abundance.

We wondered if the observed stress-induced transcript stabilization could be reversed by restoration of a favorable growth environment. To test this, we prepared 18-h hypoxia cultures, opened the vials, and agitated them for 2 min to reexpose the bacteria to oxygen before blocking transcription with RIF and sampling thereafter (Figure 3-3A, top). We found that, for all transcripts tested, half-lives were significantly decreased compared to those observed under hypoxia and similar to those observed in log phase (Figure 3-3B). While the mechanisms of stress-induced mRNA stabilization are largely unknown, multiple studies have reported inverse correlations between mRNA abundance and half-life in bacteria (Bernstein et al., 2002; Redon et al., 2005; Rustad et al., 2013; Nouaille et al., 2017). mRNA abundance was decreased for most transcripts tested in hypoxia-adapted *M. smegmatis*. We therefore considered the possibility that the dramatic increase in mRNA degradation upon reexposure to oxygen was triggered by a burst of transcription. Indeed, we found increased expression levels for four of five genes tested after 2 min of reaeration, showing that transcription is rapidly induced upon return to a favorable environment (Figure 3-3C). To test the idea that mRNA is destabilized by reaeration as a consequence of a transcriptional burst and/or increased mRNA abundance, we modified our reaeration experiment by blocking transcription with RIF 1 min prior to reaeration (Figure 3-3A).

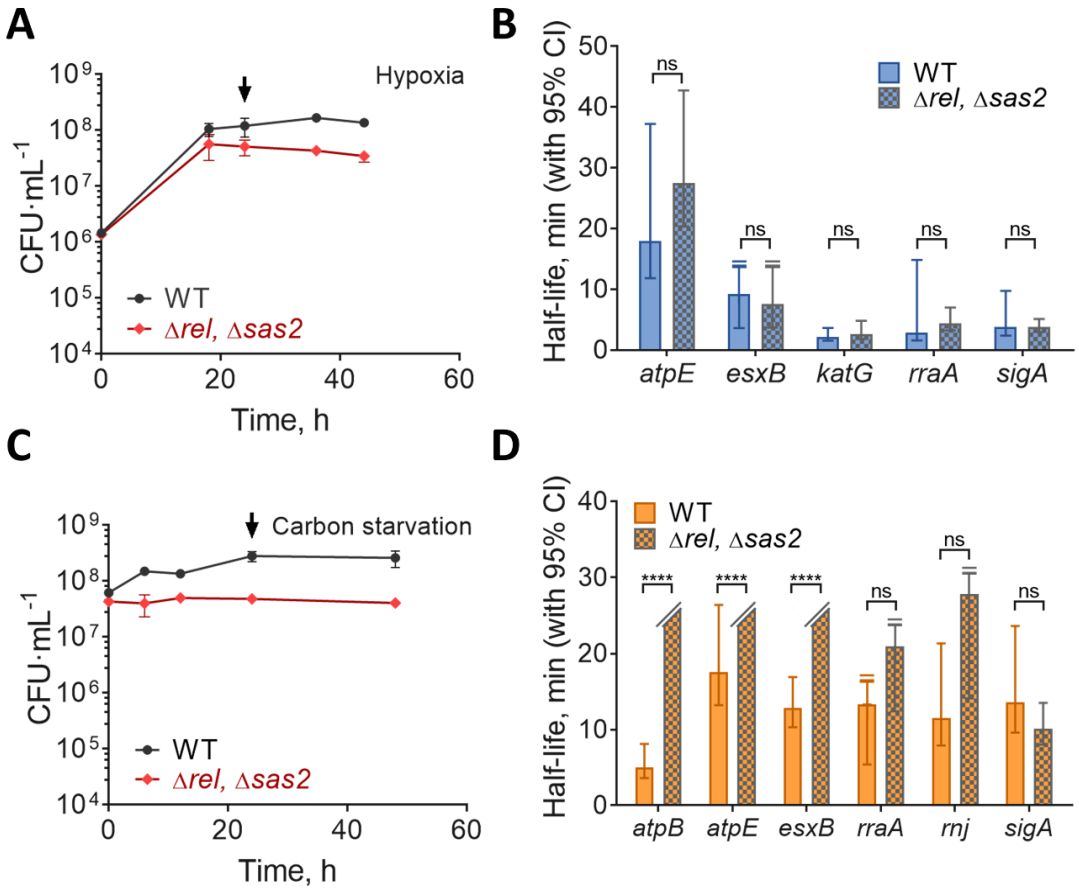

Figure 3-2. Transcript stabilization in hypoxia and carbon starvation are not dependent on the stringent response. (A) Growth kinetics for *M. smegmatis* mc^{2}155 (wild type [WT]) and Δ*rel* Δ*sas2* strains cultured in 7H9 in flasks sealed at time zero. (B) Transcript half-lives for a set of genes 24 h after sealing of the hypoxia bottles (arrow in panel A). RNA samples were collected after transcription was blocked with 150 µg/mL RIF (degassed). (C) Bacteria were grown to log phase in 7H9 supplemented with ADC, glycerol, and Tween 80 and then transferred to 7H9 supplemented with only Tyloxapol at time zero. (D) Transcript stability for a set of genes 22 h after transfer to carbon starvation medium (arrow in panel C). (A and C) The means and SD of triplicate cultures are shown. (B and D) Half-lives were compared using linear regression analysis (n=3). Error bars are 95% CI. ****, P<0.0001; ns, not significant (P>0.05). In cases where no degradation was observed or when the upper 95% CI limit was unbounded, the bar or upper error bar were clipped, respectively.

Surprisingly, every transcript tested was destabilized by reaeration despite the absence of new transcription. For most transcripts, the reaeration half-lives were indistinguishable, regardless of whether RIF was added prior to opening the vials or 2 min after (Figure 3-3B). Our results therefore do not support the idea that changes in mRNA abundance alone can explain the mRNA stabilization and destabilization observed in response to changes in energy status.

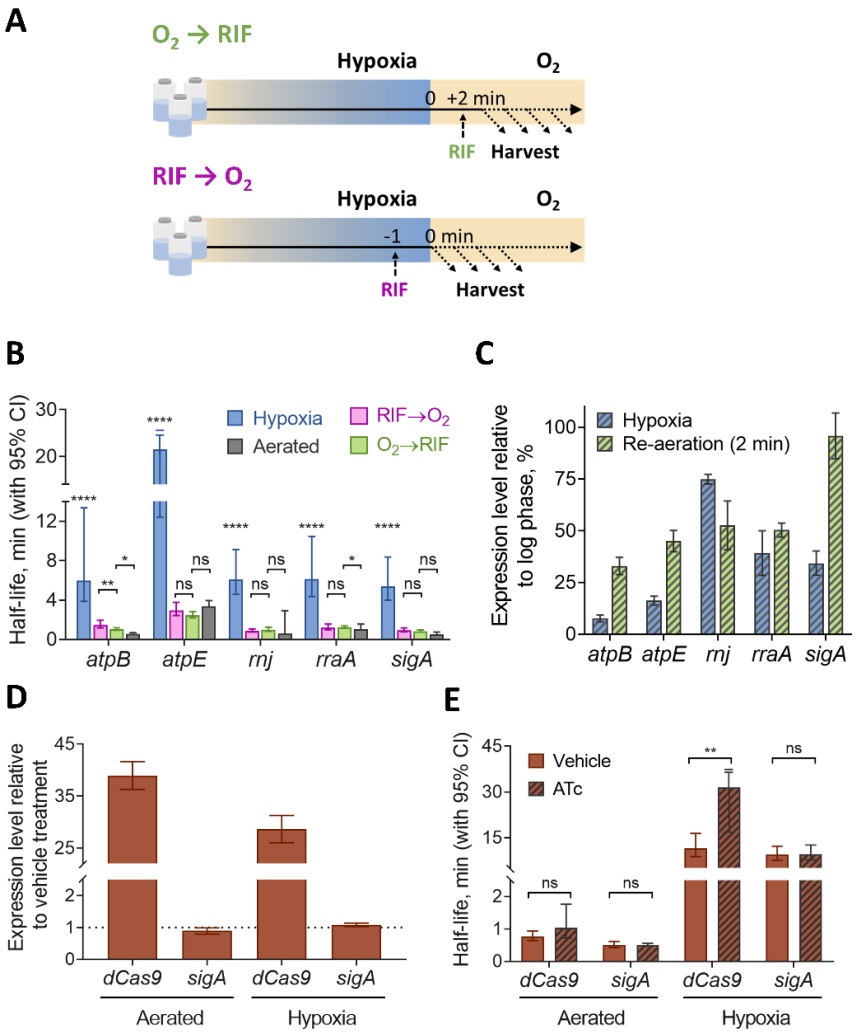

Figure 3-3. Hypoxia-induced mRNA stability is reversible and independent of mRNA abundance. (A) *M. smegmatis* was sealed in vials for 18h to produce a hypoxic environment and then reexposed to oxygen for 2 min before transcription was inhibited with RIF (top) or injected with RIF 1 min prior to opening of the vials and reexposing them to oxygen (bottom). (B) Transcript half-lives for a set of genes are displayed for log-phase normoxia cultures, hypoxia (18h), and reaeration with RIF added either before or after opening of the vials. Half-lives were compared by linear regression analysis (n=3). (C) Expression levels of transcripts under hypoxia (18h) or with a 2-min reaeration relative to the expression levels in log-phase normoxia cultures (percentages). Error bars are SD. (D) Expression levels of transcripts under hypoxia (18h) or log-phase normoxia after being treated with 200ng/mL ATc for 1h or 10min, respectively, to induce *dCas9* overexpression, relative to the expression levels in cultures treated with an H_2O vehicle (percentages). Error bars are SD. (E) Transcript half-lives for *dCas9* and *sigA* for log-phase normoxia and hypoxia (18h) after induction of *dCas9* with ATc or after vehicle treatment as shown in panel D. (B and E) Degradation rates were compared using linear regression (n=3), and half-lives were determined by the negative reciprocal of the best-fit slope. Error bars are 95% CI. *, P<0.05; **, P<0.01; ****, P<0.0001; ns, P>0.05. RIF added to hypoxic cultures was degassed prior to its addition.

We wanted to further explore whether mRNA abundance alone could influence transcript degradation. We obtained a strain bearing *dCas9* and a nonspecific sgRNA under the control of an anhydrotetracycline (ATc)-inducible promoter (Rock et al., 2017) and compared the *dCas9* transcript stability under hypoxia and normoxia after ATc induction or at basal levels. We found that despite a 34-fold transcript upregulation following ATc induction, the half-life of *dCas9* mRNA was not significantly different from that of the uninduced control in log phase. Under hypoxia, its 28-fold upregulation was associated with an increase in *dCas9* mRNA half-life compared to in the no-drug control (Figure 3-3D and E). Together, our results show that increased mRNA abundance does not necessarily result in a faster decay rate.

mRNA stability is modulated independently of RNase protein levels.

Another potential explanation for increased mRNA degradation after reaeration is the upregulation of mRNA degradation proteins, such as RNase E. To assess the role of a sudden burst in protein levels, we used two approaches. First, we constructed strains encoding FLAG-tagged RNase E, cMyc-tagged PNPase, or cMyc-tagged msmeg_1930 (predicted RNA helicase). We determined protein levels by Western blotting in log phase, with 18 h of hypoxia, and after 18 h of hypoxia followed by 2 min of reaeration. Levels of all three of these predicted RNA degradation proteins remained unchanged under the three conditions (Figure 3-4A).

Because we do not know all of the proteins that contribute to mRNA degradation in mycobacteria, our second approach was to test the global importance of translation in reaeration-induced mRNA destabilization. We blocked translation with chloramphenicol (CAM) in 18-h hypoxia cultures and then added RIF. Samples were collected for cultures that remained under hypoxia as well as those that were reaerated for 2 min (Figure 3-4B). For three of the five genes tested, we found that CAM caused increased mRNA stability under hypoxia. This is consistent with CAM's mechanism of action and published work (Shaila et al., 1973; Wu et al., 2015; Srivastava et al., 2016). CAM inhibits elongation by preventing peptidyl

transfer (Wolfe and Hahn, 1965; Yukioka and Morisawa, 1971; Drainas et al., 1987) and causing ribosomal stalling (Lopez et al., 1998). Global stabilization of mRNA pools has been reported when elongation inhibitors, but not initiation inhibitors, are used for example in log-phase cultures of *E. coli* (Lopez et al., 1998) or in yeast (Chan et al., 2018). We hypothesize that stalled ribosomes may increase mRNA stability by masking RNase cleavage sites. However, despite the stabilization caused by CAM itself, we observed mRNA destabilization in response to reaeration (Figure 3-4C). These results suggest that reaeration-induced destabilization does not require synthesis of new RNA degradation proteins. Taken together, our data suggest that tuning of protein levels is not the primary explanation for mRNA stabilization during early adaptation to hypoxia.

mRNA stability is modulated in response to changes in metabolic status.

The rapidity of mRNA destabilization following reaeration suggested that mRNA degradation is tightly regulated in response to changes in energy metabolism. We tested this hypothesis by treating log-phase cultures with 5 μg/mL bedaquiline (BDQ), a potent inhibitor of the ATP synthase F_oF_1 (Lakshmanan et al., 2013). We used minimal medium that contained acetate as the only carbon source (minimal medium acetate [MMA]) in order to make the respiratory chain the sole source of ATP synthesis. After 30 min of exposure, intracellular ATP levels were reduced by more than 90% compared to levels in cells treated with vehicle (dimethyl sulfoxide [DMSO]), without affecting viability (Figure 3-5A and B).

We then measured half-lives for a set of transcripts under these conditions. mRNA half-lives were dramatically increased in BDQ-treated cells for most of the genes that we tested (Figure 3-5C), indicating that mRNA degradation rates are rapidly altered in response to changes in energy metabolism status.

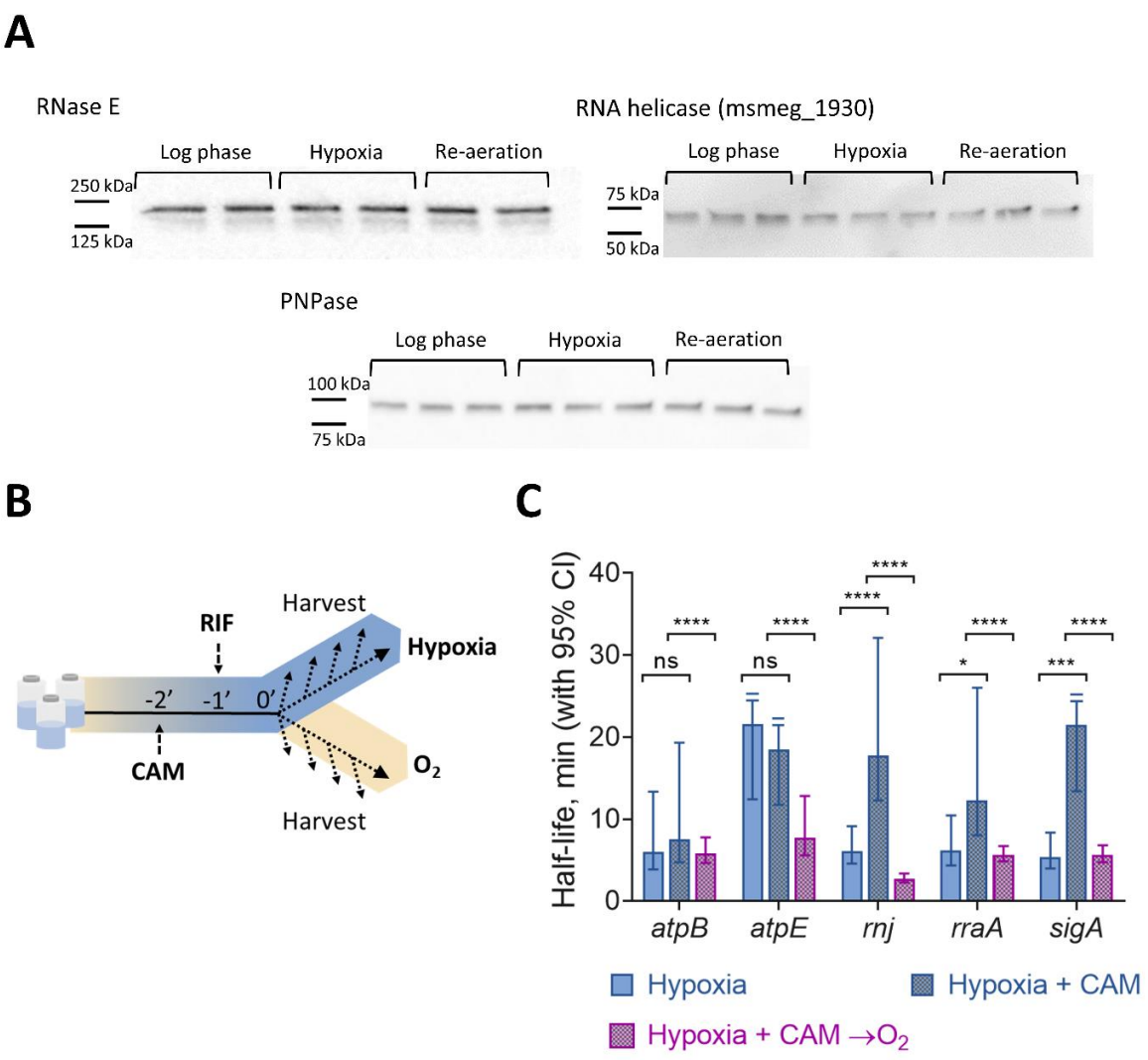

Figure 3-4. mRNA stability is regulated independently of degradation protein levels. (A) Western blotting for FLAG-tagged RNase E and cMyc-tagged PNPase or RNA helicase (msmeg_1930) in *M. smegmatis* under log-phase normoxia and hypoxia (18h) and with a 2-min reaeration. Samples were normalized to the total protein level, and levels were similar on a per-OD basis under all conditions. (B) Translation was inhibited in hypoxic cultures by 150μg/mL CAM 1min before the addition of 150μg/mL RIF. RNA was harvested at time points beginning 2min after the addition of CAM. (C) Transcript half-lives for samples from hypoxic cultures with the drug vehicle (ethanol), for hypoxic cultures after translation inhibition, and for cultures with 2min of reaeration after translation inhibition. Degradation rates were compared using linear regression (n=3), and half-lives were determined by the negative reciprocal of the best-fit slope. Error bars are 95% CI. ns, P>0.05; *, P<0.05; ***, P<0.001; ****, P<0.0001. Drugs and drug vehicles added to the hypoxic cultures were degassed prior to their addition.

We then wondered if we could increase mRNA degradation rates by increasing intracellular ATP levels. To test this, we treated *M. smegmatis* cultures with isoniazid (INH), a prodrug that interferes with the synthesis of mycolic acids and also leads to an accumulation of intracellular ATP due to increased oxidative phosphorylation (Shetty and Dick, 2018). We exposed *M. smegmatis* to 500 μg/mL INH for 6.5 h to confirm that we had achieved bacteriostasis (the *M. smegmatis* doubling time in MMA medium is ∼6 h). As shown in Figure 3-5D, INH caused a dramatic increase in intracellular ATP after 6.5 h without affecting cell viability (Figure 3-5E). Remarkably, mRNA half-lives were significantly decreased in response to INH (Figure 3-5F). To our knowledge, this is the first report of bacterial mRNA being destabilized rather than stabilized in response to a growth-impairing stressor. Our results indicate that mRNA stability is regulated not in response to growth status *per se* but rather to energy metabolism. Although we interpreted ATP levels as a reflection of metabolic status in our INH and BDQ assays, the coupling between mRNA degradation and metabolic status does not appear to be mediated by ATP directly.

To our knowledge, this is the first report of bacterial mRNA being destabilized rather than stabilized in response to a growth-impairing stressor. Our results indicate that mRNA stability is regulated not in response to growth status *per se* but rather to energy metabolism. Although we interpreted ATP levels as a reflection of metabolic status in our INH and BDQ assays, the coupling between mRNA degradation and metabolic status does not appear to be mediated by ATP directly. We measured ATP levels in cultures during the transition to hypoxia-induced growth arrest and found that although ATP levels ultimately decrease under hypoxia as has been reported elsewhere (Rao et al., 2008; Eoh and Rhee, 2013), mRNA stabilization precedes the drop in ATP levels (Figure 3-5G).

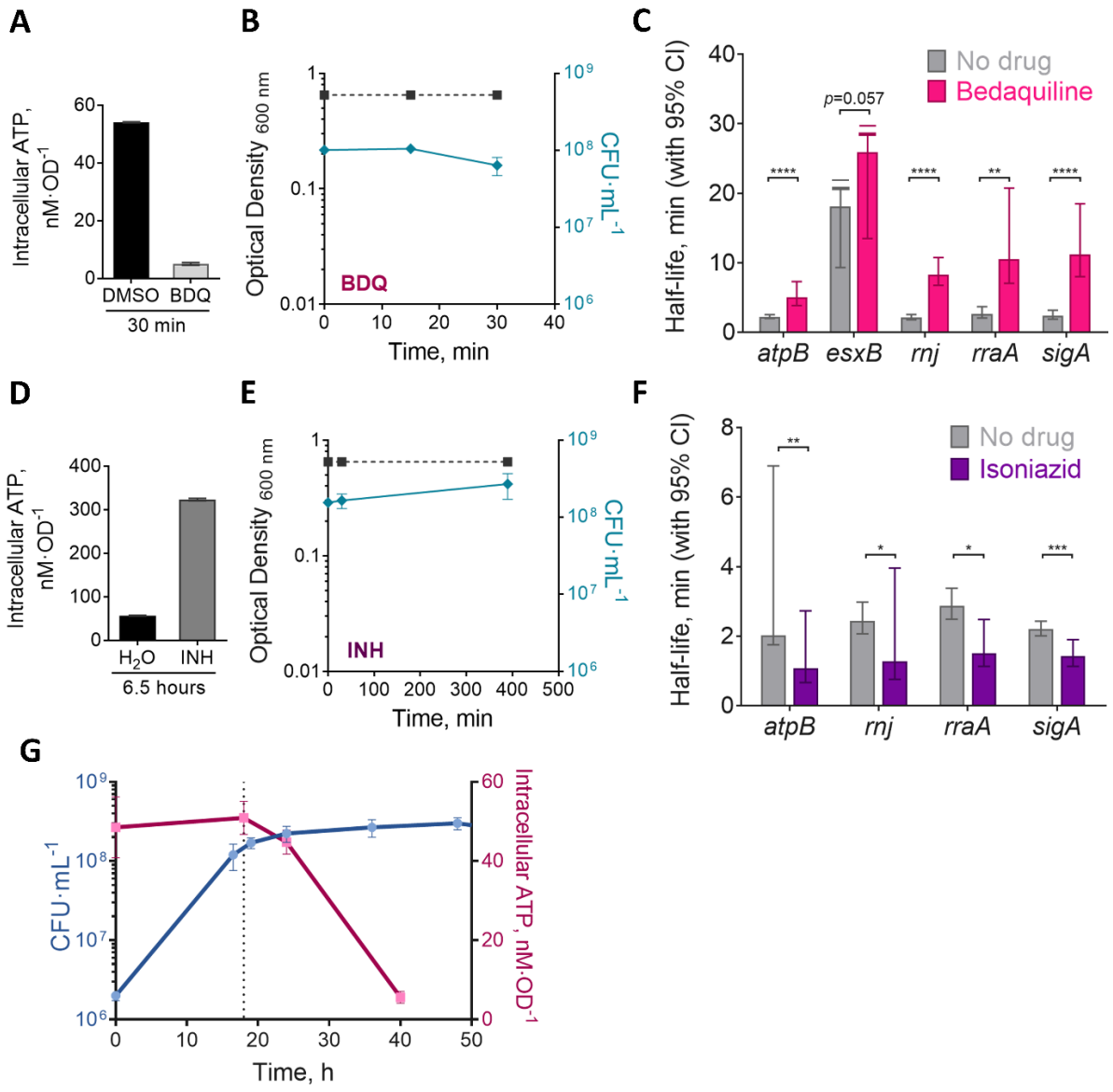

Figure 3-5. mRNA stability is modulated in response to changes in metabolic status. (A) *M. smegmatis* was cultured in MMA media for 22 h to OD_{600} 0.8 before being treated with 5 µg/mL BDQ or the vehicle (DMSO) for 30 min. Intracellular ATP was determined using the BacTiter-Glo kit. (B) Growth kinetics for *M. smegmatis* from panel A in the presence of BDQ. (C) Transcript half-lives for a subset of transcripts collected during intracellular ATP depletion (30 min with BDQ) or at the basal levels (30 min with DMSO). (D) As in panel A, but for *M. smegmatis* treated with 500 µg/mL INH or the vehicle (H_2O) for 6.5 h. (E) Growth kinetics for *M. smegmatis* from panel D in the presence of INH. (F) Transcript half-lives for a subset of transcripts after 6.5 h of INH or vehicle treatment. (G) Growth kinetics for *M. smegmatis* transitioning into hypoxia, and intracellular ATP levels at different stages. Bottles were sealed at time zero. The dotted line represents the time at which transcript stability analyses were made for the hypoxia (18 h) condition for Figure 1, 3, and 4. In C and F, half-lives were compared using linear regression analysis ($n=3$). Error bars are 95% CI. *, $P<0.05$; **, $P<0.01$; ***, $P<0.001$; ****, $P<0.0001$. ATP was measured in biological triplicate cultures and is representative of at least two independent experiments.

Discussion

Stressors that cause bacteria to slow or stop growth are typically associated with increased mRNA stability (Albertson et al., 1990; Georgellis et al., 1993; Sakamoto and Bryant, 1997; Thorne and Williams, 1997; Redon et al., 2005; Anderson et al., 2006; Rustad et al., 2013; Esquerre et al., 2014; Chen et al., 2015; Ignatov et al., 2015). Many of these same stressors reduce energy availability (Rao et al., 2008; Eoh and Rhee, 2013), requiring reductions in energy consumption and optimization of resource allocation. We speculate that the decreased mRNA turnover that accompanies such conditions may be an energy conservation mechanism. For *M. tuberculosis*, hypoxia can lead to generation of bacterial subpopulations with various degrees of antibiotic tolerance (Deb et al., 2009; Kim et al., 2013; Smith et al., 2013), facilitating bacterial survival and the acquisition of drug resistance-conferring mutations. Understanding the mechanisms that support the transitions into non-growing states and subsequent survival in these states is therefore a priority.

The transcriptome of *M. tuberculosis* has been shown to be stabilized under cold shock and hypoxia (Rustad et al., 2013). Here, we found that *M. smegmatis* also dramatically stabilized its mRNA in response to carbon starvation and hypoxia. For the first time, to our knowledge, we tested the speed at which this stabilization is reversed in mycobacteria upon restoration of energy availability. Remarkably, mRNAs are rapidly destabilized within minutes of reaeration of hypoxic cultures, suggesting that tuning of mRNA degradation rates is an early step in the response to changing energy availability.

The most straightforward explanation for stress-induced mRNA stabilization seems to be downregulation of the mRNA degradation machinery. Indeed, RNase E is downregulated at the transcript level under hypoxia, and abundance of cleaved RNAs is reduced (Martini et al., 2019). However, we found that protein levels were unchanged for RNase E and two other proteins predicted to be core components of the mRNA degradation machinery. This is largely consistent with what was reported for *M. tuberculosis* in a

quantitative proteomics study (Schubert et al., 2015), although in that case there was an apparent reduction in levels of an RNA helicase. To address this question in a more agnostic fashion, we tested the importance of translation for transcript destabilization upon reexposure of hypoxic cultures to oxygen. However, reaeration triggered increased transcript degradation even in the absence of new protein synthesis. Regulation of degradation protein levels therefore does not appear to contribute to mRNA stabilization during the initial response to energy stress. However, we found that upon longer periods of hypoxia, transcripts were stabilized to a greater extent than what we observed 18 h after sealing the vials. This suggests that mRNA stabilization progressively increases and may involve multiple mechanisms. As this work focused on the initial transition into hypoxia-induced growth arrest, we cannot discount the possibility that downregulation of the RNA degradation machinery is important for further mRNA stabilization in later hypoxia stages.

Interestingly, we found greater mRNA stabilization in hypoxic cultures treated with CAM. This may result from stalled ribosomes (Wolfe and Hahn, 1965; Drainas et al., 1987) masking RNase cleavage sites. Furthermore, the burst of transcription upon reaeration is blocked by the presence of CAM, causing up to a 4-fold decrease in transcript abundance in the CAM-treated cultures compared to that in the vehicle-treated cultures. This is consistent with the idea that transcription and translation are physically coupled, and blocking translation therefore prevents RNA polymerase from efficiently carrying out transcript elongation, as was reported for *E. coli* (Miller et al., 1970; Burmann et al., 2010; Proshkin et al., 2010; Zhang et al., 2014; Fan et al., 2017). The results obtained from the *Δrel Δsas2* strain are also consistent with the idea that the presence of ribosomes affects mRNA stability. Under carbon starvation, this strain had rRNA levels 3-fold higher than those of the WT strain, consistent with the known role of (p)ppGpp in downregulating ribosome biogenesis (Tedin and Bremer, 1992; Krasny and Gourse, 2004; Stallings et al., 2009). Interestingly, some transcripts were hyperstabilized in the *Δrel Δsas2* strain under carbon

starvation, showing virtually no degradation (**Fig. 2D**). We speculate that the observed mRNA hyperstabilization is caused by increased ribosome abundance, resulting in augmented mRNA-ribosome associations that ultimately protect transcripts from RNases. Alternatively, the increased abundance of rRNA may protect mRNA indirectly by providing alternative targets that compete for interaction with RNases (Lopez et al., 1998).

Transcript abundance has been found to be inversely correlated with mRNA stability in exponentially growing bacteria (Bernstein et al., 2002; Redon et al., 2005; Rustad et al., 2013; Esquerre et al., 2015; Nouaille et al., 2017), and experimental manipulation of transcription rates of subsets of genes affected their degradation rates (Rustad et al., 2013; Nouaille et al., 2017). Together, these studies suggest that high rates of transcription inherently increase degradation rates. We report here that during oxygen depletion, transcript levels are reduced in *M. smegmatis*, which led us to ask whether increased transcript half-lives under stress are a direct result of reduced mRNA levels. However, our data are inconsistent with this idea; mRNA is rapidly destabilized upon reaeration even in the absence of new transcription. We note that one study reported a weak positive correlation between mRNA abundance and stability in log-phase *E. coli* (Chen et al., 2015), while another reported mRNA abundance to be positively correlated with stability in carbon-starved *Lactococcus lactis* (Redon et al., 2005). Together, these observations and our own suggest that the relationship between mRNA stability and abundance is not yet fully understood and may be fundamentally different in growth-arrested bacteria.

The rapid reversibility of hypoxia-induced mRNA stabilization suggests that mRNA decay and energy metabolic status are closely linked. Consistently with this, we have shown that drug-induced energy stress causes mRNA stabilization but that mRNA decay is increased by a drug that induces a hyperactive metabolic state. To our knowledge, this is the first demonstration that the rate of bacterial mRNA degradation can be decoupled from growth rate and suggests that mRNA decay is controlled by energy

status rather than growth rate *per se*. The mechanism by which energy status and mRNA decay are coupled remains elusive; the stringent response is not required, and the stabilization of mRNA during adaptation to hypoxia precedes a decrease in ATP levels. Our data are consistent with two general (nonexclusive) models: mRNA decay may be regulated (i) by protection of transcripts from RNase attack and/or (ii) by direct regulation of the activities of the RNases. Possible explanations that fall within one or both of these frameworks include changes in ribosome occupancy, the presence of other RNA-binding proteins, regulation of the subcellular localization of mRNAs and/or the RNA degradation machinery, and altered degradosome composition. These possibilities should be investigated in future work.

Materials and Methods

Strains and culture conditions.

Mycobacterium smegmatis strain mc^2155 or its derivatives (Table 3-1) were grown in rich medium, Middlebrook 7H9 with albumin dextrose catalase (ADC; final concentrations, 5 g/liter bovine serum albumin fraction V [BSA], 2 g/liter dextrose, 0.85 g/liter NaCl, and 3 mg/liter catalase), 0.2% glycerol, and 0.05% Tween 80, which was shaken at 200 rpm and 37°C to an optical density at 600 nm (OD_{600}) of ~0.8, unless specified otherwise. For hypoxic cultures, we modified Wayne and Hayes model (Wayne and Hayes, 1996). Bacteria were cultured in 30.5- by 58-mm serum bottles (Wheaton; item 223687, 20 mL) using rich medium and an initial OD_{600} of 0.01. Bottles were sealed with a vial crimper (Wheaton; item W225303) using rubber stoppers (Wheaton; item W224100-181) and aluminum seals (Wheaton; item 224193-01). Oxygen levels were qualitatively monitored using methylene blue.

For carbon starvation cultures, cells were grown to log phase (OD_{600} = 0.8) in rich medium, pelleted, and rinsed three times with carbon starvation medium (Middlebrook 7H9 with 5 g/liter BSA, 0.85 g/liter NaCl,

3 mg/liter catalase, and 0.05% Tyloxapol) at 4°C and then resuspended in carbon starvation medium to an OD_{600} of 0.8 and incubated at 200 rpm and 37°C.

The RNase E-tagged strain (SS-M_0296) was built using a two-step process. Plasmid pSS250 was derived from pJM1 (Farrow and Rubin, 2008) and contained 1 kb of the sequence upstream and downstream of the *rne* (msmeg_4626) start codon, with the sequence encoding 6×His-3×FLAG-TEV-4×Gly inserted after the start codon. Constructs were built using NEBuilder HiFi (E2621). Integrants were selected with 200 µg/mL hygromycin and confirmed by sequencing. Counterselection with 15% sucrose was followed by PCR screening to identify isolates that underwent second crossovers resulting in loss of the plasmid and retention of tagged *rne*.

The PNPase-tagged strain (SS-M_0412) was built by inserting a second copy of *pnp* (msmeg_2656) with an N-terminal cMyc-4×Gly construct and its predicted native promoter and 5' untranslated region (UTR) at the Giles phage integration site (plasmid pSS282) into strain SS-M_0296. The RNA helicase-tagged strain (SS-M_0416) was constructed in a similar way but with a C-terminal 4×Gly-cMyc tag on msmeg_1930 (plasmid pSS285).

RNA extraction and determination of mRNA stability.

Biological triplicate cultures were treated with rifampin (RIF) to a final concentration of 150 µg/mL to halt transcription, and RNA was extracted at various time points thereafter. For exponential and carbon starvation cultures, 7 mL was collected per replicate and time point and snap-frozen in liquid nitrogen (LN2). For hypoxic samples, degassed RIF was injected using a 30-gauge needle, and all samples were sacrificially collected per time point and replicate (7 mL) and snap-frozen in LN2 within 6 s of unsealing.

Samples were stored at −80°C and thawed on ice immediately before RNA extraction. Cells were pelleted at 4°C, resuspended in 1 mL TRIzol (Invitrogen), transferred to 2-mL disruption tubes (OPS Diagnostics; 100-µm zirconium lysing matrix, molecular grade), and lysed using a FastPrep-24 5G instrument (MP Biomedical) (3 cycles of 7 m/s for 30 s, with 2 min on ice between cycles). Chloroform (300 µL) was added, samples were centrifuged for 15 min at 21,130 × *g* and 4°C, and RNA was recovered from the aqueous layer and purified with a Direct-zol RNA Miniprep kit according to the manufacturer's instructions with an in-column DNase treatment. Agarose gels were used to verify RNA integrity.

For cDNA synthesis, 600 ng of total RNA was mixed with 0.83 µL 100 mM Tris, pH 7.5, and 0.17 µL 3-mg/mL random primers (NEB) in 5.25 µL, denatured at 70°C for 10 min, and snap-cooled. Reverse transcription was performed for 5 h at 42°C using 100 U ProtoScript II reverse transcriptase (NEB), 10 U RNase inhibitor (murine; NEB), a mix containing 0.5 mM each deoxynucleoside triphosphate (dNTP), and 5 mM dithiothreitol (DTT) in a final volume of 10 µL. RNA was degraded with 5 µL each 0.5 mM EDTA and 1 N NaOH at 65°C for 15 min, followed by 12.5 µL of 1 M Tris-HCl, pH 7.5. cDNA was purified using the MinElute PCR purification kit (Qiagen) according to the manufacturer's instructions. mRNA abundance (A) over time (t) was determined for different genes (primers in Table 3-2) by quantitative PCR (qPCR) using iTaq SYBR green (Bio-Rad) with 400 pg of cDNA and 0.25 µM each primer in 10-µL reaction mixtures, with 40 cycles of 15 s at 95°C and 1 min at 61°C (Applied Biosystems 7500). Abundance was expressed as the negative threshold cycle ($-C_T$) [reflecting the $\log_2 A(t)$]. Linear regression was performed on $-C_T$ values versus time where the negative reciprocal of the best-fit slope estimates mRNA half-life (see Supplemental Methods and Figure S3-1). In many cases, the decay curves were biphasic, with a rapid period of decay followed by a period of slow or undetectable decay. In these cases, only the initial, steeper slope was used for calculation of half-lives.

mRNA stability during reaeration and translational inhibition.

Translation was halted by 150 µg/mL chloramphenicol, rifampin was added 1 min later, and samples were collected starting 1 min after that. For reaeration experiments, 18-h hypoxia cultures were opened and the contents transferred to 50-mL conical tubes, and triplicate samples were taken 2, 7, 12, 17, and 32 min after we opened the bottles and snap-frozen in LN2. Rifampin was added either 1 min before (transcription inhibition during hypoxia) or 2 min after (transcription inhibition after reaeration) we opened the bottles.

BDQ and INH treatments.

Cultures were grown to an OD_{600} of ~1.0 in rich medium, rinsed twice in minimal medium acetate (MMA) wash (final concentrations, 0.5 g/liter l-asparagine, 1 g/liter KH_2PO_4, 2.5 g/liter Na_2HPO_4, 0.5 g/liter $MgSO_4 \cdot 7H_2O$, 0.5 mg/mL $CaCl_2$, 0.1 mg/mL $ZnSO_4$, 0.1% CH_3COONa, 0.05% tyloxapol, pH 7.5) at 4°C, resuspended in MMA (MMA wash plus 50 mg/liter ferric ammonium citrate) to an OD_{600} of 0.07, and grown for 24 h to an OD_{600} of ~0.8. To remove the extracellular ATP, 30 min before drug treatment, cells were pelleted and rinsed in prewarmed MMA wash, resuspended in prewarmed MMA, and returned to the incubator. Bedaquiline (BDQ), isoniazid (INH), or their vehicles were added to final concentrations of 5 µg/mL (BDQ) or 500 µg/mL (INH). Samples were taken 30 min after the addition of BDQ or 6.5 h after the addition of INH for half-life and ATP determinations.

For half-life measurements, BDQ cultures were sampled 0, 3, 6, 9, 12, 15, and 21 min after addition of RIF, and INH cultures were sampled 0, 4, 8, and 12 min after addition of RIF. RNA extractions were performed as described above, with the following modifications: cell disruption was performed using 2-mL tubes prefilled with lysing matrix B (MP Biomedical) and 3 cycles of 10 m/s for 40 s, RNA was recovered from the aqueous layer by isopropanol precipitation and resuspension in H_2O, and samples were treated with

5 U of Turbo DNase (Ambion) in the presence of 80 U of RNase inhibitor, murine (NEB) for 1 h at 37°C with agitation. RNA was purified with an RNeasy Mini Kit (Qiagen) according to the manufacturer's specifications.

Intracellular ATP estimation.

ATP was estimated by BacTiter-Glo (Promega). For BDQ or INH treatments, 1 mL of culture was pelleted at ~21°C for 1 min at 21,130 × *g*, the supernatant removed, and cells resuspended in 1 mL of prewarmed MMA containing BDQ, INH, or vehicle to match the prior treatment conditions. Immediately after, 20-µL samples were transferred to a white 384-well plate (Greiner bio-one) containing 80 µL of BacTiter-Glo reagent and mixed for 5 min at room temperature. Luminescence was measured in a Victor^3 plate reader (PerkinElmer) (intracellular ATP). We included controls for the supernatant collected (extracellular ATP), media plus drug/vehicle (background), and ATP standards for constructing standard curves.

To estimate intracellular ATP in normoxia and hypoxia cultures, 20-µL samples were collected at 37°C and immediately combined with the reagent to measure total ATP (intracellular plus extracellular). From the same cultures, 1-mL samples were syringe filtered (PES; 0.2 µm) and the filtrate was combined with the reagent to measure extracellular ATP. Luminescence was measured as described above. Intracellular ATP was calculated by subtracting the extracellular ATP values from the total ATP values. Hypoxia samples were sacrificially harvested per time point/replicate and combined with the reagent in <6 s.

Acknowledgements

This work was supported by NSF CAREER award 1652756 to S.S.S. D.A.V.-B. was partially supported by the Fulbright Foreign Student Program. We thank all members of the Shell lab for technical assistance and

helpful discussions. We thank Christina Stallings, Jeremy Rock, and Sarah Fortune for generously providing strains.

References

Ait-Bara, S., and Carpousis, A.J. (2010). Characterization of the RNA degradosome of *Pseudoalteromonas haloplanktis*: conservation of the RNase E-RhlB interaction in the gammaproteobacteria. *J Bacteriol* 192(20)**,** 5413-5423. doi: 10.1128/JB.00592-10.

Albertson, M.H., Nyström, T., and Kjelleberg, S. (1990). Functional mRNA half-lives in the marine *Vibrio* sp. S14 during starvation and recovery. *Microbiology* 136(11)**,** 2195-2199.

Anderson, K.L., Roberts, C., Disz, T., Vonstein, V., Hwang, K., Overbeek, R., et al. (2006). Characterization of the *Staphylococcus aureus* heat shock, cold shock, stringent, and SOS responses and their effects on log-phase mRNA turnover. *J Bacteriol* 188(19)**,** 6739-6756. doi: 10.1128/JB.00609-06.

Apirion, D., and Gitelman, D.R. (1980). Decay of RNA in RNA processing mutants of *Escherichia coli*. *Mol Gen Genet* 177(2)**,** 339-343.

Artsimovitch, I., Patlan, V., Sekine, S., Vassylyeva, M.N., Hosaka, T., Ochi, K., et al. (2004). Structural basis for transcription regulation by alarmone ppGpp. *Cell* 117(3)**,** 299-310.

Atkinson, G.C., Tenson, T., and Hauryliuk, V. (2011). The RelA/SpoT homolog (RSH) superfamily: distribution and functional evolution of ppGpp synthetases and hydrolases across the tree of life. *PLoS One* 6(8)**,** e23479. doi: 10.1371/journal.pone.0023479.

Avarbock, D., Avarbock, A., and Rubin, H. (2000). Differential regulation of opposing RelMtb activities by the aminoacylation state of a tRNA.ribosome.mRNA.RelMtb complex. *Biochemistry* 39(38)**,** 11640-11648.

Battesti, A., and Bouveret, E. (2006). Acyl carrier protein/SpoT interaction, the switch linking SpoT-dependent stress response to fatty acid metabolism. *Mol Microbiol* 62(4)**,** 1048-1063. doi: 10.1111/j.1365-2958.2006.05442.x.

Bayas, C.A., Wang, J., Lee, M.K., Schrader, J.M., Shapiro, L., and Moerner, W.E. (2018). Spatial organization and dynamics of RNase E and ribosomes in *Caulobacter crescentus*. *Proc Natl Acad Sci U S A* 115(16)**,** E3712-E3721. doi: 10.1073/pnas.1721648115.

Belton, M., Brilha, S., Manavaki, R., Mauri, F., Nijran, K., Hong, Y.T., et al. (2016). Hypoxia and tissue destruction in pulmonary TB. *Thorax* 71(12)**,** 1145-1153. doi: 10.1136/thoraxjnl-2015-207402.

Bernstein, J.A., Khodursky, A.B., Lin, P.H., Lin-Chao, S., and Cohen, S.N. (2002). Global analysis of mRNA decay and abundance in *Escherichia coli* at single-gene resolution using two-color fluorescent DNA microarrays. *Proc Natl Acad Sci U S A* 99(15)**,** 9697-9702. doi: 10.1073/pnas.112318199.

Bouvet, P., and Belasco, J.G. (1992). Control of RNase E-mediated RNA degradation by 5'-terminal base pairing in E. coli. *Nature* 360(6403)**,** 488-491. doi: 10.1038/360488a0.

Burmann, B.M., Schweimer, K., Luo, X., Wahl, M.C., Stitt, B.L., Gottesman, M.E., et al. (2010). A NusE:NusG complex links transcription and translation. *Science* 328(5977)**,** 501-504. doi: 10.1126/science.1184953.

Carpousis, A.J., Van Houwe, G., Ehretsmann, C., and Krisch, H.M. (1994). Copurification of *E. coli* RNAase E and PNPase: evidence for a specific association between two enzymes important in RNA processing and degradation. *Cell* 76(5)**,** 889-900.

Chakraburtty, R., and Bibb, M. (1997). The ppGpp synthetase gene (relA) of *Streptomyces coelicolor* A3(2) plays a conditional role in antibiotic production and morphological differentiation. *J Bacteriol* 179(18)**,** 5854-5861.

Chan, L.Y., Mugler, C.F., Heinrich, S., Vallotton, P., and Weis, K. (2018). Non-invasive measurement of mRNA decay reveals translation initiation as the major determinant of mRNA stability. *Elife* 7. doi: 10.7554/eLife.32536.

Chen, C., and Deutscher, M.P. (2005). Elevation of RNase R in response to multiple stress conditions. *J Biol Chem* 280(41)**,** 34393-34396. doi: 10.1074/jbc.C500333200.

Chen, C., and Deutscher, M.P. (2010). RNase R is a highly unstable protein regulated by growth phase and stress. *RNA* 16(4)**,** 667-672. doi: 10.1261/rna.1981010.

Chen, H., Shiroguchi, K., Ge, H., and Xie, X.S. (2015). Genome-wide study of mRNA degradation and transcript elongation in *Escherichia coli*. *Mol Syst Biol* 11(1)**,** 781. doi: 10.15252/msb.20145794.

Commichau, F.M., Rothe, F.M., Herzberg, C., Wagner, E., Hellwig, D., Lehnik-Habrink, M., et al. (2009). Novel activities of glycolytic enzymes in *Bacillus subtilis*: interactions with essential proteins involved in mRNA processing. *Mol Cell Proteomics* 8(6)**,** 1350-1360. doi: 10.1074/mcp.M800546-MCP200.

Corrigan, R.M., Bellows, L.E., Wood, A., and Grundling, A. (2016). ppGpp negatively impacts ribosome assembly affecting growth and antimicrobial tolerance in Gram-positive bacteria. *Proc Natl Acad Sci U S A* 113(12)**,** E1710-1719. doi: 10.1073/pnas.1522179113.

Csanadi, A., Faludi, I., and Miczak, A. (2009). MSMEG_4626 ribonuclease from *Mycobacterium smegmatis*. *Mol Biol Rep* 36(8)**,** 2341-2344. doi: 10.1007/s11033-009-9454-1.

Dahl, J.L., Arora, K., Boshoff, H.I., Whiteford, D.C., Pacheco, S.A., Walsh, O.J., et al. (2005). The relA homolog of *Mycobacterium smegmatis* affects cell appearance, viability, and gene expression. *J Bacteriol* 187(7)**,** 2439-2447. doi: 10.1128/JB.187.7.2439-2447.2005.

Deb, C., Lee, C.M., Dubey, V.S., Daniel, J., Abomoelak, B., Sirakova, T.D., et al. (2009). A novel in vitro multiple-stress dormancy model for *Mycobacterium tuberculosis* generates a lipid-loaded, drug-tolerant, dormant pathogen. *PLoS One* 4(6)**,** e6077. doi: 10.1371/journal.pone.0006077.

Donovan, W.P., and Kushner, S.R. (1986). Polynucleotide phosphorylase and ribonuclease II are required for cell viability and mRNA turnover in *Escherichia coli* K-12. *Proc Natl Acad Sci U S A* 83(1)**,** 120-124.

Drainas, D., Kalpaxis, D.L., and Coutsogeorgopoulos, C. (1987). Inhibition of ribosomal peptidyltransferase by chloramphenicol. Kinetic studies. *Eur J Biochem* 164(1)**,** 53-58.

Dressaire, C., Picard, F., Redon, E., Loubiere, P., Queinnec, I., Girbal, L., et al. (2013). Role of mRNA stability during bacterial adaptation. *PLoS One* 8(3)**,** e59059. doi: 10.1371/journal.pone.0059059.

Eoh, H., and Rhee, K.Y. (2013). Multifunctional essentiality of succinate metabolism in adaptation to hypoxia in *Mycobacterium tuberculosis*. *Proc Natl Acad Sci U S A* 110(16)**,** 6554-6559. doi: 10.1073/pnas.1219375110.

Esquerre, T., Laguerre, S., Turlan, C., Carpousis, A.J., Girbal, L., and Cocaign-Bousquet, M. (2014). Dual role of transcription and transcript stability in the regulation of gene expression in *Escherichia coli* cells cultured on glucose at different growth rates. *Nucleic Acids Res* 42(4)**,** 2460-2472. doi: 10.1093/nar/gkt1150.

Esquerre, T., Moisan, A., Chiapello, H., Arike, L., Vilu, R., Gaspin, C., et al. (2015). Genome-wide investigation of mRNA lifetime determinants in *Escherichia coli* cells cultured at different growth rates. *BMC Genomics* 16**,** 275. doi: 10.1186/s12864-015-1482-8.

Fan, H., Conn, A.B., Williams, P.B., Diggs, S., Hahm, J., Gamper, H.B., Jr., et al. (2017). Transcription-translation coupling: direct interactions of RNA polymerase with ribosomes and ribosomal subunits. *Nucleic Acids Res* 45(19)**,** 11043-11055. doi: 10.1093/nar/gkx719.

Farrow, M.F., and Rubin, E.J. (2008). Function of a mycobacterial major facilitator superfamily pump requires a membrane-associated lipoprotein. *J Bacteriol* 190(5)**,** 1783-1791. doi: 10.1128/JB.01046-07.

Frederix, M., and Downie, A.J. (2011). Quorum sensing: regulating the regulators. *Adv Microb Physiol* 58**,** 23-80. doi: 10.1016/B978-0-12-381043-4.00002-7.

Gao, J., Lee, K., Zhao, M., Qiu, J., Zhan, X., Saxena, A., et al. (2006). Differential modulation of *E. coli* mRNA abundance by inhibitory proteins that alter the composition of the degradosome. *Mol Microbiol* 61(2), 394-406. doi: 10.1111/j.1365-2958.2006.05246.x.

Gatewood, M.L., and Jones, G.H. (2010). (p)ppGpp inhibits polynucleotide phosphorylase from *Streptomyces* but not from *Escherichia coli* and increases the stability of bulk mRNA in *Streptomyces coelicolor*. *J Bacteriol* 192(17), 4275-4280. doi: 10.1128/JB.00367-10.

Gentry, D.R., Hernandez, V.J., Nguyen, L.H., Jensen, D.B., and Cashel, M. (1993). Synthesis of the stationary-phase sigma factor sigma s is positively regulated by ppGpp. *J Bacteriol* 175(24), 7982-7989.

Georgellis, D., Barlow, T., Arvidson, S., and von Gabain, A. (1993). Retarded RNA turnover in *Escherichia coli*: a means of maintaining gene expression during anaerobiosis. *Mol Microbiol* 9(2), 375-381.

Grunberg-Manago, M. (1999). Messenger RNA stability and its role in control of gene expression in bacteria and phages. *Annu Rev Genet* 33, 193-227. doi: 10.1146/annurev.genet.33.1.193.

Ignatov, D.V., Salina, E.G., Fursov, M.V., Skvortsov, T.A., Azhikina, T.L., and Kaprelyants, A.S. (2015). Dormant non-culturable *Mycobacterium tuberculosis* retains stable low-abundant mRNA. *BMC Genomics* 16, 954. doi: 10.1186/s12864-015-2197-6.

Iost, I., Guillerez, J., and Dreyfus, M. (1992). Bacteriophage T7 RNA polymerase travels far ahead of ribosomes in vivo. *J Bacteriol* 174(2), 619-622.

Kim, J.H., O'Brien, K.M., Sharma, R., Boshoff, H.I., Rehren, G., Chakraborty, S., et al. (2013). A genetic strategy to identify targets for the development of drugs that prevent bacterial persistence. *Proc Natl Acad Sci U S A* 110(47), 19095-19100. doi: 10.1073/pnas.1315860110.

Kim, K.S., Manasherob, R., and Cohen, S.N. (2008). YmdB: a stress-responsive ribonuclease-binding regulator of *E. coli* RNase III activity. *Genes Dev* 22(24), 3497-3508. doi: 10.1101/gad.1729508.

Kovacs, L., Csanadi, A., Megyeri, K., Kaberdin, V.R., and Miczak, A. (2005). Mycobacterial RNase E-associated proteins. *Microbiol Immunol* 49(11), 1003-1007.

Krasny, L., and Gourse, R.L. (2004). An alternative strategy for bacterial ribosome synthesis: *Bacillus subtilis* rRNA transcription regulation. *EMBO J* 23(22), 4473-4483. doi: 10.1038/sj.emboj.7600423.

Lakshmanan, M., and Xavier, A.S. (2013). Bedaquiline - The first ATP synthase inhibitor against multi drug resistant tuberculosis. *J Young Pharm* 5(4), 112-115. doi: 10.1016/j.jyp.2013.12.002.

Lopez, P.J., Marchand, I., Yarchuk, O., and Dreyfus, M. (1998). Translation inhibitors stabilize *Escherichia coli* mRNAs independently of ribosome protection. *Proc Natl Acad Sci U S A* 95(11), 6067-6072.

Martinez-Costa, O.H., Fernandez-Moreno, M.A., and Malpartida, F. (1998). The relA/spoT-homologous gene in *Streptomyces coelicolor* encodes both ribosome-dependent (p)ppGpp-synthesizing and -degrading activities. *J Bacteriol* 180(16), 4123-4132.

Martini, M.C., Zhou, Y., Sun, H., and Shell, S.S. (2019). Defining the transcriptional and post-transcriptional landscapes of *Mycobacterium smegmatis* in aerobic growth and hypoxia. *Frontiers in Microbiology* 10, 591.

McDowall, K.J., Lin-Chao, S., and Cohen, S.N. (1994). A+U content rather than a particular nucleotide order determines the specificity of RNase E cleavage. *J Biol Chem* 269(14), 10790-10796.

Miczak, A., Kaberdin, V.R., Wei, C.L., and Lin-Chao, S. (1996). Proteins associated with RNase E in a multicomponent ribonucleolytic complex. *Proc Natl Acad Sci U S A* 93(9), 3865-3869.

Miller, O.L., Jr., Hamkalo, B.A., and Thomas, C.A., Jr. (1970). Visualization of bacterial genes in action. *Science* 169(3943), 392-395.

Nouaille, S., Mondeil, S., Finoux, A.L., Moulis, C., Girbal, L., and Cocaign-Bousquet, M. (2017). The stability of an mRNA is influenced by its concentration: a potential physical mechanism to regulate gene expression. *Nucleic Acids Res* 45(20)**,** 11711-11724. doi: 10.1093/nar/gkx781.

Proshkin, S., Rahmouni, A.R., Mironov, A., and Nudler, E. (2010). Cooperation between translating ribosomes and RNA polymerase in transcription elongation. *Science* 328(5977)**,** 504-508. doi: 10.1126/science.1184939.

Prud'homme-Genereux, A., Beran, R.K., Iost, I., Ramey, C.S., Mackie, G.A., and Simons, R.W. (2004). Physical and functional interactions among RNase E, polynucleotide phosphorylase and the cold-shock protein, CsdA: evidence for a 'cold shock degradosome'. *Mol Microbiol* 54(5)**,** 1409-1421. doi: 10.1111/j.1365-2958.2004.04360.x.

Py, B., Causton, H., Mudd, E.A., and Higgins, C.F. (1994). A protein complex mediating mRNA degradation in *Escherichia coli*. *Mol Microbiol* 14(4)**,** 717-729.

Py, B., Higgins, C.F., Krisch, H.M., and Carpousis, A.J. (1996). A DEAD-box RNA helicase in the *Escherichia coli* RNA degradosome. *Nature* 381(6578)**,** 169-172. doi: 10.1038/381169a0.

Rao, S.P., Alonso, S., Rand, L., Dick, T., and Pethe, K. (2008). The protonmotive force is required for maintaining ATP homeostasis and viability of hypoxic, nonreplicating *Mycobacterium tuberculosis*. *Proc Natl Acad Sci U S A* 105(33)**,** 11945-11950. doi: 10.1073/pnas.0711697105.

Redko, Y., Aubert, S., Stachowicz, A., Lenormand, P., Namane, A., Darfeuille, F., et al. (2013). A minimal bacterial RNase J-based degradosome is associated with translating ribosomes. *Nucleic Acids Res* 41(1)**,** 288-301. doi: 10.1093/nar/gks945.

Redon, E., Loubiere, P., and Cocaign-Bousquet, M. (2005). Role of mRNA stability during genome-wide adaptation of *Lactococcus lactis* to carbon starvation. *J Biol Chem* 280(43)**,** 36380-36385. doi: 10.1074/jbc.M506006200.

Regonesi, M.E., Del Favero, M., Basilico, F., Briani, F., Benazzi, L., Tortora, P., et al. (2006). Analysis of the *Escherichia coli* RNA degradosome composition by a proteomic approach. *Biochimie* 88(2)**,** 151-161. doi: 10.1016/j.biochi.2005.07.012.

Rock, J.M., Hopkins, F.F., Chavez, A., Diallo, M., Chase, M.R., Gerrick, E.R., et al. (2017). Programmable transcriptional repression in mycobacteria using an orthogonal CRISPR interference platform. *Nat Microbiol* 2**,** 16274. doi: 10.1038/nmicrobiol.2016.274.

Roux, C.M., DeMuth, J.P., and Dunman, P.M. (2011). Characterization of components of the *Staphylococcus aureus* mRNA degradosome holoenzyme-like complex. *J Bacteriol* 193(19)**,** 5520-5526. doi: 10.1128/JB.05485-11.

Russell, J.H., and Keiler, K.C. (2009). Subcellular localization of a bacterial regulatory RNA. *Proc Natl Acad Sci U S A* 106(38)**,** 16405-16409. doi: 10.1073/pnas.0904904106.

Rustad, T.R., Minch, K.J., Brabant, W., Winkler, J.K., Reiss, D.J., Baliga, N.S., et al. (2013). Global analysis of mRNA stability in *Mycobacterium tuberculosis*. *Nucleic Acids Res* 41(1)**,** 509-517. doi: 10.1093/nar/gks1019.

Sakamoto, T., and Bryant, D.A. (1997). Temperature-regulated mRNA accumulation and stabilization for fatty acid desaturase genes in the cyanobacterium *Synechococcus* sp. strain PCC 7002. *Mol Microbiol* 23(6)**,** 1281-1292.

Schubert, O.T., Ludwig, C., Kogadeeva, M., Zimmermann, M., Rosenberger, G., Gengenbacher, M., et al. (2015). Absolute Proteome Composition and Dynamics during Dormancy and Resuscitation of *Mycobacterium tuberculosis*. *Cell Host Microbe* 18(1)**,** 96-108. doi: 10.1016/j.chom.2015.06.001.

Shaila, M.S., Gopinathan, K.P., and Ramakrishnan, T. (1973). Protein synthesis in *Mycobacterium tuberculosis* H37Rv and the effect of streptomycin in streptomycin-susceptible and -resistant strains. *Antimicrob Agents Chemother* 4(3)**,** 205-213. doi: 10.1128/aac.4.3.205.

Shetty, A., and Dick, T. (2018). Mycobacterial Cell Wall Synthesis Inhibitors Cause Lethal ATP Burst. *Front Microbiol* 9**,** 1898. doi: 10.3389/fmicb.2018.01898.

Siculella, L., Damiano, F., di Summa, R., Tredici, S.M., Alduina, R., Gnoni, G.V., et al. (2010). Guanosine 5'-diphosphate 3'-diphosphate (ppGpp) as a negative modulator of polynucleotide phosphorylase activity in a 'rare' actinomycete. *Mol Microbiol* 77(3)**,** 716-729. doi: 10.1111/j.1365-2958.2010.07240.x.

Smith, T., Wolff, K.A., and Nguyen, L. (2013). Molecular biology of drug resistance in *Mycobacterium tuberculosis*. *Curr Top Microbiol Immunol* 374**,** 53-80. doi: 10.1007/82_2012_279.

Snapper, S.B., Melton, R.E., Mustafa, S., Kieser, T., and Jacobs, W.R., Jr. (1990). Isolation and characterization of efficient plasmid transformation mutants of *Mycobacterium smegmatis*. *Mol Microbiol* 4(11)**,** 1911-1919.

Srivastava, A., Asahara, H., Zhang, M., Zhang, W., Liu, H., Cui, S., et al. (2016). Reconstitution of Protein Translation of *Mycobacterium* Reveals Functional Conservation and Divergence with the Gram-Negative Bacterium *Escherichia coli*. *PLoS One* 11(8)**,** e0162020. doi: 10.1371/journal.pone.0162020.

Stallings, C.L., Stephanou, N.C., Chu, L., Hochschild, A., Nickels, B.E., and Glickman, M.S. (2009). CarD is an essential regulator of rRNA transcription required for *Mycobacterium tuberculosis* persistence. *Cell* 138(1)**,** 146-159. doi: 10.1016/j.cell.2009.04.041.

Tamura, M., Moore, C.J., and Cohen, S.N. (2013). Nutrient dependence of RNase E essentiality in *Escherichia coli*. *J Bacteriol* 195(6)**,** 1133-1141. doi: 10.1128/JB.01558-12.

Tedin, K., and Bremer, H. (1992). Toxic effects of high levels of ppGpp in Escherichia coli are relieved by *rpoB* mutations. *J Biol Chem* 267(4)**,** 2337-2344.

Thorne, S.H., and Williams, H.D. (1997). Adaptation to nutrient starvation in *Rhizobium leguminosarum* bv. phaseoli: analysis of survival, stress resistance, and changes in macromolecular synthesis during entry to and exit from stationary phase. *J Bacteriol* 179(22)**,** 6894-6901.

Tomcsanyi, T., and Apirion, D. (1985). Processing enzyme ribonuclease E specifically cleaves RNA I. An inhibitor of primer formation in plasmid DNA synthesis. *J Mol Biol* 185(4)**,** 713-720.

Vanzo, N.F., Li, Y.S., Py, B., Blum, E., Higgins, C.F., Raynal, L.C., et al. (1998). Ribonuclease E organizes the protein interactions in the *Escherichia coli* RNA degradosome. *Genes Dev* 12(17)**,** 2770-2781.

Via, L.E., Lin, P.L., Ray, S.M., Carrillo, J., Allen, S.S., Eum, S.Y., et al. (2008). Tuberculous granulomas are hypoxic in guinea pigs, rabbits, and nonhuman primates. *Infect Immun* 76(6)**,** 2333-2340. doi: 10.1128/IAI.01515-07.

Wayne, L.G., and Hayes, L.G. (1996). An in vitro model for sequential study of shiftdown of *Mycobacterium tuberculosis* through two stages of nonreplicating persistence. *Infect Immun* 64(6)**,** 2062-2069.

Weiss, L.A., and Stallings, C.L. (2013). Essential roles for *Mycobacterium tuberculosis* Rel beyond the production of (p)ppGpp. *J Bacteriol* 195(24)**,** 5629-5638. doi: 10.1128/JB.00759-13.

Wolfe, A.D., and Hahn, F.E. (1965). Mode of Action of Chloramphenicol. Ix. Effects of Chloramphenicol Upon a Ribosomal Amino Acid Polymerization System and Its Binding to Bacterial Ribosome. *Biochim Biophys Acta* 95**,** 146-155.

Wu, M.L., Tan, J., and Dick, T. (2015). Eagle Effect in Nonreplicating Persister Mycobacteria. *Antimicrob Agents Chemother* 59(12)**,** 7786-7789. doi: 10.1128/AAC.01476-15.

Yukioka, M., and Morisawa, S. (1971). Enhancement of the phenylalanyl-oligonucleotide binding to the peptidyl recognition center of ribosomal peptidyltransferase and inhibition of the chloramphenicol binding to ribosomes. *Biochim Biophys Acta* 254(2)**,** 304-315.

Zhang, Y., Mooney, R.A., Grass, J.A., Sivaramakrishnan, P., Herman, C., Landick, R., et al. (2014). DksA guards elongating RNA polymerase against ribosome-stalling-induced arrest. *Mol Cell* 53(5)**,** 766-778. doi: 10.1016/j.molcel.2014.02.005.

Tables

Table 3-1. Strains used

Strain	Characteristics	Source
mc^2155	*M. smegmatis*, WT	(Snapper et al., 1990)
SS-M_0072	mc^2155 derivative transformed with plasmid pSS162, containing an ATc-inducible copy of *rraA*.	This work
SS-M_0296	mc^2155 in which the native copy of RNase E (*rne*) is N-terminally tagged with 6xHis-3xFLAG-TEV-4xGly linker (CACCACCACCACCACCACGATTACAAGGATCACGATGGCGATTACAAGGATCATGACATCGACTATAAGGACGATGACGATAAGGAGAACCTGTACTTCCAGGGCGGCGGCGGC).	This work
SS-M_0412	SS-M_0296 derivative containing a second copy of PNPase (msmeg_2656) with its predicted native promoter and 5' UTR, and N-terminally tagged with c-Myc-4xGly-linker (GAGCAGAAGCTGATCTCGGAAGAGGACCTCGGCGGCGGCGGC) contained on a Giles-integrating plasmid pSS282 (Hyg^r).	This work
SS-M_0416	SS-M_0296 derivative containing a second copy of RNA helicase (msmeg_1930) with its predicted native promoter and 5' UTR, and C-terminally tagged with 4x Gly linker-c-Myc (GGCGGCGGCGGCGAGCAGAAGCTGATCTCGGA) contained on a Giles-integrating plasmid pSS285 (Hyg^r).	This work
Δrel_{Msm}	mc^2155 derivative, Δ*rel* Δ*sas2*	(Weiss and Stallings, 2013)
SS-M_0203	mc^2155 derivative transformed with plasmid pJR962, containing an ATc regulated *dCas9*.	(Rock et al., 2017)

Table 3-2. Primers for qPCR

Primer name	Gene	Directionality	Sequence 5’ → 3’
SSS903	*atpB* (msmeg_4942)	Forward	TGTTCGTGTTCGTCTGCTAC
SSS904	*atpB* (msmeg_4942)	Reverse	CGGCTTGGCGAGTTCTT
SSS909	*atpE* (msmeg_4941)	Forward	GGGTAACGCGCTGATCTC
SSS910	*atpE* (msmeg_4941)	Reverse	GAAGGCCAGGTTGATGAAGTA
SSS1241	*dCas9*	Forward	GACAAGTCGAAGTTCCTGATGTA
SSS1242	*dCas9*	Reverse	GATCTGCTTGTTCGGGTAGTT
SSS537	*esxB* (msmeg_0065)	Forward	GGTGAGGACACAGGGAAATAAG
SSS538	*esxB* (msmeg_0065)	Reverse	CGGAGATGCGCTCGAAAT
SSS856	*katG* (msmeg_6384)	Forward	GGCCCAATCAGCTCAATCT
SSS857	*katG* (msmeg_6384)	Reverse	CGGACCGGTAGTCGAAATC
SSS706	*rnj* (msmeg_2685)	Forward	TCATCCTCTCATCGGGTTTC
SSS707	*rnj* (msmeg_2685)	Reverse	TTCGCGCTCAACCTTCT
SSS697	*rraA* (msmeg_6439)	Forward	AACTACGGCGGCAAGAT
SSS698	*rraA* (msmeg_6439)	Reverse	GTCGAGAGGATCGACTTCAG
JR273*	*sigA* (msmeg_2758)	Forward	GACTACACCAAGGGCTACAAG
JR274*	*sigA* (msmeg_2758)	Reverse	TTGATCACCTCGACCATGTG

*Source: Rock et al., 2017.

Supplemental Methods

mRNA half-life experiments were conducted using purified RNA that was reverse-transcribed into cDNA. cDNA samples were purified as described in Methods, which allowed us to quantify cDNA concentrations and use the same amount of cDNA in each qPCR reaction. Because total RNA is composed mostly of rRNA, our cDNA was also primarily composed of rRNA sequences. rRNA is much more stable than mRNA and does not appreciably decay over the RIF treatment periods that we used for measuring mRNA decay rates, as evidenced by our observations that total RNA per OD unit or per CFU was unaltered during these treatment periods. Hence, we assumed that as mRNA decays, its abundance will change relative to total RNA abundance. When performing qPCR for a gene of interest, we therefore interpreted the cycle threshold (C_T) as a reflection of the $\log_2$ abundance of that transcript relative to total RNA levels. By performing qPCR on a defined amount of carefully quantified cDNA, we were able to measure abundance of specific mRNAs relative to total RNA content which consists mostly of stable rRNA.

Half-lives were estimated as the negative reciprocal of the slope of the regression line for $\log_2$ mRNA abundance versus time. If we assume that the overall abundance of mRNA at time t (min) after transcription is arrested, $A(t)$, follows an exponential decay curve, then

$$A(t) = A(0) \cdot 2^{-t/\tau},$$

where $A(0)$ is the initial abundance of mRNA and τ is the half-life (min). Taking the logarithm (base 2) of both sides gives

$$\log_2 A(t) = \log_2 A(0) - \frac{t}{\tau}.$$

To measure $A(t)$, we freeze samples after t minutes and determine the cycle threshold, $C_T(t)$, which is the number of duplications required to reach a fixed threshold (A^*) when starting with $A(t)$. Thus,

$$A^* = A(t) \cdot 2^{C_T(t)}$$

$$A(t) = A^* \cdot 2^{-C_T(t)}$$

Substituting into both sides of the equation for $\log_2$ abundance over time,

$$\log_2\left(A^* \cdot 2^{-C_T(t)}\right) = \log_2\left(A^* \cdot 2^{-C_T(0)}\right) - \frac{t}{\tau}$$

$$\log_2 A^* - C_T(t) = \log_2 A^* - C_T(0) - \frac{t}{\tau}$$

$$-C_T(t) = -C_T(0) - \frac{t}{\tau}.$$

Thus, when $-C_T$ (which represents abundance on a $\log_2$ scale) is plotted as a function of time, the half-life τ = -1/slope. An example is shown in Figure S3-1 in the Supplemental Methods.

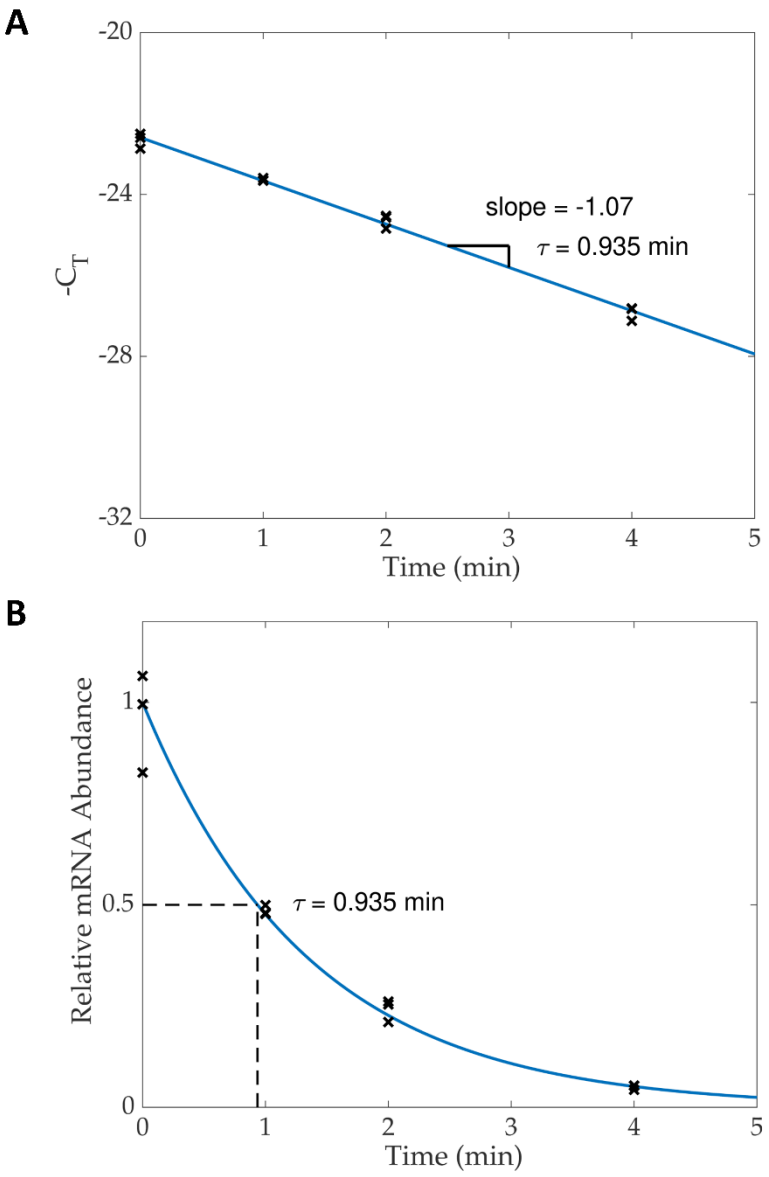

Figure S3-1. mRNA decay curves for a sample gene, *rraA*. The *x* axis denotes the time after transcription was blocked by addition of RIF. (A) $-C_T$ versus time data for *rraA*, giving a half-life estimate of 0.935 min. (B) Estimated mRNA abundance for *rraA* relative to the time of RIF addition, giving a half-life estimate of 0.935 minutes.

Chapter 4 : The effects of ribosome occupancy on mRNA stability in *Mycobacterium smegmatis*

The effects of ribosome occupancy on mRNA stability in *Mycobacterium smegmatis*

Abstract

As part of the bacterial stress response, mycobacteria quickly regulate gene expression. Because transcription and translation are impacted by these stress responses, it is possible that global mRNA stabilization could be a consequence of changes in translation elongation or ribosome occupancy. In *E. coli,* it has been shown that translation can interfere with transcript degradation by causing RNase occlusion. Moreover, stalled ribosomes can act as 5' blockers that impair linear scanning by RNase E. Therefore, we wondered if changes in translation as a response to stress, such as hypoxia, could lead to global mRNA stability. We have previously reported mRNA stabilization in hypoxia using a small set of transcripts. Here, we validated those findings by measuring mRNA half-lives transcriptome-wide in *M. smegmatis* in hypoxia and log phase. Then, to determine if translation or ribosome occupancy impact global mRNA degradation, we used three approaches.

First, we used a translational inhibitor to cause ribosome stalling on mRNA templates. Our results showed that in chloramphenicol-treated hypoxic *M. smegmatis*, mRNAs become more stable when compared to the vehicle treatment, and the observed mRNA stability was preserved even after reaeration. We also used a different translation inhibitor, puromycin, which showed dual effects on mRNA stability. Our second approach consisted of comparing mRNA degradation rates for two transcripts (*mCherryOS* and *mCherryUT*), once of which was modified to be untranslatable (*mCherryUT*). Unexpectedly, we found that *mCherryUT* was remarkably more stable than its counterpart. We reconciled these results as we found evidence of coupled transcription-translation that could have obscured our findings. Our third approach was to use polysome profiling to detect ribosome occupancy in *M. smegmatis* either in rich media or

under carbon starvation. Our results were surprising, as we found that during starvation most ribosomes were present as separate subunits, while a significantly smaller fraction corresponded to monosomes and polysomes. To discard the possibility of mRNA being associated with 30S and 50S subunits, we measured transcript abundance for different fractions corresponding to our polysome profiling samples. Our results showed different association profiles for distinct transcripts, but most importantly, that a greater proportion of each mRNA remained unassociated from ribosomes or subunits in carbon starvation compared to log phase. Altogether, we conclude that ribosome occupancy is not a mechanism of global stabilization as a response to carbon starvation stress in *M. smegmatis*.

Introduction

Bacterial adaptation to stress involves a stress response. To be effective and ensure survival, the stress response must be immediate. As such, bacteria actively sense the environment and within seconds alter the translatome, the collection of all mRNAs actively undergoing translation. Because the ultimate goal of bacteria is to survive and multiply, it is not surprising that transcription—an energetically demanding process—is tightly regulated. However, while transcription-oriented regulatory mechanisms have been broadly study in bacteria, those pertinent to mRNA degradation remains elusive.

We and others have shown that mRNA degradation rates are slowed as part of bacterial stress responses [for example (Dressaire et al., 2013; Rustad et al., 2013; Vargas-Blanco et al., 2019; Morin et al., 2020)]. We also have proposed that mRNA stabilization is directly dependent on metabolic activity rather than growth rate, at least in *M. smegmatis* (Vargas-Blanco et al., 2019), and similar findings were later reported in *E. coli* (Morin et al., 2020). Several studies have highlighted an inverse correlation between growth rate and mRNA degradation in *Bacillus subtilis* (Melin et al., 1989), *E. coli* (Esquerre et al., 2014; Esquerre et al., 2015; Esquerre et al., 2016) and *Salmonella dublin* (Paesold and Krause, 1999). Moreover, analysis of

transcript degradation in *E. coli* at different growth rates reinforced the concept of mRNA degradation linked to gene function, as transcripts from the "Coenzyme transport and metabolism" and "Intracellular trafficking, secretion and vesicular transport" COGs were highly stabilized during slow growth conditions, while transcripts from the "Carbohydrate metabolism" COG comprised some of the most stable genes during normal growth rates (Esquerre et al., 2014; Esquerre et al., 2015).

Stress-induced transcript stabilization could also be a consequence of changes in translation elongation, a parameter associated with growth rate (Dalbow and Young, 1975; Pedersen, 1984; Klumpp et al., 2013). In *E. coli*, nutrient limitation and hyperosmotic stress conditions caused slower elongation rates compared to rich media conditions (Dai et al., 2018; Zhu and Dai, 2019). Similar findings were also reported for *E. coli* under cold-induced stress (Dai et al., 2016; Zhang et al., 2018; Tollerson and Ibba, 2020). Interestingly, the relationship between cell growth and translation elongation rate is not linear. *E. coli* cells with doubling times of <60 min had an elongation rate (k) of ~17 aa·s^{-1}, while those with a doubling time of 20 hours had a k of ~8 aa·s^{-1}, as determined by a β-galactosidase induction assay for LacZ and other LacZ-derived proteins (Dai et al., 2016). These results suggest that even under stress conditions there is a basal level of translation with physiological relevance, and *E. coli* cells are capable of rapidly resuming protein synthesis upon encountering favorable conditions (Dai et al., 2016). Recent work on alternative ribosomes in *M. smegmatis*, found only under stress conditions, evidenced unusual translational patterns compared to canonical ribosomes, including preference for certain codons and a 5' positional polarity shift (Chen et al., 2020). Do these translational changes during stress conditions impact transcript fate? We think this is plausible, as changes in ribosome trafficking, translational elongation rates and even translational defects can impair RNases access to the mRNA, presumably resulting in altered transcriptome degradation rates.

In *E. coli*, active translation seems to prevent RNases from degrading transcripts. For example, experiments using distinct translation inhibitors resulted in disturbances in the degradation rate of the

RNA pool (Fry et al., 1972; Pato et al., 1973). However, while the presence of ribosomes on transcripts can impact transcript fate, it is not always associated with active translation, as shown for *ermC* and *ompA* (Hambraeus et al., 2002). Stalled ribosomes located at the 5' end of a transcript can act as an obstacle during RNase E's linear transcript scanning function, impairing its endonucleolytic activity (Richards and Belasco, 2019). For example, in *Bacillus subtilis* a stalled ribosome near the 5' end of *emrC* increases its half-life (Bechhofer and Dubnau, 1987; Bechhofer and Zen, 1989). Other studies have shown that ribosomal binding site (RBS) mutations resulted in shorter half-lives of their associated transcripts (Hue et al., 1995; Jurgen et al., 1998; Hambraeus et al., 2002). Given the ability of ribosomes to protect transcripts even when not actively translating, as well as the increased rRNA:mRNA ratio that we have observed in energy-starved mycobacteria, we wondered if mRNA-ribosome associations are involved in the regulation of mRNA degradation as part of the mycobacterial response to stress.

In the work described in this chapter, we used multiple approaches to study mycobacterial mRNA stabilization in response to stress. We used RNA-seq to calculate mRNA half-lives in a transcriptome-wide manner for *Mycobacterium smegmatis* cultures subject to hypoxic stress and normoxic conditions, reinforcing the concept of mRNA stabilization as a global stress response as detailed in Chapter 3. To address the question whether ribosomes are involved in regulation of mRNA degradation, we used three different approaches. First, we used two drugs (chloramphenicol and puromycin) to assess the role of ribosomal occupancy as a determinant of mRNA stability in *M. smegmatis*. Next, we designed three reporter constructs with different translational profiles to evaluate the role of translation in mRNA degradation. Finally, we used polysome profiling and qPCR to directly compare ribosome occupancy under carbon starvation and rich media conditions. Our results suggest that while mRNA half-lives can be modulated by active translation and stalled ribosomes, these associations do not regulate global mRNA stabilization as a response to energy stress.

Results

mRNA is globally stabilized as a response to hypoxic stress in *Mycobacterium smegmatis*.

We have previously shown that in *M. smegmatis* the *atpB*, *aptE*, *katG*, *rnj*, *rraA,* and *sigA* transcripts had increased half-lives under hypoxia and carbon starvation, compared to those of log phase normoxic cultures (Vargas-Blanco et al., 2019). Based on the diversity of transcript-specific features in our tested genes, as well as reports of global mRNA stabilization in *M. tuberculosis* as a response to hypoxia (Rustad et al., 2013), we offered the educated guess that stress-induced mRNA stabilization is also a global phenomenon in *M. smegmatis*. However, we had not provided evidence of stress-induced mRNA stabilization in a transcriptome-wide manner. Therefore, we used RNA-seq to determine transcript half-lives in *M. smegmatis* under hypoxia and log phase normoxic cultures. We generated a hypoxic environment for *M. smegmatis* using a variation of the Wayne and Hanes model (Wayne and Hayes, 1996), consisting of a gradual transition from aerated growth to hypoxia-induced growth arrest over 19 hours, as detailed in Chapter 3 of this dissertation. *M. smegmatis* samples were collected in biological triplicate at different time points after transcription inhibition by degassed rifampicin. Total RNA was extracted from all samples, ribosomal RNA (rRNA) was depleted and RNA-seq libraries were constructed. The removal of rRNA meant that rRNA could not be used to normalize mRNA abundance as we did when determining mRNA half-lives by quantitative PCR (qPCR). Instead, we created a normalization factor by using qPCR to measure mRNA abundance for eight transcripts [msmeg_0065 (*esxB*), msmeg_2758 (*sigA*), msmeg_4626 (*rne*), msmeg_4665 (*iolE*), msmeg_4941 (*atpE*), msmeg_5691 (putative RBP), msmeg_6439 (*rraA*), and msmeg_6941 (putative RBP)] in each sample. The RNA-seq reads were then transformed using the normalization factor and used to determine transcript half-lives (see *Materials and Methods*). As expected, hypoxic conditions lead to transcriptome-wide stabilization with a median half-life of 29.9 min for 3179 *M. smegmatis* genes. The median half-life for normoxia in *M. smegmatis* is 0.9 min (Figure 4-1).

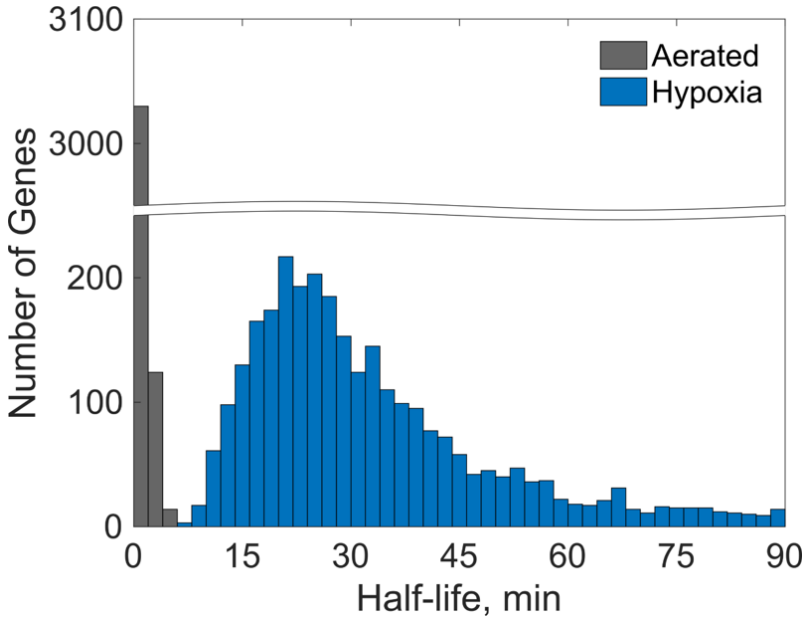

Figure 4-1. *Mycobacterium smegmatis* stabilizes its mRNA transcriptome-wide as a response to hypoxia. RNA-seq analysis shows dramatic mRNA stabilization for *M. smegmatis* cells under early hypoxic stress when compared to log phase.

Chloramphenicol-induced ribosome stalling increases mRNA stability in *Mycobacterium smegmatis* under hypoxic stress.

In Chapter 3 we have shown that chloramphenicol, an elongation inhibitor that prevents peptidyl transfer causing ribosome stalling along the transcript (Wolfe and Hahn, 1965; Lopez et al., 1998), causes mRNA stabilization for at least some genes in hypoxic *M. smegmatis* (Figure 4-2A, also shown in Chapter 3). This implies that some level of translation continues in hypoxia, and that increased ribosome occupancy protects mRNA from the already-slow degradation that occurs in this condition. Having previously shown that reaeration of hypoxic *M. smegmatis* causes swift resumption of mRNA degradation (Vargas-Blanco et al., 2019), we wondered if we could use chloramphenicol to preserve the ribosome-mRNA associations present in hypoxic conditions, carrying over transcript stability into a reaeration phase. We therefore redesigned our hypoxia experiment with two modifications. First, we included a reaeration step 2 minutes after translation inhibition. Second, we blocked transcription either one minute before or two minutes after reaeration (Figure 4-2B and C, bottom) in order to test the impact of transcriptional changes that

occur upon alteration of metabolic status. Our results showed that for each of our five tested genes, mRNA half-lives were higher for mycobacteria treated with chloramphenicol, regardless of whether transcription had been blocked before or after reaeration (Figure 4-2B and C, top).

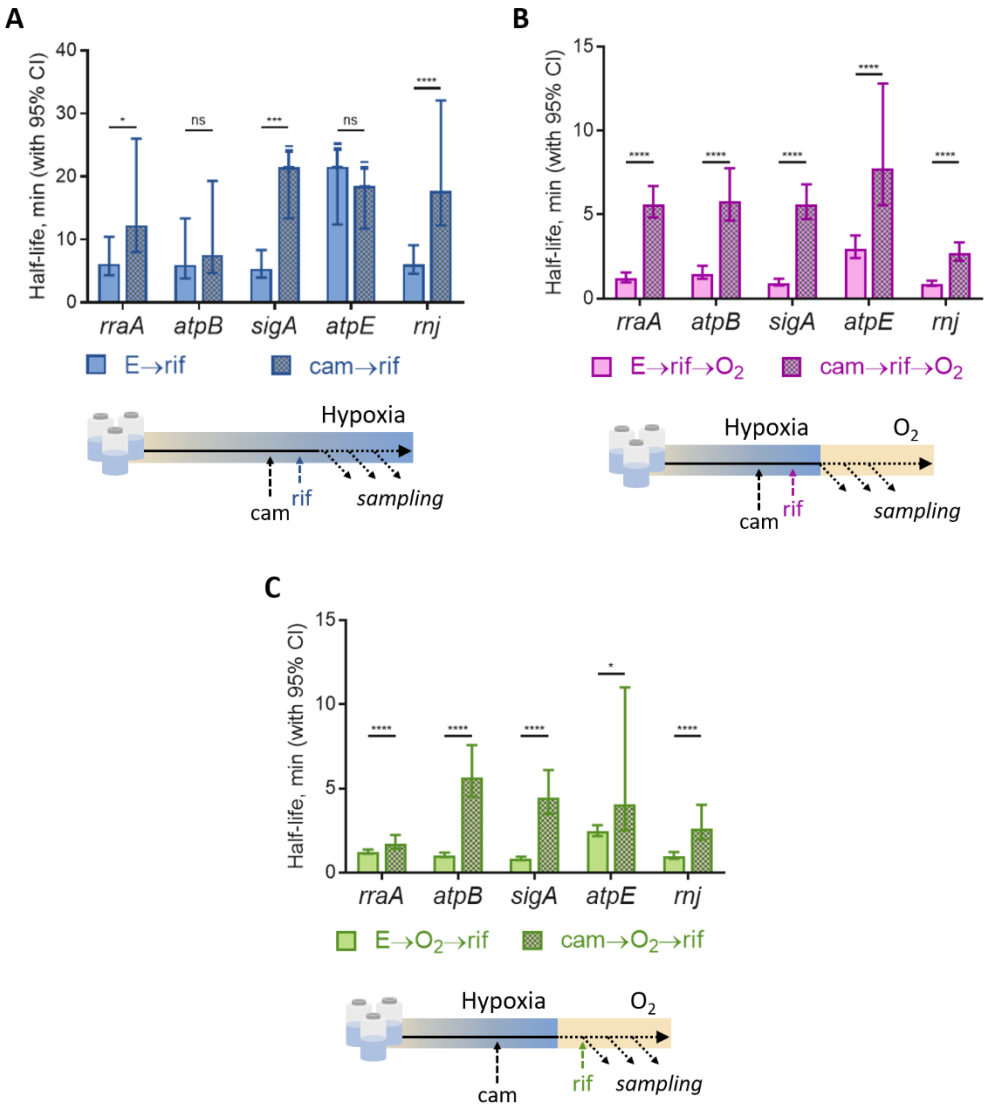

Figure 4-2. Ribosome stalling increases *Mycobacterium smegmatis* mRNA half-lives in hypoxia and re-aeration. (A) Chloramphenicol-treated *M. smegmatis* cultures further stabilize their transcripts under hypoxic stress, suggesting that stalled ribosomes enhance protection from RNases. (B and C) Re-aeration of hypoxic *M. smegmatis* cultures leads to swift transcript degradation, a phenomenon that is prevented by the addition of chloramphenicol. Transcripts from chloramphenicol-treated cells show slower mRNA degradation upon reaeration, regardless of whether transcription inhibition occurred before (B) or after (C) disrupting the hypoxic environment. Error bars: 95% confidence intervals. * = $p<0.05$, **** = $p<0.0001$, ns = not significant; linear regression test, $n=3$. The → indicates the order of the events; E: ethanol (drug vehicle), cam: chloramphenicol, rif: rifampicin, O_2: re-aeration.

Next, we analyzed the expression levels of our tested genes. In hypoxic *M. smegmatis* cultures, gene expression increased in two minutes of reaeration in the absence of chloramphenicol, as shown for three/five of our tested transcripts (Figure 4-3A). Interestingly, we found that *atpB*, *atpE*, *rnj* and *sigA* had similar expression levels for cells treated with chloramphenicol, regardless of when transcription was halted (i.e., *chloramphenicol → reaeration → rifampicin* or *chloramphenicol → rifampicin → reaeration*) as shown in Figure 4-3B. Chloramphenicol therefore prevented the transcriptional burst that occurred during two minutes of reaeration in untreated cells. Thus, as discussed below, it seems possible that in *M. smegmatis* translation and transcription are physically coupled.

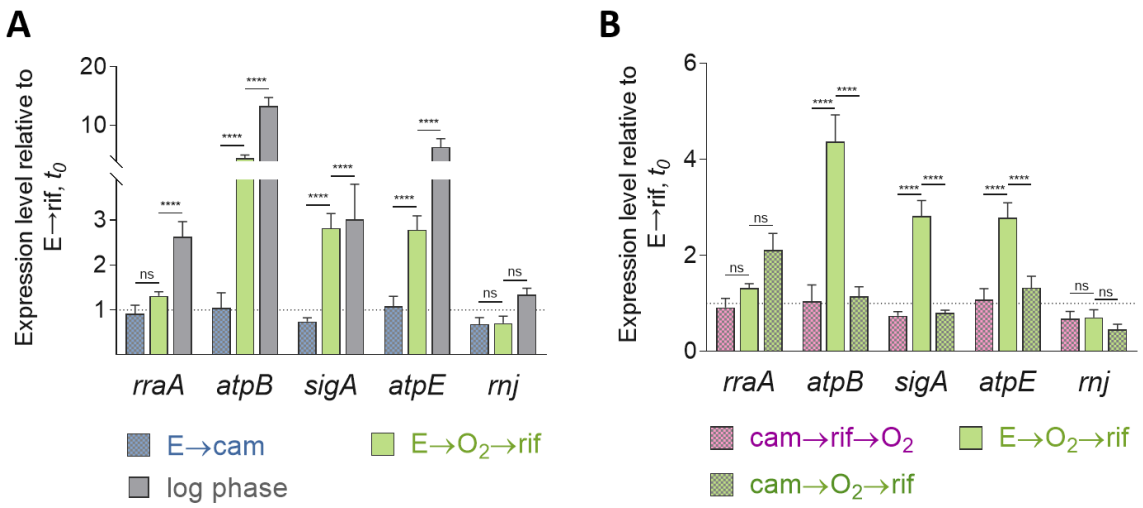

Figure 4-3. Translation inhibition impacts transcription in *Mycobacterium smegmatis*. (A) Expression level of transcripts under hypoxia + cam, re-aeration or normoxia (log phase) relative to hypoxia. (B) Expression level for five tested genes from re-aeration of hypoxic *M. smegmatis* cultures using rifampicin and chloramphenicol or the drug vehicle. After re-aeration, cultures treated with chloramphenicol had lower expression levels (for *atpB*, *sigA*, *atpE* and *rnj)* than those treated with ethanol, suggesting a possible coupling of translation and transcription processes. The → indicates the order of the events; E: ethanol (drug vehicle), cam: chloramphenicol, rif: rifampicin, O_2: re-aeration. Error bars: standard deviation. *** = p<0.001, **** = p<0.0001, ns = not significant; ANOVA, Dunnett, n=3.

Translation inhibition by puromycin has dual effects on mRNA stability in *Mycobacterium smegmatis*.

Having shown that stalled ribosomes can lead to mRNA stabilization, we hypothesized that in *M. smegmatis,* ribosome-depleted transcripts would have shorter half-lives compared to transcripts associated with ribosomes. In *E. coli*, puromycin was reported to cause faster RNA decay (Varmus et al., 1971; Pato et al., 1973). Puromycin is a translation inhibitor that competes with aminoacyl tRNAs to bind the A site in the peptidyl transferase reaction, leading to premature chain termination (Traut and Monro, 1964; Azzam and Algranati, 1973). Hence, if puromycin causes ribosomes to release from the transcripts, RNases would be more effective at accessing the unprotected transcripts. To test this hypothesis, we used *M. smegmatis* cultures in logarithmic phase (OD_{600} = 0.8) and inhibited transcription with rifampicin 30 seconds prior adding puromycin. Samples were collected at different time points thereafter (Figure 4-4A). We also used chloramphenicol and ethanol (the drug vehicle) as control treatments. Contrary to our expectations, we observed that mRNA half-lives were longer for both puromycin-treated and chloramphenicol-treated cultures compared to the ethanol treatment (Figure 4-4B). In puromycin-treated cells, transcript half-lives were 1.1- to 2.8-fold those from the vehicle drug (Figure 4-4B). Nevertheless, the longest mRNA half-lives corresponded to chloramphenicol-treated cells, which were 2.1- to 7.1-fold those of the vehicle drug treatment (Figure 4-4B).

We and others often observe biphasic and triphasic mRNA decay curves (Hambraeus et al., 2003; Selinger et al., 2003; Chen et al., 2015; Vargas-Blanco et al., 2019; Nguyen et al., 2020). Biphasic curves have a period of rapid decay followed by a slowing of decay at later time points. Triphasic curves also have an initial delay before the rapid decay phase. We attribute the “slow-fast” degradation pattern to continued synthesis of mRNA by RNA polymerases that had already begun elongation when rifampicin was added, as this drug only inhibits transcription initiation. Both of these typical bi- and triphasic decay patterns can

be seen in the vehicle control (Figure 4-4D). However, examination of the mRNA degradation pattern in puromycin-treated mycobacteria revealed an unusual pattern in which a short period of very rapid decay preceded the main decay period (Figure 4-4C). For all three genes tested, a faster mRNA degradation period, characterized by a steeper negative slope, took places between 0 and 30 seconds after transcription inhibition (Figure 4-4C). Interpretation of these results will be further discussed below.

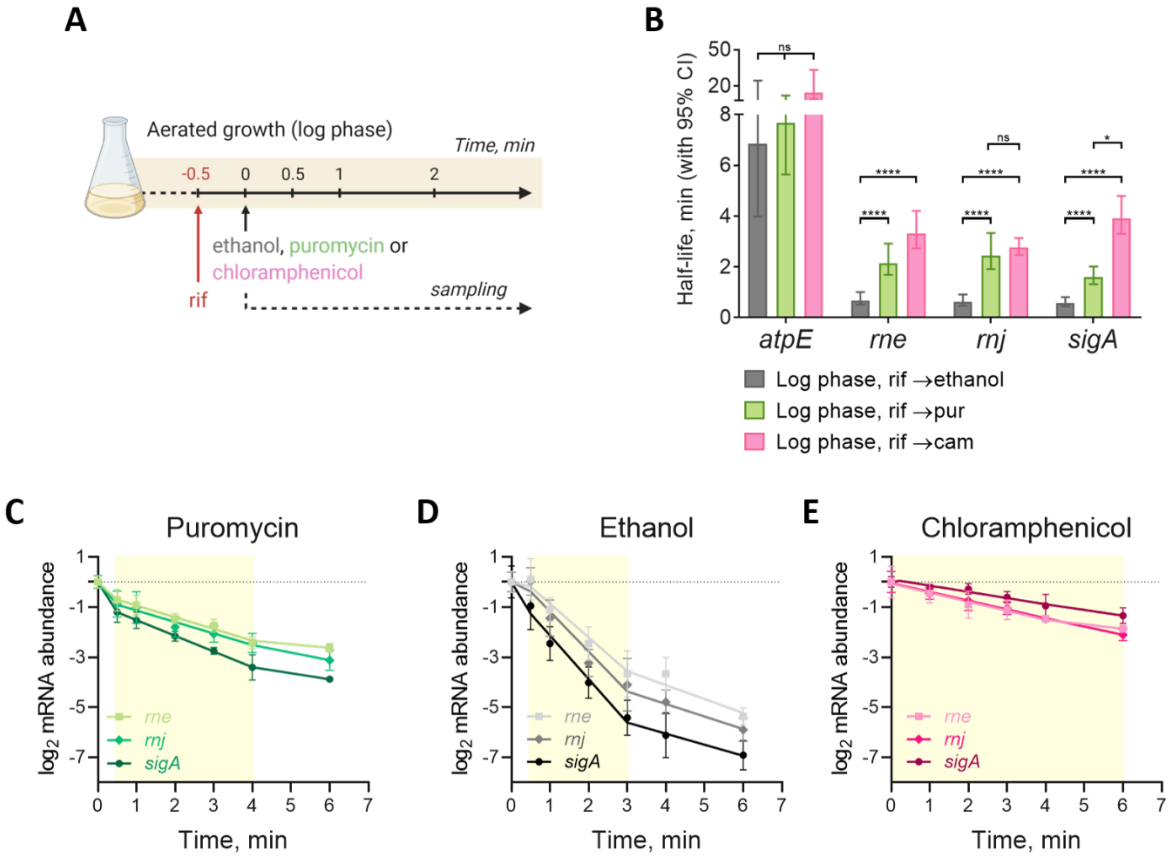

Figure 4-4. Puromycin has a dual effect on mRNA stability in *Mycobacterium smegmatis*. (A) Analysis of mRNA degradation in log phase *M. smegmatis* cultures treated with rifampicin (rif) and 30 seconds after with ethanol, puromycin (pur) or chloramphenicol (cam). (B) Drugs that cause ribosome stalling and premature ribosome release both lead to increased mRNA half-lives in log phase. mRNA half-life was calculated using the time points from the longest linear regression section in the transcript degradation plots (*see next panels, region highlighted in yellow*). * = p<0.05, **** = p<0.0001, ns= not significant; linear regression test, n=3. (C) Segmental linear regression for *rifampicin → puromycin*. A segmental fitting shows a faster mRNA degradation trend for the first 30 seconds, followed by two slower mRNA degradation trends. (D), Segmental linear regression for *rifampicin → ethanol* showing a faster mRNA degradation trend for the first 4 minutes, followed by a slower mRNA degradation trend. In the case of *rifampicin → chloramphenicol* (E) only a single degradation rate is observed. The yellow highlighted region in panels (C), (D) and (E) shows the time points used for half-life determinations in panel B. Error bars for (C), (D), (E) are standard deviation.

The effects of start codon mutations on stability of a reporter transcript

In order to further assess the impact of translation on mRNA stability we designed three reporter constructs using the coding sequence of mCherry in *M. smegmatis*. Our first reporter is *unmodified mCherry*, which contains the intact coding sequence for mCherry. Our two other reporters, *mCherryOS* and *mCherryUT,* both have mutations throughout their sequence to eliminate all possible start codons (GTG, ATG, and TTG) with the goal of reducing spurious ribosome binding. Most of the mutations were synonymous, but 11 amino acid residues were replaced by residues with chemically similar sidechains (see methods). *mCherryOS* is a translatable reporter that has 10 methionine-to-leucine replacements (M#L) and one lysine-to-arginine replacement at position 97 (K97R), keeping only M1 as a start codon. K97R was made to avoid the potential of coding for methionine in a different reading frame. *mCherryUT* is an untranslatable reporter in which we also made the M1L replacement (Figure 5A). Our three constructs were designed to be leaderless to avoid interactions with ribosomes upstream of the start codon.

M. smegmatis with either unmodified *mCherry*, *mCherryOS*, or *mCherryUT* was grown to logarithmic phase (OD_{600} = 0.40). We inhibited transcription with rifampicin, collected samples at different time points, and used qPCR to determine mRNA half-lives as described before. Our results were surprising; the transcript half-lives of unmodified *mCherry* and *mCherryUT* were similar, while *mCherryOS* had a significantly shorter half-life compared to the other two reporters (Figure 4-5B). Moreover, the abundance of unmodified *mCherry* was 5.6-fold higher than *mCherryOS*, and 20-fold higher than *mCherryUT* (Figure 4-5C and D). We had expected a modest difference in the expression levels of our reporters; however, these findings again suggest the possibility of physically coupled translation and transcription processes, with transcription consequently being reduced in the absence of translation. We revisited the coding sequence of *mCherry* and observed that two internal methionine codons (M10 and M17) could potentially

serve as start codons, as both were preceded by SD-like sequences. To explore this possibility, we designed two constructs in which the sequence upstream of M10 or M17 was removed to create Δ9 *mCherry* and Δ16 *mCherry*, respectively (Figure 4-6A).

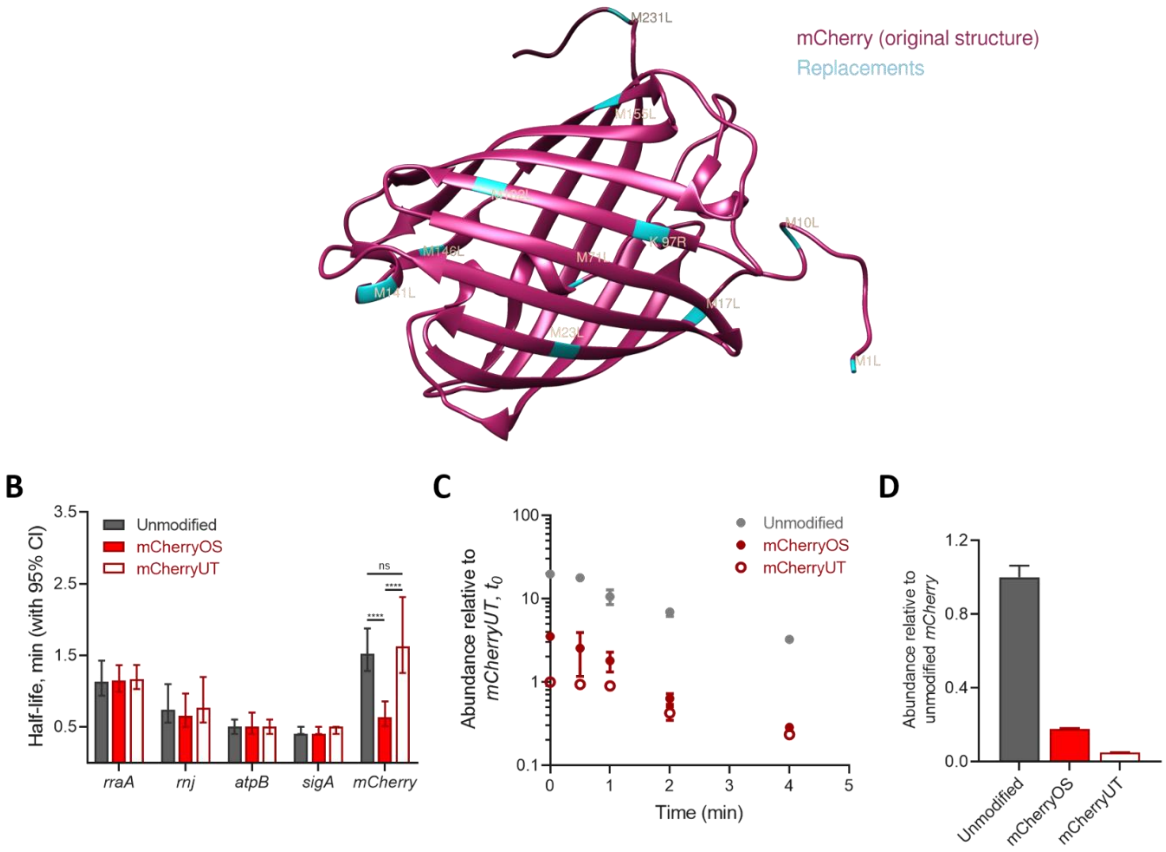

Figure 4-5. Start codon mutations lead to changes in transcript stability. (A) Protein model structure showing the original sequence of mCherry in red, with amino acid residues replacements in cyan. Methionine (M) to leucine (L), and lysine (K) to arginine (R) replacements were introduced in the protein coding sequence to generate an untranslatable version of mCherry (*mCherryUT*), as well as other synonymous mutations. A translatable version with a single start codon was also created (*mCherryOS*), with no replacement at M1. (B) mRNA half-lives for the mCherry transcripts, as well as four transcripts used as controls. *M. smegmatis* cultures were in log phase (OD_{600} = 0.1) and aerated conditions. There was a significant difference between the mRNA half-lives of *mCherryOS* and *mCherryUT*. **** = p<0.0001, ns= not significant; linear regression test, n=3. (C) mRNA degradation pattern for the different versions of the mCherry transcript, from cells in log phase and aerated conditions. (D) Steady-state abundance of *mCherryOS* and *mCherryUT* transcripts relative to the unmodified *mCherry* mRNA, from 0-minute samples in (B and C). Error bars for (C) and (D): standard deviation.

Using microscopy, we observed strong fluorescence intensity from *M. smegmatis* transformed with Δ9 *mCherry* but not from the Δ16 *mCherry* strain (Figure 4-6B) (Franca, 2020). These results show that codon M10 can also be used as a start site, and may in fact be the primary start site. This is consistent with a

previous report from *M. tuberculosis* (Carroll et al., 2014). Hence, ribosomes could have stalled near L10 and L17 in *mCherryUT*, protecting the transcript from degradation and posing challenges that would confound our ability to compare mRNA levels and mRNA degradation trends between our constructs (see Discussion).

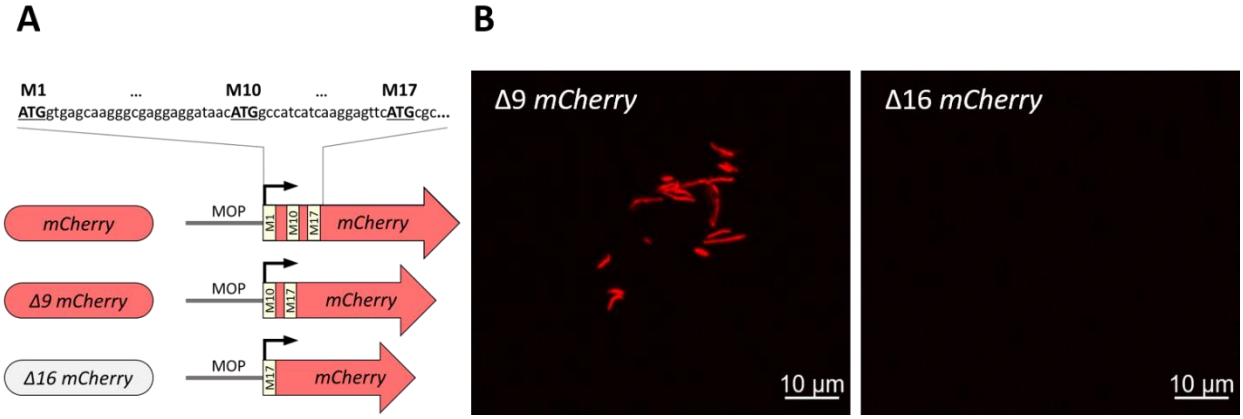

Figure 4-6. The coding sequence of *mCherry* has three possible start sites. (A) mCherry constructs modified to start either at the annotated M1 start, or at codons M10 (Δ9 mCherry) and M17 (Δ9 mCherry). (B) mCherry fluorescence is restricted to the strains carrying the unmodified mCherry gene or the M10 (Δ9 mCherry) variant.

mRNA association with ribosomes does not explain transcript stabilization under carbon starvation in *M. smegmatis.*

Based on the high rRNA to mRNA ratio in *M. smegmatis* under carbon starvation stress (Vargas-Blanco et al., 2019), we hypothesized that mRNAs may be associated with more ribosomes or ribosomal subunits than in log phase growth, protecting transcripts from RNases and therefore increasing the transcriptome half-life. To capture a snapshot of the biological interactions between *M. smegmatis* ribosomes and mRNA, we performed polysome profiling on log phase and carbon-starved cells. We first exposed *M. smegmatis* to carbon starvation for 24 hours, leading to growth cessation but maintaining cell viability (Figure 4-7A). As reported previously, we determined mRNA half-lives of *M. smegmatis* in carbon starvation stress and in rich media. Our results showed increased mRNA stability in the former condition for each assessed gene (Figure 4-7B). Using additional cultures, we recovered *M. smegmatis* cells by rapid

filtration at room temperature (~23°C) and immediately froze them in liquid nitrogen; we also added frozen lysis buffer containing chloramphenicol. Frozen cells were lysed using a Retsch CryoMill at -196°C to preserve the structural integrity of RNA and ribosomal associations. We then used a sucrose gradient to separate subunits, monosomes, and polysomes, creating a polysome profiling chart while simultaneously binning each sample into 72 fractions.

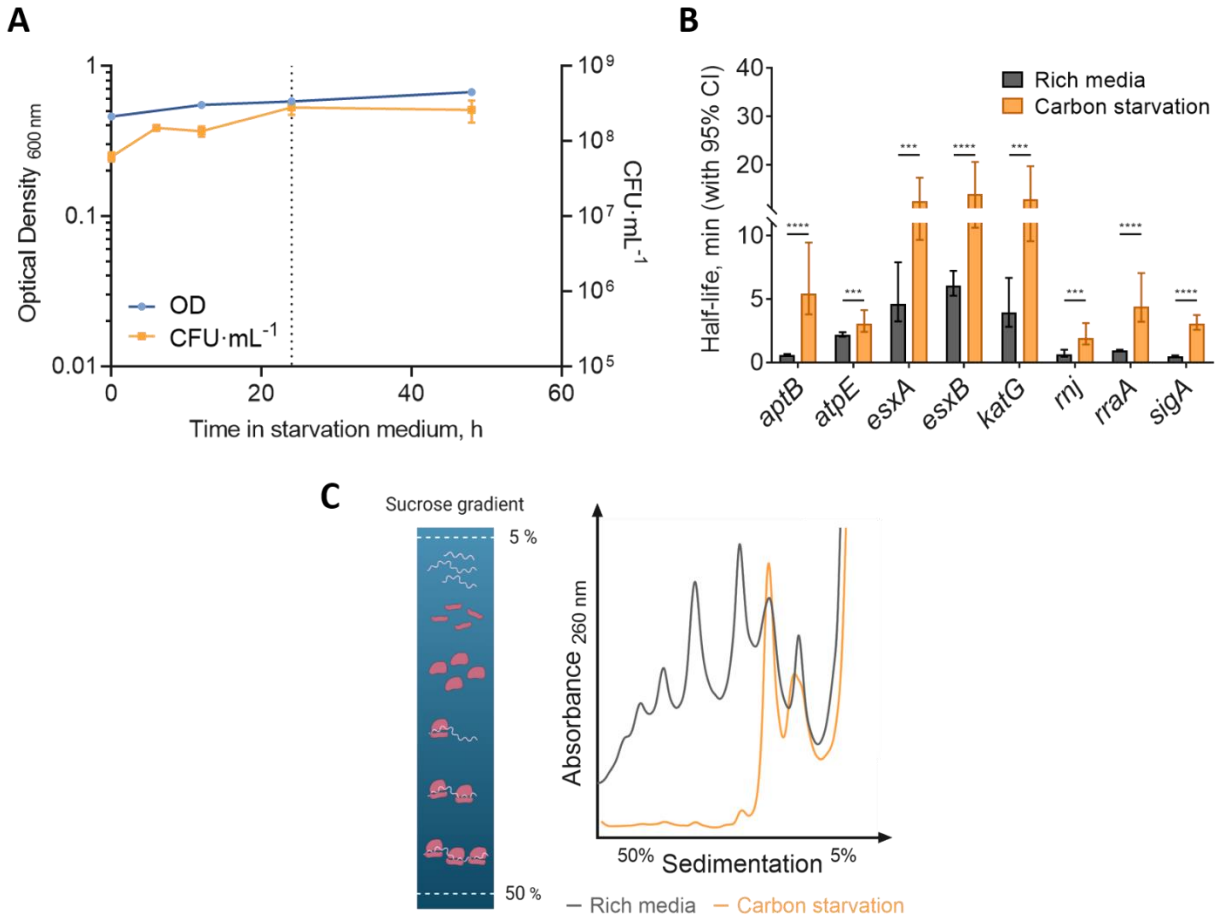

Figure 4-7. Ribosome occupancy is altered during carbon starvation in *Mycobacterium smegmatis*. (A) *M. smegmatis* growth curve, displaying viability and optical density (OD) measurements. The dotted line indicates the time at which samples were processed for mRNA half-life analysis (24 hours). (B) mRNA half-lives for *M. smegmatis* under carbon starvation stress (24 hours) or in rich media (log phase, OD: 0.8) showing dramatic transcript stabilization for cells under energy stress. *** = $p<0.001$, **** = $p<0.0001$; linear regression test, $n=3$. (C) Polysome profiling analysis to determine ribosome occupancy under carbon starvation. The polysome profiles of *M. smegmatis* in rich media and carbon starvation greatly differ, with the latter showing mostly 30S and 50S subunit peaks.

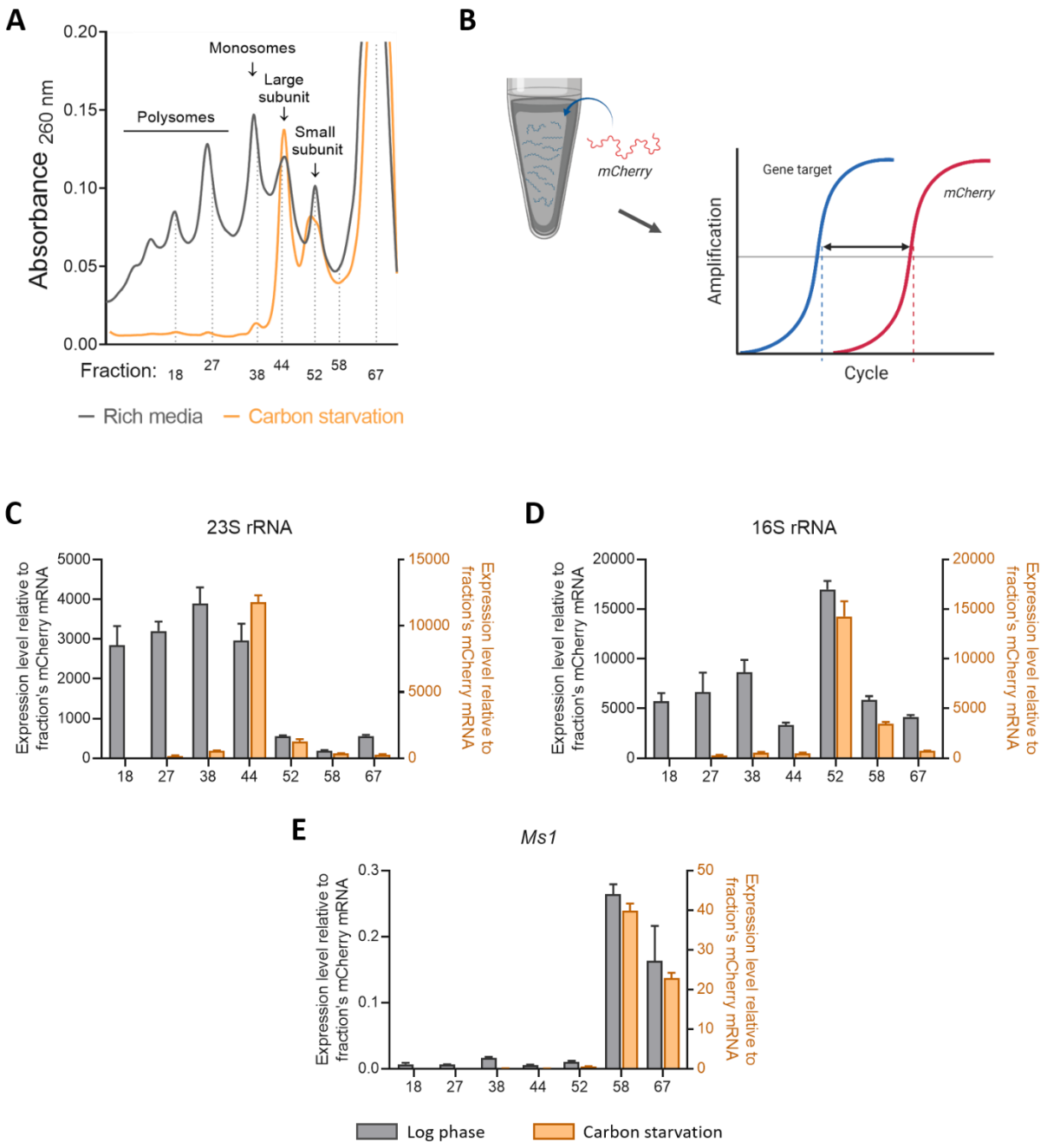

Figure 4-8. *in vitro* transcribed *mCherry* can be used to normalize transcript abundance in polysome profiling samples.(A) Polysome profiling fractions used for subsequent mRNA-ribosomal association analysis. (B) We spiked each sample with *in vitro* transcribed mCherry mRNA to compare the relative abundance of transcripts across polysome profiling fractions. Transcript abundance was estimated from qPCR data by normalizing the abundance of a target transcript to *mCherry* transcript abundance. (C) Expression levels of the controls targets 23S rRNA (large subunit); 16S rRNA (small subunit) (D); and the sRNA MS1, expected not to be associated with ribosomes/subunits (E).

Our results showed dramatically different profiles for the two conditions. In log phase samples the majority of ribosomes were present as monosomes and polysomes, consistent with active translation. In carbon starvation, most ribosomes existed as individual 30S and 50S subunits (Figure 4-7C). We confirmed which subunits were present in each peak by assessing rRNA size and abundance with a Fragment Analyzer (data not shown). These data suggested that transcripts were unlikely to have increased ribosome occupancy in carbon starvation compared to log phase growth. However, the possibility remained that mRNAs were associated with individual subunits in carbon-starved *M. smegmatis.* To exclude this possibility, we chose seven fractions corresponding to the highest concentrations of polysomes, monosomes, subunits and free mRNA for each condition (Figure 4-8A) and determined mRNA abundance in each fraction for a set of transcripts. To determine the mRNA abundance of a given transcript by qPCR we would typically normalize the sample to total RNA content (most of which is rRNA) or to a housekeeping gene. Such an approach was not possible in this experiment since samples contained varying amounts of both mRNA and rRNA. Thus, we transcribed *mCherry in vitro* and spiked 1 ng of *mCherry* mRNA into each of our seven fractions (Figure 4-8A and B). To verify our fractionation and normalization methods we included qPCR targets within both 16S and 23S rRNA and the small RNA *Ms1*. The 16S and 23S rRNA were abundant in the fractions corresponding to the small and large subunits, respectively, as well as distributed throughout the monosome and polysome fractions (Figure 4-8C and D), while *Ms1* remained dissociated from rRNA (Figure 4-8E), as we had predicted.

Then, we determined mRNA abundance for 4 target genes relative to that of *mCherry*. Our results showed that in carbon starvation samples, ribosomal associations with mRNA varied by gene (Figure 4-9). For example, a large proportion of *sigA* was associated with monosomes, while *atpE* was mostly associated with polysomes (Figure 4-9). On the other hand, the proportions of transcripts that interacted with monosomes and polysomes, interacted with 30S and 50S subunits, or did not interact with any were

similar for both *rnj* and *rraA* (Figure 4-9). In log phase samples there was also variability among genes with respect to the relative abundance of mRNA in various fractions. However, there was a consistent trend in which the distribution of mRNA abundance across fractions was heavily skewed toward the polysome and monosome fraction in log phase samples. This skew was absent or weaker in the carbon starvation samples. We can therefore conclude that mRNAs do not generally have greater ribosome occupancies in carbon starvation compared to log phase. Overall, while mRNA associations with ribosomes can lead to transcript stabilization in other contexts, ribosomes do not seem to be part of the global mRNA stabilization response to low energy stress.

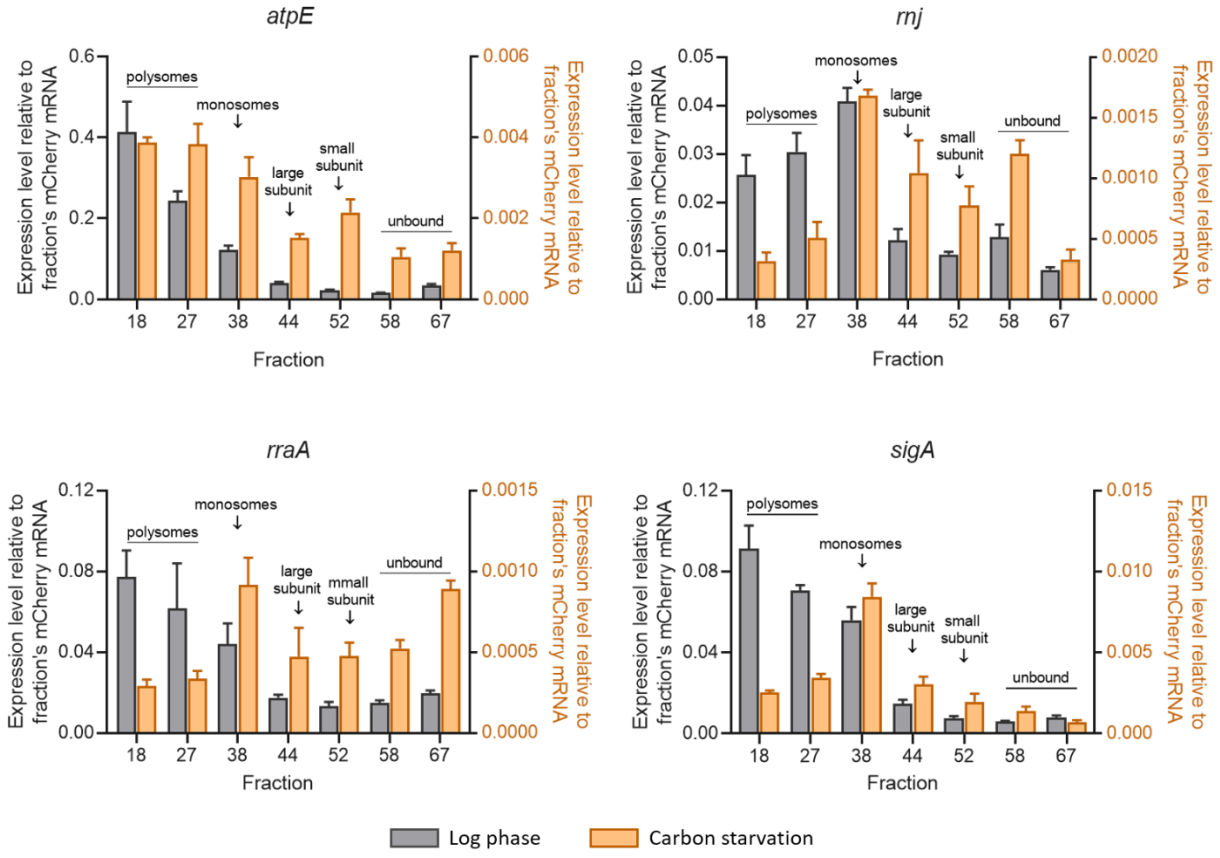

Figure 4-9. mRNA association with ribosomes does not explain transcript stabilization under carbon starvation in *Mycobacterium smegmatis*. mRNA abundance for four tested genes to determine association of mRNA and ribosomes. Carbon starvation fractions show distinct mRNA-ribosomal association profiles, which does not explain global transcript stabilization under energy stress.

Discussion

Rustad et al. reported that hypoxic conditions lead to transcriptome stabilization in *M. tuberculosis* (Rustad et al., 2013). We have previously shown that *M. smegmatis* plausibly has a similar stress response, as we reported increased mRNA half-lives for a set of transcripts during hypoxia (Vargas-Blanco et al., 2019). But, is mRNA stabilization also a transcriptome-wide phenomenon in *M. smegmatis*? Here, we complemented our previous findings by reporting transcriptome-wide half-life data for *M. smegmatis* under normoxic and hypoxic conditions. We measured half-lives for 3179 of the ~6625 genes in *M. smegmatis*, considering only genes for which we had high-confidence half-life predictions in both normoxia and hypoxia. The median mRNA half-life for *M. smegmatis* when entering a non-growing phase in early-stage hypoxia is 29.9 min. In contrast, the average mRNA half-life for *M. smegmatis* in normoxic log phase growth (OD = 0.8) for the same set of genes is 0.8 min (Figure 4-1). We also observed that the average log phase mRNA half-life for *M. smegmatis* is shorter compared to that of log phase *M. tuberculosis* (9.5 min) (Rustad et al., 2013), a difference we attribute to the ~10-fold difference in doubling time between these mycobacteria. Furthermore, our median mRNA half-life for *M. smegmatis* in log phase is 6-fold lower than that obtained by Rustad et al., most likely due to the time-points used. Rustad et al. only considered 0, 5 and 10 min. In contrast, we obtained data for 0, 1, 2, 3, 4, 8 and 16 min after transcription was blocked, and only the first five time-points were used to determine half-lives, as degradation slows for most genes after 4 min. Regardless of these technique differences, our RNA-seq results validate our findings on transcript stabilization during hypoxia in *M. smegmatis* (Vargas-Blanco et al., 2019). As such, in subsequent sections we make the key assumption that mRNA half-life trends observed for a subset of genes using qPCR are generally representative of transcriptome-wide responses.

We and others have shown that in low energy stress conditions the ratio of rRNA to mRNA greatly increases in *M. smegmatis* (Vargas-Blanco et al., 2019) and other bacteria (Betts et al., 2002; Wood et al.,

2005), suggesting that the ratio of ribosomes to mRNA is correspondingly increased. Although active translation is presumably low in non-growing, energy-starved cells, it is plausible that large numbers of ribosomes or ribosomal subunits associate non-productively with mRNA leading to occlusion of RNase cleavage sites. We therefore wondered if increased ribosome occupancy could explain the global transcript stabilization we observed in mycobacteria during hypoxia.

Translation can cause RNase occlusion, ultimately interfering with transcript degradation as we reviewed before (Vargas-Blanco and Shell, 2020). Experiments in *E. coli* using translation inhibitors showed major shifts in mRNA degradation, a role primarily attributed to ribosome stalling (Fry et al., 1972; Pato et al., 1973). This means that active translation is not always necessary for ribosomes to protect mRNA from degradation. Indeed, ribosomes could act as obstacles during scanning function of endonucleases, such as RNase E in *E. coli* (Richards and Belasco, 2019). Our results are in agreement with these statements, as ribosome stalling in chloramphenicol-treated *M. smegmatis* caused mRNAs to become more stable when compared to the vehicle treatment in conditions of hypoxia and log phase (Figure 4-2A, Figure 4-4B and Figure 4-4E). We also induced ribosome stalling under hypoxia with chloramphenicol to determine if mRNA-ribosome associations formed under stress could confer mRNA stability even after reaeration. Indeed, transcript stabilization remained after *M. smegmatis* was re-exposed to O_2 (Figure 4-2B and C). Importantly, we allowed chloramphenicol-treated mycobacteria to resume transcription for two minutes after reaeration (*chloramphenicol → reaeration → rifampicin*) and compared this treatment with another in which rifampicin was added before reaeration (*chloramphenicol → rifampicin → reaeration*). Surprisingly, the expression levels for most transcripts were similar between these two treatments, in contrast to untreated cells which demonstrated a burst of transcription in the two minutes following reaeration. We propose two explanations for these results. In the absence of ribosome translocation RNA polymerase could be less effective at transcript elongation, supporting the possibility that translation and

transcription are physically coupled processes in *M. smegmatis* as we suggested in Chapter 3, as well as others had previously shown for *E. coli* (Miller et al., 1970; Burmann et al., 2010; Proshkin et al., 2010; Zhang et al., 2014; Fan et al., 2017). Another possibility is that the chloramphenicol-induced translation stress causes an increased ratio of rRNA transcription to mRNA transcription, which would confound our ability to compare mRNA levels across conditions since we use total RNA as a normalizer.

We reasoned that if ribosomes protect transcript from RNases, depleting ribosomes from mRNA would render transcripts more susceptible to degradation. Thus, we treated *M. smegmatis* cultures with puromycin to strip off ribosomes from mRNA templates. Unexpectedly, puromycin led to transcript stabilization, similarly to the outcome of chloramphenicol-treated cells but not to those with the drug vehicle (Figure 4-4). Upon closer inspection of the mRNA degradation trends, we observed an initial fast degradation phase from 0 s to 30 s in puromycin-treated cells, something not commonly found in other multiphasic degradation trends (Hambraeus et al., 2003; Selinger et al., 2003; Chen et al., 2015; Moffitt et al., 2016; Vargas-Blanco et al., 2019; Nguyen et al., 2020). We conceived a few explanations for this phenomenon, as it is possible that puromycin has direct and indirect effects on mRNA degradation. Puromycin could initially cause ribosomes to fall off, enabling RNases access to degrade most unprotected transcripts, as expected. A ribosome-to-mRNA ratio increase could explain the increase in transcript stability during the third phase; regardless of completing translation, ribosomes would be more likely to bind the RBS blocking the 5'end from RNase interactions. Alternatively, if ribosomes fall off rapidly upon puromycin addition, the RNA polymerase could end transcription prematurely, preventing residual transcription from elongating RNAPs which are unaffected by rif. This would further support transcription and translation being physically coupled in *M. smegmatis*, as we have previously discussed. Furthermore, studies in *E. coli* have shown that puromycin leads to faster degradation of *lacZ* and the RNA pool (Varmus et al., 1971; Pato et al., 1973). Conversely, another study reported that puromycin, as well as other

translational inhibitors, lead to mRNA stabilization (Lopez et al., 1998). A probable explanation for these contradictory findings is whether transcription was blocked before adding a translation inhibitor or not. In the case of Pato et al., transcription was blocked with rifampicin 2 min before adding puromycin. Varmus et., al used ^{3}H-uridine *lac* labelling in a pulse-chase approach, where labelling was terminated 1 min before adding puromycin. In the case of Lopez et al., the translation inhibitor was added 20 min before transcription was switched off for an IPTG-regulated gene reporter. Moreover, another group showed that kasugamycin—a drug that prevents initiation (Schluenzen et al., 2006)—also caused an increase in mRNA half-life when used 15 min before blocking transcription with rifampicin (Moffitt et al., 2016). Therefore, puromycin and other translational inhibitors could cause mRNA stability to increase if they promote a sudden increase in rRNA synthesis, a substrate that can titrate the activity of RNase E and other RNases. This was possible in the Lopez et al. and Moffitt et al. studies where cells were exposed to translation inhibitors in the absence of transcription inhibitors. In our experiments, mRNA stabilization in response to puromycin cannot be explained by increased rRNA transcription because we added rifampicin prior to puromycin. It is also possible that a combination of factors contribute to the biphasic degradation patterns we observed.

To further explore the role of ribosomal occupancy on mRNA degradation we used *mCherryUT*, an untranslatable transcript, and compared its half-life with that of *mCherryOS*, a transcript with a single translation start site, and with the unmodified mCherry transcript. Our results were surprising; the half-lives of *mCherry* and *mCherryUT* were approximately 1.5 min, while that of *mCherryOS* was ~0.6 min (Figure 4-5B). We had expected that a transcript unable to associate with ribosomes would be better targeted by RNases. Moreover, the expression level of mCherry was 5.6-fold higher than *mCherryOS*, and 20-fold higher than the level of *mCherryUT* (Figure 4-5C and D), which could potentially explain the absence of fluorescence in *mCherryOS* (data not shown). We had expected a modest difference in the

expression levels of our reporters; however, these findings supported transcription and translation as physically coupled processes. We revisited the coding sequence of mCherry and observed that M10 and M17 could potentially serve as start codons, as both were preceded by SD-like structures (Figure 4-6A). Thus, it was possible that *mCherryUT* had a shorter half-life because of stalled ribosomes near L10 and L17, protecting the transcript from degradation. Indeed, we confirmed that M10 acted as the preferred start site in *mCherry* for *M. smegmatis* as shown in Figure 4-6B and by (Franca, 2020), findings also reported for *mCherry* in *M. tuberculosis* (Carroll et al., 2014).

In *E. coli* at a fast growth rate (doubling time = 20 min) the number of ribosomes per cell was calculated to be ~70,000 (Bremer and Dennis, 2008), while in similar conditions the number of mRNA is ~10-fold lower (Bartholomaus et al., 2016). Therefore, it possible to have ~10 ribosomes committed to a single mRNA if we assume (1) an average mRNA length of 1,000 nucleotides (Ochman and Jones, 2000) and (2) a similar translation efficiency for each mRNA. Furthermore, considering a ribosome footprint of 23nt (Neuhaus et al., 2017; Mohammad et al., 2019) we estimated that ribosomes could be ~70 nucleotides apart from each other on the mRNA strand, similarly to reported estimates (Bremer and Dennis, 2008). These numbers, however, could drastically change in stress conditions that cause reductions in mRNA levels as shown by us and others (Betts et al., 2002; Wood et al., 2005; Vargas-Blanco et al., 2019). Hence, we hypothesized that an increased ratio of ribosomes to mRNA during low energy stress would lead to augmented mRNA-ribosome associations as part of the bacterial stress response, resulting in transcriptome stabilization. However, polysome profiling of *M. smegmatis* under carbon starvation revealed reduced mRNA associations with ribosomes compared to bacteria growing in rich media (Figure 4-7C). Interestingly, we observed higher levels of individual 30S and 50S subunits compared to monosomes or polysomes in carbon starved cells. To determine the relative amounts of mRNA in ribosome-bound versus unbound states, we measured abundance levels of different transcripts across

our fractionated polysome profiling samples. We discovered that our transcript targets had distinct association patters with ribosomes and subunits in mycobacteria under carbon starvation stress (Figure 4-9). More importantly, a greater proportion of *rraA* and *rnj,* and *sigA,* was not associated with ribosomes or ribosomal subunits in stressed mycobacteria compared to log phase mycobacteria (Figure 4-9). Yet, these transcripts were significantly stabilized under carbon starvation stress conditions. Overall, we conclude that while ribosomes do impact the fate of mRNA, transcriptome stabilization as a response to carbon starvation stress does not depend on mRNA-ribosome associations.

Materials and methods

Strains and culture conditions.

Mycobacterium smegmatis strain mc^2155 or its derivatives (Table 4-1) were grown in rich medium, Middlebrook 7H9 with albumin dextrose catalase (ADC; final concentrations, 5 g/L bovine serum albumin fraction V [BSA], 2 g/L dextrose, 0.85 g/L NaCl, and 3 mg/L catalase), 0.2% glycerol, and 0.05% Tween 80, which was shaken at 200 rpm and 37°C to an optical density at 600 nm (OD_{600}) of ~0.8, unless specified otherwise. For hypoxic cultures, we modified the Wayne and Hayes model as described in Chapter 3. Samples for all hypoxia RNA determinations were taken 18.5 to 19 hours after sealing the vials.

For carbon starvation cultures, cells were grown to log phase (OD_{600} = 0.8) in rich medium, pelleted, and rinsed three times with carbon starvation medium (Middlebrook 7H9 with 5 g/liter BSA, 0.85 g/liter NaCl, 3 mg/liter catalase, and 0.05% Tyloxapol) at 4°C and then resuspended in carbon starvation medium to an OD_{600} of 0.8 and incubated at 200 rpm and 37°C. *M. smegmatis* remained in these conditions for 24 hours before been used for RNA determination experiments.

The *mCherryOS* strain (SS-M_0395) was built using the MOP promoter (Mycobacterial Optimized Promoter) (Hickey et al., 1996) in plasmid pSS271 with the synthetically synthesized one-start *mCherry*

sequence, and a **synthetic bidirectional terminator region (ttsbiB)** enclosed by two buffer regions. The strain *mCherryUT* (SS-M_0397) was similarly built using pSS273, except the starting codon was **ATC** (**ATG**GTAAGCAAGGGCGAGGAGGATAACCTCGCCATCATCAAGGAGTTCCTCCGCTTCAAGGTACACCTCGAGGG CTCCGTAAACGGCCACGAGTTCGAGATCGAGGGCGAGGGCGAGGGCCGCCCCTACGAGGGCACCCAGACCGCCA AGCTCAAGGTAACCAAGGGAGGCCCCCTCCCCTTCGCCTGGGACATCCTCTCCCCTCAGTTCCTCTACGGCTCCAA GGCCTACGTAAAGCACCCCGCCGACATCCCCGACTACTTAAAGCTCTCCTTCCCCGAGGGCTTCCGCTGGGAGCGC GTACTCAACTTCGAGGACGGCGGCGTAGTAACCGTAACCCAGGACTCCTCCCTCCAGGACGGCGAGTTCATCTAC AAGGTAAAGCTCCGCGGCACCAACTTCCCCTCCGACGGCCCCGTACTCCAGAAGAAGACCCTCGGCTGGGAGGCC TCCTCCGAGCGGCTCTACCCCGAGGACGGCGCCCTCAAGGGCGAGATCAAGCAGAGGCTCAAGCTCAAGGACGG CGGCCACTACGACGCAGAGGTCAAGACCACCTACAAGGCCAAGAAGCCCGTACAGCTCCCCGGCGCCTACAACGT CAACATCAAGTTAGACATCACCTCCCACAACGAGGACTACACCATCGTAGAACAGTACGAACGCGCCGAGGGCCG CCACTCCACCGGCGGCCTCGACGAGCTCTACAAGTAG)tagggcgttgcctcaatcggcctgctgcctgcc**aaaaaaaaaagcgccg caactgcggcgctttttttttt**atcagttctggaccagcgagtatcgatgtcgacgtagttaacta). The strain *mCherry* (SS-M_0362) was built in a similar manner, using pSS264 with the unmodified sequence for *mCherry* (ATGGTGAGCAAGGGCGAGGAGGATAACATGGCCATCATCAAGGAGTTCATGCGCTTCAAGGTGCACATGGAGG GCTCCGTGAACGGCCACGAGTTCGAGATCGAGGGCGAGGGCGAGGGCCGCCCCTACGAGGGCACCCAGACCGC CAAGCTGAAGGTGACCAAGGGTGGCCCCCTGCCCTTCGCCTGGGACATCCTGTCCCCTCAGTTCATGTACGGCTCC AAGGCCTACGTGAAGCACCCCGCCGACATCCCCGACTACTTGAAGCTGTCCTTCCCCGAGGGCTTCAAGTGGGAG CGCGTGATGAACTTCGAGGACGGCGGCGTGGTGACCGTGACCCAGGACTCCTCCCTGCAGGACGGCGAGTTCATC TACAAGGTGAAGCTGCGCGGCACCAACTTCCCCTCCGACGGCCCCGTAATGCAGAAGAAGACCATGGGCTGGGA GGCCTCCTCCGAGCGGATGTACCCCGAGGACGGCGCCCTGAAGGGCGAGATCAAGCAGAGGCTGAAGCTGAAG GACGGCGGCCACTACGACGCTGAGGTCAAGACCACCTACAAGGCCAAGAAGCCCGTGCAGCTGCCCGGCGCCTA CAACGTCAACATCAAGTTGGACATCACCTCCCACAACGAGGACTACACCATCGTGGAACAGTACGAACGCGCCGA GGGCCGCCACTCCACCGGCGGCATGGACGAGCTGTACAAGGCAGCAAACGACGAAAACTACGCTCTGGCCGCGT

AG). Constructs were built using NEBuilder HiFi (E2621). Integrants were selected with 50 µg/mL kanamycin and confirmed by sequencing.

The mCherryOS protein sequence was designed using the BLOSUM62 scoring matrix for amino acid substitutions, and its structural sequence was modelled using MODELLER 9.18 (Sali and Blundell, 1993) and UCSF Chimera (Pettersen et al., 2004) using as template the crystal structure of mCherry, PDB entry 2HQ5 (Shu et al., 2006).

RNA extraction and determination of mRNA stability by qPCR.

Biological triplicate cultures were treated with rifampicin to a final concentration of 150 µg/mL to halt transcription. For most culture conditions samples of 7 mL were frozen using liquid nitrogen and RNA was extracted at various time points thereafter. Details about cell culture sampling and RNA processing for qPCR analyses are described in detail in Chapter 3.

Transcript abundance (A) over time (t) was determined for different genes (primers in Table 4-2) by quantitative PCR (qPCR) using iTaq SYBR green (Bio-Rad) with 400 pg of cDNA and 0.25 µM each primer in 10-µL reaction mixtures, with 40 cycles of 15 s at 95°C and 1 min at 61°C (Applied Biosystems 7500). Abundance was expressed as the negative threshold cycle ($-C_T$) [reflecting the $\log_2 A\,(t)$]. Linear regression was performed on $-C_T$ values versus time where the negative reciprocal of the best-fit slope estimates mRNA half-life (see Chapter 3, supplemental material).

RNA processing and determination of mRNA stability by RNA-seq.

Samples for hypoxic and normoxic cultures were obtained as described before and stored at −80°C. Cell cultures were thawed immediately before RNA extraction. Cells were pelleted, lysed and RNA was recovered as described in Chapter 3, with the following modifications: DNase treatment was not included

as an in-column step, instead we used 2.5 U of TURBO™ DNase and 80,000 U of NEB RNase inhibitor to treat 600 ng of RNA for 1 hour at 37°C, with mild agitation. A second RNA clean-up step followed using a Zymo RNA Clean & Concentrator™-25 kit according to the manufacturer's instructions, but using 3 Wash Buffer steps. mRNA abundance was determined by qPCR, as described by the protocol detailed in Appendix I. RNA-seq libraries were constructed and sequenced by the Broad Institute Microbial 'Omics Core.

RNA-seq data was normalized for each time point using transcript abundance information collected by qPCR for eight transcript targets (shown in Table 4-2). Read counts per sample were expressed as RPKM (Reads Per Kilobase of transcript, per Million) and the summation of RPKMs within a qPCR target region was denoted $\sum RPKM$. For each of the 8 qPCR targets a calculated $\sum RPKM$ at any given time ($calc.\sum RPKM_n$) can be obtained using the transcript abundance at any given time (A_n), the average transcript abundance at time zero ($\langle A_0 \rangle$) and the average $\sum RPKM$ at time zero ($exp.\sum RPKM_0$) according to:

$$calc.\sum RPKM_n = \left(\frac{A_n}{\langle A_0 \rangle}\right) \times \langle exp.\sum RPKM_0 \rangle$$

A_n and A_0 are determined from the qPCR data. An RNA-seq normalization factor per gene can be obtained by dividing the $calc.\sum RPKM_n$ by its corresponding experimentally determined $\sum RPKM_n$:

$$Normalization\ Factor = \frac{calc.\sum RPKM_n}{exp.\sum RPKM_n}$$

RNA-seq data was normalized by multiplying each RPKM by the Normalization Factor average obtained for the eight qPCR transcript targets.

mRNA stability after translational inhibition in hypoxia and reaeration.

Hypoxia cultures were used 18.5 hours after sealing the vials. For the chloramphenicol → rifampicin treatments, translation was halted by 150 µg/mL chloramphenicol, 150 µg/mL rifampicin was added 1 min later, and samples were taken 1 min afterwards. For the reaeration version of the previous treatment, samples were taken after a 1-min reaeration period. For the chloramphenicol → reaeration → rifampicin treatment, chloramphenicol was added 2 min before reaeration and rifampicin 2 min after reaeration. Chloramphenicol, ethanol (drug vehicle) and rifampicin solutions were degassed under vacuum for 20 min before use. Collected samples were immediately frozen in liquid nitrogen and stored at -80°C.

mRNA stability after translational inhibition in exponential phase.

M. smegmatis cells in logarithmic phase (OD_{600} = 0.8) were treated with 150 µg/mL rifampicin and 0.5 min after with 150 µg/mL chloramphenicol, 500 µg/mL puromycin or an equally matching volume of the drug vehicle (135 µL of ethanol). Samples were collected immediately after the translational inhibitor—or the drug vehicle—was added (Figure 4-4A).

Polysome profiling.

Biological triplicate cultures of *M. smegmatis* in logarithmic phase (OD_{600} = 0.94, 300 mL) or in 22-h carbon starvation (OD_{600} = 0.94, 600 mL) were filtered over 0.20 µm filters (VWR part number 10040-468) using a vacuum pump at room temperature (~23°C), and cells were scraped into 50 mL of liquid nitrogen. Lysis buffer (20 mM Tris pH 8, 10 mM $MgCl_2$, 100 mM NH_4Cl, 5 mM $CaCl_2$, 0.4% Triton-X 100, 0.1% Igepal (NP-40), 1 mM chloramphenicol, 100 U/mL RNase-free DNase) was carefully added to the same liquid nitrogen, forming small crystal spheres. Frozen cell pellets and crystalized lysis buffer were ground in a Retsch CryoMill using 10 mL grinding jars and a single 7 mm stainless steel ball (6 cycles of 3 min at 15 Hz, with a 1 min pause in between). Cell lysates were thawed at 30° for 2 min and then on ice for 30 min. Lysates

were clarified by centrifugation at 21,130 x g and 4°C for 10 min. Three aliquots of 1 mg of RNA in 150 µL of RNase-free water, per sample, were layered onto a 5%-50% linear sucrose gradient (gradients made using a Biocomp Gradient Master). Sucrose gradients were fractioned using an Optima L90K ultra centrifuge (SW 41 Ti rotor) at 35,000 RPM (151,000 x g) for 2 h 45 min at 4°C, and analyzed using an EM-1 Econ UV Monitor (Bio-Rad) while creating 72 x 150 µL fractions. A detailed protocol is included as Appendix J.

in vitro mRNA synthesis and quantification of low-abundance mRNA samples.

The *mCherry* (M10) sequence + T7 terminator (782 bp) was obtained from plasmid pSS374 using EcoRI. RNA was *in vitro* generated with a HiScribe T7 Quick High Yield RNA Synthesis Kit (NEB, E2050S) followed by RNA purification using the LiCl protocol, according to the manufacturer's instructions. Size confirmation was done by the agarose gel electrophoresis.

To estimate mRNA abundance from polysome profiling fractions, an 80 µL fraction aliquot was spiked with 1 ng of *mCherry* mRNA. RNA was purified using acid phenol:chloroform:IAA (125:24:1, pH 4-5) and cDNA was synthesized as described in Appendix K. mRNA abundance was quantified by qPCR as described before. mRNA expression levels were calculated with respect to the *mCherry*'s abundance, per sample.

References

Azzam, M.E., and Algranati, I.D. (1973). Mechanism of puromycin action: fate of ribosomes after release of nascent protein chains from polysomes. Proc Natl Acad Sci U S A 70(12), 3866-3869.

Bartholomaus, A., Fedyunin, I., Feist, P., Sin, C., Zhang, G., Valleriani, A., et al. (2016). Bacteria differently regulate mRNA abundance to specifically respond to various stresses. Philos Trans A Math Phys Eng Sci 374(2063). doi: 10.1098/rsta.2015.0069.

Bechhofer, D.H., and Dubnau, D. (1987). Induced mRNA stability in *Bacillus subtilis*. Proc Natl Acad Sci U S A 84(2), 498-502. doi: 10.1073/pnas.84.2.498.

Bechhofer, D.H., and Zen, K.H. (1989). Mechanism of erythromycin-induced ermC mRNA stability in *Bacillus subtilis*. J Bacteriol 171(11), 5803-5811. doi: 10.1128/jb.171.11.5803-5811.1989.

Betts, J.C., Lukey, P.T., Robb, L.C., McAdam, R.A., and Duncan, K. (2002). Evaluation of a nutrient starvation model of *Mycobacterium tuberculosis* persistence by gene and protein expression profiling. Mol Microbiol 43(3), 717-731.

Bremer, H., and Dennis, P.P. (2008). Modulation of Chemical Composition and Other Parameters of the Cell at Different Exponential Growth Rates. EcoSal Plus 3(1). doi: 10.1128/ecosal.5.2.3.

Burmann, B.M., Schweimer, K., Luo, X., Wahl, M.C., Stitt, B.L., Gottesman, M.E., et al. (2010). A NusE:NusG complex links transcription and translation. Science 328(5977), 501-504. doi: 10.1126/science.1184953.

Carroll, P., Muwanguzi-Karugaba, J., Melief, E., Files, M., and Parish, T. (2014). Identification of the translational start site of codon-optimized mCherry in *Mycobacterium tuberculosis*. BMC Res Notes 7, 366. doi: 10.1186/1756-0500-7-366.

Chen, H., Shiroguchi, K., Ge, H., and Xie, X.S. (2015). Genome-wide study of mRNA degradation and transcript elongation in *Escherichia coli*. Mol Syst Biol 11(1), 781. doi: 10.15252/msb.20145794.

Chen, Y.X., Xu, Z.Y., Ge, X., Sanyal, S., Lu, Z.J., and Javid, B. (2020). Selective translation by alternative bacterial ribosomes. Proc Natl Acad Sci U S A 117(32), 19487-19496. doi: 10.1073/pnas.2009607117.

Dai, X., Zhu, M., Warren, M., Balakrishnan, R., Okano, H., Williamson, J.R., et al. (2018). Slowdown of Translational Elongation in *Escherichia coli* under Hyperosmotic Stress. mBio 9(1). doi: 10.1128/mBio.02375-17.

Dai, X., Zhu, M., Warren, M., Balakrishnan, R., Patsalo, V., Okano, H., et al. (2016). Reduction of translating ribosomes enables *Escherichia coli* to maintain elongation rates during slow growth. Nat Microbiol 2, 16231. doi: 10.1038/nmicrobiol.2016.231.

Dalbow, D.G., and Young, R. (1975). Synthesis time of beta-galactosidase in *Escherichia coli* B/r as a function of growth rate. Biochem J 150(1), 13-20. doi: 10.1042/bj1500013.

Dressaire, C., Picard, F., Redon, E., Loubiere, P., Queinnec, I., Girbal, L., et al. (2013). Role of mRNA stability during bacterial adaptation. PLoS One 8(3), e59059. doi: 10.1371/journal.pone.0059059.

Esquerre, T., Bouvier, M., Turlan, C., Carpousis, A.J., Girbal, L., and Cocaign-Bousquet, M. (2016). The Csr system regulates genome-wide mRNA stability and transcription and thus gene expression in *Escherichia coli*. Sci Rep 6, 25057. doi: 10.1038/srep25057.

Esquerre, T., Laguerre, S., Turlan, C., Carpousis, A.J., Girbal, L., and Cocaign-Bousquet, M. (2014). Dual role of transcription and transcript stability in the regulation of gene expression in *Escherichia coli* cells cultured on glucose at different growth rates. Nucleic Acids Res 42(4), 2460-2472. doi: 10.1093/nar/gkt1150.

Esquerre, T., Moisan, A., Chiapello, H., Arike, L., Vilu, R., Gaspin, C., et al. (2015). Genome-wide investigation of mRNA lifetime determinants in *Escherichia coli* cells cultured at different growth rates. BMC Genomics 16, 275. doi: 10.1186/s12864-015-1482-8.

Fan, H., Conn, A.B., Williams, P.B., Diggs, S., Hahm, J., Gamper, H.B., Jr., et al. (2017). Transcription-translation coupling: direct interactions of RNA polymerase with ribosomes and ribosomal subunits. Nucleic Acids Res 45(19), 11043-11055. doi: 10.1093/nar/gkx719.

Franca, K. P. (2020). Investigating RNase E Autoregulation in *Mycobacterium smegmatis*. Retrieved from https://digitalcommons.wpi.edu/mqp-all/7545

Fry, M., Israeli-Reches, M., and Artman, M. (1972). Stabilization and breakdown of *Escherichia coli* messenger ribonucleic acid in the presence of chloramphenicol. Biochemistry 11(16), 3054-3059. doi: 10.1021/bi00766a017.

Hambraeus, G., Karhumaa, K., and Rutberg, B. (2002). A 5' stem-loop and ribosome binding but not translation are important for the stability of *Bacillus subtilis* aprE leader mRNA. Microbiology 148(Pt 6), 1795-1803. doi: 10.1099/00221287-148-6-1795.

Hambraeus, G., von Wachenfeldt, C., and Hederstedt, L. (2003). Genome-wide survey of mRNA half-lives in *Bacillus subtilis* identifies extremely stable mRNAs. Mol Genet Genomics 269(5), 706-714. doi: 10.1007/s00438-003-0883-6.

Hickey, M.J., Arain, T.M., Shawar, R.M., Humble, D.J., Langhorne, M.H., Morgenroth, J.N., et al. (1996). Luciferase in vivo expression technology: use of recombinant mycobacterial reporter strains to evaluate antimycobacterial activity in mice. Antimicrob Agents Chemother 40(2), 400-407. doi: 10.1128/AAC.40.2.400.

Hue, K.K., Cohen, S.D., and Bechhofer, D.H. (1995). A polypurine sequence that acts as a 5' mRNA stabilizer in *Bacillus subtilis*. J Bacteriol 177(12), 3465-3471. doi: 10.1128/jb.177.12.3465-3471.1995.

Jurgen, B., Schweder, T., and Hecker, M. (1998). The stability of mRNA from the gsiB gene of *Bacillus subtilis* is dependent on the presence of a strong ribosome binding site. Mol Gen Genet 258(5), 538-545. doi: 10.1007/s004380050765.

Klumpp, S., Scott, M., Pedersen, S., and Hwa, T. (2013). Molecular crowding limits translation and cell growth. Proc Natl Acad Sci U S A 110(42), 16754-16759. doi: 10.1073/pnas.1310377110.

Lopez, P.J., Marchand, I., Yarchuk, O., and Dreyfus, M. (1998). Translation inhibitors stabilize *Escherichia coli* mRNAs independently of ribosome protection. Proc Natl Acad Sci U S A 95(11), 6067-6072.

Melin, L., Rutberg, L., and von Gabain, A. (1989). Transcriptional and posttranscriptional control of the *Bacillus subtilis* succinate dehydrogenase operon. J Bacteriol 171(4), 2110-2115. doi: 10.1128/jb.171.4.2110-2115.1989.

Miller, O.L., Jr., Hamkalo, B.A., and Thomas, C.A., Jr. (1970). Visualization of bacterial genes in action. Science 169(3943), 392-395.

Moffitt, J.R., Pandey, S., Boettiger, A.N., Wang, S., and Zhuang, X. (2016). Spatial organization shapes the turnover of a bacterial transcriptome. Elife 5. doi: 10.7554/eLife.13065.

Mohammad, F., Green, R., and Buskirk, A.R. (2019). A systematically-revised ribosome profiling method for bacteria reveals pauses at single-codon resolution. Elife 8. doi: 10.7554/eLife.42591.

Morin, M., Enjalbert, B., Ropers, D., Girbal, L., and Cocaign-Bousquet, M. (2020). Genomewide Stabilization of mRNA during a "Feast-to-Famine" Growth Transition in *Escherichia coli*. mSphere 5(3). doi: 10.1128/mSphere.00276-20.

Neuhaus, K., Landstorfer, R., Simon, S., Schober, S., Wright, P.R., Smith, C., et al. (2017). Differentiation of ncRNAs from small mRNAs in Escherichia coli O157:H7 EDL933 (EHEC) by combined RNAseq and RIBOseq - ryhB encodes the regulatory RNA RyhB and a peptide, RyhP. BMC Genomics 18(1), 216. doi: 10.1186/s12864-017-3586-9.

Nguyen, T.G., Vargas-Blanco, D.A., Roberts, L.A., and Shell, S.S. (2020). The impact of leadered and leaderless gene structures on translation efficiency, transcript stability, and predicted transcription rates in *Mycobacterium smegmatis*. J Bacteriol. doi: 10.1128/JB.00746-19.

Ochman, H., and Jones, I.B. (2000). Evolutionary dynamics of full genome content in *Escherichia coli*. EMBO J 19(24), 6637-6643. doi: 10.1093/emboj/19.24.6637.

Paesold, G., and Krause, M. (1999). Analysis of rpoS mRNA in *Salmonella dublin*: identification of multiple transcripts with growth-phase-dependent variation in transcript stability. J Bacteriol 181(4), 1264-1268.

Pato, M.L., Bennett, P.M., and von Meyenburg, K. (1973). Messenger ribonucleic acid synthesis and degradation in *Escherichia coli* during inhibition of translation. J Bacteriol 116(2), 710-718.

Pedersen, S. (1984). Escherichia coli ribosomes translate in vivo with variable rate. EMBO J 3(12), 2895-2898.

Pettersen, E.F., Goddard, T.D., Huang, C.C., Couch, G.S., Greenblatt, D.M., Meng, E.C., et al. (2004). UCSF Chimera--a visualization system for exploratory research and analysis. J Comput Chem 25(13), 1605-1612. doi: 10.1002/jcc.20084.

Proshkin, S., Rahmouni, A.R., Mironov, A., and Nudler, E. (2010). Cooperation between translating ribosomes and RNA polymerase in transcription elongation. Science 328(5977), 504-508. doi: 10.1126/science.1184939.

Richards, J., and Belasco, J.G. (2019). Obstacles to Scanning by RNase E Govern Bacterial mRNA Lifetimes by Hindering Access to Distal Cleavage Sites. Mol Cell 74(2), 284-295 e285. doi: 10.1016/j.molcel.2019.01.044.

Rock, J.M., Hopkins, F.F., Chavez, A., Diallo, M., Chase, M.R., Gerrick, E.R., et al. (2017). Programmable transcriptional repression in mycobacteria using an orthogonal CRISPR interference platform. Nat Microbiol 2, 16274. doi: 10.1038/nmicrobiol.2016.274.

Rustad, T.R., Minch, K.J., Brabant, W., Winkler, J.K., Reiss, D.J., Baliga, N.S., et al. (2013). Global analysis of mRNA stability in *Mycobacterium tuberculosis*. Nucleic Acids Res 41(1), 509-517. doi: 10.1093/nar/gks1019.

Sali, A., and Blundell, T.L. (1993). Comparative protein modelling by satisfaction of spatial restraints. J Mol Biol 234(3), 779-815. doi: 10.1006/jmbi.1993.1626.

Schluenzen, F., Takemoto, C., Wilson, D.N., Kaminishi, T., Harms, J.M., Hanawa-Suetsugu, K., et al. (2006). The antibiotic kasugamycin mimics mRNA nucleotides to destabilize tRNA binding and inhibit canonical translation initiation. Nat Struct Mol Biol 13(10), 871-878. doi: 10.1038/nsmb1145.

Selinger, D.W., Saxena, R.M., Cheung, K.J., Church, G.M., and Rosenow, C. (2003). Global RNA half-life analysis in *Escherichia coli* reveals positional patterns of transcript degradation. Genome Res 13(2), 216-223. doi: 10.1101/gr.912603.

Shu, X., Shaner, N.C., Yarbrough, C.A., Tsien, R.Y., and Remington, S.J. (2006). Novel chromophores and buried charges control color in mFruits. Biochemistry 45(32), 9639-9647. doi: 10.1021/bi060773l.

Snapper, S.B., Melton, R.E., Mustafa, S., Kieser, T., and Jacobs, W.R., Jr. (1990). Isolation and characterization of efficient plasmid transformation mutants of *Mycobacterium smegmatis*. Mol Microbiol 4(11), 1911-1919.

Tollerson, R., 2nd, and Ibba, M. (2020). Translational regulation of environmental adaptation in bacteria. J Biol Chem 295(30), 10434-10445. doi: 10.1074/jbc.REV120.012742.

Traut, R.R., and Monro, R.E. (1964). The Puromycin Reaction and Its Relation to Protein Synthesis. J Mol Biol 10, 63-72. doi: 10.1016/s0022-2836(64)80028-0.

Vargas-Blanco, D.A., and Shell, S.S. (2020). Regulation of mRNA Stability During Bacterial Stress Responses. Front Microbiol 11, 2111. doi: 10.3389/fmicb.2020.02111.

Vargas-Blanco, D.A., Zhou, Y., Zamalloa, L.G., Antonelli, T., and Shell, S.S. (2019). mRNA Degradation Rates Are Coupled to Metabolic Status in *Mycobacterium smegmatis*. mBio 10(4). doi: 10.1128/mBio.00957-19.

Varmus, H.E., Perlman, R.L., and Pastan, I. (1971). Regulation of lac transcription in antibiotic-treated *E. coli*. Nat New Biol 230(10), 41-44. doi: 10.1038/newbio230041a0.

Wayne, L.G., and Hayes, L.G. (1996). An in vitro model for sequential study of shiftdown of *Mycobacterium tuberculosis* through two stages of nonreplicating persistence. Infect Immun 64(6), 2062-2069.

Wolfe, A.D., and Hahn, F.E. (1965). Mode of Action of Chloramphenicol. Ix. Effects of Chloramphenicol Upon a Ribosomal Amino Acid Polymerization System and Its Binding to Bacterial Ribosome. Biochim Biophys Acta 95, 146-155.

Wood, D.N., Chaussee, M.A., Chaussee, M.S., and Buttaro, B.A. (2005). Persistence of *Streptococcus pyogenes* in stationary-phase cultures. J Bacteriol 187(10), 3319-3328. doi: 10.1128/JB.187.10.3319-3328.2005.

Zhang, Y., Burkhardt, D.H., Rouskin, S., Li, G.W., Weissman, J.S., and Gross, C.A. (2018). A Stress Response that Monitors and Regulates mRNA Structure Is Central to Cold Shock Adaptation. Mol Cell 70(2), 274-286 e277. doi: 10.1016/j.molcel.2018.02.035.

Zhang, Y., Mooney, R.A., Grass, J.A., Sivaramakrishnan, P., Herman, C., Landick, R., et al. (2014). DksA guards elongating RNA polymerase against ribosome-stalling-induced arrest. Mol Cell 53(5), 766-778. doi: 10.1016/j.molcel.2014.02.005.

Zhu, M., and Dai, X. (2019). Maintenance of translational elongation rate underlies the survival of *Escherichia coli* during oxidative stress. Nucleic Acids Res 47(14), 7592-7604. doi: 10.1093/nar/gkz467.

Tables

Table 4-1. Strains used and sources

Strain	Characteristics	Reference or source
mc^2155	*M. smegmatis*, WT	(Snapper et al., 1990)
SS-M_0362	mc^2155 derivative containing *mCherry* on an L5-integrating plasmid pSS264 (Kan^r).	This work
SS-M_0395	mc^2155 derivative containing *mCherryOS* on an L5-integrating plasmid pSS271 (Kan^r).	This work
SS-M_0397	mc^2155 derivative containing *mCherryUT* on an L5-integrating plasmid pSS273 (Kan^r)	This work
SS-M_0436	mc^2155 derivative containing Δ9 *mCherry* on an L5-integrating plasmid pSS300 (Kan^r)	(Franca, 2020)
SS-M_0437	mc^2155 derivative containing Δ16 *mCherry* on an L5-integrating plasmid pSS301 (Kan^r)	(Franca, 2020)

Table 4-2. Primers for qPCR

Primer name	Feature	Directionality	Sequence 5' → 3'
SSS903	*atpB* (msmeg_4942)	Forward	TGTTCGTGTTCGTCTGCTAC
SSS904	*atpB* (msmeg_4942)	Reverse	CGGCTTGGCGAGTTCTT
SSS909	*atpE* (msmeg_4941)	Forward	GGGTAACGCGCTGATCTC
SSS910	*atpE* (msmeg_4941)	Reverse	GAAGGCCAGGTTGATGAAGTA
SSS706	*rnj* (msmeg_2685)	Forward	TCATCCTCTCATCGGGTTTC
SSS707	*rnj* (msmeg_2685)	Reverse	TTCGCGCTCAACCTTCT
SSS697	*rraA* (msmeg_6439)	Forward	AACTACGGCGGCAAGAT
SSS698	*rraA* (msmeg_6439)	Reverse	GTCGAGAGGATCGACTTCAG
JR273*	*sigA* (msmeg_2758)	Forward	GACTACACCAAGGGCTACAAG
JR274*	*sigA* (msmeg_2758)	Reverse	TTGATCACCTCGACCATGTG
SSS566	*mCherry*	Forward	GATGGTGTAGTCCTCGTTGTG
SSS1233	*mCherry*	Reverse	GAGGTCAAGACCACCTACA
SSS537	*esxB* (msmeg_0065)	Forward	GGTGAGGACACAGGGAAATAAG
SSS538	*esxB* (msmeg_0065)	Reverse	CGGAGATGCGCTCGAAAT
SSS1113	*Ms1*	Forward	GCCGGAAGAGAAGGCTAGAT
SSS1114	*Ms1*	Reverse	CGTCCGCTTTTCGAAACTAC
SSS1107	16S rRNA	Forward	AAGCGCAAGTGACGGTATGTG
SSS1108	16S rRNA	Reverse	AAGCTGTGAGTTTTCACGAACAAC
SSS1111	23S rRNA	Forward	AGCCTGTAGGGAGTCAGATAG
SSS1112	23S rRNA	Reverse	GCAGCATAGGATCACCGAAT
SSS846	*rne* (msmeg_4626)	Forward	TCAACACCGGCAAGTTCA
SSS847	*rne* (msmeg_4626)	Reverse	CCATGTCGATGAAGTCGATGA
SSS1298	*iolE* (msmeg_4665)	Forward	GCCTGGAACTCGGTGTG
SSS1299	*iolE* (msmeg_4665)	Reverse	ACATCTCCGGGATGACGA
SSS2041	putative RBP (msmeg_5691)	Forward	GCCAACATGCCCGGTTA
SSS2042	putative RBP (msmeg_5691)	Reverse	GCACGAGCACCAGTTCA
SSS2019	putative RBP (msmeg_6941)	Forward	CGAGGACGATCTCGAAGAG
SSS2020	putative RBP (msmeg_6941)	Reverse	GAAGTCCAGGAGGTCCAAA

*Source: Rock et al., 2017.

Chapter 5 : Conclusions and future directions

The role of a mycobacterial leader in transcription, translation, and transcript stability

Approximately 14% of the annotated genes in both *M. tuberculosis* and *M. smegmatis* are expressed as leaderless transcripts (Cortes et al., 2013; Shell et al., 2015; Martini et al., 2019) (Figure 2-1), an unusually large proportion of messages compared to other bacteria. Surprisingly, not much is known about the role of 5' UTRs—or their absence—in the regulation of gene expression in mycobacteria. We wondered if transcripts lacking 5' UTRs are differently transcribed, translated and/or degraded compared to their leadered counterparts, possibly revealing a major regulatory trait. To investigate the role of 5' UTRs in mycobacterial gene expression, we made a leadered construct using the YFP transcript (*yfp*) under the control of the p_{myc1}*tetO* promoter and its associated 5' UTR ($UTR_{pmyc1tetO}$) (Ehrt et al., 2005), or the promoter alone for a leaderless *yfp* construct. We also made the construct UTR_{sigA} consisting of YFP associated to the 5' UTR of *sigA*, a short-lived transcript in *M. tuberculosis* and *M. smegmatis*. We discovered that YFP levels were ~100-fold and ~10-fold higher for $UTR_{pmyc1tetO}$ and UTR_{sigA} *yfp* compared to their leaderless counterparts, respectively (Figure 2-4B). Transcription rate and steady-state abundance were also highly increased for the leadered constructs compared to their leaderless counterpart. Yet, transcript half-lives were similar for UTR_{sigA}-leadered and leaderless *yfp*, but twice as long for the $UTR_{pmyc1tetO}$-leader *yfp* (Figure 2-4F).

We also wondered, is translation efficiency generally higher or lower for leaderless transcripts? While our results for $UTR_{pmyc1tetO}$ seemed to suggest yes, the increased protein abundance produced by the UTR_{sigA}-leader *yfp* could be mostly explained by its steady-state mRNA level. Because our results were restricted to one transcript using different 5' UTRs, we complemented our analysis with an evaluation of published proteomics (Schubert et al., 2015) and transcriptome data (Shell et al., 2015) for *M. tuberculosis*. We considered ~475 leadered and 503 leaderless transcripts and their products and found a correlation

between mRNA and protein abundance (Figure 2-4E). These correlations were similar for leadered and leaderless transcripts, causing us to conclude that leader status is not a generalizable predictor of translation efficiency *in M. tuberculosis*.

Indeed, it has been difficult to predict the influence of 5' UTRs mRNA fate and translation efficiency in other organisms as well. In *E. coli*, the composition of the leader can cause premature termination by affecting the rate of translation (Lale et al., 2011; Lodato et al., 2012). The stability of some mRNAs has also been shown to be impacted by ribosomal binding and secondary structures in the leader region, particularly for *B. subtilis* (Agaisse and Lereclus, 1996; Hambraeus et al., 2002; Sharp and Bechhofer, 2003). Moreover, some proteins have been shown to contribute to mRNA stabilization and translation by interacting with the 5' UTR, highlighting the complexity of the functions of the leader region. The chaperone CsrA is one of them, protecting ~78 mRNAs in *E. coli* from degradation by binding to their 5' UTRs (Esquerre et al., 2016), also increasing expression (Yakhnin et al., 2013). Overall, it is clear that many 5' UTRs have regulatory roles in mRNA stability and translation. But, because of the complex combination of leader composition and the specificity of diverse leader-interacting elements, it may be impossible to predict consistent transcriptome-wide regulatory patterns.

mRNA degradation is dependent on energy metabolism status

To understand how mRNA stabilization is regulated during stress in mycobacteria, we conducted analyses on *M. smegmatis* under hypoxic and carbon starvation conditions. In order to identify elements that could regulate mRNA degradation rates, we used a set of transcripts with distinct features (e.g., monocistronic/polycistronic, leader/leaderless, short/long half-lives) whose half-lives were determined using qPCR. For each of these transcripts we observed stabilization under stress conditions. But are these transcripts representative of the global behavior of the transcriptome? Our research suggests they are, as we complemented our qPCR results using RNA-seq for *M. smegmatis* in normoxic and hypoxic conditions,

showing that mRNA stabilization is a global response to stress (Figure 4-1). Moreover, RNA-seq processing and analysis of *M. smegmatis* mRNA half-lives under 24-hour carbon starvation is underway.

As we aimed to understand how mRNA stabilization occurred under stress we wondered if stress-induced mRNA stabilization could be reversed and if so, how rapidly. The answer to this compelling question is yes, at least for *M. smegmatis* in early-stage hypoxia. We observed that it only takes a few seconds of reaeration for *M. smegmatis* to resume mRNA degradation with rates similar to those observed in normoxic log phase conditions. Fascinatingly, we also gathered evidence that transcription and translation are closely coordinated processes in *M. smegmatis* and presumably in other mycobacteria. As reported for *E. coli*, it is likely that ribosome stalling impairs RNA polymerase activity or even causes premature termination (Miller et al., 1970; Burmann et al., 2010; Proshkin et al., 2010; Zhang et al., 2014; Fan et al., 2017). We observed that the usual burst of transcription upon reaeration was prevented by chloramphenicol. These results were similar regardless of when transcription inhibition took place, either before or after reaeration (Figure 4-3). This conclusion is further supported by additional experiments, as discussed below.

Our discovery of the rapid reversibility of mRNA stabilization shaped our thinking of how mRNA degradation is likely to be regulated, narrowing the list of candidate mechanisms for stress-induced mRNA stabilization. For example, we suspected that regulation of mRNA degradation by RNase abundance modulation was not feasible, as synthesis and degradation of proteins is a relatively slow process. Western blotting analysis of PNPase, RNase E, and a predicted RNA helicase (msmeg_1930) confirmed our predictions (Figure 3-4A). On the other hand, elements that would allow a more immediate response, such as the stringent response or energy metabolism status, became potential candidates. In the actinomycetes *Streptomyces coelicolor* and *Nonomuraea,* the alarmone that regulates the stringent response, (p)ppGpp, inhibits the activity of the ribonuclease PNPase (Gatewood and Jones, 2010; Siculella

et al., 2010). We hypothesized that (p)ppGpp leads to mRNA stabilization by repression of PNPase. Hence, we used a strain unable to synthesize (p)ppGpp, and determined mRNA half-lives for transcripts under hypoxia, carbon starvation and rich media log phase conditions. However, in absence of (p)ppGpp we observed no defect in mRNA stabilization under stress, meaning the stringent response does not act as a transcriptome stabilization mechanism.

Given that ATP is used by RNA helicases, components of the RNA degradosome, we wondered if changes in ATP levels would influence the mRNA degradation machinery activity. This hypothesis was short-lived as we determined that mRNA stabilization precedes a drop in ATP levels when *M. smegmatis* transitions into hypoxia-induced growth arrest. Yet, the presence of oxygen is sufficient to resume mRNA degradation, as shown in reaeration of hypoxic *M. smegmatis* cultures (Figure 3-3B). Therefore, we decided to use ATP as a proxy to measure energy status by regulating its levels with bedaquiline (ATP synthase F_oF_1 inhibitor) or isoniazid (ATP synthesis stimulator). We discovered that alteration of metabolic status also causes changes in mRNA degradation rates. Fast mRNA degradation is observed after a burst of ATP, while mRNA stabilization is a response to ATP depletion (Figure 3-5). As both of these drugs are bacteriostatic, we designed our experiment to induce ATP depletion or ATP synthesis in non-growing bacteria. Therefore, we also discovered that mRNA stability in *M. smegmatis* is dependent on metabolic status rather than growth rate *per se*, as literature had previously suggested ((Nilsson et al., 1984; Resnekov et al., 1990; Esquerre et al., 2014; Esquerre et al., 2015)). Recently, similar findings were reported for *E. coli* (Morin et al., 2020).

Energy metabolism impacts multiple cellular processes, but which is responsible for direct mRNA stabilization? This question remains unanswered. Future efforts should focus on addressing which is the signaling molecule that triggers mRNA degradation or stabilization. A possibility is GTP, a molecule with multiple regulatory functions. For example, in *Myxococcus xanthus*, the GTP cycle of MglA regulates cell

polarization (Zhang et al., 2010). In other microorganisms, GTP participates in the regulation of diverse cell functions via Obg and other GTPases. Some examples are cell differentiation in *Streptomyces coelicolor* (Okamoto and Ochi, 1998), sporulation in *Streptomyces griseus* (Okamoto et al., 1997), and late log phase growth in *M. tuberculosis* (Sasindran et al., 2011). We suggest measuring GTP levels in *M. smegmatis* under 18-h hypoxia, as mRNA was shown to be stabilized at that time-point while ATP levels were similar to those in normoxic log phase cells. A difference in GTP levels between stressed and non-stressed mycobacteria would encourage further investigation on GTP as a regulator of mRNA stabilization.

Recent findings on bacterial mRNA caps encountered only during stress conditions suggest that nucleotide modifications can alter mRNA stability (Bird et al., 2016; Luciano et al., 2018; Hudecek et al., 2020; Luciano and Belasco, 2020). However, even if nucleotide modifications exist in hypoxic mycobacterial mRNA, we have shown that pre-existing mRNA is promptly degraded once mycobacteria are re-exposed to oxygen. There are not reported mechanisms of cap modification consistent with such a rapid timescale. Yet, it is plausible that such mRNA modifications may contribute to mRNA fate if decapping enzymes undergo conformational changes as a response to metabolic status changes, having active and inactive forms (e.g., acetylation). A similar logic can be applied to RNases, in particular RNase E, as conformational changes could alter the efficiency or assembly of the degradosome. Moreover, BR-bodies have shown to be active centers of mRNA degradation in *C. crescentus* (Al-Husini et al., 2018; Al-Husini et al., 2020), future work should also focus on determining if similar structures exist in mycobacteria and if they play a role in stress response. Finally, it is possible that different mechanisms are involved in the stabilization of the mRNA pool at different stages in the progression into non-growing states. We have observed that 40 hours after sealing the bottles in our hypoxia model, mRNAs are more stable than at 18 hours, so much so that half-lives can no longer be measured by our methodologies. Furthermore, only some transcripts were rapidly destabilized when 40-h hypoxia cultures were reaerated (data not shown). It is conceivable that some of

the mechanisms that we have excluded as contributors to stabilization at 18 hours do indeed have roles as cells progress further into semi-dormant states.

The ribosome machinery stabilizes mRNA but is not responsible for global stabilization in response to energy stress

Translation is regulated as part of the stress response. There is ample evidence that ribosome occupancy alters mRNA degradation, at least on a transcript-specific basis, for example (Emory and Belasco, 1990; Hue et al., 1995; Arnold et al., 1998; Jurgen et al., 1998). Therefore, we wondered if ribosomes can also contribute to transcriptome stabilization as a part of the mycobacterial stress response. We answered this question using three approaches: (1) by causing ribosome stalling and ribosome depletion on mRNA using chloramphenicol and puromycin, respectively; (2) by using translatable and untranslatable synthetic transcripts; (3) by doing polysome profiling of mycobacteria in rich media and carbon starvation and measuring the presence of mRNA associated to ribosome subunits, monosomes and polysomes. In the first case, we used an elongation inhibitor (chloramphenicol) to cause ribosome stalling in hypoxic mycobacteria and measured mRNA half-life in a set of transcripts. We discovered that some of our transcript targets were further stabilized while others remained similar compared the drug vehicle control (Figure 4-2A). These findings encouraged a link between ribosome occupancy and global mRNA degradation. We then validated our hypothesis that ribosome stalling in hypoxic mycobacteria would preserve mRNA stability, even after reaeration (Figure 4-2B and C). If stalled ribosomes protect the mRNA from degradation, would the absence of ribosomes make a transcript prone to faster degradation? We tested this hypothesis using *M. smegmatis* cultures in log phase treated with puromycin, a translation inhibitor that causes ribosomes to dissociate from the mRNA strand. Our results revealed a short period of mRNA hyper-degradation followed by stabilization. It is plausible that transcript degradation takes place faster when the mRNA is depleted from ribosomes. However, our results using puromycin had

unforeseen effects, possibly due to transcription and translation being coupled. Alternatively, it is possible that transcript stabilization occurs as part of a programed response to translation-related stress. Whether this response is caused by BR-bodies being sequestered or RNase activity being impaired by undefined regulators are just speculations that require further testing. In Chapter 4 we discussed these and other scenarios that could explain why puromycin also stabilizes mRNA. However, the question of whether mRNA degradation occurs faster in the absence of translation in mycobacteria remains unanswered.

For the second approach, we compared degradation rates for two transcripts that were identical except for the presence (*mCherryOS*) or absence (*mCherryUT*) of a start codon. We hypothesized that *mCherryUT* would be less stable (no ribosome association) compared to *mCherryOS* (protected by translating ribosomes). Yet, our results were unexpected as *mCherryUT* had a longer half-life than *mCherryOS* and the unmodified *mCherry* transcript. What made *mCherryUT* less prone to degradation? We reconciled these results as we discovered that in *M. smegmatis* the translation of *mCherry* relies on a preferred start site (M10) located 10 codons downstream the annotated start site. These findings were similar to those reported for mCherry in *M. tuberculosis* (Carroll et al., 2014). Therefore, *mCherryUT* and *mCherryOS* contained an unintentional leader region with the potential to act as ribosome binding site, even though M10 was mutated to Leu to prevent translation from that position. It is conceivable that ribosomes would engage the ribosome binding site upstream of L10 in *mCherryUT*, increasing transcript stability by interfering with the linear scanning function of RNase E (Richards and Belasco, 2019). If true, this would suggest that in *M. smegmatis* ribosomes can impact mRNA stability even in the absence of translation.

We also observed that the expression level of *mCherryUT* was 20-fold lower than *mCherry* and 3-fold lower than *mCherryOS*. These results could be explained by translation and transcription being physically coupled, with RNA polymerase being less efficient at transcribing *mCherryUT* in the absence of translation. The unexpected complications with *mCherryOS* and *mCherryUT* led us to redesign our untranslatable

transcript approach. Specifically, we created new mCherry constructs to be under the control of the T7 promoter using M10 as the start codon. The resulting *M. smegmatis* strains transcribe *mCherry* using the bacteriophage T7 RNA polymerase, such that transcription is effectively uncoupled from translation (Iost et al., 1992). However, measuring the *mCherry* half-lives requires further work, as neither rifampicin nor actinomycin-D block T7 RNA polymerase transcription (data not shown). We envisioned using a strain that constitutively expresses *mCherry* under a Tet-Off *dCas9*-regulated T7 promoter, that can quickly stop *mCherry* transcription in the presence of ATc. This would allow us to track mRNA degradation for a particular gene, without affecting the transcriptome degradation rate.

Is the mycobacterial transcriptome stabilized by ribosome occupancy as a response to stress? To answer this question, our third approach was based on polysome profiling for *M. smegmatis* cells grown in rich media (7H9) or under carbon starvation. The readouts revealed that carbon-starved mycobacteria are characterized by a large accumulation of 30S and 50S ribosome subunits, while monosome and polysome peaks were dramatically lower than in log phase growth (Figure 4-7C). To eliminate the hypothesis that mRNA stabilization is driven by transcript association with individual subunits, we quantified mRNA abundance by qPCR in different polysome profiling fractions. We discovered that in carbon starvation different transcripts had distinct ribosome-association profiles (Figure 4-9). Although we observed some association of mycobacterial mRNA with monosomes and polysomes during stress, there was overall a greater proportion of free mRNA compared to log phase. We therefore concluded that mRNA stabilization is not a consequence of increased ribosome occupancy during carbon starvation.

References

Agaisse, H., and Lereclus, D. (1996). STAB-SD: a Shine-Dalgarno sequence in the 5' untranslated region is a determinant of mRNA stability. Mol Microbiol 20(3), 633-643. doi: 10.1046/j.1365-2958.1996.5401046.x.

Al-Husini, N., Tomares, D.T., Bitar, O., Childers, W.S., and Schrader, J.M. (2018). alpha-Proteobacterial RNA Degradosomes Assemble Liquid-Liquid Phase-Separated RNP Bodies. Mol Cell 71(6), 1027-1039 e1014. doi: 10.1016/j.molcel.2018.08.003.

Al-Husini, N., Tomares, D.T., Pfaffenberger, Z.J., Muthunayake, N.S., Samad, M.A., Zuo, T., et al. (2020). BR-Bodies Provide Selectively Permeable Condensates that Stimulate mRNA Decay and Prevent Release of Decay Intermediates. Mol Cell 78(4), 670-682 e678. doi: 10.1016/j.molcel.2020.04.001.

Arnold, T.E., Yu, J., and Belasco, J.G. (1998). mRNA stabilization by the ompA 5' untranslated region: two protective elements hinder distinct pathways for mRNA degradation. RNA 4(3), 319-330.

Bird, J.G., Zhang, Y., Tian, Y., Panova, N., Barvik, I., Greene, L., et al. (2016). The mechanism of RNA 5' capping with NAD+, NADH and desphospho-CoA. Nature 535(7612), 444-447. doi: 10.1038/nature18622.

Burmann, B.M., Schweimer, K., Luo, X., Wahl, M.C., Stitt, B.L., Gottesman, M.E., et al. (2010). A NusE:NusG complex links transcription and translation. Science 328(5977), 501-504. doi: 10.1126/science.1184953.

Carroll, P., Muwanguzi-Karugaba, J., Melief, E., Files, M., and Parish, T. (2014). Identification of the translational start site of codon-optimized mCherry in *Mycobacterium tuberculosis*. BMC Res Notes 7, 366. doi: 10.1186/1756-0500-7-366.

Cortes, T., Schubert, O.T., Rose, G., Arnvig, K.B., Comas, I., Aebersold, R., et al. (2013). Genome-wide mapping of transcriptional start sites defines an extensive leaderless transcriptome in *Mycobacterium tuberculosis*. Cell Rep 5(4), 1121-1131. doi: 10.1016/j.celrep.2013.10.031.

Ehrt, S., Guo, X.V., Hickey, C.M., Ryou, M., Monteleone, M., Riley, L.W., et al. (2005). Controlling gene expression in mycobacteria with anhydrotetracycline and Tet repressor. Nucleic Acids Res 33(2), e21. doi: 10.1093/nar/gni013.

Emory, S.A., and Belasco, J.G. (1990). The ompA 5' untranslated RNA segment functions in *Escherichia coli* as a growth-rate-regulated mRNA stabilizer whose activity is unrelated to translational efficiency. J Bacteriol 172(8), 4472-4481. doi: 10.1128/jb.172.8.4472-4481.1990.

Esquerre, T., Bouvier, M., Turlan, C., Carpousis, A.J., Girbal, L., and Cocaign-Bousquet, M. (2016). The Csr system regulates genome-wide mRNA stability and transcription and thus gene expression in *Escherichia coli*. Sci Rep 6, 25057. doi: 10.1038/srep25057.

Esquerre, T., Laguerre, S., Turlan, C., Carpousis, A.J., Girbal, L., and Cocaign-Bousquet, M. (2014). Dual role of transcription and transcript stability in the regulation of gene expression in *Escherichia coli* cells cultured on glucose at different growth rates. Nucleic Acids Res 42(4), 2460-2472. doi: 10.1093/nar/gkt1150.

Esquerre, T., Moisan, A., Chiapello, H., Arike, L., Vilu, R., Gaspin, C., et al. (2015). Genome-wide investigation of mRNA lifetime determinants in *Escherichia coli* cells cultured at different growth rates. BMC Genomics 16, 275. doi: 10.1186/s12864-015-1482-8.

Fan, H., Conn, A.B., Williams, P.B., Diggs, S., Hahm, J., Gamper, H.B., Jr., et al. (2017). Transcription-translation coupling: direct interactions of RNA polymerase with ribosomes and ribosomal subunits. Nucleic Acids Res 45(19), 11043-11055. doi: 10.1093/nar/gkx719.

Gatewood, M.L., and Jones, G.H. (2010). (p)ppGpp inhibits polynucleotide phosphorylase from streptomyces but not from *Escherichia coli* and increases the stability of bulk mRNA in Streptomyces coelicolor. J Bacteriol 192(17), 4275-4280. doi: 10.1128/JB.00367-10.

Hambraeus, G., Karhumaa, K., and Rutberg, B. (2002). A 5' stem-loop and ribosome binding but not translation are important for the stability of *Bacillus subtilis* aprE leader mRNA. Microbiology 148(Pt 6), 1795-1803. doi: 10.1099/00221287-148-6-1795.

Hudecek, O., Benoni, R., Reyes-Gutierrez, P.E., Culka, M., Sanderova, H., Hubalek, M., et al. (2020). Dinucleoside polyphosphates act as 5'-RNA caps in bacteria. Nat Commun 11(1), 1052. doi: 10.1038/s41467-020-14896-8.

Hue, K.K., Cohen, S.D., and Bechhofer, D.H. (1995). A polypurine sequence that acts as a 5' mRNA stabilizer in *Bacillus subtilis*. J Bacteriol 177(12), 3465-3471. doi: 10.1128/jb.177.12.3465-3471.1995.

Iost, I., Guillerez, J., and Dreyfus, M. (1992). Bacteriophage T7 RNA polymerase travels far ahead of ribosomes in vivo. J Bacteriol 174(2), 619-622.

Jurgen, B., Schweder, T., and Hecker, M. (1998). The stability of mRNA from the gsiB gene of *Bacillus subtilis* is dependent on the presence of a strong ribosome binding site. Mol Gen Genet 258(5), 538-545. doi: 10.1007/s004380050765.

Lale, R., Berg, L., Stuttgen, F., Netzer, R., Stafsnes, M., Brautaset, T., et al. (2011). Continuous control of the flow in biochemical pathways through 5' untranslated region sequence modifications in mRNA expressed from the broad-host-range promoter Pm. Appl Environ Microbiol 77(8), 2648-2655. doi: 10.1128/AEM.02091-10.

Lodato, P.B., Hsieh, P.K., Belasco, J.G., and Kaper, J.B. (2012). The ribosome binding site of a mini-ORF protects a T3SS mRNA from degradation by RNase E. Mol Microbiol 86(5), 1167-1182. doi: 10.1111/mmi.12050.

Luciano, D.J., and Belasco, J.G. (2020). Np4A alarmones function in bacteria as precursors to RNA caps. Proc Natl Acad Sci U S A 117(7), 3560-3567. doi: 10.1073/pnas.1914229117.

Luciano, D.J., Vasilyev, N., Richards, J., Serganov, A., and Belasco, J.G. (2018). Importance of a diphosphorylated intermediate for RppH-dependent RNA degradation. RNA Biol 15(6), 703-706. doi: 10.1080/15476286.2018.1460995.

Martini, M.C., Zhou, Y., Sun, H., and Shell, S.S. (2019). Defining the Transcriptional and Post-transcriptional Landscapes of *Mycobacterium smegmatis* in Aerobic Growth and Hypoxia. Front Microbiol 10, 591. doi: 10.3389/fmicb.2019.00591.

Miller, O.L., Jr., Hamkalo, B.A., and Thomas, C.A., Jr. (1970). Visualization of bacterial genes in action. Science 169(3943), 392-395.

Morin, M., Enjalbert, B., Ropers, D., Girbal, L., and Cocaign-Bousquet, M. (2020). Genomewide Stabilization of mRNA during a "Feast-to-Famine" Growth Transition in *Escherichia coli*. mSphere 5(3). doi: 10.1128/mSphere.00276-20.

Nilsson, G., Belasco, J.G., Cohen, S.N., and von Gabain, A. (1984). Growth-rate dependent regulation of mRNA stability in *Escherichia coli*. Nature 312(5989), 75-77. doi: 10.1038/312075a0.

Okamoto, S., Itoh, M., and Ochi, K. (1997). Molecular cloning and characterization of the obg gene of *Streptomyces griseus* in relation to the onset of morphological differentiation. J Bacteriol 179(1), 170-179. doi: 10.1128/jb.179.1.170-179.1997.

Okamoto, S., and Ochi, K. (1998). An essential GTP-binding protein functions as a regulator for differentiation in *Streptomyces coelicolor*. Mol Microbiol 30(1), 107-119. doi: 10.1046/j.1365-2958.1998.01042.x.

Proshkin, S., Rahmouni, A.R., Mironov, A., and Nudler, E. (2010). Cooperation between translating ribosomes and RNA polymerase in transcription elongation. Science 328(5977), 504-508. doi: 10.1126/science.1184939.

Resnekov, O., Rutberg, L., and von Gabain, A. (1990). Changes in the stability of specific mRNA species in response to growth stage in *Bacillus subtilis*. Proc Natl Acad Sci U S A 87(21), 8355-8359. doi: 10.1073/pnas.87.21.8355.

Richards, J., and Belasco, J.G. (2019). Obstacles to Scanning by RNase E Govern Bacterial mRNA Lifetimes by Hindering Access to Distal Cleavage Sites. Mol Cell 74(2), 284-295 e285. doi: 10.1016/j.molcel.2019.01.044.

Sasindran, S.J., Saikolappan, S., Scofield, V.L., and Dhandayuthapani, S. (2011). Biochemical and physiological characterization of the GTP-binding protein Obg of *Mycobacterium tuberculosis*. BMC Microbiol 11, 43. doi: 10.1186/1471-2180-11-43.

Schubert, O.T., Ludwig, C., Kogadeeva, M., Zimmermann, M., Rosenberger, G., Gengenbacher, M., et al. (2015). Absolute Proteome Composition and Dynamics during Dormancy and Resuscitation of *Mycobacterium tuberculosis*. Cell Host Microbe 18(1), 96-108. doi: 10.1016/j.chom.2015.06.001.

Sharp, J.S., and Bechhofer, D.H. (2003). Effect of translational signals on mRNA decay in *Bacillus subtilis*. J Bacteriol 185(18), 5372-5379. doi: 10.1128/jb.185.18.5372-5379.2003.

Shell, S.S., Wang, J., Lapierre, P., Mir, M., Chase, M.R., Pyle, M.M., et al. (2015). Leaderless Transcripts and Small Proteins Are Common Features of the Mycobacterial Translational Landscape. PLoS Genet 11(11), e1005641. doi: 10.1371/journal.pgen.1005641.

Siculella, L., Damiano, F., di Summa, R., Tredici, S.M., Alduina, R., Gnoni, G.V., et al. (2010). Guanosine 5'-diphosphate 3'-diphosphate (ppGpp) as a negative modulator of polynucleotide phosphorylase activity in a 'rare' actinomycete. Mol Microbiol 77(3), 716-729. doi: 10.1111/j.1365-2958.2010.07240.x.

Yakhnin, A.V., Baker, C.S., Vakulskas, C.A., Yakhnin, H., Berezin, I., Romeo, T., et al. (2013). CsrA activates flhDC expression by protecting flhDC mRNA from RNase E-mediated cleavage. Mol Microbiol 87(4), 851-866. doi: 10.1111/mmi.12136.

Zhang, Y., Franco, M., Ducret, A., and Mignot, T. (2010). A bacterial Ras-like small GTP-binding protein and its cognate GAP establish a dynamic spatial polarity axis to control directed motility. PLoS Biol 8(7), e1000430. doi: 10.1371/journal.pbio.1000430.

Zhang, Y., Mooney, R.A., Grass, J.A., Sivaramakrishnan, P., Herman, C., Landick, R., et al. (2014). DksA guards elongating RNA polymerase against ribosome-stalling-induced arrest. Mol Cell 53(5), 766-778. doi: 10.1016/j.molcel.2014.02.005.

APPENDICES

Appendix A. Cell density and viability analysis for *M. smegmatis* in hypoxia

To generate a hypoxic environment for *M. smegmatis* strains, we modified the Wayne and Hayes hypoxia model (Wayne and Hayes, 1996). First, we tested serum vials of 40 mL and 20 mL capacity (Wheaton, cat. 223687); each of these bottles had a maximum volume of 54 mL and 27 mL, respectively. In order to maintain a 1:1 headspace to culture volume ratio, we used cultures of 27 mL (large vial) and 13.5 mL (small vial). In each case we cultured *M. smegmatis* mc^2155 in 7H9 at 37°C and 125 rpm in an orbital shaker, starting at an initial OD_{600} of 0.01. Vials were sealed with a vial crimper (Wheaton, cat. W225303) using rubber stoppers (Wheaton, cat. W224100-181) and aluminum seals (Wheaton, cat. 224193-01). Culture density (OD_{600}) and viability (Colony Forming Units per mL, $CFU \cdot mL^{-1}$) were monitored at different time points using three biological replicates (individual vials) per time point. Oxygen levels were qualitatively monitored using methylene blue. Our results indicated that size of the culture did not affect the viability or culture density, but methylene blue discoloration was reached at 36 h when using the small vials compared to 40 h when using the large ones (Fig. A-1A).

We observed that with a low shaking speed (125 rpm) bacteria were not homogeneously dispersed, as a sediment formed in the vials when the cultures reached the non-growing phase, exacerbating thereafter. Hence, we compared cell density and viability between cultures at 125 and 200 rpm (Fig. A-1B). As expected, cultures subject to a more vigorous agitation did not form the sediment and reached higher cell density and viability compared to the low agitation cultures, and as a consequence oxygen depletion occurred faster (methylene blue discoloration at 24 h). In addition to strain mc^2155, we also evaluated SS-M_0424 under hypoxia. SS-M_0424 is an mc^2155 derivative that contains an ATc regulated *dCas9* and a nonspecific sgRNA. This strain was used in Chapter 4. As expected, SS-M_0424 behaved similarly to mc^2155 under hypoxia (Fig. A-1C).

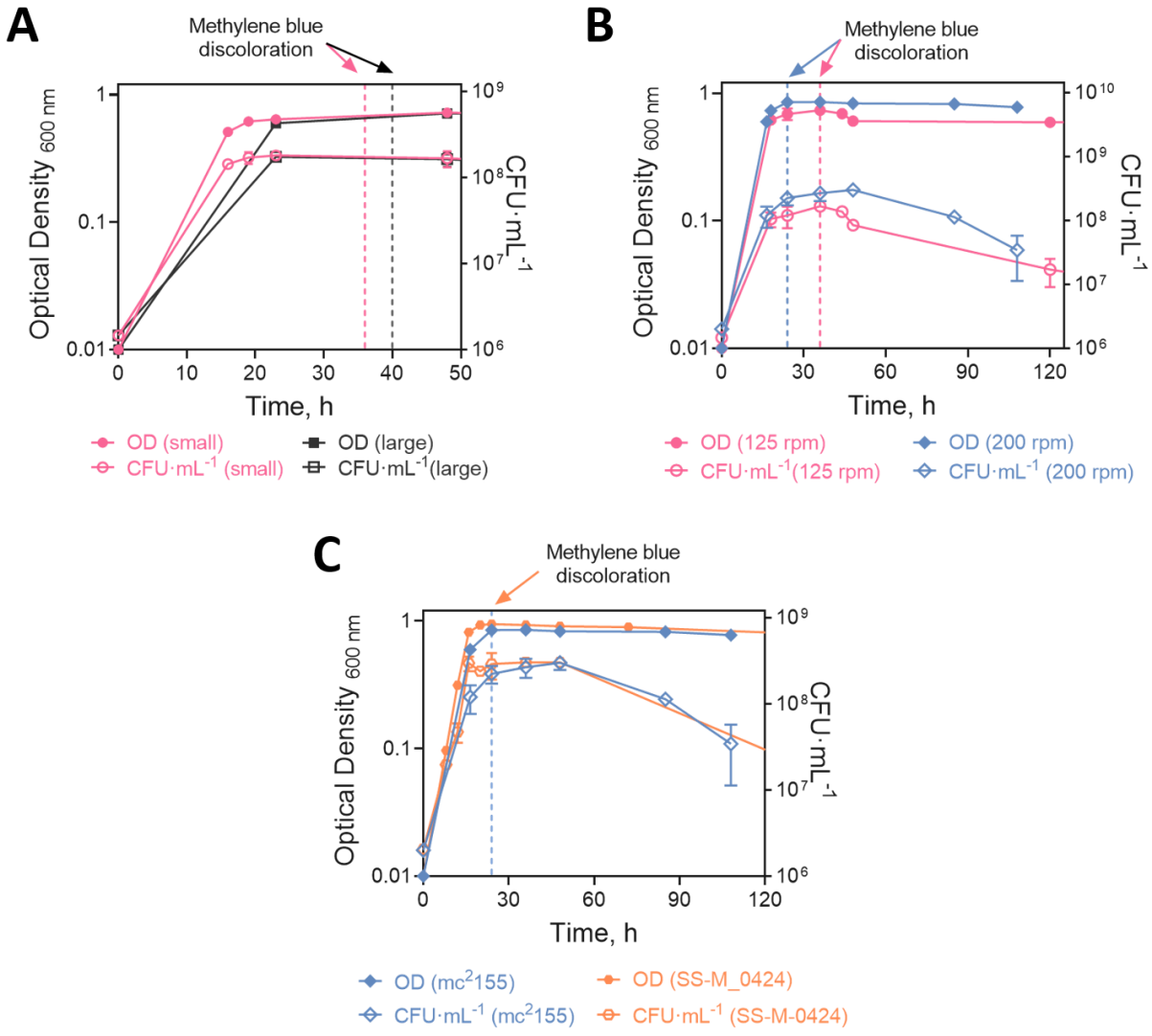

Fig. A-1. Cell density and viability analysis for *M. smegmatis* strains in hypoxia. (A) Growth curve of mc^{2}155 using 13.5 mL cultures (small) or 27 mL cultures (large). Dotted lines show the time at which methylene blue discoloration (qualitative indicator of oxygen levels) occurred. (B) as in (A), but using the small flask system (13.5 mL cultures) and varying culture agitation from 125 rpm to 200 rpm. (C) Growth curve of SS-M_0424 and mc^{2}155 using the small flask system and an agitation of 200 rpm. SS-M_0424 is an mc^{2}155 derivative that contains an ATc regulated *dCas9* and a nonspecific sgRNA (strain used in Chapter 4).

References

Wayne, L.G., and Hayes, L.G. (1996). An in vitro model for sequential study of shiftdown of *Mycobacterium tuberculosis* through two stages of nonreplicating persistence. *Infect Immun* 64(6), 2062-2069.

Appendix B. Considerations for intracellular ATP determinations

Reagent: BacTiter-Glo (Promega), Ref: G8230, G8230, G8230 or G8230.

The following are results from experiments designed to assess intracellular ATP determinations for *M. smegmatis* under our experimental conditions. The BacTiter-Glo reagent contains a lysing reagent to release ATP from bacterial cells, as well as Mg^{2+}, luciferin and luciferase, which under the presence of ATP catalyze the mono-oxygenation of luciferase to emit light (Fig. B-1). Luminescence measurements were done using a Victor^3 plate reader (PerkinElmer). We estimated the half-life of the reagent at room temperature to be 36.2°C min (data not shown). However, because our ATP readings required immediate sampling from *M. smegmatis* cultures at 37°C, we estimated the half-life of the reagent at that temperature to be 27.5 min (Fig. B-2A).

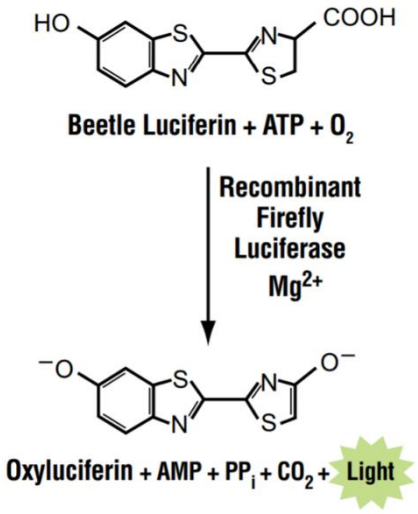

Fig. B-1. BacTiter-Glo luminescence reaction for the determination of ATP. In the presence of ATP, O_2 and Mg^{2+}, luciferin undergoes mono-oxygenation catalyzed by luciferase. *Source:* (Technical Bulletin: BacTiter-Glo™ Microbial Cell Viability Assay, 2020).

We also determined the BacTiter-Glo reagent can be used after 8 hours at room temperature (23°C), providing similar readings when compared to BacTiter-Glo used after a short (~15 min) period of equilibration (Fig. B-2B). This makes BacTiter-Glo adequate for time-sensitive and sequential readings over large periods of time without having to freeze the reagent. An ATP standard must be used within every determination. We recommend an equilibration time of 60 min, as the reagent is stored at -80/-20°C.

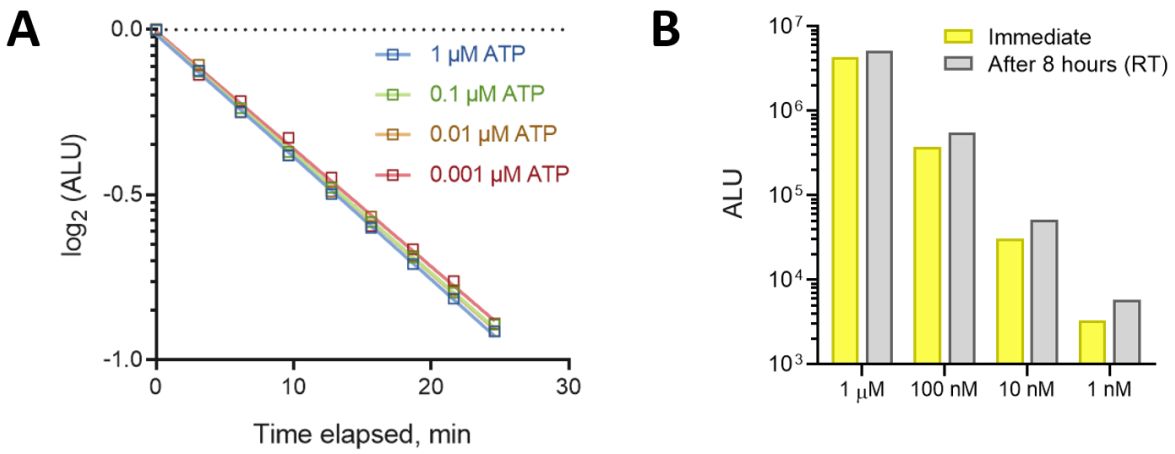

Fig. B-2. BacTiter-Glo is stable at room temperature but its enzymatic half-life in reaction is short. (A) Half-life determination of *BacTiter-Glo* at 37 °C. The results of one representative reading are displayed as $\log_2$ of Arbitrary Luminescence Units. *BacTiter-Glo* Luminescence reaction half-life = 27.5 min. (B) Efficiency of the *BacTiter-Glo* reagent used immediately or after being exposed to room temperature for 8 hours. Both (A) and (B) used four different concentrations of pure ATP, as indicated.

ATP determination of *M. smegmatis* cultures using centrifugation at RT (23°C) or at 4°C provided similar results (Fig. B-3A). However, when *M. smegmatis* was exposed to 4°C for ~15 min, bacteria increased the production of ATP without releasing it to the media (Fig. B-3B). Additional experiments showed that the production of ATP by *M. smegmatis* is very sensitive, as even shorter periods of time or the exposure of bacteria to cold media triggered increased ATP synthesis (data not shown).

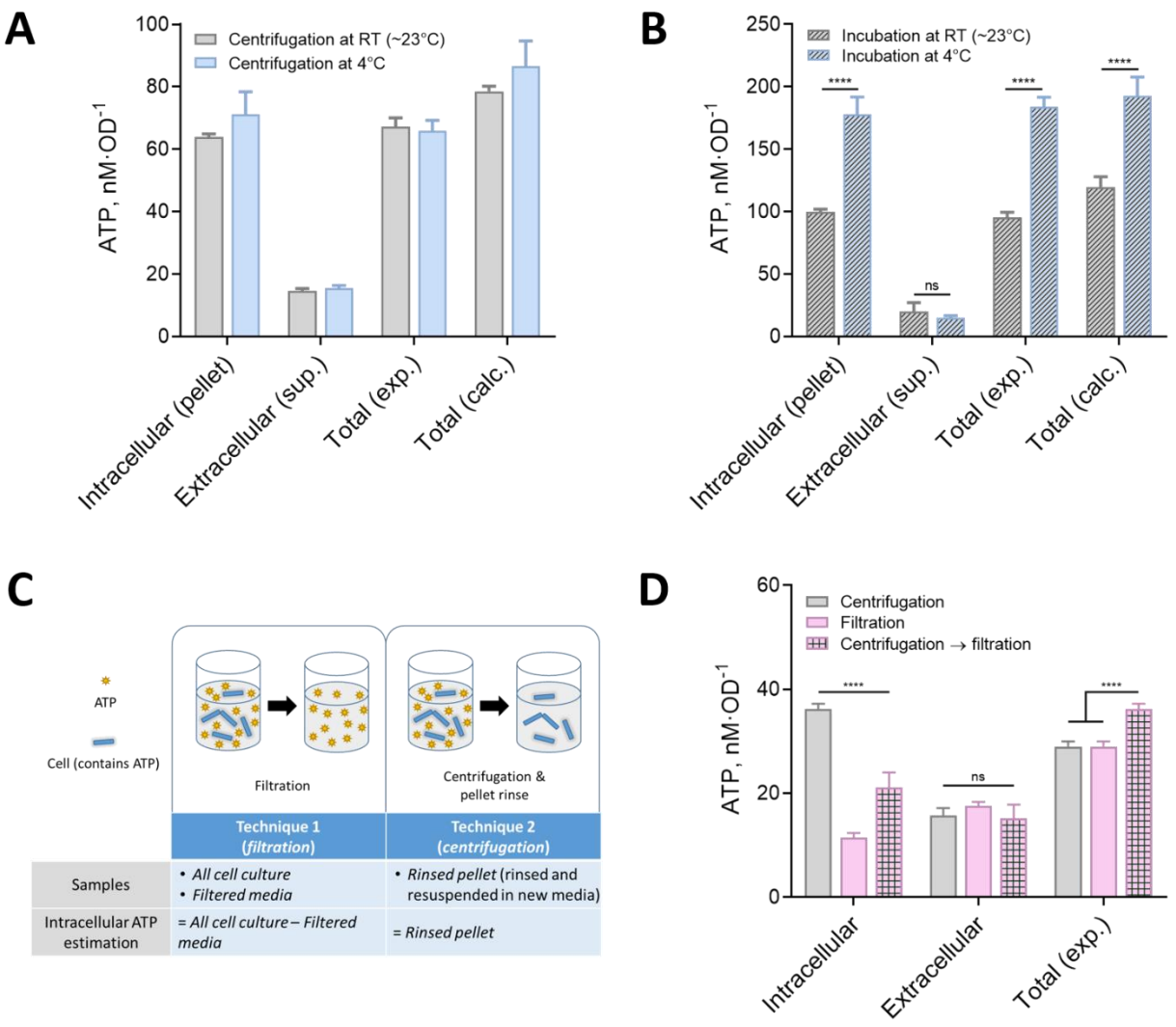

Fig. B-3. Different techniques used to determine ATP highlighting their differences on intracellular ATP estimations. ATP levels determined after centrifugation at 4°C or at RT (~23°C), no significant difference between treatments. (B) Cell cultures were incubated for 15 min at 4°C or RT (~23°C) before measurement of ATP levels. (C) Techniques used to estimate intracellular ATP: *Filtration* (measures extracellular ATP and total ATP, intracellular ATP is the difference) and *Centrifugation* (intracellular ATP is measured directly from a rinsed pellet). (D) ATP levels determined at RT (~23°C) using *Filtration* or *Centrifugation*. Due to the difference between these techniques, we also included a *Centrifugation* followed by *Filtration* experiment (pellet rinsed and resuspended in new media [technique 2] was filtered [technique 1] to obtain the data shown). In this experiment, "total" indicates the reading of the centrifuged cells following resuspending in new media. Statistics: ANOVA and Sidak for (A) and (B), or ANOVA and Tuckey's HSD for (D). **** = $p<0.0001$; ns = no significant. Error bars: standard deviation. Measurements from (A), (B) and (D) do not correspond to the same cell culture growth stage, hence the difference in readings. Total (exp.) represents the total amount of ATP experimentally measured. Total (calc.) represents the total amount of ATP calculated from intracellular and extracellular ATP measurements.

ATP determinations can be done using a 30 s centrifugation of *M. smegmatis* cultures (~1 mL), resuspending the cell pellet in prewarmed media. The luminescence reading of the initial *M. smegmatis* culture minus the luminescence reading of resuspended pelleted cells will provide the intracellular ATP. Alternatively, ATP determinations can be done using filtration with a 0.2 µm syringe filter, determining the intracellular ATP by subtracting the luminescence values from the cell culture with the filtered media (Fig. B-3C). In both cases ATP measurements must be normalized to cell culture OD_{600}.

The determinations of intracellular ATP with centrifugation and filtration differ (Fig. B-3D). Cells that have been pelleted and resuspended in media produce high levels of ATP; summing the total ATP in the pellet plus the supernatant results in a higher value than obtained from the total culture prior to centrifugation. On the other hand, cell filtration seems to provide a more accurate ATP profile of intracellular ATP readings. However, because determination of ATP is based on 1) lysis of cells to release ATP, and 2) the luminescence reaction using the released ATP, cell-free samples (e.g., filtered media) will emit luminescence faster and at a higher intensity than those with cells, as cell lysis is required for the latter ones. This disparity is accounted for in our ATP determination protocols by reading luminescence from cell cultures after reading luminescence from cell-free samples. The use of centrifugation allows higher sample uniformity, as the initial culture and the resuspended pelleted cells are both read simultaneously (equal lysis and luminescence reaction times). However, the intracellular ATP levels appear to increase during the process of centrifugation and are therefore not an accurate reflection of levels in the culture. Additionally, this technique cannot be used to estimate intracellular ATP levels from *M. smegmatis* hypoxic cultures, as cells also produce high levels of ATP within seconds of reaeration (see Appendix E).

References

Promega.com (2020). Technical Bulletin: Bactiter-Glo™ Microbial Cell Viability Assay. [online] Available at: <https://www.promega.com/-/media/files/resources/protocols/technical-bulletins/101/bactiter-glo-microbial-cell-viability-assay-protocol.pdf?la=en> [Accessed 12 October 2020].

Appendix C. ATP determination protocols

Reagent: BacTiter-Glo (Promega), Ref: G8230, G8230, G8230 or G8230.

Plates: White solid 384-well plates (Greiner-bio-one), Ref: 781080.

Note 1: Record the OD of the cultures used for ATP estimation.

1. Equilibrate the BacTiter-Glo reagent to room temperature for ~60 min.
2. Prepare ATP standards using fresh media: 1 µM, 100 nM, 10 nM and 1 nM.
3. Add 25 µL of the BacTiter-Glo reagent to each well to be used (e.g., for the standard, samples). If using a 96-well plate, add 50 µL instead.
4. Equilibrate the plate with the reagent at 37°C for a few minutes.

Note 2: For a more accurate ATP determination combine the reagent and the samples at 37°C, as *M. smegmatis* can synthesize ATP at low temperatures.

Note 3: Intracellular ATP estimations can be done using two techniques as explained in Appendix B: (1) Filtering the cell culture using 0.2 µm syringe filters, and measuring ATP in both the filtered media and the cell culture; or (2) by centrifugation of the cell culture for 30 s at ~20,000 x g at RT, removing the supernatant and resuspending the cells in 1 mL of fresh media. ATP is then measured in the resuspended pellet, in the supernatant and in the cell culture. Nonetheless, centrifuged cells show higher levels of intracellular ATP, so we do not recommend the latter technique for most ATP estimations. Below we describe in detail the protocol using the filtration technique.

5. Add 25 µL of mycobacteria cultures (**cell culture** for *total* ATP determinations) to their respective wells containing the reagent, and mix by pipetting up and down a few times. Additionally, filter ~1-2 mL of the samples (**filtered media** for *extracellular* ATP determinations). Add 25 µL of the ATP standards, media controls and **Filtered media** to their respective wells (Fig. B-3C).
6. Mix the content of the plate for 1 minute using an orbital shaker.

7. Bring the plate to a plate reader with capable of doing luminescence readings (e.g., Victor^3 multi label reader, PerkinElmer) and follow the next steps:

    a) Shake: 180 s, normal speed, shaker diameter 5 mm, orbital mode.

    b) Delay 10 s.

    c) Measurement 1: CPS/luminescence reading (the settings usually come determined by default).

    d) Delay 2 min.

    e) Measurement 2: CPS/luminescence reading.

8. Estimate the ATP as follows:

    a) Use the results from Measurement 1 to obtain the luminescence readings for the standard, media control and **filtered media**.

    b) Use the results from Measurement 2 to obtain the luminescence readings for the **cell culture**.

    c) Use the media control to normalize for background luminescence. Use the ATP standards to estimate the ATP content.

    d) Normalize ATP content to OD.

Note 3: Extracellular ATP (**filtered media**) as well as ATP from the standards do not require cell lysis. Thus, free ATP molecules will react with the reagent faster. We did internal tests to determine reliable time points for sampling and measuring luminescence based on luminescence decay. Additionally, cells need to be exposed to the reagent for a longer time to reach a maximum ATP release point, which occurs close to 10 min after getting in contact with the reagent (~5 min of sample processing/loading time before being inserted in the plate reader + ~5 min within the plate reader). If these conditions are met, the results are highly reproducible, but we encourage the use of standards with every reading.

Appendix D. Minimal Media 0.1% Acetate (MMA)

Note: This media was used in Chapter 3 for determination of intracellular ATP in combination with drugs that affect ATP production (e.g. bedaquiline).

2x Minimal media base (1 L)

- 1 g asparagine
- 1 g KH_2PO_4
- 5 g Na_2HPO_4
- 100 mg ferric ammonium citrate
- Adjust to 1 L using dH_2O

Sterilize by autoclave and store at 4°C.

1000x Salts (100 mL)

- 50 g $MgSO_4 \cdot 7H_2O$
- 50 mg $CaCl_2$
- 10 mg $ZnSO_4$
- Adjust to 100 mL using dH_2O

Sterilize by autoclave and store at room temperature.

20x Carbon source (acetate) (100 mL)

- 33.2 g $C_2H_9NaO_5$
- Adjust to 100 mL using dH_2O

Sterilize by filtration (0.22 µm) and store at 4°C

20% Tyloxapol (20 mL)

- 4 mL tyloxapol
- Adjust to 20 mL using dH_2O

Dissolve at 55°C, sterilize by filtration (0.22 µm) and store at 4°C.

Media Preparation (1 L)

Combine 500 mL of 2x Minimal media base, 1 mL of 1000x Salts, 5 mL of 20% Carbon source and 2.5 mL of 20% tyloxapol. Adjust volume to 1 liter using dH_2O. Adjust pH to 7-7.5, if necessary. Store at 4°C.

Appendix E. Intracellular ATP profile after reaeration of hypoxic cultures

Reaeration of 40-hour hypoxic cultures of *M. smegmatis* led to a rapid production of ATP (Fig. E-1A), reaching similar ATP levels to those of log phase cells 3 to 5 minutes after re-oxygenation. Interestingly, this phenomenon was not observed for mycobacteria in earlier hypoxia stages. For example, reaeration of 24-hours and 18-hours hypoxic cultures leads to a drop in intracellular ATP (Fig. E-1B, C and D). It is possible that because intracellular ATP levels are highly reduced in late hypoxia, cellular components depending on ATP are present in reduced levels (i.e., proteins degrade, molecules dilute after cell division). Hence, once *M. smegmatis* resumes production of ATP after reaeration there is no immediate use for this molecule, resulting in a positive energy balance. On the other hand, for early hypoxia cultures ATP levels are ~60% of those observed in log phase. As such, cellular elements dependent on ATP are likely to be present but not active. Thus, we propose a scenario where upon reaeration the ATP demand is greater than its production, resulting in a negative energy balance, at least for a short period of time. Consistent with this idea, mRNA synthesis resumes quickly in 18-hour hypoxic *M. smegmatis* cultures upon re-exposure to oxygen, but slowly in 40-hour hypoxic cultures re-exposed to oxygen.

We also observed that altering the agitation speed of the cultures lead to changes in the extracellular ATP levels for 24-h hypoxia cultures (Fig. E-1B and D), and we suspect this is caused by better access to nutrients, including oxygen, and reduced cell death.

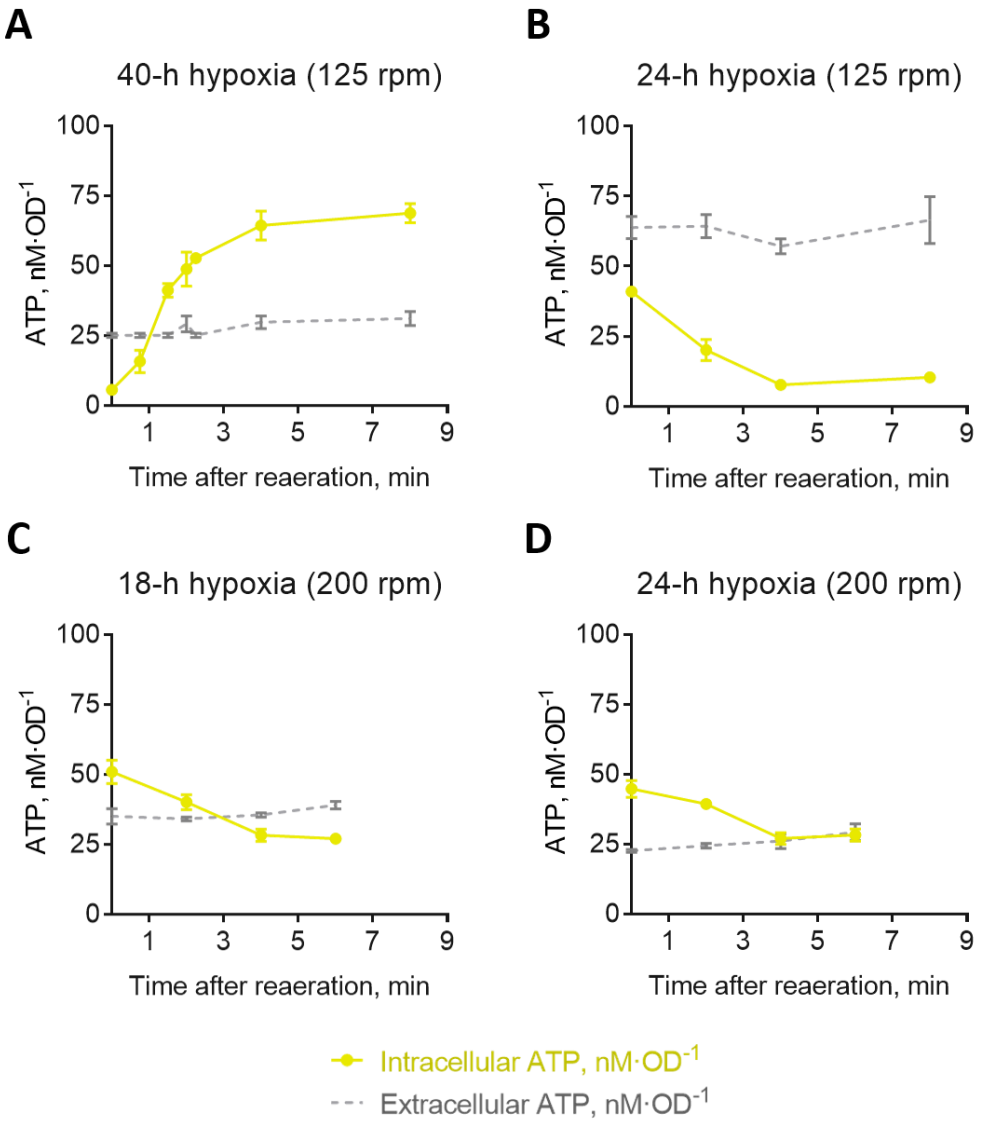

Fig. E-1. Determination of ATP in *M. smegmatis* after reaeration. Intracellular and extracellular ATP levels of *M. smegmatis* cells after reaeration using *BacTiter-Glo* (filtration technique). Mycobacteria samples were collected from cultures agitated at 125 rpm and (A) 40 hours or (B) 24 hours after sealing the vials, reflecting late and early hypoxic conditions, respectively. For (C) and (D) cultures were instead agitated at 200 rpm and samples collected (C) 18 hours or (D) 24 hours after sealing the vials. Error bars denote standard deviation.

Appendix F. Rifampicin induces increased intracellular ATP levels

Following our work with isoniazid and its effect on ATP levels in *M. smegmatis* (Chapter 3), we wondered if rifampicin could also have an impact on intracellular ATP levels. We used *M. smegmatis* in logarithmic phase in Minimal Media 0.1% Acetate (MMA, see Appendix D), and treated them with 150 $\mu g \cdot mL^{-1}$ rifampicin (RIF) or DMSO (vehicle control). We then measured ATP with BacTiter-Glo using our centrifugation protocol. Our results show that 40 min after RIF was added, the intracellular ATP level had increased almost 3-fold compared to the DMSO treatment while the extracellular ATP levels did not change (Fig. F-1A). Similar results were observed after 2.5 h (data not shown). A possible explanation for the sudden burst of ATP is that RIF makes mycobacteria more permeable, allowing ATP to be released more readily upon exposure to the BacTiter-Glo reagent. To rule out this possibility, we reasoned that if RIF triggers ATP synthesis, cells unable to generate new ATP will not have a burst of ATP upon RIF treatment. Therefore, we used *M. smegmatis* in MMA and treated them for 30 min with 5 $\mu g \cdot mL^{-1}$ bedaquiline (BDQ), a potent inhibitor of the F_1F_0 ATP synthase (Lakshmanan et al., 2013) (Fig. F-1B). Then, we treated the same cultures with either DMSO or RIF for 30 min before measuring ATP. Indeed, cells treated with BDQ and then RIF did not show an increase in intracellular ATP levels (Fig. F-1C), but rather had decreased ATP levels compared to cells treated with BDQ alone. These results suggest that in the absence of BDQ, RIF stimulates the synthesis of ATP in *M. smegmatis*. An alternative explanation for the increase in ATP levels following RIF treatment is that there could be an accumulation of nucleotides that would otherwise be incorporated into mRNA. Bedaquiline-treated cells likely have reduced rates of mRNA synthesis, given that they have slower rates of mRNA decay (Chapter 3) but do not have noticeably higher steady-state RNA abundance (data not shown). To assess if a RIF-induced ATP burst also occurred in rich media, we treated *M. smegmatis* in 7H9 with RIF and measured intracellular levels of ATP after 5, 10 or 15 min. Our results show that within 5 min, RIF caused a 3-fold increase in intracellular ATP compared to DMSO, and this increase was sustained for the whole length of the experiment (Fig. F-1D).

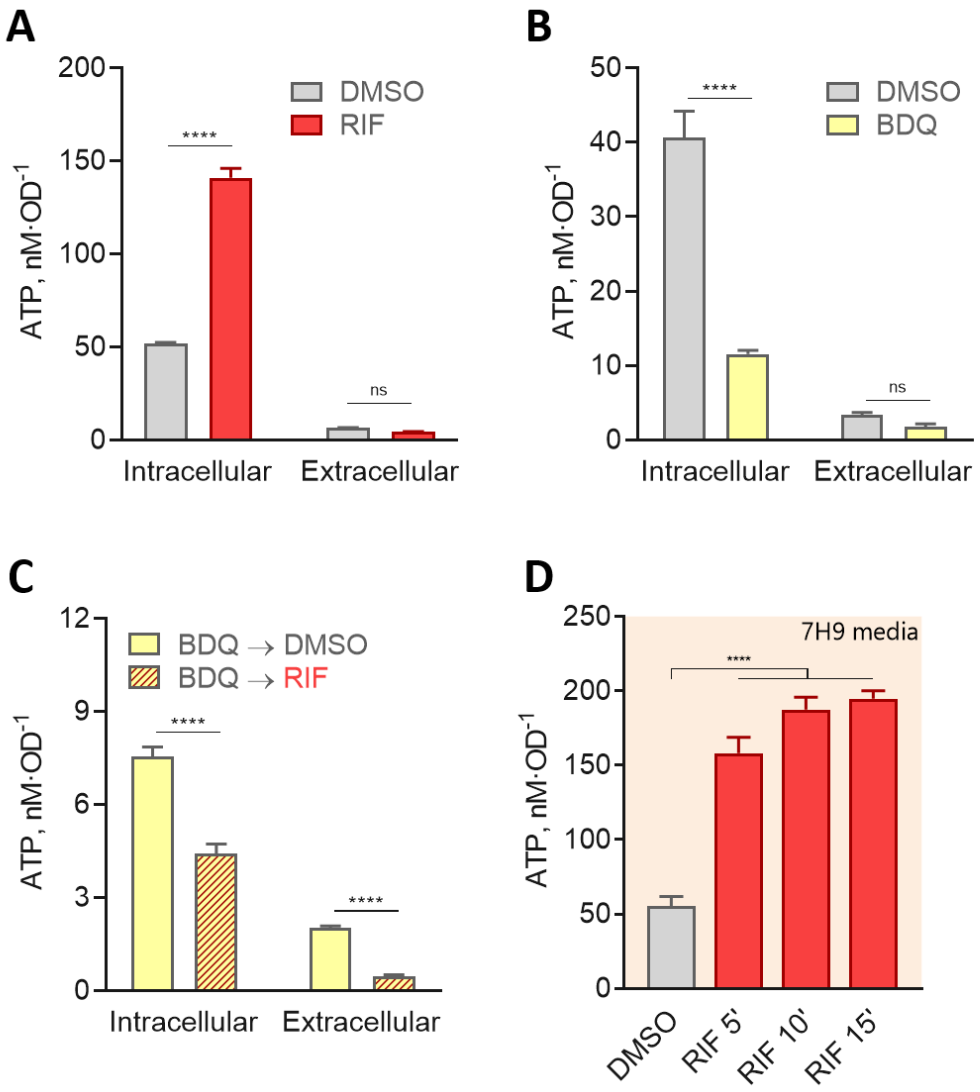

Fig. F-1. Rifampicin triggers ATP synthesis in *M. smegmatis*. (A) ATP levels from *M. smegmatis* cultures in Minimal Media 0.1% Acetate (MMA) treated with 150 µg·mL^{-1} rifampicin (RIF) or the drug vehicle (DMSO) for 40 minutes. (B) *M. smegmatis* treated with 5 µg·mL^{-1} bedaquiline (BDQ) or DMSO for 30 min. When cells are grown in MMA, BDQ prevents the synthesis of ATP, as acetate is the sole carbon source and ATP therefore cannot be synthesized by glycolysis. (C) *M. smegmatis* cultures in MMA were treated with BDQ for 30 min, followed by 30 min with DMSO or RIF. (D) *M. smegmatis* cultures in rich media (7H9) were treated with RIF for 5, 10 or 15 minutes ('), or with the drug vehicle DMSO. Intracellular ATP levels are displayed as bars. Statistics: *t-test* for (A), (B) and (C); ANOVA and Holm-Sidak for (D). **** = p<0.0001; ns = not significant. Error bars: standard deviation; n = 3. "Intracellular" and "Extracellular" refer to intracellular and extracellular ATP levels, respectively. ATP determinations were done using BacTiter-Glo and the centrifugation protocol. All cultures correspond to logarithmic growth phase *M. smegmatis* cells.

References

Lakshmanan, M., and Xavier, A.S. (2013). Bedaquiline - The first ATP synthase inhibitor against multi drug resistant tuberculosis. *J Young Pharm* 5(4), 112-115. doi: 10.1016/j.jyp.2013.12.002.

Appendix G. Overexpression of *dCas9* by ATc in log phase and hypoxic *M. smegmatis* cultures

As reported in chapter 3, we used a strain expressing *dCas9* and a non-specific sgRNA (SS-M_0203) under the control of anhydrotetracycline (ATc). We evaluated the expression level of *dCas9* in *M. smegmatis* cultures during hypoxia (18.5 hours after sealing the vials, OD_{600}: 0.81) and during logarithmic growth (OD ~0.82). *M. smegmatis* cultures were treated with ATc to a final concentration of 200 ng/mL, and samples collected at 0, 5, 10, and 20 min (log phase) or at 0, 5, 10, 20, 40 and 60 min (hypoxia). We normalized the expression levels of *dCas9* to *sigA* (data not shown) and to *dCas9* basal levels (no ATc, time zero). Our results show that the highest levels of *dCas9* overexpression (~38-fold) are reached 10 to 20 minutes after ATc treatment for hypoxia (Fig. G-1A). For log phase cultures, a similar increase in expression (~45-fold) was reached between 10 and 20 min (Fig. G-1B).

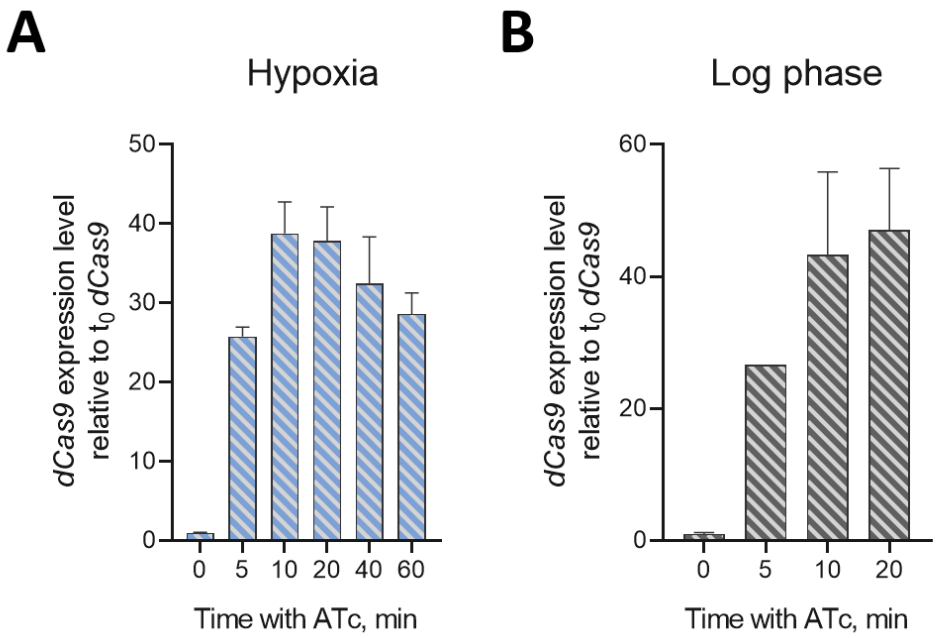

Fig. G-1. Overexpression of *dCas9* under the control of ATc is rapidly regulated. Expression levels of *dCas9* from *M. smegmatis* from (A) hypoxic cultures (18.5 h) or (B) log phase cultures after being treated with 200 ng/ml ATc for the indicated times to induce *dCas9* overexpression. Expression levels are relative to *dCas9* expression level at time 0 min. Error bars: standard deviation; *n*=2 [for (B), only one replicate was used at 5 min]. Log phase data collected with help of Gregory Zamalloa Gutierrez.

Appendix H. Tests for qPCR sensitivity at low sample concentrations using mCherry mRNA

Quantitative PCR (qPCR) is a very sensitive technique. It is possible to obtain inaccurate data because of technical errors (user technique) or sample abundance (low amounts of template). During mRNA degradation analysis, later time points contain smaller amounts of mRNA compared to the first ones. This is of relevance, particularly for hypoxia samples (or similar stress conditions) where the levels of mRNA are inherently low. To confirm that our methods result in accurate quantification of mRNA at various abundance levels, we used purified *M. smegmatis* RNA aliquots of 600 ng (corresponding to the sample "hypoxia, time 0 min A – 9.21.18 – DVB") and spiked in *in vitro* transcribed mCherry mRNA (*mCherry*) at concentrations ranging from 0.012 pg to 200 pg in two-fold increments.

cDNA was made by mixing spiked RNA samples with 0.83 µL 100 mM Tris (pH 7.5) and 0.17 µL 3-mg/mL random primers (NEB), adjusting with DNase/RNase-free water to 5.25 µL. RNA was denatured at 70°C for 10 min, and snap-cooled. Reverse transcription was performed using 100 U ProtoScript II reverse transcriptase (NEB); 10 U RNase inhibitor, murine (NEB); 0.5 µL of a mix of deoxynucleoside triphosphates (0.5 mM each dNTP), and 0.5 µL 5 mM dithiothreitol (DTT) in a final volume of 10 µL. The reverse transcription reaction was performed for 5 h at 42°C. RNA was degraded with 5 µL each 0.5 mM EDTA and 1 N NaOH at 65°C for 15 min, followed by 12.5 µL of 1 M Tris-HCl, pH 7.5. cDNA was purified using the MinElute PCR purification kit (Qiagen) according to the manufacturer's instructions. mRNA abundance was determined for *mCherry* and *sigA* targets by quantitative qPCR using samples of 400 pg of purified cDNA, 0.25 µM each primer and iTaq SYBR green (Bio-Rad) in 10-µL reaction mixtures. Amplification conditions were set to 40 cycles of 15 s at 95°C and 1 min at 61°C (Applied Biosystems 7500). mRNA abundance for mCherry dilutions at the different ranges are displayed in Fig. H-1A and B, in both cases following a linear trend and confirming the technique sensitivity.

Moreover, *mCherry* abundance was normalized to each sample's respective levels of *sigA* (housekeeping gene). The resulting expression levels matched our expectations for the full range of *mCherry* spiked in samples (Fig. H-1C).

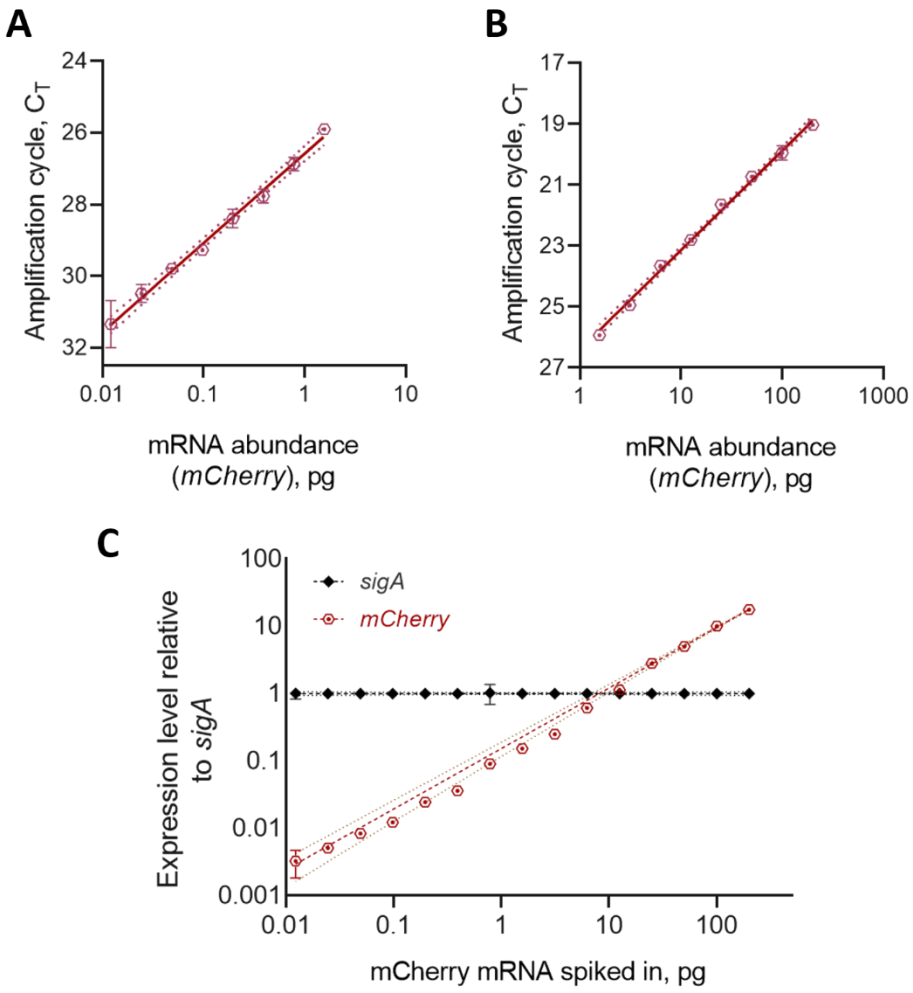

Fig. H-1. Analysis of *mCherry* mRNA abundance using qPCR highlights the technique's sensitivity. Amplification of an mCherry target sequence by qPCR. Purified mCherry mRNA *in vitro* transcribed was used to determine the linear range of qPCR detection. mCherry was spiked at the indicated concentrations (0.01 pg to 200 pg) to *M. Smegmatis* RNA samples (600 ng) before cDNA synthesis. (A) Lower range of mRNA abundance (R^2 = 0.995). (B) Higher range of mRNA abundance (R^2 = 0.9964). Both results originated from two independent qPCR experiments. Error bars: standard deviation and 95% CI (linear regression); *n* = 2. (C) Expression level of *mCherry* spiked in *M. smegmatis* RNA samples, normalized to the mRNA abundance of the housekeeping gene *sigA*. Error bars: standard deviation and 95% CI (non-linear fit); *n* = 2.

Appendix I. RNA extraction and cleanup for RNA-seq samples

Suitable for *M. smegmatis* cultures, OD_{600}= ~0.74, volume= 5-7 mL.

Before starting: Turn on the centrifuge and microcentrifuge and set the temperature to 4°C

Part 1: Cell lysis, RNA extraction and first purification

Required: Invitrogen TRIzol reagent (cat. 15596026). OPS Diagnostics 100 µm zirconium lysing matrix, molecular grade (cat. PFMB 100-100-12).

1. Centrifuge the cultures at 3,900 rpm for 5 min at 4°C. Remove supernatant.
2. Fast-spin for 5 to 10 sec and remove any supernatant remaining with a micropipette.
3. On ice and in a fume hood: Add 1 mL of TRIzol *to each sample*. Then, resuspend the pellet and transfer it to a labelled bead-beating tube.
4. Lyse the cells in the MP FastPrep 5G using 3 cycles of 7 m/s, 30 seconds each, placing samples on ice for 2 min after each cycle.
5. On ice and in a fume hood: Add 300 µL of chloroform.
6. Vortex for 15 sec and centrifuge at 15,000 rpm for 15 min at 4°C.
7. In the meantime, label and fill a 1.5 mL tube with 500 µL of 100% ethanol, per sample.
8. Carefully, transfer 500 µL of the aqueous phase to the tubes containing ethanol. *Avoid disruption of the other phases*. Mix thoroughly.

Note: Centrifugation steps are now at 15,000 x g for 30 s and at room temperature.

9. Transfer 500 µL of the mix to the column and centrifuge. Carefully, discard the flow through by aspiration using a p1000 micropipette (you may re-use the tip).
10. Transfer the remaining 500 µL of the mix and centrifuge. Discard the flow through.
11. Add 400 µL of Direct-zol RNA Pre-wash to the column and centrifuge. Discard the flow through. Repeat step 6.

12. Add 700 µL of RNA Wash Buffer to the column and centrifuge for 2 min. Transfer column to a labeled 1.5 mL tube.
13. Add 50 µL of RNase-free H_2O, directly to the matrix, and centrifuge.
14. Vortex for <2 s three times at low speed to ensure a proper RNA resuspension.
15. Take a 1.4 µL aliquot in a PCR tube, per sample, and determine the concentration loading 1 µL in a Nanodrop.
16. Store samples at -80°C or continue with DNase treatment.

Part 2: DNase treatment

Required: TURBO™ DNase, 2 U/µL (cat. AM2238). NEB RNase Inhibitor, murine, 40,000 U/mL (cat. M0314).

1. Use up to 20 µg of RNA per sample resuspended in RNase-free H_2O to a final volume of 85.5 µL.
2. Prepare a DNase master mix as follows:

Reagent	1x
10x Turbo Buffer	10 µL
TURBO™ DNase (2 U/µL)	2.5 µL
RNase Inhibitor, Murine (40,000 U/mL)	2 µL
TOTAL (per sample)	14.5 µL

3. Add 14.5 µL of DNase master mix to each sample.
4. Incubate samples for 1 h at 37°C with agitation.
5. Proceed immediately with RNA Clean Up.

Part 3: Second RNA purification

Required: Zymo RNA Clean & Concentrator™-25, catalog number: R1017 or R1018

Note: Centrifugation steps at 15,000 x g for 30 s and at room temperature.

1. Quick spin (1-3 s) to bring the content to the bottom of the tube.

2. Add two volumes of Binding Buffer (200 µL) to each sample and mix well.
3. Add one volume of 100% ethanol (300 µL) to each sample and mix well. Transfer to a Zymo column with a collection tube.
4. Centrifuge and carefully discard the flow through by aspiration using a p1000 micropipette (you may re-use the tip).
5. Add 400 µL of Prep Buffer. Centrifuge. Discard flow through.
6. Add 500 µL of Wash Buffer. Centrifuge. Discard flow through.
7. Add 700 µL of Wash Buffer. Centrifuge. Discard flow through.
8. Add 400 µL of Wash Buffer. **Centrifuge for 2 min**. Transfer column to a labeled 1.5 mL tube.
9. Add 40 µL of RNase-free H_2O, directly to the matrix, and centrifuge.
10. Briefly vortex at low speed to resuspend the RNA.
11. Take a 1.4 µL aliquot in a PCR tube, per sample, and determine the concentration loading 1 µL in a Nanodrop.
12. Store clean RNA samples at -80°C.

Appendix J. Polysome profiling and sample fractioning protocols

Lysis Buffer reagents and preparation

10x salts (5 mL, 100 mM $MgCl_2$, 1 M NH_4Cl, 200 mM Tris pH 8.0)

- 101.65 mg $MgCl_2$
- 267.45 mg NH_4Cl
- 121.14 mg Tris
- 4 mL DEPC H_2O
- ~210 µL HCl to regulate pH to 8.0
- Adjust to 5 mL using DEPC H_2O

Store at -20°C

10x Igepal (5 mL, 1%):

- 50 µL Igepal (previously known as NP-40)
- 4950 µL DEPC H_2O

Store at room temperature

10x Triton X-100 (5 mL, 4%):

- 200 µL X-100 Triton
- 4.8 mL DEPC H_2O

Store at room temperature

10x Chloramphenicol (1 mL, 10 mM):

- 323.13 µg chloramphenicol (Cam)
- Adjust to 1 mL using DEPC H_2O

Store at -20°C

10x $CaCl_2$ (5 mL, 50 mM):

- 27.75 mg $CaCl_2$
- Adjust to 5 mL using DEPC H_2O

Store at -20°C

Prepare 1x Lysis Buffer before using due to this solution is unstable (recommended: <24 hours before milling). Combine 65 µL of each of the previously prepared 10x solutions + 6.5 µL (10 $U \cdot \mu L^{-1}$) of Recombinant DNase I, RNase-free (Roche, cat. 04716728001) and complete with 318.5 µL DEPC H_2O to a final volume of 650 µL per sample.

Lysis Buffer 1x concentrations: 10 mM $MgCl_2$, 100 mM NH_4Cl, 5 mM $NaCl_2$, 1 mM Cam, 100 $U \cdot mL^{-1}$ DNase, 0.4% Triton-X 100, 0.1% Igepal, 20 mM Tris pH 8.0.

Gradient buffer composition

10x gradient buffer (40 mL, 1M NaCl, 0.1M $MgCl_2$, 0.3M Tris-HCl pH7.5)

- 813.2 mg $MgCl_2$
- 2.34 g NaCl
- 1.46 g Tris
- Adjust to 38 mL with DEPC H_2O
- Adjust pH to 7.5
- Adjust to 40 mL using DEPC H_2O

Store at 4°C

Note: Prepare a parallel solution to estimate how much HCl is needed to adjust the pH to 7.5. Using Henderson-Hasselbalch equation, we estimated 200 µL.

50% sucrose (40 mL), prepare two:

- 4 mL 10x Gradient Buffer
- 36 mL DEPC H_2O
- 20 g sucrose (RNase free/DNase free)

5% sucrose (40 mL), prepare two:

- 4 mL 10x Gradient Buffer
- 36 mL DEPC H_2O
- 2 g sucrose (RNase free/DNase free)

Store solutions at 4°C

Sample collection

Culture information: >300 mL of M. smegmatis *cells*

Fill ~40 mL of liquid nitrogen in a 50 mL conical tube. Collect cells by filtration using a 500 mL filter upper cup (VWR, cat. 10040-468) and a vacuum pump at room temperature. Scrape cells before media runs out using ~3 cell scrapers (VWR, cat. 70-1180) and transfer them to the liquid nitrogen tube. Add 650 µL of lysis buffer, drop by drop, to the liquid nitrogen tube to form small crystal spheres. Keep samples on ice/dry ice until liquid nitrogen evaporates. Store samples at -80°C.

Polysome recovery protocol (using a CryoMill)

1. Turn on CryoMill and the liquid nitrogen supply.
2. Fill a large container with ~1 gallon of liquid nitrogen. Inside, pre-chill a 10 mL jar (Retsch, cat. 014620331) and a 7 mm stainless steel grinding ball (Retsch, cat. 053680035) for approx. 5 min.
3. While jar is being chilled, work on dry ice to carefully detach the cells and lysis buffer from their collection tubes using a chilled plastic spatula (plastic cell scrapers also work).
4. Transfer Lysis Buffer and cells with the chilled plastic spatula to jar, place in the 7 mm stainless steel ball, close the jar and insert the jar in the CryoMill. Do not tighten strongly.
5. Perform 6 cycles of 3 min at 15 Hz, with 1 min pauses in between.
6. In the meantime, pre-chill plastic spatula and a plastic funnel in liquid nitrogen. Pre-chill a 5 mL conical tube on dry ice.
7. Transfer the pulverized samples using the funnel and a pre-chilled plastic spatula into the 5 mL conical tube (**note:** for carbon starvation cells the powder should be slightly yellow/orange; for log phase cells the powder should be white, a yellowish coloration indicates inefficient milling).
8. Store samples at -80°C or continue with the next step.

Lysate preparation

Prepare only one or two biological replicate samples at a time and within 24 hours of using them. Each biological replicate will produce three aliquots (technical replicates) for the gradient separation step.

1. Initiate the thawing of pulverized samples at 30°C for 2 min and then on ice for 20 to 30 min.
2. Transfer samples to a 1.5 mL tube and centrifuge at max speed and at 4°C for 10 min.
3. Transfer supernatant to a new 1.5 mL tube. Repeat steps 2 and 3.
4. Take 1 µL and dilute with 99 µL of RNase-free H_2O to measure the concentration.
5. Calculate and set up three aliquots of 1 mg of RNA (or two aliquots of similar mass if less than 1 mg RNA). Adjust with RNase-free H_2O to a final volume of 150 µL. These are technical replicates.
6. Continue with a separation in sucrose gradient, or flash freeze in LN_2 and store at -80°C until further use (within 24 hours).

Gradient formation

Required: RNase-free polypropylene tubes (Beckman Coulter, cat. 331372), Polypropylene/Polyallomer centrifuge tubes, 14X89mm (VWR, cat. BK331372). Biocomp Gradient Master model 107.

1. Load a 50 mL syringe with the 5% sucrose solution. Add 5% sucrose gradient buffer until the 6 mL mark is reached in the polypropylene tubes (use the Gradient Master calibrated holders).
2. Load a 50 mL syringe with the 50% sucrose solution. Carefully introduce the metal needle until reaching the bottom of the tube and release 6 mL of 50% sucrose gradient buffer.
3. Prepare the gradient using the Gradient Master 11-step protocol (see Table J-1). Allow the tubes to stabilize for at least 20 min at 4°C.

   Store at 4°C until use.

Table J-1. Gradient Master protocol for gradients of sucrose 5-50% w/v using 11 Steps.

Step	*Time, s*	*Angle, °*	*Speed, RPM*	Step	*Time, s*	*Angle, °*	*Speed, RPM*
1	0.05	87	30	7	0.05	87	30
2	0:15	87	0	8	0:15	87	0
3	0.05	87	30	9	0.05	87	30
4	0:15	87	0	10	0:15	87	0
5	0.05	87	30	11	0:19	80	20
6	0:15	87	0				

Gradient separation

Required: Optima L90K ultra centrifuge with a SW 41 Ti rotor

1. Remove 500 µL of the top sucrose layer, weigh and bring each tube to a similar weight (<0.01 g difference between tubes).
2. Carefully load the gradient tubes with 150 µL of the lysate sample and load them in the centrifuge buckets. Then, insert the buckets into the rotor. Insert the rotor into the centrifuge.
3. Start the vacuum function setting the temperature to 4°C and pressing “Vacuum”.
4. Set speed = 35,000 RPM (151,000 x g), temp = 4°C, time = 2 h 45 min and enter. Start.
5. Wait until the RPMs reach to 35,000 and the vacuum shows <20 µ.
6. Once the centrifugation has finished, press vacuum and wait until the door unlocks. Allow the tubes to sit in the rotor for ~15 min after the centrifugation to stabilize the gradients.
7. Unload the contents, clean the centrifuge and the rotor, write down the revolutions counter in the log book and turn off the centrifuge.

Sample analysis and fractionation

Required: Econ EM-1 UV monitor (Bio-Rad) and a fraction collector device. Sarstedt 1.5ml capless tubes (VWR, cat. 101093-233) and Push caps (VWR, cat. 101093-502)

Note: Turn the monitor and lamp at least 15 min before starting the fractioning analysis.

1. Turn ON the Fraction Collector, set to manual collection. Parameters should be: delay time: 0.00; collect start to end; rack code 1 or 0; do not press START.

2. Turn on the pump and using the capillary tube run dH_2O through the device for ~15 min. Then, run 50% sucrose for ~5 min. (Dead volume is ~2 mL.)

3. Log in to the PC controlling the equipment and open "Gradient Profiler". Select COM4, "alper" as user, and hit "continue". Select preset run "polysome150uL.txt" for ~150 µL fractions. Parameters should be: AUFS as EM-1 (2.0). Hit "Okay" and DO NOT set AutoZero using the software (instead, use the hardware button). Hit "Graph". Name the run, hit "Graph".

4. Make sure the Y axis maximum is the same as AUFS or greater. Set the window size to 113.2 mm.

5. Place and lock the collection tubes in the Fraction Collector apparatus. Make sure the fraction Collector is in the "Home" position.

6. Clean the capillary tube with a tissue and carefully insert it into the gradient near the wall, to avoid disrupting the gradient.

7. Simultaneously press "frac adv" (software) and start the pump. Collect fractions and hit "stop recording". Save run. Hit "end". If planned, start another run by hitting "New Run?" and repeat steps 7-10.

8. Once finished, rinse with dH_2O for 20 min. Fill the Flow Cell with 20% ethanol in water and seal openings with parafilm.

Appendix K. Low-volume/low-concentration RNA purification protocol

For extraction of RNA from polysome profiling fractions or other solutions; not for extraction from cultures.

Sample volume: 80 µL, but the protocol can be adapted to different volumes.

RNA purification: as low as 3 ng of RNA were recovered in a final volume of 10 µL.

Normalizing sample RNA abundance by spike in (*optional*): add 2 µL of 0.5 ng/µL *mCherry* (or another RNA) to RNA samples in step 1.

Note 2: Warm an aliquot of acid phenol:chloroform:IAA (125:24:1, pH 4-5; Sigma, cat. 77619) to 65°C.

1. Prepare 80 µL aliquot samples in Eppendorf tubes.
2. Add 14.5 µL of 10% SDS (Promega, cat. V6551) to samples.
3. Add 127.3 µL of, 65°C pre-warmed, acid phenol:chloroform:IAA to the samples and wrap tube in parafilm. Vortex.
4. Incubate for 5 min at 65°C.
5. Incubate for 5 min on ice.
6. Centrifuge at max speed, RT for 2 min.
7. Transfer upper phase to a new tube containing 127.3 µL of phenol:chloroform:IAA at RT. Vortex.
8. Incubate for 5 min at RT.
9. Centrifuge at max speed, RT for 2 min.
10. Transfer upper phase to a new tube containing 127.3 µL of chloroform (to remove the phenol). Vortex.
11. Centrifuge at max speed, RT for 2 min.
12. For this step, use 0.5 mL in 1.5 mL nested tubes (USA Scientific, cat. 1405-9700). Transfer upper phase to a new tube, measure volume. Add 0.1 volume (~7 µL) of 3M sodium acetate (pH 5.5, Invitrogen, cat. AM9740) + 1 volume (~70 µL) of isopropanol. Vortex.
13. Precipitate at -20°C for ~3 hours to overnight, or for 1.5 hour at -80°C.

14. Centrifuge for 15 minutes at max speed and at 4°C.
15. Remove supernatant and add 400 µL of 70% ethanol. Centrifuge for 10 min at 4°C. Repeat step.
16. Incubate for 5 min at RT.
17. Centrifuge at max speed, RT for 2 min.
18. Dry pellet at RT for ~10 min.
19. Remove any remaining liquid using a p2 pipette.
20. Resuspend pellet in 10 µL of RNase-free H_2O.
21. Take a 1.3 µL aliquot in a PCR tube, per sample, and determine the concentration loading 1 µL in a Nanodrop.
22. Store samples at -80°C or use immediately.